CoQ10 Deficiency: The Lysosomal Paradigm

By: Robert Alexander Heaton

A thesis submitted in partial fulfilment of the requirements of Liverpool John Moores University for the degree of Doctor of Philosophy (PhD)

October - 2021

I Robert Alexander Heaton conform, that the work presented in this thesis is my own. Where information has been derived from other sources, I can confirm that this has been indicated and acknowledged in the thesis.

Signed ……

Date 29/10/2021

Abstract

Coenzyme Q_{10} (CoQ_{10}) deficiency currently represents the only treatable disorder of the mitochondrial electron transport chain (METC). Generally, in patients with CoQ_{10} deficiency there is some form of neurological impairment typically presenting as either ataxia and/or seizures. Currently the preponderance of research relating to a CoQ_{10} deficiency has focused on its effect on mitochondrial function, and there is a paucity of information on how this may affect other organelles. Interestingly, the lysosome has been found to have a large concentration of CoQ_{10} localised in its membrane which is thought to play a role in the normal acidification of the lysosomal lumen. In order to investigate the effect of a CoQ_{10} deficiency on lysosomal acidification, we established a neuronal cell model of CoQ_{10} deficiency via the treatment of the cell line SH-SY5Y with Para-AminoBenzoic Acid (PABA) a competitive inhibitor of the CoQ_{10} biosynthetic enzyme, para-hydroxybenzoate—polyprenyltransferase (COQ2). A single 1 mM (5 days) treatment with PABA resulted in a significant decrease of up to 58% in cellular CoQ_{10} status ($p < 0.05$). This decrease in cellular CoQ_{10} status was then found to be associated with a significant decrease in both the LysoSensor (23%) and LysoTracker 167 (35%) fluorescence; probes used to measure lysosomal lumen pH ($p < 0.05$). This suggests that the lysosomal pH has been significantly increased as the result of a deficit in CoQ_{10} status. Additionally, a third pH probe was used, LysoSensor 160, which was able to accurately determine the pH of the lysosomal lumen. It was found that a decrease in neuronal CoQ_{10} status of (58%) resulted in a significant increase in lysosomal pH from 4.1 in control cells, to 6.3 in the CoQ_{10} deficient state. This finding provides evidence of the vulnerability of the lysosomal pH to changes in CoQ_{10} status and is the first study of its kind to investigate this phenomenon.

Subsequently, the neuronal cell model was utilised to evaluate whether the observed increase in lysosomal pH associated with a CoQ_{10} deficiency and could it be reversed via supplementation with CoQ_{10} at levels reported to improve mitochondrial function in patient fibroblast studies. Treatment with CoQ_{10} (5 μM, 3 days) was found to restore cellular CoQ_{10} concentration above controls ($p < 0.005$) and this was associated with an increase in both LysoTracker and LysoSensor 167 fluorescence to around 90% of

control levels ($p < 0.05$), suggesting that lysosomal pH had been restored to 90% of its original level. Analysis of the LysoSensor 160 probe showed CoQ_{10} supplementation was associated with a reduction in lysosomal pH from 6.3 to around 4.7.

In addition to the increase in lysosomal pH, a number of other cellular aspects were also investigated in an attempt to determine some possible mechanisms causing the increase in lysosomal pH in CoQ_{10} deficient neuronal cells. General METC function was measured using the fluorescent probes JC-1 and MTG together with measurements of the mitochondrial marker enzyme, citrate synthase (CS) and assessments of total cellular ATP concentration. JC-1 is a specific probe which measures mitochondrial membrane potential ($\Delta\Psi_m$) and using this probe it was found that there was no significant difference in the fluorescence between the control and CoQ_{10} deficient cells. Additionally, MTG, a probe that assesses mitochondrial mass also found no significant difference between control cells and CoQ_{10} deficient cells. In contrast, CS activity and cellular ATP concentration were found to be significantly different between control and CoQ_{10} deficient neurones. CS activity was significantly increased ($p< 0.005$) in the CoQ_{10} deficient neurones contradicting the MTG result. In addition, cellular ATP concentration was found to be significantly decreased (15% lower than controls) in the CoQ_{10} deficient neurones. The deficit in cellular ATP status may impact upon the lysosomal pH given the requirement of the lysosomal V-ATPase for cytosolic ATP. In this study we also measured total cellular reactive oxygen species (ROS) levels due to because of CoQ_{10}'s role as a potent antioxidant and the lysosomes sensitivity to oxidative stress induced impairment. Commensurate with the deficit in neuronal cellular CoQ_{10} status a significant increase in cellular ROS levels (29% $p< 0.005$) was determined which could also contribute to lysosomal alkalisation.

In conclusion, this PhD thesis has been successful in providing an insight into the association between lysosomal pH and cellular CoQ_{10} status. It has provided evidence to support the possibility that a deficit in cellular CoQ_{10} status may result in an impairment of lysosomal acidification which may impinge on the function of this

organelle.

Table of Contents

Table of Figures

Table of Tables

List of Abbreviations

3-hydroxy-3-methylglutaryl-CoA ……	HMG-CoA
5, 5'-dithio-bis (2-nitrobenzoic acid) ……..	DTNB
Acetyl-coenzyme a ……	acetyl-CoA
Adenosine tri phosphate …….	ATP
Alzheimer's disease …….	AD
Blood-brain barrier …….	BBB
Blue Native Poly-Acrylamide Gel Electrophoresis	BN-PAGE
Cerebellar ataxia ……	CA
Cerebellar ataxia ……	CA
Chaperone-mediated autophagy ……	CMA
Chorismate lyase ……	UBiC
Citrate Synthase ……..	CS
Coenzyme $Q_{10.}$ ……	CoQ_{10}
Dimethyl sulphoxide. ……	DMSO
Dulbecco's modified Eagle's medium …….	DMEM
Electron transferring protein ……	ETP
Enzyme replacement therapy ……	ERT
Farnesyl pyrophosphate ……	FPP
Farnsworth–Munsell 100 Hue test ……	FMT
Flavin adenine dinucleotide …….	FAD
Fluorescent 2', 7'- dichlorofluorescein ……	DCF
Foetal bovine serum ……	FBS
Forward scatter …….	FSC
Gaucher Disease ……	GD
Glucocerebrosidase …….	GBA
Glucosylceramide …….	GlcCer
High performance liquid chromatography. …..	HPLC
Hydroxy-3-methylglutaryl-CoA reductase ……	HMGR
Inorganic phosphate ……	Pi
Iron-sulphur protein ……	ISP
Isopentenyl pyrophosphate …….	IPP
Liquid nitrogen ……	LN2
Lysosomal membrane protein 2 …….	LIMP2
Mevalonate kinase …….	MK
Mitochondrial electron transport chain ……	METC
Mitochondrial encephalomypathy lactic acidosis.	MELAS
Mitochondrial membrane potential ……	ΔΨm
Mitochondrial ROS …….	mtROS
NADH oxidase …….	NOX
National Institute of Health Stroke Scale …….	NIHSS
Niemann Pick C …….	NPC
Oxidative phosphorylation. …….	OXPHOS
Para-aminobenzoic acid ……	PABA
Penicillin streptomycin ……	PC
Phosphate buffer saline ……	PBS

Phosphate buffer saline ……	PBS
Phosphomevalonate kinase ……	PMK
Programmed cell death ……	PCD
Propidium Iodide ……	PI
Proton Motive Force ……	Δp
Reactive nitrogen species ……	RNS
Reactive oxygen species ……	ROS
Side scatter ……	SSC
Sterol regulatory element binding proteins ….	SREBP
Trans-polyprenyl-transferase ……	TPT
Transcription Factor EB ……	TFEB
Tricarboxylic acid ……	TCA
Senescence associated β-galactosidase ……	SA-βgalactosidase
β-galactosidase ……	β-gal

Acknowledgements

I would like to dedicate this thesis to everyone that has contributed to my development both as a scientist and as a person. Firstly, I would like to thank my partner Chelsie for her unwavering support throughout my PhD during both the low and high point for which there where many. Knowing I could go home to complain about every day mundane things and have someone just listen has been a blessing. I would also like to thank my family for their unbridled questioning of what it is I actually do. Specifically, I would like to thank my mum and dad who have shown me no matter the challenge, I can overcome it. Thanks to my dad's extraordinary work ethic and my mums caring nature, coupled with their never-ending support I have never felt any challenge was too large for me to overcome. I would also like to thank my nan for her support, always trying to relate to me via her "time in the lab" back in the dark ages.

I would like to thank my PhD supervisor team; Iain Hargreaves, Khalid Rahman and Simon Heales for their support and imparting some of their wealth of knowledge. Iain has been an amazing supervisor and over the course of my PhD and has become a close friend I have come to rely on. Although his hieroglyphic handwriting almost sent me off the edge more than once, I can honestly say I couldn't have asked for a better supervisor.

I would also like to thank all the people who have helped me, contributing to this project in a multitude of ways. Specifically, Darren Sexton who has put up with my constant badgering on all things flow cytometry. Also, to the ladies that keep the LSB running, Nicola browning and Jenny Thompson, who I have relied upon not only in a professional capacity but also as close friends who I could chat to (sometimes for far too long).

Finally, I would like to thank all my amazing friends at LJMU. Specifically, Nadia, Talhat, Petra and Andy. You all have put up with my nonsense through easily the toughest time in my PhD. Our small group quickly became one of my most utilised support networks, despite our extremely competitive nature (I defiantly won).

General Introduction

1. CoQ_{10} Structure

Coenzyme Qs (CoQs) are a ubiquitous group of coenzymes found in animals, plants and microorganisms (Hargreaves, 2003). Originally characterised by Festenstein et al. (1955), CoQs were dubbed the "275 mμ molecule" as a result of its substantial absorbance at 272 nm. Later it was re-named ubiquinone, because of its quinone structure and ubiquitous nature by Wolf et al. (1958). The complex chemical structure is now known as, 2, 3-dimethoxy, 5-methyl, 6-polyisoprene parabenzoquinone [Figure 1]. The species of CoQ is determined by the length of the polyisoprenoid side chain, varying from 6 to 10 isoprene units (CoQ_6 – CoQ_{10}). The predominant species found in humans is CoQ_{10} which has a side chain made up of ten isoprenoid units, however, small amounts of CoQ_9 (2-7%) can also be found in human tissues (Turunen et al., 2004).

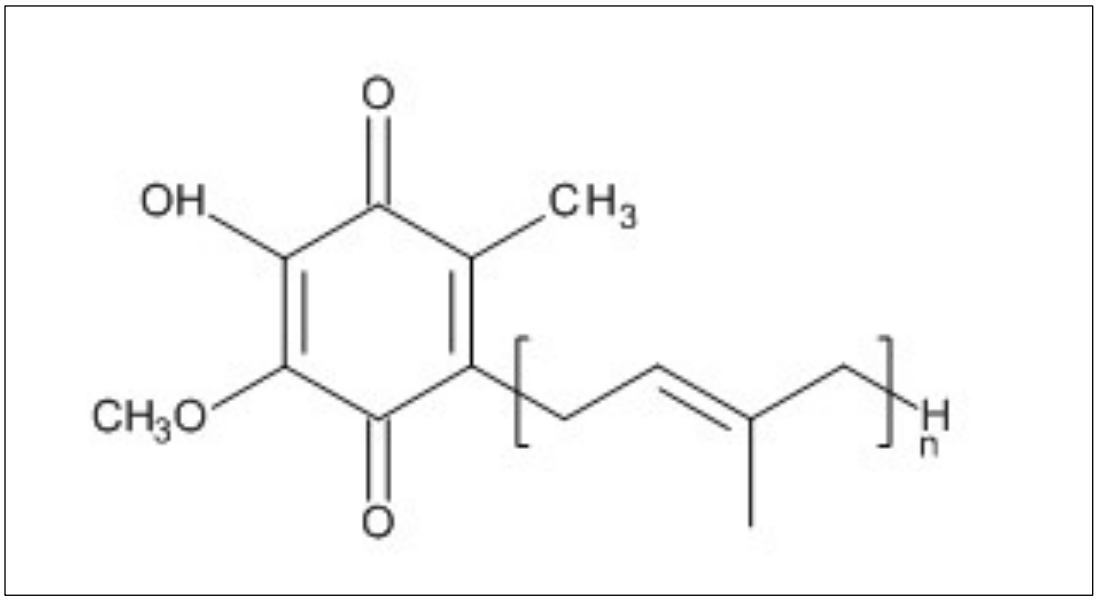

Figure 1. Chemical Structure of Coenzyme Q, N = Number of Isoprenoid Units

2. CoQ_{10} Biosynthesis

CoQ_{10} is a product of the mevalonate pathway (figure 2) and has been studied extensively in yeast and bacteria; however, in comparison, little is understood about the pathway in mammals. In the first stage of the pathway, acetyl-coenzyme (acetylCoA) is utilised to synthesize farnesyl pyrophosphate (FPP). FPP is then condensed to 4-hydroxybenzoate derived from tyrosine. In the final stages of the pathway a series of ring modifications occurs on the benzoquinone core (figure 1). at this point the difference between procryptic and eukaryotic becomes apparent, as the order of synthetic events in the terminal pathways differs. In yeast (prokaryotes) the modification order is decarboxylation, hydroxylation and methylation, however in bacteria the methylation takes place before decarboxylation and then hydroxylation (Tran and Clarke, 2007, Kawamukai, 2009).

2.1 Biochemistry of the Mevalonate Pathway

The mevalonate pathway is reasonable for the production of a number of important biological molecules, most notably cholesterol and CoQ_{10} (figure 2). The pathway is reasonable for the formation of (FPP) from acetyl-CoA. FPP can be considered to be the linchpin of the pathway as it is the universal intermediate for all its products (Fisher et al., 2000, Brown and Goldstein, 1986).

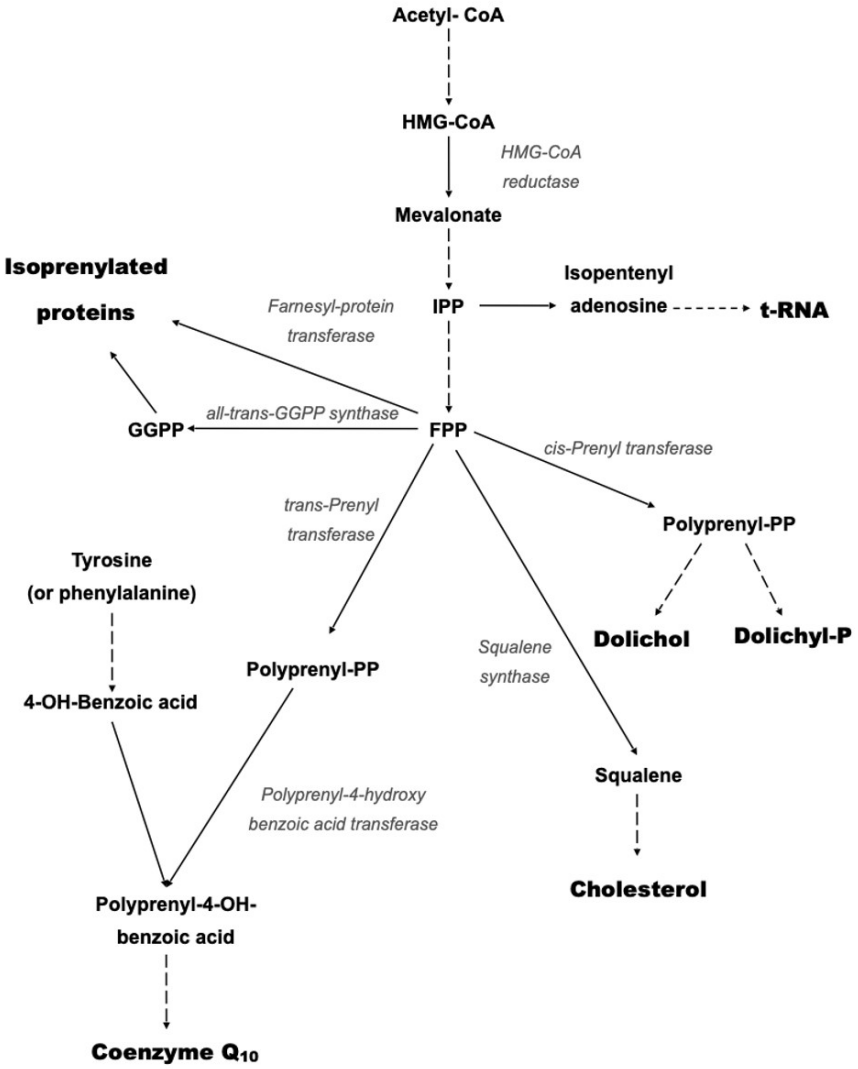

Figure 2. The Mevalonate Pathway.

CoQ_{10} is synthesised from Acetyl CoA through a complex pathway. Additionally, this pathway is responsible for the synthesis of cholesterol, dolichol, t-RNA and isoprenylated proteins. The farnesyl pyrophosphate branching point appears to be a key regulation point for the synthesis for all the final products. Taken from, (Buhaescu and Izzedine, 2007).

The initial steps of the pathway involve the synthesis of 3-hydroxy-3-methylglutarylCoA (HMG)-CoA from acetyl-CoA, this step is facilitated by two enzymes, acetoacetyl-CoA thiolase and HMG-CoA synthase. The enzyme hydroxy-3methylglutaryl-CoA reductase (HMGR) can then catalyse the conversion of HMGCoA into mevalonate. HMGR is considered to be one of the main rate-limiting enzymes in the pathway and is one of the most regulated enzymes in nature (Goldstein and Brown, 1990). This enzyme has been extensively studied in the synthesis of cholesterol, although with its position within the pathway it can be assumed its mediation has an effect on CoQ_{10} biosynthesis (figure 2). Evidence has

shown that gene transcription of HMGR can be activated by a family of transcription factors called sterol regulatory element binding proteins (SREBPs) (Weber et al., 2004). Additionally, there is evidence that SREBPs can activate the gene expression of all enzymes in the mevalonate pathway, suggesting a level of genetic control of CoQ_{10} biosynthesis (Sakakura et al., 2001).

The second stage of the pathway involves the phosphorylation of mevalonate into isopentenyl pyrophosphate (IPP) and then FPP. This stage is mediated by two more enzymes; mevalonate kinase (MK) and phosphomevalonate kinase (PMK). MK is responsible for phosphorylation of mevalonate into IPP. Although not as closely controlled as HMGR, MK can be considered yet another supervisory enzyme for the pathway, with MK being shown to be regulated via feedback from downstream intermediates in the mevalonate pathway (Hinson et al., 1997). PMK can then catalyse the conversion of IPP and ATP into FPP and ADP. FPP can then be utilsed to create the final products of the pathway, cholesterol, dolichol, CoQ_{10} or isoprenylated proteins. This is catalysed by one of the four enzymes: squalene synthase, *cis*prenyltransferase, *trans*-prenyltransferase and farnesyl-protein transferase. These enzymes are also considered to be regulatory points for the latter stages of the pathway, as they can limit or increase the formation of any of the four products depending on the cells current needs, via feedback loops (Buhaescu and Izzedine, 2007).

2.2. Synthesis of 4-hydroxy Benzoate

The precursor for the synthesis of the benzoquinone ring of CoQ_{10} is 4-hydroxy benzoate (4-HB). Prokaryotic organisms can synthesize 4-HB through *de novo* pathways. In E.coli for example, its synthesis is catalysed by the enzyme chorismite lyase (UbiC) (Meganathan, 2001). However, in eukaryotic organisms this does not occur and synthesis of 4-HB must rely on dietary sources for the essential amino acids, as a result, tyrosine and phenylalanine are utilised in order to synthesise 4-HB (Tran and Clarke, 2007).

2.3 CoQ Species Determination

The species of CoQ is determined by the length of the isoprenoid side chain, and the predominant form can vary depending on which animal it is present in. This has been shown extensively in a number of studies. For example, the predominant species of CoQ_{10} in rats is CoQ_9, whereas in Saccharomyces species CoQ_6 is predominantly produce, and in humans the predominant CoQ is CoQ_{10} (Tran and Clarke, 2007, Martinefski et al., 2014).

Formation of the trans-polyprenyl tail is controlled by the enzyme trans-polyprenyltransferase (TPT). TPT is encoded by the genes responsible for CoQ_1 which is in turn responsible for determining the species-specific tail length (Okada et al., 1998). In humans the side chain is determined by the TPT that is encoded by both the PDSS1 and PDSS2 genes in theCoQ_1 gene set (Saiki et al., 2005). The synthesis of the side chain also differs between eukaryotes and prokaryotes, as the side chain is synthesised in the mevalonate pathway in eukaryotes; however, in prokaryotes it is synthesised in the MEP (2-C-methyl-D-erythritol 4-phosphate) (or non-mevalonate) pathway (Meganathan, 2001). An isomer of IPP, DMAPP (dimethylallyl diphosphate) facilitates the condensation of a single IPP molecule to create an isoprenoid with a particular length (Figure 3) (Kawamukai, 2009).

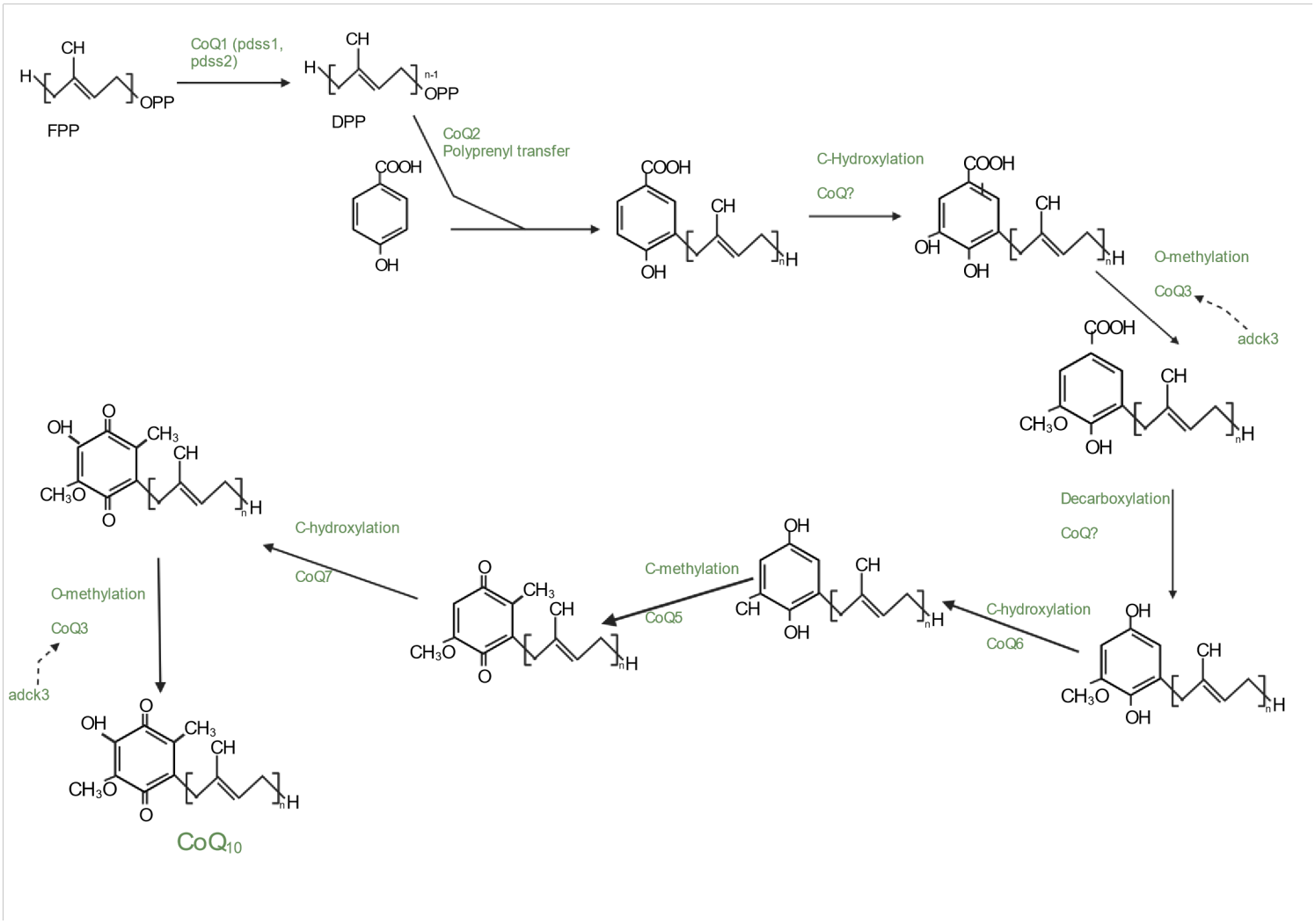

Figure 3. CoQ Biosynthetic Pathway.

Originally characterised in yeast, displays the proposed biosynthesis of CoQ. Adck3 has been suggested to act as a kinase in the phosphorylation of CoQ3 (Tauche et al., 2008). CoQ? Represents unclassified molecules.

3. CoQ_{10} function

CoQ_{10} plays a complex role in the homeostasis of the cell, with various functions from energy production to its role as an antioxidant (Crane, 2001). Arguably, one of the most important roles CoQ_{10} plays is as an electron carrier in the mitochondrial electron transport chain (METC) as depicted in figure 2. Crane (1957) first proposed an important role for CoQ_{10} in the oxidative phosphorylation process of the METC. This process creates a proton gradient across the mitochondrial inner membrane which is utilized for the production of ATP (Mitchell, 1966, Mitchell, 1961, Perry et al., 2011). It is now widely accepted that in humans COQ_{10} has a fundamental role in this cardinal process and changes in CoQ_{10} concentrations have been linked to a plethora of diseases associated with impaired mitochondrial function (Hargreaves, 2003).

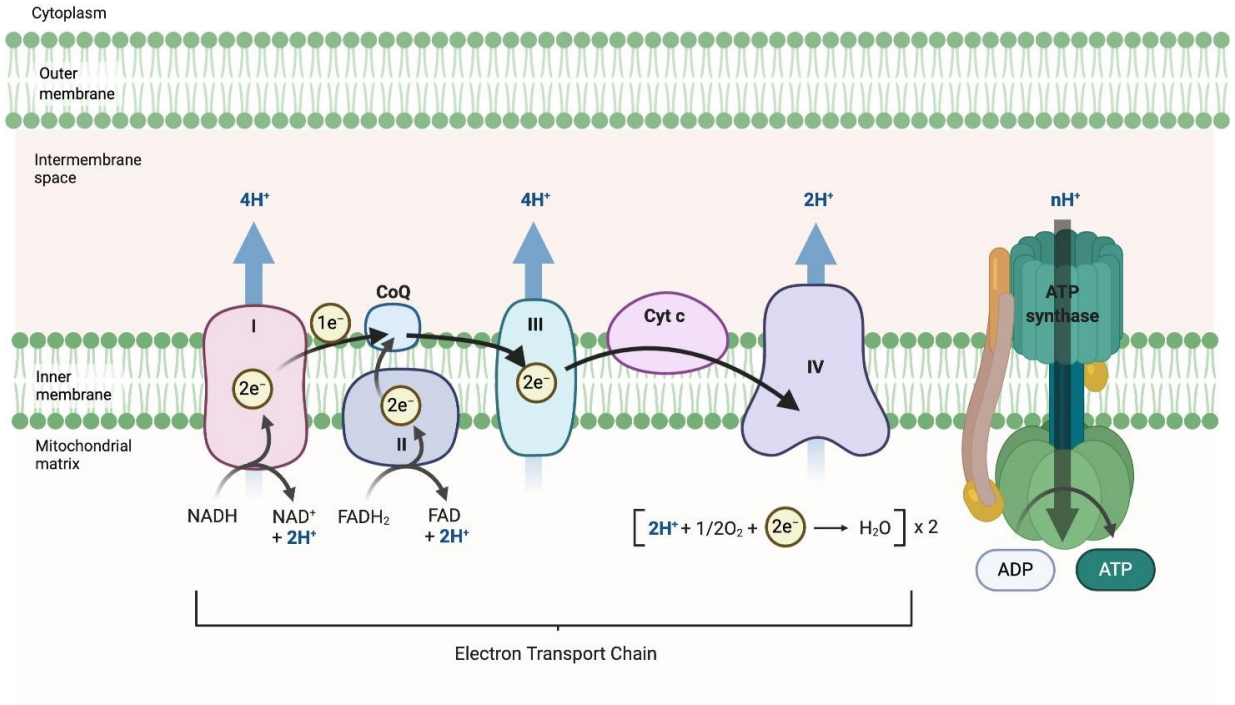

Figure 4. Mitochondrial Electron Transport Chain (ETC) + Complex V (ATP Synthase).

CoQ accepts electrons form both complex I and complex II, passing them to complex III. The electros can then be transported from complex III to complex IV via cytochrome c (shown as Cyt c). This stepwise proses facilitates the creation of a proton gradient across the mitochondrial membrane, which can then be utilised for the phosphorylation of ADP to ATP through complex V (shown as ATP synthase).

In the METC CoQ_{10} acts as an electron carrier, accepting electrons derived from Complex I (NADH ubiquinone oxidoreductase; EC 1.6.5.3) and Complex II (succinate ubiquinone reductase; ETF: QO EC 1.3.5.1) then transporting them to Complex III (ubiquinol cytochrome *c* reductase; EC 1.10.2.2) (Crane, 2001, Ernster and Dallner, 1995). The electrons are then transported via cytochrome c to the final acceptor, Complex IV (cytochrome *c* oxidase; EC 1.9.3.1). This passage of electrons creates a proton rich environment inside the mitochondrial inner membrane space, which in turn creates an energy source called the Proton-Motive Force (Alberts, 2002). This is then utilized by Complex V (ATP synthase; EC 3.6.3.14) to generate ATP.

Originally it was hypothesized that all the components of the METC were arranged in a fluid mosaic model, meaning that all the enzyme complexes where randomly distributed across the mitochondrial inner membrane and were mobile (Green and Tzagoloff, 1966). As a result of this it was presumed that electron transfer would ensue through random collisions between the complexes (Hackenbrock et al., 1986). It wasn't until Kröger et al. (1973) quantified the two-enzyme oxidation reduction of CoQ_{10} in beef bovine heart mitochondria, which suggested the existence of the CoQ_{10} pool in this organelle. Consequently, CoQ_{10} is able to behave kinetically as a freely defusing pool, ferrying electrons amongst Complexes I, II and III.

However, we now know this theory may be erroneous; through various assays including Blue Native Poly-Acrylamide Gel Electrophoresis (BN-PAGE) which have revealed the presence of multi-complex super structures in a multitude of different organisms such as yeast, bacteria, and mammalian mitochondria (Schägger and Pfeiffer, 2000). Interestingly, it has been found that complexes I, II and IV commonly form super-complexes, allowing for the direct transfer of electrons between them depending on the stoichiometric ratio and through the use of electron carriers (CoQ_{10} and cytochrome c). Indeed, it has been suggested that 70% of the Complex I enzyme present in the METC is associated with the super complexes (Schägger and Pfeiffer, 2000). In addition to this, the METC appears to act as a single component and any changes in the function of one unit can lead to global impairment (Kholodenko et al., 1995).

3.1 The METC Complexes

3.1.1 Complex I

Consisting of 45 subunits and with a molecular mass of 980kDa, Complex I represent the largest enzyme in the METC. Complex I was initially characterised using electron microscopy, with more detailed analysis carried out using X-ray crystallography in the bacterium, Thermus thermophilus and the fungus, Yarrowia lipolytica (Fassone and Rahman, 2012).

METC Complex I is responsible for the oxidation of NADH and the resulting reduction of CoQ_{10}. Reduction facilitates the movement of H^+ ions across the inner mitochondrial membrane (Brandt, 1999). Proton Motive Force (Δp) is created from three successive steps of rapid electron transfer, from a Flavin mononucleotide along a succession of iron-sulphur clusters; this then facilitates Complex V in the production of ATP (Maloney et al., 1974, Rao et al., 2008). When Complex I oxidises NADH creating NAD+ two electrons are also produced, these electrons are then responsible for the reduction of CoQ_{10} to $CoQ_{10}H_2$. $CoQ_{10}H_2$ then translocated to Complex III where it is re-oxidised (Hirst, 2010).

The METC is also a major contributor to reactive oxygen species (ROS) production within the cell, with Complex I being one of the major sites of leakage of this free radical (Dunn et al., 2015). It was first recognised that Complex I was a major contributor to cellular ROS generation by Hinkle et al. (1967), who identified the ROS production following the reduction of CoQ_{10}; also H_2O_2 production in submitochondrial partials and the subsequent production of O2- (superoxide) by Complex I in the presence of NADH. Additionally, Cadenas et al. (1977) found that O_2 production is increased after the addition of the Complex I inhibitor (rotenone), in this case ROS is produced when there is a low concentration of ATP and a high NADH/NAD+ ratio.

3.1.2 Complex II

Complex II represents the only METC complex that contributes to both the Krebs cycle and the METC. Complex II is responsible for the reduction of fumarate in the Krebs cycle, leading to the reduction of CoQ_{10} and the replenishment of the $CoQH_2$ pool (Ackrell, 2000). Additionally, Complex II is also the only enzyme complex entirely nuclear encoded, whilst the other complexes are both nuclear and mitochondrial DNA encoded (Bezawork-Geleta et al., 2017).

Complex II is bound to the mitochondrial inner membrane by an iron-sulfur protein (SDHB) and two hydrophobic transmembrane subunits (SDHC and SDHD); the transmembrane components are composed of cytochrome b, haem b and a CoQ_{10} binding cites (Ackrell, 2000).

In the process of succinate oxidation, the cofactor, flavin adenine dinucleotide (FAD) accepts two hydride ions to form $FADH_2$. The reduced $FADH_2$ can then pass electrons down the iron-sulphur clusters [2Fe-2S] and [4Fe-4S] to the terminal acceptor [3Fe-4S], where CoQ_{10} is then reduced with the transitional creation of a semi-ubiquinone (Anderson et al., 2005).

3.1.3 Complex III

Complex III consists of 11 subunits, 6 low-molecular weight proteins, 3 respiratory, and 2 core units (Rieske, 1976, Solmaz and Hunte, 2008). Most subunits are manufactured in the nucleus with the exception of cytochrome b which is synthesised in the mitochondria.

Complex III is responsible for passing the electrons gained from complexes I and II onto Complex IV. For this to occur the synchronised movement of electrons from $CoQ_{10}H_2$ via two pathways needs to occur (Mitchell, 1975). The iron cluster [2Fe-2S] is the first of these electron acceptors, located on the Rieske iron sulphur protein (ISP).

Then the electrons are moved through a fixed cytochrome c1 onto the peripatetic cytochrome c2, from here the electrons can then move to Complex IV (Crofts, 2004).

The second route consists of cytochrome b_L and cytochrome b_H and a Q_i-site. The $Q_i$site catalyses the reduction of CoQ_{10} via a two-electron transfer (Crofts, 2004). The electrons needed for this process are provided by the oxidation of two molecules of $CoQ_{10}H_2$ at the Q_i-site, thus releasing four H^+ ions, giving each chain two electrons (Crofts, 2004).

Complex III has been identified as a major site for ROS production in the METC, due to the production of semiubiquinone. This is because, when the second path is blocked the movement of electrons from the intermediate semiubiquinone onto cytochrome b_L becomes limited, leading to the production of the ROS, superoxide (Turrens et al., 1985).

3.1.4 Complex IV

Complex IV, represents the final electron acceptor in the METC and is the only genuine proton pump in the METC (Wikstrom, 1977). Complex IV consists of 14 protein subunits, with 11 of them encoded by the nucleus and the remaining 3 by the mitochondria. Complex IV also has a number of metal prosthetic units, including haems, cytochrome a, and a3, and two copper centres (Brzezinski and Gennis, 2008). Four electrons are passed on to Complex IV by cytochrome c. Subsequently, protons from within the mitochondrial matrix are used to create two water molecules from one oxygen molecule. The reaction depicted below shows the 4-electron reduction of water catalysed by complex IV (Brzezinski and Gennis, 2008).

4 Fe2+-cytochrome c + 8 H+ in + O2↔4 Fe3+-cytochrome c + 2 H_2O + 4 H+ out

3.1.5 Complex V

Complex V although not strictly part of the METC, is essential for the process of oxidative phosphorylation, enabling the movement of protons (H^+ ions) from the mitochondrial inner space into the matrix with the concomitant production of ATP.

Complex V is composed of two major subunits, F_1 and F_o; the F_1 subunit resides within the mitochondrial space and the F_o subunit spans the mitochondrial inner membrane as shown in figure 5.

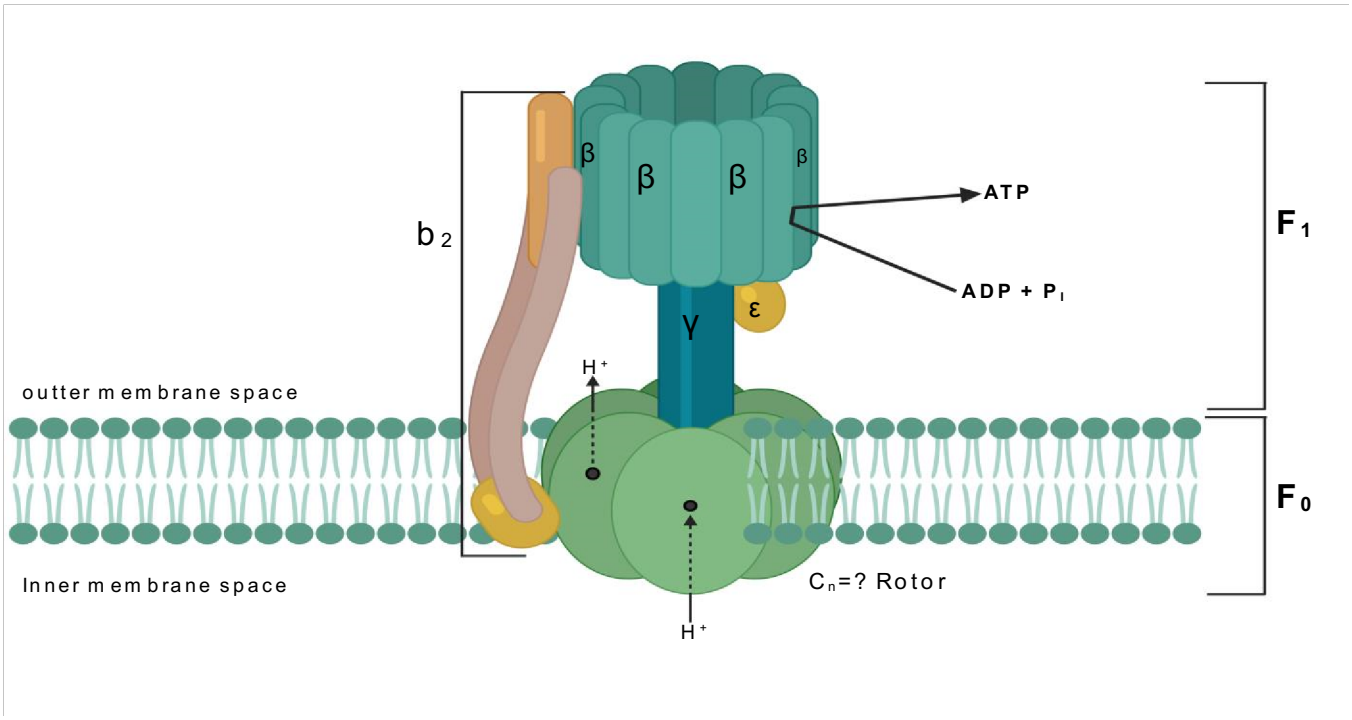

Figure 5. Complex V (ATP Synthase).

Ada pted from Okuno et al. (2011), shows the basic structure of ATP synthases and how it consists of a F_1 and F_0 subunit.

Paul Boyer won a Nobel Prize for his work on the function of Complex V proposing the Binding Change Model as its mechanism for the synthesis of ATP (Boyer, 1997). Boyer proposed that the rotation of the γ subunit leads to a binding change in the catalytic β subunits and was able to demonstrate alternating α and β subunits fixed to a γ unit (α3β3γδε) in the F_1 subunit (Boyer, 1997).

The proton motive force created by the METC allows for the flow of H^+ ions through the F_o subunit of Complex V. Arginine residues on the ATPase facilitate the passage of H^+ ions through a c-ring subunit, which then pushes the c-ring to rotate. The c-ring is directly attached to the γ subunit in the F_1 region, this leads to the rotation of the γ unit and a series of conformational changes in the catalytic nucleotide binding sites

which allows the addition of P_i groups onto ADP, thus synthesising ATP (von Ballmoos et al., 2008). Interestingly, it has also been reported that the arginine residue may also play a role in discriminating between binding substrates, ensuring the appropriate ones are bound; additionally, certifying that the correct substrate is released i.e., ATP is released rather than ADP+Pi from the catalytic site during ATP synthesis, and in contrast that ADP+Pi are released in hydrolysis (Menz et al., 2001).

Interestingly, a number of studies have shown that in some conditions, Complex V can work in the opposite direction, and instead of synthesizing ATP it catabolizes the nucleotide to generate energy to move protons against the concentration gradient (Chinopoulos, 2011).

3.2 Flavoprotein Quinone Oxidoreductase

Although the major source of cellular energy is the METC, the cell can also utilise a number of other processes for energy generation including fatty acid β-oxidation (Bartlett and Eaton, 2004). In the process of fatty acid β-oxidation two carbon units are removed from a long-chain acyl-CoA, through the recurrent cycle of oxidation, hydration, oxidation and thiolysis. A medium-chain acyl-CoA dehydrogenase will oxidise an octanoyl-CoA to oct-2-3-enoyl-CoA, then the medium-chain acyl-CoA dehydrogenase is itself re-oxidised through two electron transferring protein (ETP); which in turn is re-oxidised by ETP-QO, this then allows the transfer of electrons to the mitochondrial CoQ pool (Watmough and Frerman, 2010). These electrons can then be utilised by the METC for oxidative phosphorylation for the synthesis of ATP.

3.3. The antioxidant Function of CoQ10

3.3.1. Oxidative stress

Oxidative stress represents an imbalance between the production of reactive oxygen species (ROS) and the organism's ability to neutralise the reactive intermediates or repair the damage created (Sies, 2000). Although ROS are utilized in the cell as signalling mechanism, an increased concentration of ROS can lead to the damage of all cellular components, including DNA, lipids and proteins (Sies, 2000). Equally a decrease in ROS production can lead to a number of complications due to their

responsibility in cell signalling (Martin and Barrett, 2002).

3.3.2. Mitochondrial Oxidative Stress

In mammalian cells almost all the oxygen consumption (around 90%) can be associated with mitochondrial ATP production. As a result of this, the mitochondrion can also be held responsible for the majority of cellular ROS production (around 1-2% of mitochondrial oxygen consumption) (Rolfe and Brown, 1997, Skulachev, 1998). Although mitochondrial ATP synthesis is highly efficient, this process requires oneelectron oxidation and reduction reactions which causes the mitochondria to be predisposed to ROS generation. Which in turn means that the mitochondria are predisposed to the creation of ROS. In fact, it has been reported that the mitochondrial matrix has a 5 to 10 fold higher concentration of free radicals than any other of the cellular organelles (Cadenas and Davies, 2000).

3.3.3. CoQ_{10} as an Antioxidant

CoQ_{10} is found in almost all cellular membranes at a relatively high concentration, in some cases 30 times greater than that of other antioxidants such as vitamin E (Kagan et al., 2000, Frei et al., 1990). In view of this, CoQ_{10} can be found in close proximity to an abundance of unsaturated lipids; these lipids are pre-disposed to lipid peroxidation and thus the free radical scavenging ability of CoQ_{10} is paramount in maintaining cellular homeostasis. A multitude of studies have demonstrated the ability of CoQ_{10} to protect the cell against oxidative damage, for example Frei et al. (1990), Eskelinen (2006) suggested that the reduced form of CoQ_{10}, ubiquinol, is considered to be more effective than its counterpart vitamin E. Although the exact reason for this finding is yet to be elucidated, one hypothesis could be that CoQ_{10} has two active sites, where one CoQ_{10} molecule can interact with two superoxide molecules (Dutton et al., 2000) (figure 6). Additionally, it has been shown that ubiquinol is able to restore Vitamin E concentrations through the α-tocopheroxyl radical (Ernster and Forsmark-Andree, 1993). A study by Stoyanovsky et al. (1995) found evidence that the one electron reduction of CoQ_{10} was able to induce the redoxcycling of α-tocopherol (a form of vitamin E) from its phenoxyl radical, consequently preventing the loss of α-tocopherol (Stoyanovsky et al., 1995). In light of this role, the regeneration of ubiquinol is fundamental to the maintenance of its antioxidant

functions within the cell and its status is maintained by the METC (Åberg et al., 1992). Outside of the mitochondria however, three distinct enzymes have been noted to maintain the ubiquinol concentration in cellular membranes and even in blood plasma, these enzymes are: NADH cytochrome b5 reductase; NADH/NADPH oxidoreductase and NADPH coenzyme Q reductase (Villalba and Navas, 2000). Both NADH, cytochrome b5 reductase and NADPH coenzyme Q reductase can reduce semiubiquinone to ubiquinol via one electron transfer, whereas the enzyme DT diaphorase can facilitate the two-electron reduction, thus reducing the intermediate ubisemiquinone (Figure 6). Interestingly, upon enhanced oxidative stress levels the concentration of CoQ_{10} has been found to increase, along with a relative increase in DT diaphorase activity, providing further support for the important contribution CoQ_{10} makes to the antioxidant capacity of the cell (Navarro et al., 1999).

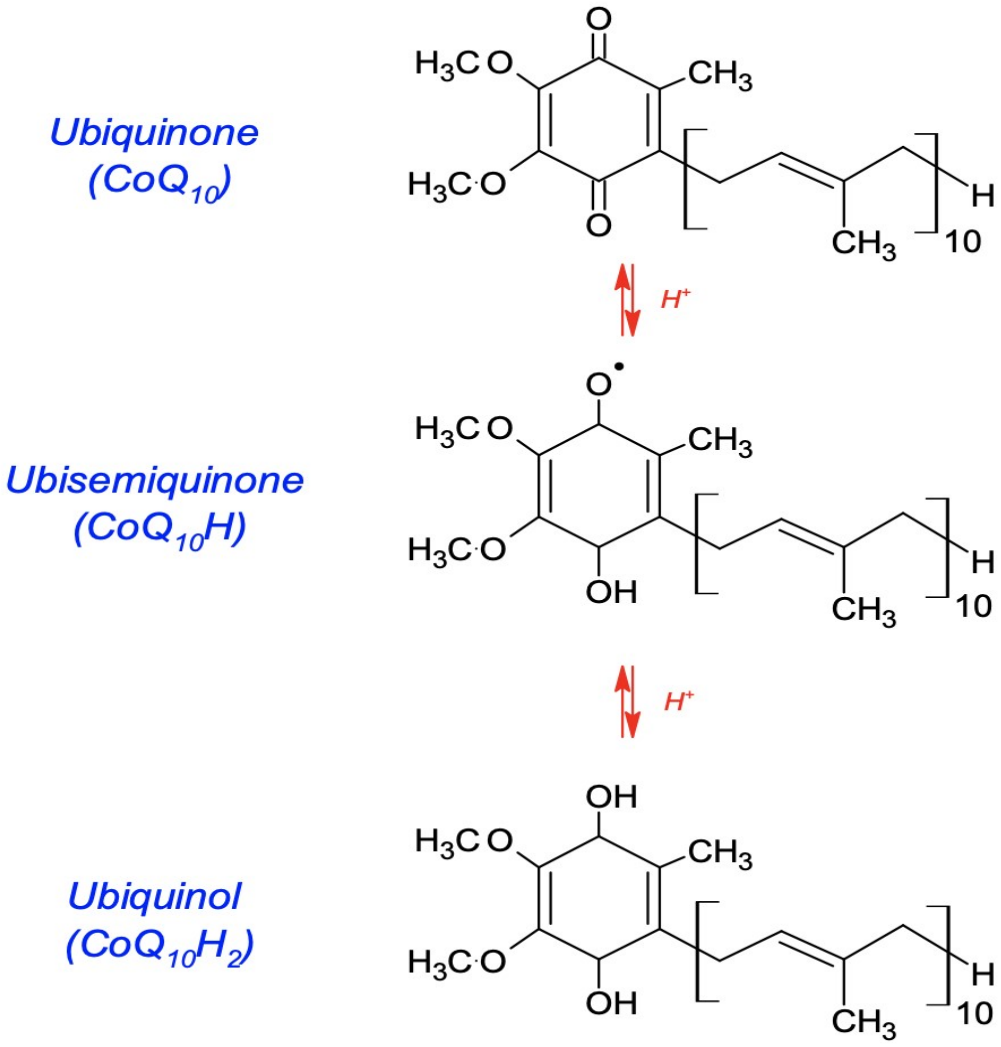

Figure 6. The Redox States of CoQ10

The ability of ubiquinol to reduce vitamin E back into its active *a*-tocopherol form is also evidence of its importance in protecting the cell against oxidative stress. It has been found that even a relatively low concentration of ubiquinol (which is commonly found in lipoproteins), is proficient at the regeneration of the active form of vitamin E, thus increasing the antioxidant concentrations (Schneider and Elstner, 2000, Thomas et al., 1999). Additionally, although it is well documented that the cellular antioxidant, reduced glutathione is responsible for the bulk of vitamin C regeneration studies have shown this can also take place via the plasma membrane electron transport chain (section 3), which involves the electron carrier function of CoQ_{10} (Crane, 2001).

The efficiency of CoQ_{10} as an antioxidant has been demonstrated in both yeast models by Poon et al. (1997) and CoQ_{10} deficient patient fibroblasts by Quinzii et al. (2010). In both models of CoQ_{10} deficiency, increased ROS concentrations were detected. In yeast, the CoQ_{10} deficiency was associated with an increased lipid peroxide concentration (Poon et al., 1997); and in the fibroblast model with a CoQ_{10} deficiency of 30-50% compared to control levels, a significant increase in lipid peroxidation was also reported (Quinzii et al., 2010).

3.3.4. CoQ_{10} in Plasma Membrane Redox

CoQ_{10} is extremely versatile and within the mitochondrion it is able to facilitate electron transport across the plasma membrane. Eukaryotic plasma membranes have an enzyme called NADH oxidase (NOX) on the external surface, which is utilised for the movement of electrons across the plasma membrane (Moiré et al., 1988, Löw et al., 2012). Both hormones and growth factors are able to locate and activate NOX (Brightman et al., 1992, Lijnen et al., 2012). Once NOX is stimulated an internally bound quinone reductase catalyses the reduction of CoQ_{10} in the presence of NADH, regenerating the cellular pool of reduced CoQ_{10} (Crane and Löw, 2012).

NOX has been linked to a number of cellular functions such as cell growth and differentiation and has been studied in a number of different roles. An example of this is Gómez-Díaz et al. (1997), whose research showed that NOX plays a role in regulating the cytosolic NAD^+/NADH ratio. Additionally, a study undertaken by Larm et al. (1994) showed that without mitochondrial DNA the cell retains the ability to regenerate NADH in the plasma membrane. In 1994 Crane et al. (1994) suggested that the redox state of the quinone in the oxidase acts as a signalling mechanism, controlling the tyrosine kinase either by the generation of H_2O_2 or a redox-induced conformational change, this change can lead to activation of gene expression (Stirpe et al., 1991).

3.3.5. CoQ_{10} in regulating cellular membranes

It has been reported that CoQ_{10} is distributed in all cellular and organelle membranes in varying concentrations (Turunen et al., 2004, Gille and Nohl, 2000). The variation in the concentration of CoQ_{10} may be a result of the function of that membrane, with changes in CoQ_{10} and other ubiquitous lipids altering the structural and functional properties of the membrane. CoQ_{10} has a long side chain that remains in the hydrophobic portion of the bilayer, an increased concentration of CoQ_{10} would most likely increase membrane thickness and increase the permeability thus de-stabilising the membrane depending on its function. In contrast, cholesterol has a short side chain that does not remain in the inner membrane space, thus decreasing its permeability and fluidity (Van Dijck et al., 1976). As a result of this, it can be assumed that the concentration of these ubiquitous molecules is closely maintained, and they are fundamental in maintaining membrane structure and function (figure 7).

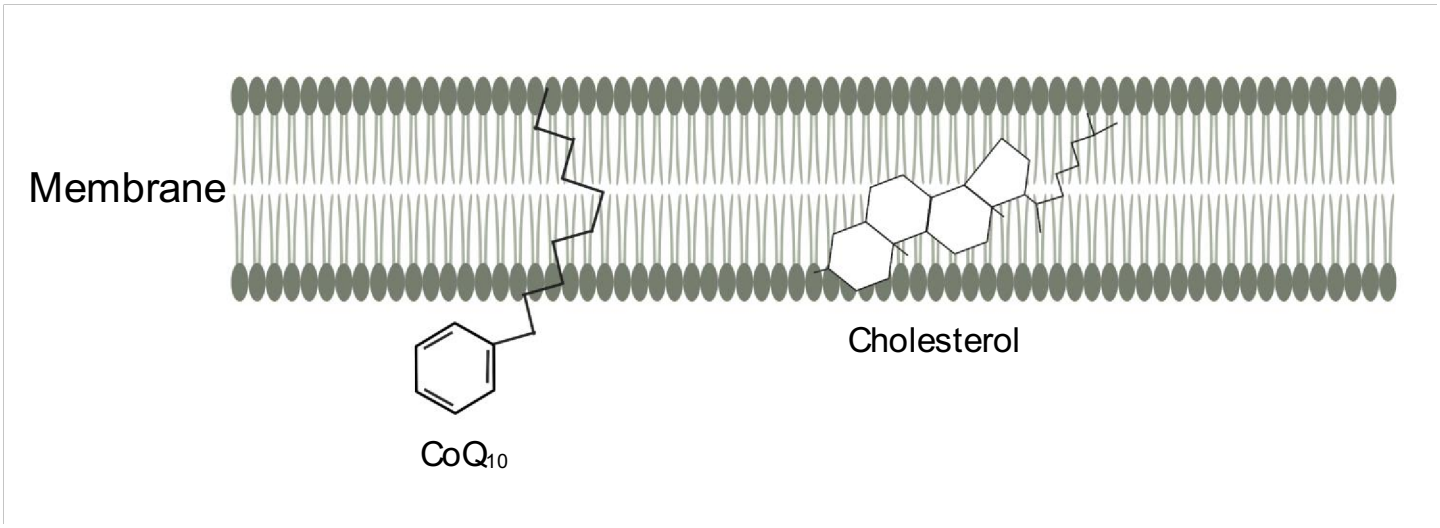

Figure 7. Intramembranous distribution of both CoQ10 and Cholesterol.

CoQ_{10}' s longer side chain is able to hold the molecule close to the membrane, whereas cholesterol's side chain is much shorter reducing its permeability and fluidity across the membrane.

In both primary and secondary CoQ_{10} deficiency, diagnosis remains an important clinical challenge. Evidence of a CoQ_{10} deficiency can be identified following assessment of METC complex I/III (NADH: cytochrome c reductase; EC 1.6.5.3 + 1.10.2.2) and/or complex II/III (succinate: cytochrome c reductase; EC. 1.3.5.1 + 1.10.2.2) whose activities are dependent upon endogenous CoQ_{10} (Montero et al., 2013). Diagnosis can be confirmed with measurement of CoQ_{10} in skeletal muscle, patient fibroblasts or blood mononuclear cells. Blood plasma has been reported to be a poor surrogate of endogenous CoQ_{10} status whose concentration is influenced by the level of circulatory lipoproteins, the major carriers of CoQ_{10} in the blood (Duncan et al., 2005). However, once biochemical evidence of a deficit in CoQ_{10} status has been detected, further studies will then be required to determine whether it is a primary or secondary CoQ_{10} deficiency (Yubero et al., 2014). The former diagnosis may require next generation sequencing diagnostic strategies and the latter, radiolabelled incorporation studies (Yubero et al., 2014).

4.1. Primary CoQ_{10} deficiency

A primary CoQ_{10} deficiency is generally an inherited autosomal recessive disease effecting genes directly involved in CoQ_{10} biosynthesis. Fist identified in 1989 by Ogasahara et al. (1989), in a pair of young siblings that presented with progressive muscle fatigue and central nervous system dysfunction. A primary CoQ_{10} deficiency has been linked with a number of the genes utilised in the CoQ_{10} biosynthetic pathway: *PDSS1, PDSS2, COQ2, COQ4, COQ6, COQ7, ADCK3, ADCK4* and *COQ9* (Duncan et al., 2009, Heeringa et al., 2011, Mollet et al., 2007, Salviati et al., 2012, Hashemi et al., 2021).

4.1.1 PDSS1 and PDSS2 Mutation

Both PDSS1 and 2 are responsible for encoding the subunits on the TPT enzyme, that in turn catalyses the formation of the isoprenoid side chain of CoQ_{10}. López et al. (2006) and colleagues reported an infant patient who was found to have a heterozygous mutation in the *PDSS2* gene (López et al., 2006). This mutation was associated with nephrotic syndrome, epilepsy, and Leigh syndrome. The study also reported a significant decrease in the activities of METC complexes I, II and III in fibroblasts. Additionally, there was a significant decrease in the CoQ_{10} content of both skeletal muscle and fibroblasts. Mollet et al. (2007) described a patient with a mutation in the *PDSS1* gene in a patient, with no other reported family related issues. The patient displayed a multisystem disease, obesity, valvular heart disease, mitochondrial encephalomypathy lactic acidosis (MELAS), and early onset hearing issues. Notably, this was the first study to report a number of these clinical symptoms in association with a primary CoQ_{10} deficiency. When the activities of the mitochondrial METC enzymes was determined, evidence of a deficiency in both complex II and complex II/III activities in addition to low concentrations of CoQ_{10} were detected in fibroblasts. However, no evidence of a deficiency in the activities of the METC enzymes was detected in skeletal muscle (Mollet et al., 2007).

4.1.2 ADCK3 Mutation

Currently the bulk of the studies assessing mutations in the *ADCK3* gene have been undertaken in the yeast, *S. cerevisiae*, in an attempt to better understand primary CoQ10 deficiency, although some studies have been undertaken in humans. The *ADCK3* enzyme is responsible for the synthesis of an atypical kinase, that plays a role in CoQ_{10} biosynthesis. Currently, however, there is little information available on its mechanism of action, although, one suggestion is that *ADCK3* has an indirect regulatory role in CoQ_{10} biosynthesis in a feedback loop regulating ATP concentration (Lagier-Tourenne et al., 2008). In a study by Liu et al. (2014) a frameshift mutation in the *ADCK3* gene was detected in two siblings and both presented with cerebellar ataxia. The CoQ_{10} concentration in the patient serum was found to be in the control

range, however the CoQ_{10} status was significantly decreased in fibroblasts. Additionally, assessment of the METC enzymes in fibroblast revealed evidence of decreased complex I and complexes II/III activities. This study also assessed the effects of CoQ_{10} supplementation, and found that it was able to significantly restore METC activity in all the effected complexes (Liu et al., 2014).

4.1.3 COQ2 Mutation

The *COQ*$_2$ gene encodes the 4HB-polyprenyl transferase (4-HBPT), enzyme. 4HBPT catalyses the reaction condensing 4-HB derived from tyrosine/phenylalanine with FPP derived from the mevalonate pathway (Figure 2) (Quinzii et al., 2006).

A study in 2006 by Quinzii et al. (2006) reported a patient with infantile encephalomyopathy, nephropathy associated with a CoQ_{10} deficiency in fibroblasts. The mutation was found to be inherited in an autosomal recessive manner in view of the parent's consanguineous relationship. Additionally, the patient had an older sibling who displayed nephropathy together with a CoQ_{10} deficiency. Assessment of the METC revealed a significant decrease in complex I, II and II/III activities in skeletal muscle (12μg/g, mean of controls = 32.1 μg/g). The CoQ_{10} deficiency was found to be more profound in the patient fibroblasts (19 ng/mg – mean of controls = 105 ng/mg) together with a more severe deficiency in METC complex I, II and II/III activities. In addition to this, the study reported a dramatic improvement in both METC activity and clinical presentation following CoQ_{10} supplementation (Quinzii et al., 2006).

4.1.4 COQ4 mutation

The *COQ*$_4$ gene is responsible for encoding a ubiquitous protein associated with the periphery of the inner mitochondrial membrane. The exact function of the human COQ_4 (ubiquinone biosynthesis protein COQ4 homolog) protein has not yet been fully

elucidated. However, studies carried out in yeast have suggested it plays some structural roles in the multi-enzyme complexes involved in the CoQ biosynthetic pathway (Marbois et al., 2009).

A study by Brea-Calvo et al. (2015) reported five patients from four unrelated family's where a CoQ_{10} deficiency was not originally diagnosed. One male patient presented with severe hypotonia, areflexia, acrocyanosis, bradycardia, and respiratory insufficiency. Assessment of METC activity revealed decreased complex II and complex II/III activities in skeletal muscle. Although, in both liver and fibroblast the activity of all METC complexes was within the reference range. CoQ_{10} supplementation was not administered as the infant died four hours after birth.

4.1.5 CoQ6 Mutation

The *COQ_6* gene encodes for a highly conserved protein required for at least one of the ring hydroxylation steps in CoQ_{10} biosynthesis. Heeringa et al. (2011) studied eleven patients from five different families. The patients displayed symptoms similar to those identified with mutations in the *PDSS1* and *COQ_2* genes, such as nephrotic syndrome associated with sensorineural hearing loss. METC activity was not assessed in this study, however, the renal epithelial cell mitochondrial membrane potential ($\Delta\Psi m$) was assessed and found to be significantly decreased compared to control levels. This was an indication of impaired ETC activity.

4.1.6 CoQ9 Mutation

First described by Duncan et al. (2009) A mutation in *COQ9* gene has been associated with a significant decrease in skeletal muscle CoQ_{10} concentration. CoQ_9 encodes for a protein with a lipid binding domain, and it is involved in a protein-protein interaction with CoQ7, which in turn is involved with the final steps of CoQ_{10} biosynthesis (Lohman et al., 2014). However, the exact function of the CoQ9 protein has yet to still be to fully elucidated.

In the study by Duncan et al. (2009), a patient with multi-systemic diseases, including real dysfunction, cardiomyopathy and intractable seizures was reported. Assessment of the METC in skeletal muscle revealed a significantly decreased CoQ_{10} concentration (37 pmol/mg, reference range: 140-580 pmol/mg) together with undetectable complex II/III activity. The activities of complexes I, II, III and IV were all within the reference range.

4.2 Secondary CoQ_{10} Deficiency

A secondary CoQ_{10} deficiency occurs as a result of mutations in genes not directly related to CoQ_{10} biosynthesis or can be induced by environmental factors (Quinzii and Hirano, 2011). A secondary deficiency is common in a number of other diseases including other METC disorders (Montero et al., 2013, Sacconi et al., 2010). Irrespective of the fact that a secondary CoQ_{10} deficiency is more common than a primary CoQ_{10} deficiency, the underlying causes are generally unknown, with a large number of cases arising from seemingly unrelated defects (Navas et al., 2021).

Symptoms of secondary CoQ_{10} deficiency vary dramatically as it is largely based upon the underlying condition, although in the majority of cases diagnosis relies upon assessment of skeletal muscle CoQ_{10} concentration and/or central nervous system involvement (Desbats et al., 2015). As with a primary CoQ_{10} deficiency, a CoQ_{10} secondary deficiency will generally manifest clinically with muscle weakness, hypotonia, exercise intolerance, myoglobinuria and a general impairment of the central nervous system (Desbats et al., 2015). Quinzii et al. (2005) reported that patients treated with CoQ_{10} supplementation often show an improvement in clinical symptoms. However, because the CoQ_{10} deficiency is a secondary factor to the disease pathophysiology, the degree of clinical improvement following CoQ_{10} supplementation is not as profound as those reported with a primary deficiency (Quinzii et al., 2005).

A number of genetic defects have been associated with a secondary CoQ_{10} deficiency. Balreira et al. (2014) described one example of mutations in the *ANO10* gene which is primarily associated ataxia. The *ANO10* gene encodes for a transmembrane protein involved in calcium signalling. Balreira et al. (2014) reported two patients with cerebella ataxia and CoQ_{10} deficiency caused by mutations in the *ANO10* gene. The study also reported that the patients responded well to CoQ_{10} supplementation and demonstrated a reduction in the severity of some symptoms. In an earlier study by Le Ber et al. (2007) mutations in the *APTX* gene were found to be associated with secondary CoQ_{10} deficiency. The study reported that five out of six patients with mutations in *APTX* who presented with ataxia-oculomotor-apraxia 1 (AOA1), had a CoQ_{10} deficiency. As with other reported secondary deficiencies, Le Ber et al. (2007) reported that patients symptoms improved following CoQ_{10} supplementation. One interesting piece of evidence reported in this study, was that hypercholesterolemia is commonly associated with *AOA1* gene mutations, this provides a tentative link between the diseases via the CoQ_{10} biosynthetic pathway.

4.3. Environmental and pharmacological CoQ_{10} inhibition

Obesity is currently one of the biggest challenges in modern medicine and high circulatory cholesterol (LDL, low density lipoprotein) is a key pathogenic factor in this disease. As a result of this drugs like statins are routinely prescribed to treat the hypercholesterolemia. Statins are competitive inhibitors of the enzyme, HMG CoAreductase, a key regulatory enzyme in the mevalonate pathway (Istvan and Deisenhofer, 2001). This target enzyme is a major regulator of both cholesterol and CoQ_{10} biosynthesis, thus its inhibition not only leads to a reduction in cholesterol synthesis but also CoQ_{10}.

Currently the preponderance of work investigating the relationship between statins and CoQ_{10} have focused on blood plasma or serum CoQ_{10} concentrations. As previously stated, these are not good surrogates for the assessment of endogenous CoQ_{10}, as the concentrations of this isoprenoid can fluctuate depending on dietary intake and/or the circulatory lipoprotein status, thus it may not represent cellular

CoQ_{10} concentrations (Hargreaves, 2003). However, studies that have focused on muscle CoQ_{10} concentrations have also shown evidence of a CoQ_{10} deficiency associated with statin treatment (Harper and Jacobson, 2010).

4.4. CoQ_{10} Supplementation

As previously discussed, both primary and secondary CoQ_{10} deficiencies respond positively to treatment with CoQ_{10}. Although treatments have shown positive results with little side effects, there is little consensus on an appropriate dose with ranges from 30 to 3000 mg/day being recommended (Shults et al., 2004). In addition, there is also a plethora of different forms of CoQ_{10} formulations such as powder, suspension, oil solution, solubilised forms, creams, tablets, wafers, hard-shell and soft-gel capsules. One of the main debates that influences the treatment in humans is the relatively low bioavailability of CoQ_{10}; this is one of the main reasons as to why there is such a variety of products (Pravst et al., 2020).

5. The Lysosome

Lysosomes are single membrane, membrane bound organelles, responsible for the degeneration and recycling of cellular waste products (De Duve, 1963). Ubiquitous across mammalian cells (with the exception of red blood cells), the lysosome was originally underappreciated in research and simply branded as the cells "waste bin" due to its role at the terminal point of the endocytic pathway. However, in recent years research has intensified and has revealed that this organelle has a number of functions fundamental to cell homeostasis as well as roles in disease prevention and progression (Murphy and LeVine, 2010, Parkinson-Lawrence et al., 2010, Platt et al., 2012, Schwake et al., 2013, Gómez-Sintes et al., 2016, Gordon and Martinez-Pomares, 2017).
Considering this information, the lysosomal function is now an important focus of clinical research as both potential avenues for treatment and prevention of disease.

Originally discovered in 1955 by Christian De Duve whilst researching the enzyme glucose 6-phosphatase, an enzyme involved in sugar metabolism. The original experiments to investigate glucose 6-phosphatase failed, as a result of inadequate purification of the enzyme; because of this De Duve and his team changed the procedure to whole cell fractionation, separating out cellular components based on their size. This change in method led to the surreptitious discovery of the lysosome. De Duve and colleagues found that in freshly prepared fractions the activity of acid phosphatase (a liver enzyme), was only 10% of its expected value when compared to the control enzyme. However, when the samples were refrigerated for five days the enzyme activity was restored to the expected level. This led to further assessment of the enzyme and the conclusion that it must be contained within a membrane, as well as this, the five days of refrigeration had allowed the enzyme to diffuse across the membrane, explaining the disparity in activity over time. De Duve and his team then developed a more discriminative separation process, using enzyme markers and found another five enzymes in the same cellular fractionation as acid phosphatase. Later the same year De Duve and colleagues were able to take the first electron micrographs of the lysosome (De Duve et al., 1955, Klionsky, 2008). These studies showed that the lysosome was an enzyme rich organelle with a heterogenous shape and size (figure 8). De Duve later won the Nobel prize in 1974 for his work on the discovery of the lysosome.

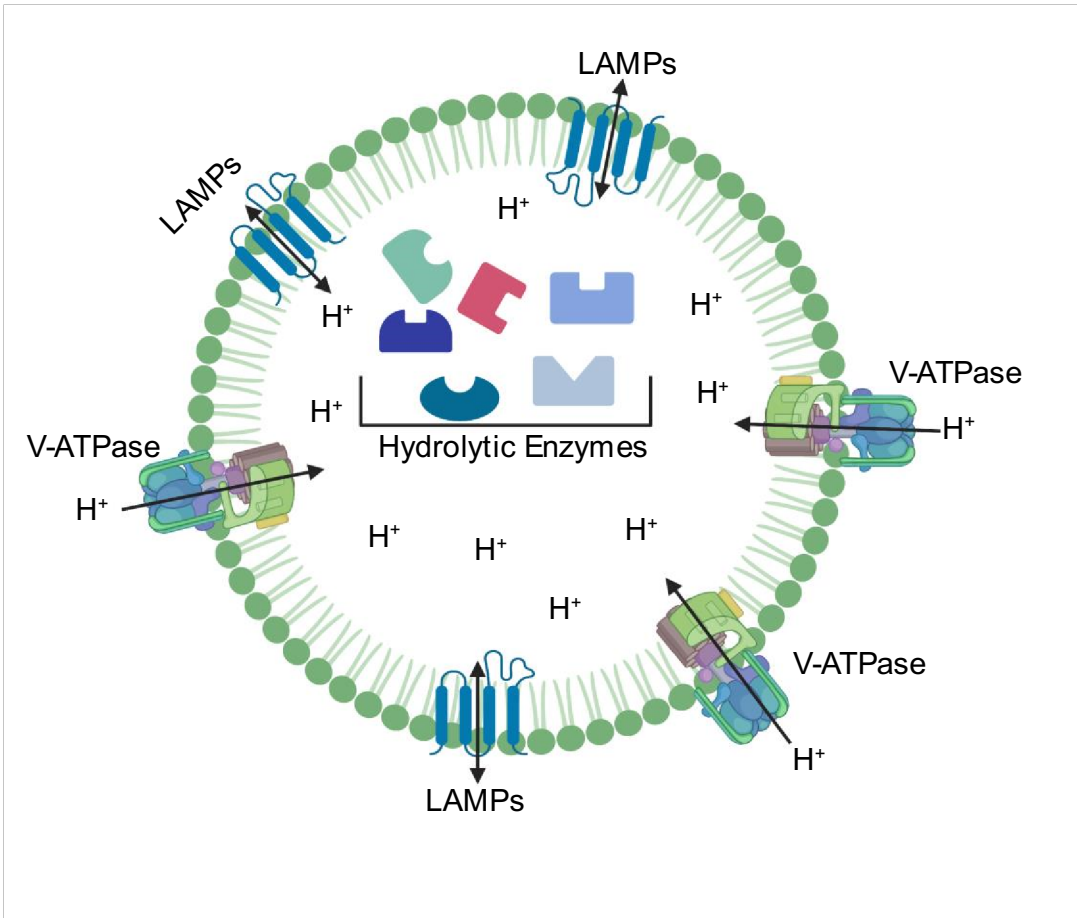

Figure 8. Basic Features of the Lysosome.

A variety of transmembrane proteins with a litany of different functions. The lysosomal lumen has an acidic pH which is maintained by the movement of H^+ ions against the concentration gradient. Also shows several different soluble proteins such as the hydrolytic enzymes crucial to lysosomal

5.1 The lysosomal membrane *function.*

In view of the acidic environment and plethora of digestive enzymes, the lysosomal membrane is key in preventing cellular damage caused by these factors. The inner portion of the membrane is known as the glycocalyx because it is highly glycosylated. This mainly consists of (about 50%) the lysosomal membrane associated proteins (LAMP) 1 and 2, which among other roles help prevent the acidic hydrolases of the lysosome from digesting the membrane (Saftig et al., 2010, Hunziker et al., 1996). Along with LAMP the membrane is known to contain at least 50 other proteins contributing to lysosomal function. In comparison to the trafficking and transport of the lysosomal hydrolases to the lysosomal lumen, little is understood about how the

lysosomal membrane proteins are targeted to the lysosome (Saftig and Klumperman, 2009). However, a number of gene mutations associated with aberrant lysosomal membrane transport have been reported to cause lysosomal dysfunction. For example, mutations in the HGSNAT gene have been associated with Sanfilippo C Syndrome (Fedele and Hopwood, 2010) or mutations in the CLN3 gene have been associated with juvenile neuronal ceroid lipofuscinosis (Saftig and Klumperman, 2009). Additionally, there is evidence that proteins associated with the lysosomal membrane can impose specific functions onto other organelles, such as the endoplasmic reticulum (ER) through which a number of lysosomal membranes proteins are transported (Saftig and Klumperman, 2009).

Considering the lysosome`s function, the membrane has to not only constrain the acidic environment within the organelle, but also has to allow the influx of a wide variety of different molecules that range vastly in size. To facilitate this, the lysosomal membrane has an array of different membrane transporters and channels. One example is the LMP cystionosin, a seven-domain transmembrane protein responsible for the transport of the amino acid cystine out of the lysosomal lumen (Huizing and Gahl, 2020, Gahl et al., 2001).

5.1. Lysosomal cellular signalling

As lysosomal research has intensified it has become increasingly apparent that the lysosome along with its role in macromolecule degradation is a versatile signalling hub, playing a role in a multitude of cellular possesses such as cellular response to nutrient availability and cell proliferation/death (Lawrence and Zoncu, 2019). The important cell signalling role of the lysosome is indicated by its abundance of luminal Ca^{2+}, which can be released into the cytosol upon stimulation of the organelle, eliciting a number of cellular processes such as membrane fusion and restructuring of lysosomes (Morgan et al., 2011). Numerous lysosomal membranes associated proteins also play a role in cell signalling, for example the protein complex mTORC1. This multifaceted complex is responsible for the phosphorylation of several different substrates relating to cell proliferation; one of these is the transcription factor EB (TFEB) (Eltschinger and Loewith, 2016). Activation of TFEB leads to an increase in cellular mass and surface area as the result of enhanced protein synthesis, turnover, and lipid production. It has been reported that TFEB is influenced by downstream regulators and responds to a number of different cellular signals; for example, it has been reported during cellular starvation, TFEB becomes dephosphorylated, leading to its translocation into the nucleus to regulate cell growth and lysosomal synthesis (Schmelzle and Hall, 2000).

5.2. Lysosomal Hydrolases

The lysosomal lumen is home to over 50 different hydrolytic enzymes, all responsible for the degradation of macromolecules transported to the lysosome. Majority of these enzymes are encoded for by the TFEB gene, which is responsible for organising expression of the lysosomal hydrolases and associated membrane proteins. Additionally, TFEB is able to activate many genes associated with autophagy (Settembre et al., 2011, Sardiello et al., 2009).

The lysosomal hydrolases themselves are synthesized in the ER and then modified in

the Golgi apparatus (Figura and Hasilik, 1986). As all these enzymes are manufactured away from the lysosome, a transport pathway exists to deliver the enzymes to the lysosomal lumen, where they can undergo the final step of the removing the pro-peptides and consequently, activating the enzymes (Figura and Hasilik, 1986).

5.2.1 The Mannose-6-Phosphate Transport Pathway

It is understood that most of the lysosomal enzymes are targeted and delivered to the lysosomal lumen using the mannose-6-phosphate pathway (M6PP) (Hille-Rehfeld, 1995). The pathway starts with the addition of a mannose sugar to the proteins destined for the lysosome in the ER. These proteins are then translocated to the *cis*Golgi, where a specific phosphotransferase adds a GlcNac-1-phosphate to the mannose deposits on the protein (Coutinho et al., 2012). This tagged protein can then be moved to the *trans* Golgi where the M6PP can be exposed by the removal of the GlcNac residues facilitated by phosphodiesterase in the *trans* Golgi (Ludwig et al., 1994).

These enzymes can now interface with the M6PP receptor creating a complex for transport. Facilitated by the presence of dileucine motifs the complex is then translocated to the endo-lysosomal system (Mattera et al., 2011). The complex then moves through the endo-lysosomal system, towards the acidic compartments where the M6PP receptor detaches leaving the lysosomal enzyme in the acidic environment. The enzymes are then activated by a number of other proteins such as cathepsin D (Ludwig et al., 1994).

As to be expected with such a wide verity of proteins, there are several pathways independent of the M6PP utilised to transport lysosomal components. One example of this is the transport β-glucosidase to the lysosome via the lysosomal membrane protein 2 (LIMP2) (Jadot et al., 1999). As with many other lysosomal enzymes, βglucosidase becomes bound after translocation glycosylation to the membrane. Thanks to this, β-glucosidase is brought into a space where it can interact with LIMP2 in a pH-dependent manner. LIMP2 is made up of transmembrane domains which allows for the translocation to the endosome (Blanz et al., 2015).

The aforementioned lysosomal hydrolases are all acidic enzymes meaning they require an acidic environment to function optimally (De Duve, 1963, Ballabio and Bonifacino, 2020). As a consequence, the lysosomal lumen has an acid pH of around 5 (De Duve, 1963, Ponsford et al., 2021). Various studies have also reported this pH value is generally consistent across cell types (Ponsford et al., 2021).

In order to create this acidic environment, the lysosome deploys a number of mechanisms to move protons across the lysosomal membrane form the cytosol into the lumen against the concentration gradient. One current established and well documented process for lysosomal acidification is by way of the active transport of protons across the lysosomal membrane via the lysosomal V-ATPase (Figure 9). This is a complex multi-structural transmembrane protein found at the lysosomal membrane which is not dissimilar to the ATPase reported in the mitochondria (figure 5 and figure 9). Although, unlike the mitochondrial ATPase, the V-ATPase on the lysosomal membrane is responsible for the hydrolysis of systolic ATP rather than its manufacture (Brown and Breton, 2000, Collins et al., 2020). The V-ATPase is made up of 13 subunits divided into two domains, V0 and V1 as shown in figure 9 The V0 domain is responsible for the translocation of H^+ ions from the cytoplasm into the lysosomal lumen against the concentration gradient (Yokoyama et al., 2003). The V1 domain is responsible for the hydrolysis of ATP, providing the energy required for the movement of H^+ ions (Forgac, 1989, Zoncu et al., 2011). Consequently, the VATPase is dependent on the presence of systolic ATP to function adequately and thus the lysosomal lumen pH may also be impacted by abridged ATP concentrations.

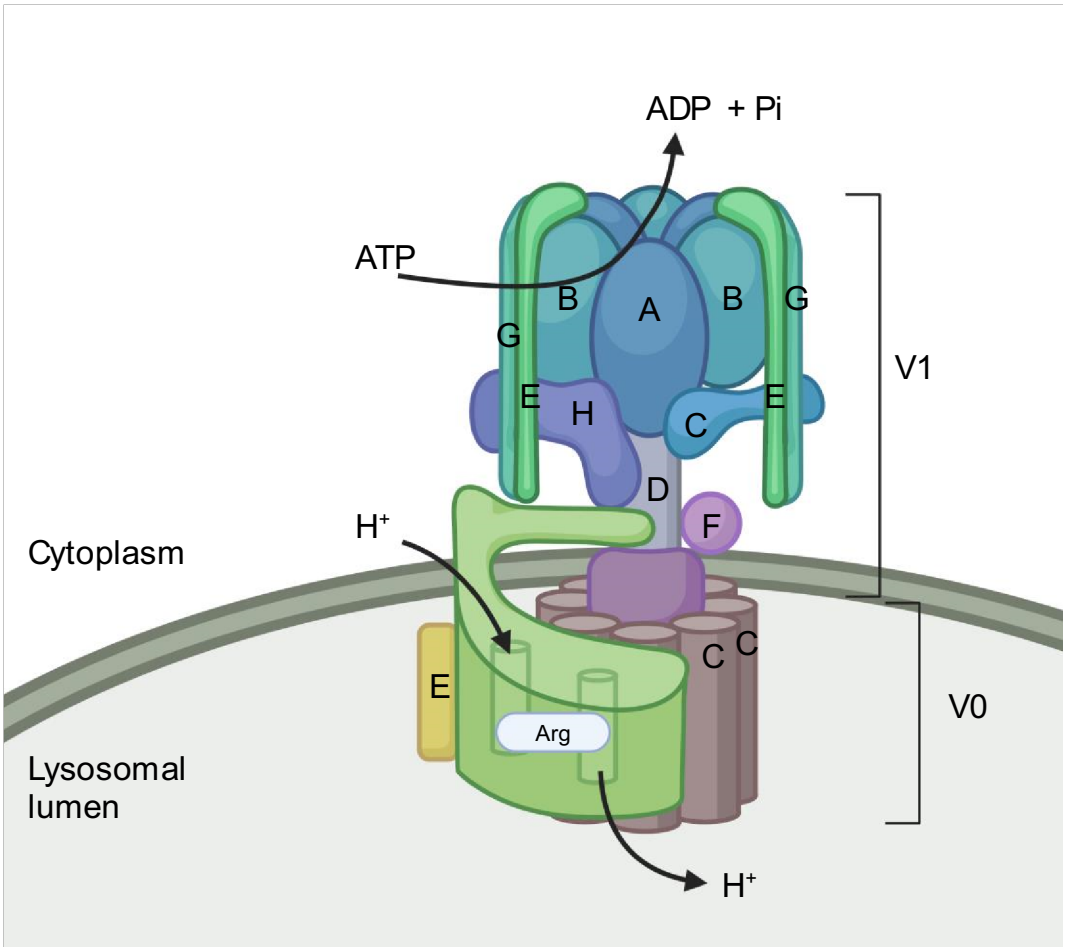

Figure 9. Structure of the Lysosomal V-ATPase.

The V-ATPase is made up of two sub domains a hydrolytic domain (V1), and a proton translocation domain (V1). The ATP binding sites are found on the A and B subunits, with the catalytic sites found mainly on the three A subunits. The two domains V1 and V0 are interconnected via a central stem made up of D, F, C, E, G, and H. The movement of H^+ is facilitated via hydrolysis of ATP in the V1 domain, which drives the rotation of the central stem, which in turn drives the rotation of the ring of proteolipid subunits (C) passed the Arg subunit in V0 which is held stationery. The movement of these subunits allow the passage of H^+ ions across the membrane. Adapted from (Hinton et al., 2009).

5.5.1 Lysosome Storage Disorders

Lysosome storage disorders (LSDs) are a group of genetic disorders associated with the accumulation of macromolecular molecules destined for breakdown by the lysosomal enzymes. There have been around 70 distinct disorders reported, although it is estimated with such an array of different features contributing to lysosomal function that there may be several more disorders as yet to elucidated (Fuller et al., 2006, Sun, 2018). Figure 9 shows a generalised view of the progression for diseases associated with lysosomal disorders.

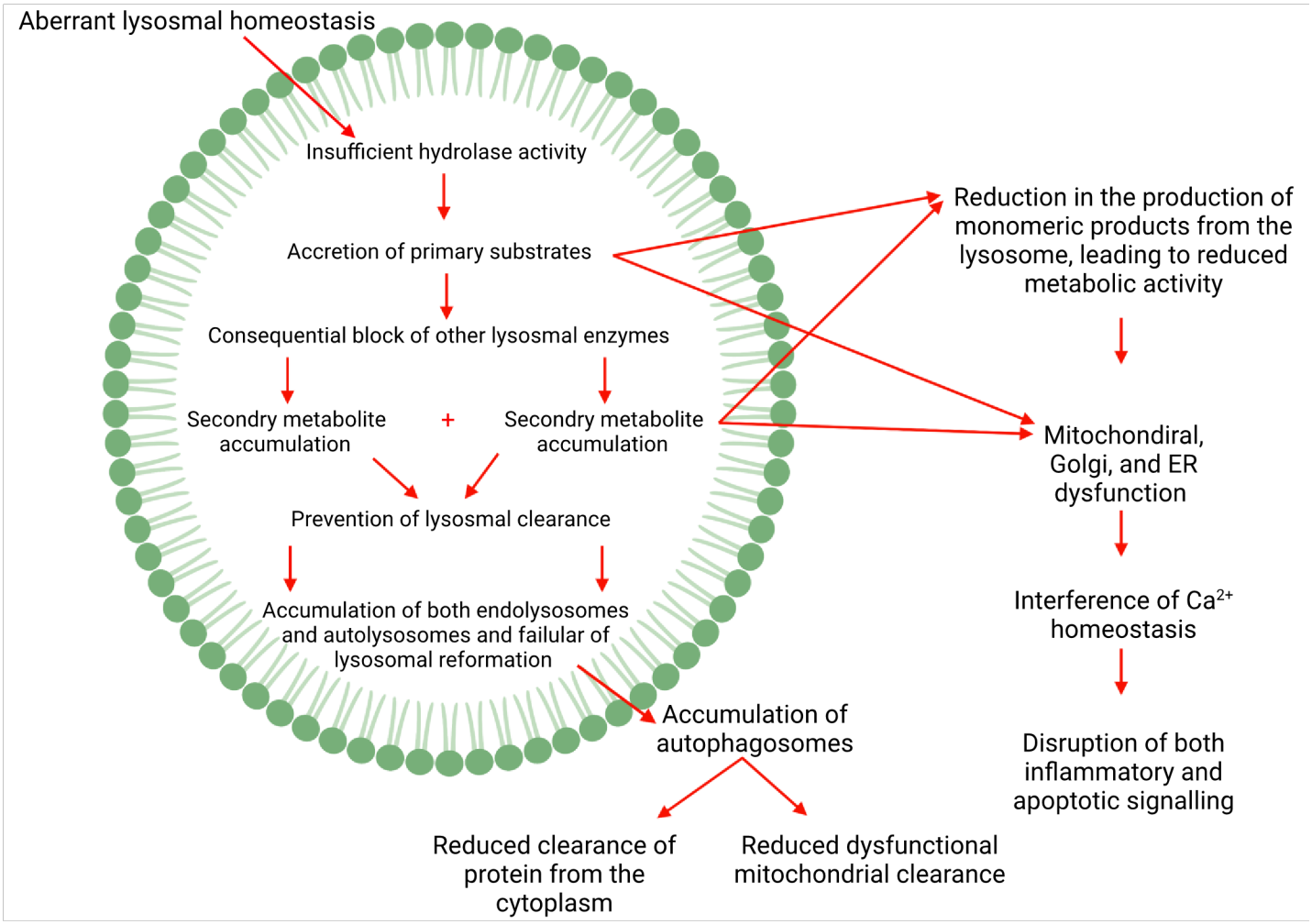

Figure 10. Generalised Schematic of Lysosomal Disease Pathogeneses.

The predominant cause of LSDs is the loss of function of the lysosomal enzymes, resulting in the build-up of the macromolecule targeted by that enzyme. The material that is affected first is considered to be the primary storage material, for example if the lysosomal proteases are affected the primary material would be considered undigested proteins; with the accumulation of other material resulting from this build up being the secondary storage material. For example, the build-up of undigested protein leads to impairment of the digestion of other materials such as complex sugars. With such an array of different materials, it is generally difficult to identify which is the primary material. This can lead to misdiagnosis and even in some cases mistreatment; this also increases the difficulty of understanding the exact mechanisms of lysosomal disease pathogenesis. Additionally, there is a significant overlap between different LSD's and secondary storage material, further increasing the difficulty in identification (Vitner et al., 2010). It is also difficult to accurately distinguish theses intertwined diseases from one another due to a plethora and overlap of clinical symptoms such as, hepatomegaly, macroglossia, and generalized muscle weakness (Mokhtariye et al., 2019, Sun, 2018).

Although, generally caused by a relatively simplistic mechanism of an inborn recessive monogenetic defect, leading to functionality changes in one or more lysosomal associated proteins; the exact mechanism responsible for the disease pathogenesis of these disorders is still to be elucidated (Cox and Cachón-González, 2012). This is mainly due to the fact that it is not always clear which macromolecule storage material is primary; to add to this, as discussed previously, many lysosomal associated proteins also exert effects on other organelles and organelles generally rely on the lysosome for signalling (discussed in section 5.2). Therefore, as a result of this, LSD's can display symptoms seemingly unrelated to lysosomal impairment (Platt et al., 2012). Whilst there are many obstacles related to understanding the progression of LSD's they do have some commonalities such as the build-up of lysosomal storage material, as outlined in Figure 9. Although not all LSD's present with these symptoms (Platt et al., 2012), some examples that do include Gaucher Disease and Niemann Pick C.

5.4.2. Gaucher Disease

First described by Gaucher (1882) Gaucher Disease (GD) is now clinically known as the most common LSD with 1 in 50,000 people in the general population displaying this disorder (Grabowski, 2012, Nalysnyk et al., 2017). GD is caused by a mutation in the GBA1 gene, which encodes for the enzyme, glucocerebrosidase (GBA). This acidic hydrolase is responsible for the catabolism of the glycosphingolipid, glucosylceramide (GlcCer) into glucose and ceramide (Gegg et al., 2012, Rijnboutt et al., 1991). Ceramide is also known as a secondary messenger in the activation of the apoptotic cascade and glucocerebroside (GBA) is an intermediary in the breakdown of plasma membrane gangliosides and globosides (Patrick, 1965). Both of these compounds are understood to be derived from apoptotic red and white blood cell membranes, which under normal circumstances would be phagocytosed by macrophages for recycling (Lee, 1968). The accumulation of glucocerebroside within the lysosome causes it to elongate and fill the cytosol, which leads to the inhibition of other cellular functions, such as normal cellular signalling. Additionally, it also causes the well documented morphological change associated with GD, giving the cytosol the appearance of crinkled paper (Arroyo and CRAWFORD, 2009). The clinical presentation of GD can include, hepatosplenomegaly, pancytopenia and in variant forms of the disease, neuropathology with wide variation in age of onset (Vitner et al., 2010, Alaei et al., 2019, Lachmann et al., 2004).

Clinical presentations of neuropathy in GD often start with either hyperextension of the neck and dysphagia or supranuclear gaze palsy. However, in common with other lysosomal disorders this is not always the case for all patients and an array of other clinical features have also been reported such as ataxia, neuropathic pain and seizures (Pastores and Hughes, 2018).

GD is classified into three groups depending on age of onset and neurological involvement: type one, two, and three (Jmoudiak and Futerman, 2005). Type one is both the most prevalent and the mildest form of GD accounting for around 95% of reported cases (Pastores and Hughes, 2018). This form of GD is a non-neuropathic

disease with clinical symptoms generally displaying around the early twenties, although, some patients may never display symptoms (Pastores and Hughes, 2018). Type two, or infantile GD, is a particularly severe form or GD with neurological signs presenting from a young age; penitents with type two GD generally perish before the age of two. Type three GD also represents with neurological symptoms and patients are generally symptomatic at an early age, however, survival to middle age is much more likely than with type two (Pastores and Hughes, 2018, Grabowski, 2012). As a result of GD type one's mild symptoms, it can go undiagnosed for a protracted period of time, with the most recurrent symptoms being an enlarged spleen or liver (as a result of excessive lipid storage) being the key factor in diagnosis. As previously discussed, type one GD is also generally regarded as a non-neuropathic condition, due too little to no patients displaying neuropathologic symptoms. However, Sidransky et al. (2009) reported the presence of GBA gene mutations in Parkinson's disease (PD) patients, suggesting that mutations in this gene are a risk factor for PD.

5.4.2.1 Treatment of GD

As a result of type two GD`s morality there is little to no treatment options. Type one GD currently has the most promising treatment options which overlap with type three; however, they are much more effective for the milder forms of the disease. Enzyme replacement therapy (ERT) is now the foremost treatment for GD, first proposed and carried out by Brady et al. (1974). The method involved injecting the patient with the purified GBA gene from human placenta (Brady et al., 1974). Nowadays, in common with most other replacements therapies the enzyme is manufactured using recombinant DNA technology. One pitfall, however, is that the enzyme is unable to cross the blood-brain barrier (BBB), and therefore is ineffective for treatments of neurological symptoms (Schapira, 2015).

5.4.3 Niemann Pick C

Originally identified in 1914 Niemann Pick C (NPC) is an autosomal recessive neurovegetative disorder, attributed to defective cholesterol trafficking as a result of mutations in either NPC1 or NPC2 genes (Vanier et al., 1996). NPC1 encodes the NPCs

membrane spanning protein and NPC2 encodes the NPC2 soluble lumen protein (Vanier et al., 1996). Both of these proteins contribute to the normal efflux of cholesterol form the lysosome and late endosome. The pathogenic cascade of NPC is extremely complex and has not yet been fully elucidated. However, it is believed that due to the inability to properly traffic cholesterol, an accumulation of unesterified cholesterol along with gangliosides and other glycolipids occurs resulting in cellular dysfunction (Schedin et al., 1997, Neufeld et al., 1999).

Clinical presentations of NPC can vary considerably from patient to patient, however, the hallmarks of NPC have generally been identified to be ataxia and vertical supranuclear gaze palsy (the inability to look vertically due to cerebral impairment); although not every patient may display these symptoms (Neufeld et al., 1999). As with other lysosomal disorders, the age of onset can be used to roughly classify patient phenotypes (Patterson et al., 2012). NPC can be divided into five subgroups: perinatal-onset, early infantile (2 months – 2 years), late infantile (2 years – 6 years), juvenile (6 years-15 years), and adolescent (>15 years) onset. Peri-natal NPC typically presents with fetal ascites, neonatal jaundice, and hepatosplenomegaly. Early infantile has been reported to display a delay in development of normal motor function, hypotonia, and hepatosplenomegaly. In late infantile NPC, patients can present with clumsiness, ataxia and less often organomegaly. Patients with juvenile NPC have been reported to most commonly present with ataxia, dysarthria, dystonia, seizures,

cataplexy, in addition to behavioral issues and learning difficulties. Lastly, adolescent onset NPC has been characterised by ataxia, dementia, psychosis, and a general progressive neurologic decline (Carstea et al., 1997, Neufeld et al., 1999, Patterson et al., 2012).

In addition to the lysosomal dysfunction associated with NPC, studies have reported evidence of mitochondrial dysfunction associated with this disorder, although the factors responsible for impairing mitochondrial function have yet to be elucidated. However, studies have suggested a number of possible causes including oxidative stress, antioxidant capacity, increased mitochondrial cholesterol accumulation and a

repression of mitochondrial biogenesis (Hargreaves et al., 2005, Vázquez et al., 2012). Interestingly, Fu et al. (2010) reported that in addition to increased levels of circulatory cholesterol there also appears to be a decreased plasma CoQ_{10} concentration.

5.4.3.1 Treatment of NPC

An effective treatment for NPC has thus remained elusive for a multitude of reasons. One of the most problematic aspects of this disease is that in the majority of patients, there is a delay of onset in clinically observable symptoms. As a result of this, delay patients may wait years before treatment begins, narrowing the window of opportunity for successful therapeutic treatment prior to the onset of disease. This delay in diagnosis means that any therapy developed must not only slow or prevent the progression of the disease, but also attempt to undo some of the damage already sustained. Another hurdle that NPC treatments must overcome is the fact that the cells most effected by the disease tend to be in the CNS. As previously discussed, the CNS environment is very tightly controlled, and any treatment developed must attempt to cross the BBB. In addition to this, the functions of the genes that are responsible for this disease have yet to be fully elucidated together with the proteins they encode, NPC1 and NPC2.

In the initial attempts to treat NPC it was thought that lowering the build-up of cholesterol through drugs like statins or low cholesterol diets would alleviate the symptoms of the disease. However, it was found that while these treatments were able to reduce the cholesterol levels in plasma, they were unable to reduce the concentration build up on a cellular level; thus this treatment was ineffective (Erickson et al., 2000). Several LSDs have previously been reported to respond positively to ERT (discussed in section 5.5.2.1). However, because NPCs principally inflicts its effects through the non-soluble membrane associated NPC 1 protein, ERT is unlikely to be able elicit any positive effects. In addition to this, gene therapy could also be considered a viable treatment. However, this also comes with its own challenges such as the ability of transporting the gene to the required region of the body in sufficient quantities.

5.5. Lysosomes in Neurodegeneration

Given the array of LSD's previously discussed, it is apparent that both neuropathic and neurodegeneration are factors to be considered in association with lysosomal dysfunction (Cox and Cachón-González, 2012). Although this is a considerable challenge when discussing treatment of LSD's, it does provide a unique model to try and investigate and understand aspects of neurodegeneration in diseases such as Alzheimer's and Parkinson's (Okouchi et al., 2007).

As previously discussed, the pathology of LSDs is particularly difficult to pinpoint. They have a complex pathogenic cascade which can result from primary storage substrates, secondary substates or even dysfunction in other organelles and physiological pathways seemingly unrelated to the lysosome itself. As a result of their complex nature LSDs could include any number of different pathological features such as: increased oxidative stress, dysregulated Ca^{2+} signalling, lipid miss-trafficking, and irregular proteolysis which leads to a build-up cellular waste product (Schöndorf et al., 2014).

5.5.1 Parkinson's Disease

Autophagy pathways are imperative for the development and survival of neurons, with research suggesting that neurons are particularly sensitive to changes in protein degradation pathways (Rubinsztein, 2006). During the early stages of neuronal development, the cell death pathway is exceptionally active, because of this degradation and turnover of material is imperative (Kole et al., 2013, Cataldo et al., 1994). It has been found that changes in lysosomal function during this time can lead to the rapid build-up of material in the cytosol, leading to neurodegeneration and prevention of the establishment of a perfectly `wired ` nervous system (Rubinsztein, 2006).

Yu et al. (2010) showed that the genetic inactivation of autophagy pathways in neurons leads to the formation of ubiquitinated intracellular inclusions and cell death. In a study by Kabuta et al. (2008) it was found that an increase in cellular α-Synuclein

could constitute a cause of PD. α-Synuclein is predominantly degraded by chaperonemediated autophagy (CMA), with the 193M mutation L1 (UCH-L1) associated with hereditary PD (Kabuta et al., 2008). Kabuta et al. (2008) found that UCH-L1 interacts

with LAMP-2A, the lysosomal receptor for the CMA pathway; this interaction subsequently enhances the 193M mutation thus leading to build up of α-Synuclein in the cell (Xilouri et al., 2008). As discussed, it is understood that a build-up of αsynuclein has a direct impact on the development of PD in a number of different ways. However, it is generally accepted that its abnormal soluble oligomeric conformation is toxic and can affect a number of different intracellular targets such as synaptic function, thus, disrupting cellular homeostasis (Stefanis, 2012). More recently it has also become apparent that the previously discussed GD is also a risk factor for PD.

Although, more work is needed to fully understand how these diseases are linked. A study performed by Manning *et al.,* (2009) established a strong possibility that Synuclein not only contributes to the cascade of events leading to GD, but also plays a role in the development of PD (Manning-Boğ et al., 2009).

5.5.2 Alzheimer's disease

Alzheimer's disease (AD) is characterized by a gradual loss of memory, orientation, judgment, and reasoning. These clinical presentations are attributed to neuronal cell loss, particularly in the regions of the brain involved with memory and cognition (Rosen et al., 1984). Currently, the exact mechanism of how the lysosome contributes to the pathogenesis of AD has yet to be elucidated.

It is widely accepted that the pathogenesis of AD is progressed by the production of β-Amyloid plaques (Murphy and LeVine, 2010). Amyloid plaques are clusters of nonfunctioning protein fragments called beta-amyloids (Masters et al., 1985). These betaamyloids can damage nerve cells and the synapses connecting them, although betaamyloids begin as a single non-functioning protein they can cluster together as they move freely through the brain (Frautschy et al., 1996). As they begin to get larger, they can become bound to receptors on neurons and once bound to the neurons they

block the communication between cells (Hardy and Higgins, 1992). This then leads to impairment in memory, thinking, planning and emotional regulation, as these betaamyloids become larger they from plaques, leading to the binding of more neurons and the progression the disease (Oddo et al., 2003).

It is understood that lysosome dysfunction plays a significant role in the formation of these plaques, as during normal conditions the lysosome is responsible for the breakdown and removal of the proteins that form the plaques (Nixon et al., 2008). As a result of this, it is easy to assume that lysosomal dysfunction significantly increases the risk of β-Amyloid plaque formation in neurons and thus increases the risk of developing AD (Nixon et al., 2001).

5.5.3 Neuroinflammation

Numerous studies have found that neuroinflammation is a common feature associated with multiple different LSDs, which is believed to be a result of the activation of macrophage like cells known as microglia (Jeyakumar et al., 2005). Microglia are responsible for the immune response in the CNS and maintaining CNS homeostasis. It has been reported that activation of these cells positively correlates with increased storage material found in animal models of LSDs, such as GD mice (Crivaro et al., 2019). The fact that chronic inflammation and microglia activation is found in multiple different LSDs suggest that the type of storage material is irrelevant and that the neuroinflammation reported in other neurodegenerative diseases may provide insights into the LSD CNS association, given that the lysosomal aspect of these other disease may have been overlooked (Vitner et al., 2010).

6. CoQ_{10} and Lysosomes

The link between COQ_{10} and lysosomes is currently a sparsely populated topic of research with little known about the relationship between the two. Currently it is understood that the lysosome is a cite of relatively high CoQ_{10} concentration with only some speculation as to its function there (Kalen et al., 1987, Nohl and Gille, 2005, Takahashi et al., 1993, Nohl and Gille, 2002, Zhang et al., 1996). One avenue of thought suspects that CoQ_{10} functions as an antioxidant protecting the lysosomal membrane from damage (Santoro, 2020). It has previously been reported that the lysosome is

practically susceptible to oxidative damage (Liton et al., 2008). This leads to the speculation that the high abundance of CoQ_{10} located on the lysosomal membrane is as a preventative measure for changes in superoxide.

Additionally, Gille and Nohl (2000) alluded to the existence of a lysosomal redox chain (figure 10). It was hypothesised that CoQ_{10} plays a fundamental role in the acidification of the lysosomal lumen by utilising its ability to accept electrons. Nohl and Gille (2002) provided evidence that CoQ_{10} is responsible for the transfer of free electrons from cytosolic NADH to dioxygen crossing the lysosomal membrane (Figure 10). This study found that in the presence of oxygen ubisemiquinone is not detectable and when oxygen was removed, NADH consumption was prevented. They also noted that the pKa of ubisemiquinone also favours the liberation of the protons derived from NADH within the lysosomal lumen, this further supports the idea that CoQ_{10} is a fundamental player in the acidification of the lysosome (Nohl and Gille, 2002).

Although, acidification of the lysosomal lumen has been observed to be carried out by the lysosomal V-ATPase as discussed in section 5.4 this is fundamentally reliant on mitochondrial production of ATP, this mechanism of proton translocation is independent of mitochondrial function. Thus, during conditions where mitochondrial function is compromised, the lysosomal lumen would be significantly less affected through the use of this second mechanism to maintain the acidic environment independent of ATP.

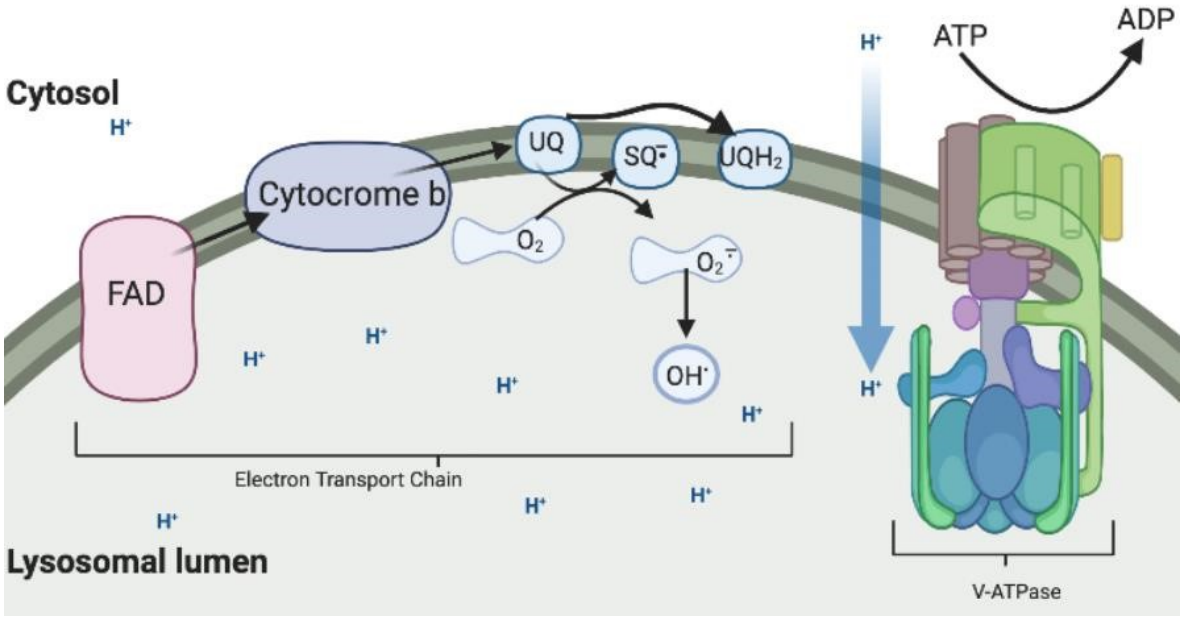

Figure 11. Schematic of the proposed Lysosomal Electron Transport Chain. Highlights the role of CoQ10 in the lysosomal electron transport chain adapted form (Gille and Nohl, 2000).

7. Aims

The original hypothesis of this study was that a significant CoQ_{10} deficiency will alter the normal homeostasis of the lysosomal lumen. Thus, the aim of the present study was to assess the effect of a pharmacologically-induced CoQ_{10} deficiency on lysosomal acidification and, subsequently, whether CoQ_{10} supplementation can be used to reverse this effect. The results of this study will provide important information about the role of CoQ_{10} in maintaining lysosomal acidification. Additionally, insights into the use of CoQ_{10} as a treatment option for diseases relating to lysosomal de-acidification.

Materials and Methods

8. Materials

The following were purchased from Sigma Aldrich (Poole, UK):

Triton X-100; SigmaUltra ≥ 99.5%; Sterile 0.4% Trypan blue; Dimethyl sulphoxide; Coenzyme Q_1~95%; β-Nicotinamide adenine dinucleotide, reduced disodium salt hydrate ≥ 97%; Rotenone ≥ 95%; BSA (Bovine Serum Albumin) ≥ 96%; Trizma-base (reagent grade); Cytochrome *c* from equine heart ≥ 95%; Antimycin A from *Steptomyces sp.*; Sodium succinate dibasic hexhydrate *ReagentPlus®*, ≥ 99%; 5,5′Dithiobis(2-nitrobenzoic acid), ≥ 98%; Acetyl coenzyme A sodium salt, ≥ 93%; Oxaloacetic acid, ≥ 97%; L-Ascorbic acid, cell culture tested; Potassium hexacyanoferrate(III), *ReagentPlus®*, ~99%; Coenzyme Q_{10}, ≥ 98%; 4-Aminobenzoic acid (PABA) ≥ 99.9%; Bafilomycin A1 ≥ 99.9%; Sodium perchlorate, 98%; 1-Propanol, chromasolv® for HPLC, ≥ 99.9%; Oligomycin from *Streptomyces sp.*; Carbonyl cyanide4-(trifluoromethoxy)phenylhydrazone, ≥ 98%; Sterile cell culture products: Dulbecco's modified eagles medium/Ham's F-12 Nutrient Mixture (DMEM/F-12) (1:1) with No Lglutamine; L-glutamine; Fetal bovine serum, heat inactivated (EU approved).

The following were purchased from VWR International Ltd (Lutterworth, UK):

Perchloric acid 60% (Hipersolv for HPLC); Ethanol 96% (Hipersolv for HPLC); nHexane (Hipersolv for HPLC); Methanol (Hipersolv for HPLC); Potassium hydroxide pellets (analar grade); 85% Orthophosphoric acid (Hipersolv for HPLC)

DC total protein assay Reagent A and Reagent B were purchased from Bio-Rad Laboratories Ltd (Hemel Hempstead, UK).

HPLC vials and caps were purchased from Agilent (Stockport, Cheshire, UK). HPLC C19 columns were gifted by Prof. Simon Heals at Neurometabolic unit (London UK) LysoTracker, LysoSensor, MitoTracker Green FM, JC-1, Propidium Iodide and H2DCFDA probes were all purchased from Invitrogen Ltd (Paisley, UK).

CellTiter-Glo kit was purchased from Promega (Promega UK).

Senescence Assay Kit (Beta Galactosidase, Fluorescence, ab228562) was purchased from Abcam (Cambridge Biomedical Campus, Cambridge, UK).

9. Cell Culture

9.1 SH-SY5Y Cell line

Originally derived from the bone marrow of a four-year-old female with a neuroblastoma of the chest, the cell line SK-N-SH had two distinctive cell lines. firstly, an epithelial cell group and a neuroblastoma group, for this study only the neuroblastoma cells were used. The neuroblastoma cells were sub cloned three times thus producing the SH-SY5Y cell line (Biedler et al., 1973). With a neuroblastoma morphology (figure 12) these cells have shown to have neurotransmitter activity (Biedler et al., 1978). This cell line was selected as its properties will give an insight into how a CoQ_{10} deficiency may have an impact upon neurological lysosomal function. Additionally, previous studies have demonstrated that para-aminobenzoic acid (PABA) is able to reduce the level of cellular CoQ_{10} in this cell line to a concentration deemed appropriate for CoQ_{10} deficiency assessment (Alam et al., 1975, Duberley et al., 2013a).

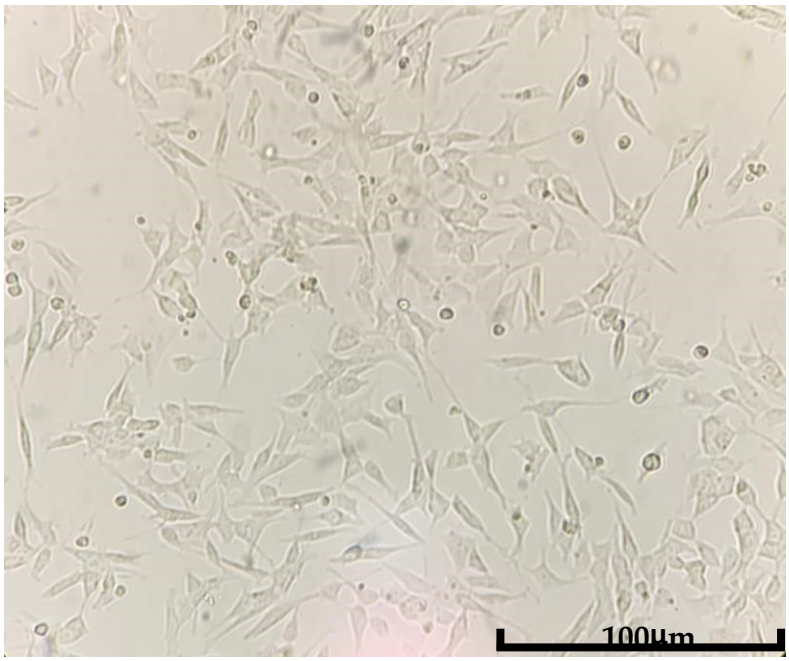

Figure 12. SH-SY5Y Cells Under Light Microscope.
Healthy, mature SH-SY5Y neurons demonstrate diffuse axonal projections connecting to neighbouring cells.

9.2. Passage

The SH-SY5Y neuroblastoma cell line was provided by -University College of London, Institute of Child Health, Guilford Street, London. Cells were seeded at a density of 1 x 104 cells/cm^2 into 75cm^2 tissue culture flasks and maintained in Dulbecco's modified Eagle's medium (DMEM) high glucose, supplemented with 10% foetal bovine serum (FBS) and 5% penicillin streptomycin (PS). Cells were grown in a cell culture incubator at +37°C in 95% air and 5% CO_2. When cells were re-animated from liquid nitrogen (LN^2), the medium was replaced the day after initial seeding. Cells were passaged at 70-80% confluency (generally 6-7 days). All cell culture and passage techniques were carried out in a laminar flow hood under sterile conditions. Once confluent media was removed and the cells were washed with 5ml of 1X phosphate buffer saline (PBS), cells could then be lifted following incubation with 3ml of trypsin-EDTA (Invitrogen) at 37°C for 3min. Cells were then inspected using a light microscope to ensure that they were fully lifted, if not they were re-incubated for a further two minutes. Once lifted trypsin was inhibited by the addition of 5ml of fresh media and the cells were then transferred to a centrifuge tube and centrifuged at 500xg for 5min at 25˚C. The supernatant was then removed, and cells were re-suspended in 5ml of fresh media, this was then mixed well on a slow vortex or by pipetting up and down. 100µl of the cell suspension was mixed 1:5 with 4g/l trypan blue and cells counted using a Neubauer improved haemocytometer (figure 13). Live cells were then counted in the four corners of the haemocytometer (figure 13 and 14) and an average was calculated. This was the used to calculate the number of cells per mL in the solution following the equation:

Average number of cells in corner squares x dilution factor x 10_4.

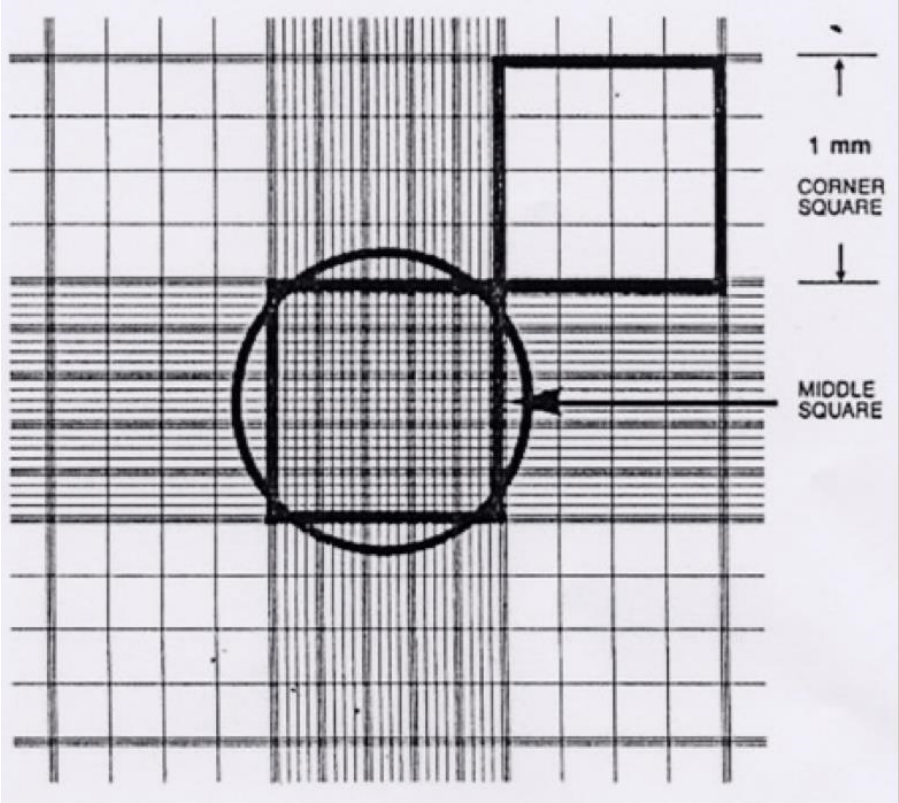

Figure 13. Haemocytometer Used for Counting Cells as seen under a Microscope.

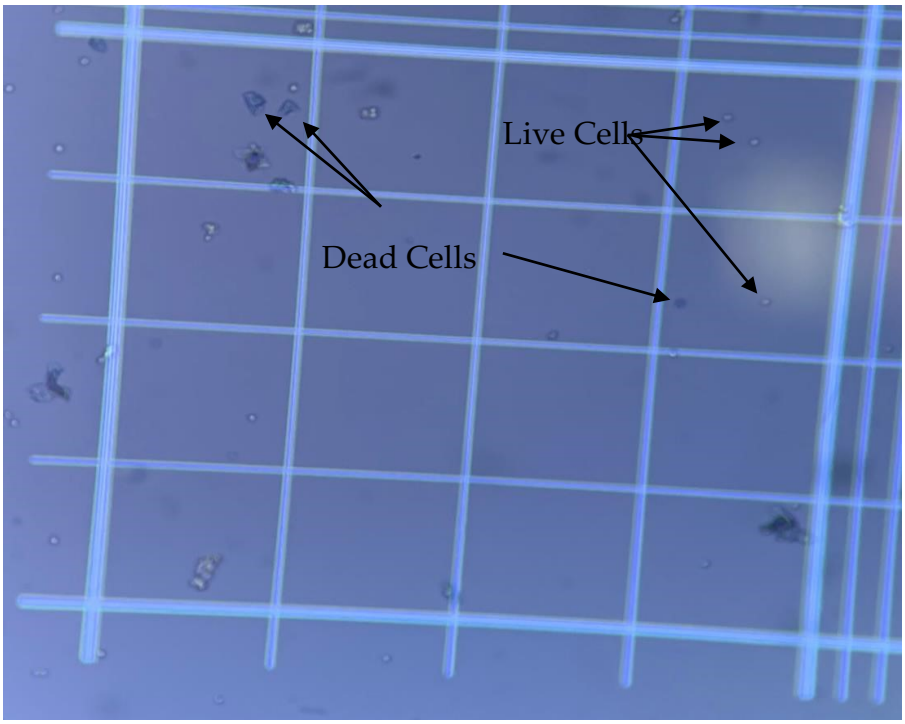

Figure 14. Haemocytometer with Trypan bule showing Dead cells (blue) vs Live cells (clear).

Passaging cells can be harsh on the cells and the number of times the process is undertaken on the cell culture must be strictly monitored. Although immortalised cells such as the ones used in this study are able to proliferate for an extended period of time compared to primary cells, their phenotype and genotype can change. Although this is not specifically reported for the SH-SY5Y cells used in this study, it was felt that it was a necessary precaution to ensure the reproducibility and reliability of the results. For this reason the passage number was maintained at between 15 and 20, and cells were always split into the same number of T-75 culture flasks (4)(Au - Shipley et al., 2016).

9.3. Long term storage and recovery

For long term storage cells were kept in Liquid nitrogen (LN_2) with a cell density of 1 x 10^6 cells/ml in a cryogenic media (40% FBS, 10% dimethyl sulphoxide (DMSO) and 50% un-supplemented media) in 1ml freezing cryotubes. Before placing in LN_2, cells were frozen in a -80°C using an isopropanol freezing vessel and then transferred to LN_2 for long term storage. When recovering cells from LN_2 cells were seeded at a density of 2 x 10^6 cells/mL.

9.4. Para-aminobenzoic Acid/ CoQ_{10} treatment

The organic compound, PABA is a natural product found in folic acid and several foods (figure 15). PABA is an intermediate product in the synthesis of folate in bacteria and plants, however humans lack the enzyme required to convert PABA into folate (Basset et al., 2004, Slock et al., 1990). PABA has been used in the treatment in a number of different conditions such as Peyronine's disease (skin disorder) and irritable bowel syndrome (Basset et al., 2004, Slock et al., 1990). However, its most notable use is in sunscreen as a UV light absorber. PABAs ability to absorb harmful light wavelengths between 290 and 320 nm but allow light between 320 and 400 nm to produce a tan made it ideal for sunscreen and in fact it was one of the first active ingredients to be used in sunscreen (Gasparro et al., 1998, Rahal et al., 2008).

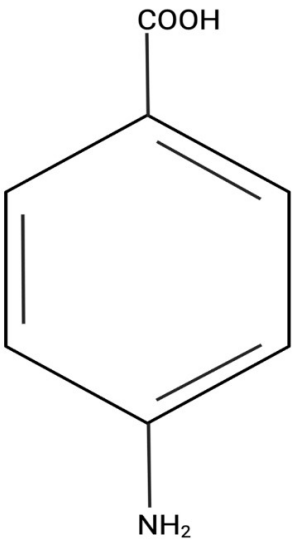

Figure 15. Basic Structure of PABA.

The method used in this study was originally described by Alam et al. (1975) and amended by Duberley et al. (2013a). Duberley et al. (2013a) used a 1mM PABA treatment over 5 days to induce a CoQ_{10} deficiency in SH-SY5Y cells. As described by Alam et al. (1975), this method works through the competitive inhibition of the active site of polyprenyl-4-hydroxybenzoate transferase by PABA, thus inhibiting CoQ_{10} biosynthesis. In agreement with previous studies, the maximum inhibition of CoQ_{10} biosynthesis in SH-SY5Y cells was induced by treatment with 1mM PABA (in PBS) and higher concentrations of PABA (> 1mM) failed to induce a further deficit in cellular CoQ_{10} status. Thus, 1mM PABA was selected to induce a CoQ_{10} deficiency in the SH-SY5Y cells used in this study (Duberley et al., 2014, Duberley et al., 2013a). Once seeded, cells were left for a minimum of one hour to allow them to attach to the surface of the flask, PABA (1mM, final concentration) could then be added and incubated with the cells for five days, control cells were treated with the same volume of fresh PBS.

To assess the effects of CoQ_{10} supplementation, the cells were subsequently treated with 5 μM CoQ_{10} for 3 days post PABA treatment. This concentration of CoQ_{10} was selected as it is the approximate concentration reached in the plasma of patients undergoing CoQ_{10} supplementation as reported by López et al. (2010). As a result of the lipophilic nature of CoQ_{10}, it was difficult to ensure that the isoprenoid was fully soluble in aqueous solution, because of this, the CoQ_{10} was suspended in ethanol. Thus, to ensure maximal solubilisation the CoQ_{10} solution was made up in fresh media and incubated for 37°C for at least 20 minutes before adding to cells. The concentration of CoQ_{10} in the media was determined using high performance liquid chromatography (HPLC) analysis as described below in section 11.3

10. Total Protein Analysis

For assessment of cellular CoQ_{10} concentrations results were standardised against total protein concentration and expressed as pmol/mg. The protein concentration was determined using the Bio-Rad DC-protein assay (Bio-Rad Laboratories Ltd, Hemel Hempstead, UK), adapted from the original method by Lowry et al. (1951). In order to calculate protein concentrations a standard curve was created using a BSA protein standard in distilled water (0 to 1mg/ml) (Figure 16). 20μl pre-prepared cell sample in PBS was added to 80μl of distilled water and mixed in an Eppendorf, once mixed 10μl of this solution was then added to 190 μl of distilled water in a fresh Eppendorf tube and vortex mixed. 100μl of reagent A (alkaline copper tartrate) and 800μl of reagent B (Folin-Ciocalteau phenol) was then added to all Eppendorf tubes (including standards). Samples were then left in the dark for 30 minutes at room temperature.
The absorbance of samples was then measured at 750nm using a spectrophotometer. The total protein concentration was then calculated from the linear regression of sample absorbance plotted against the BSA standard concentrations (Figure 16).

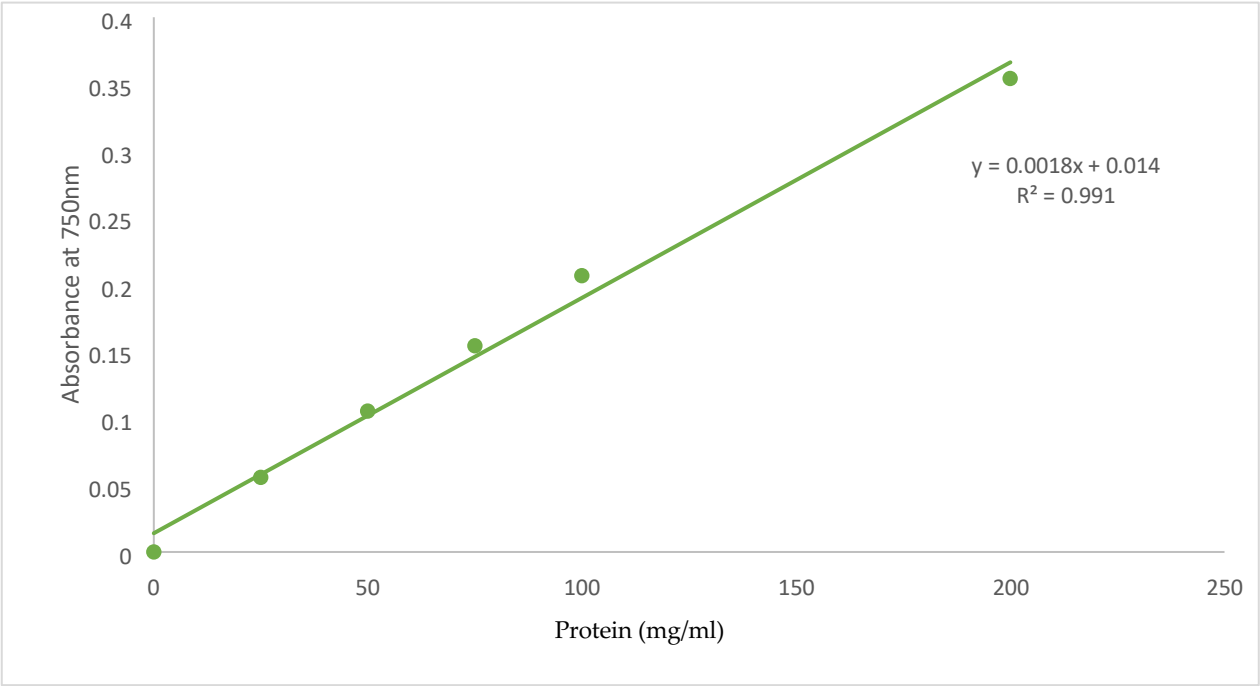

Figure 16. BSA Standard Curve.

11. CoQ10 Quantification

11.1. Internal Standard

In order to account for any losses of CoQ_{10} during the sample preparation an internal standard was used during the HPLC analysis. For this study we used the internal standard (I.S) known as dipropoxy-CoQ_{10}, a non-physiological analogue of CoQ_{10} which was first synthesised by Duncan et al. (2005). A number of previous studies have used the readily purchasable CoQ_9 as an I.S, however, this has been found to be un-reliable as it can be influenced by endogenous synthesis or dietary sources; unlike dipropoxy-CoQ_{10} which is not naturally occurring (Duncan et al., 2005). This IS also giving extremely distinctive peak on the HPLC chromatogram separate from CoQ_{10} for easy analysis (figure 17).

Dipropoxy-CoQ_{10} was synthesised according to the method set out by Duncan et al. (2005). 1 g of CoQ_{10} was dissolved into 10ml of hexane and then in 4ml of propan-1-ol with 1ml of potassium hydroxide solution in ethanol (40g/1) to catalyse the substitution of the methoxy groups with propoxy groups. The reaction was then allowed to proceed for 25 minutes at room temperature before being inhibited by the

addition of 1ml acetic acid. Dipropoxy-CoQ_{10} was then extracted from solution by the addition of 100ml of hexane, and centrifuging (100g, 5min). The upper organic layer was then removed and washed twice with distilled water, before drying down using nitrogen gas. The dipropoxy-CoQ_{10} was then re-constituted in 5ml ethanol. A standard curve was the created against known concentrations of CoQ_{10} using reverse-phase HPLC (SECTION 11.3) in order to obtain the concentration of the standard (figure 19).

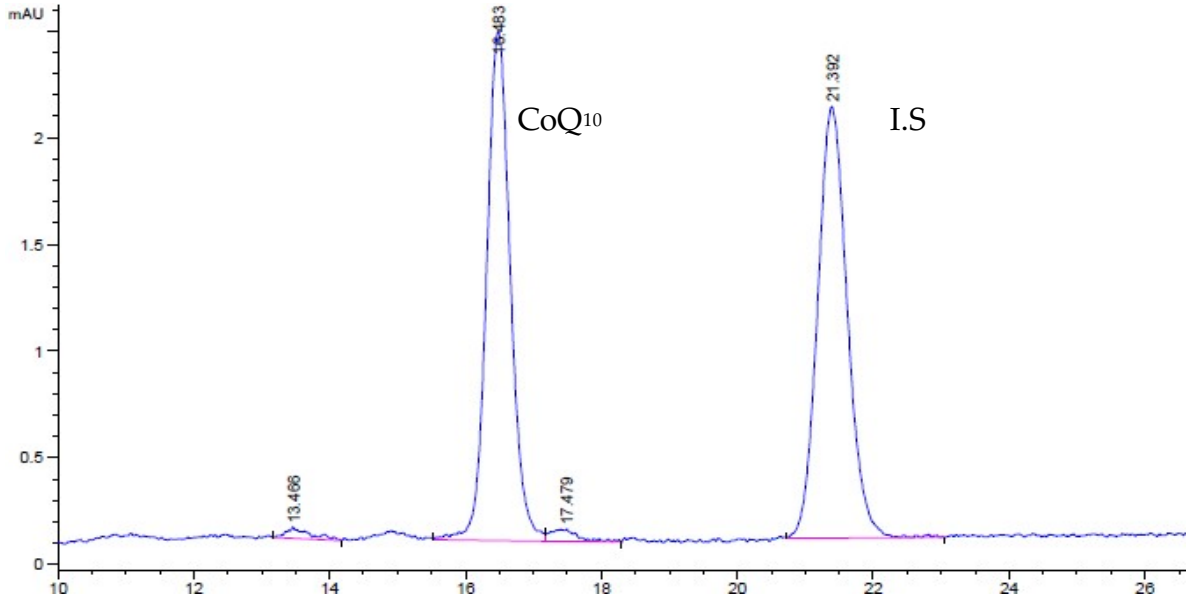

Figure 17. Typical CoQ10 and I.S HPLC chromatogram for Sh-SY5Y Cell.

11.2. CoQ_{10} Extraction

The CoQ_{10} extraction solution was prepared from 50ml of hexane and 20ml of ethanol (5:2) on the day of the experiment and stored at 4°C. Prior to extraction samples were thawed and a 50-60µl aliquot was dispensed into a new Eppendorf tube (at least 20µl of sample was retained for protein determination). 30µL of 5µM I.S was then added to samples, this gave a theoretical value of 1 for HPLC analysis. The cell membranes were then disrupted by 2 cycles of freeze/thawing the samples using liquid nitrogen and a water bath set at 30°C. Vigorously mixing of the samples was performed between the cycles using a vortex mixer. After completion of the freeze-thaw cycles 0.7ml of extraction solution was added to samples which were again vigorously mixed using a vortex mixer. Samples were then centrifuged at 15,000 rpm (100g) for 3

minutes at room temperature. The upper hexane layer (organic layer) was then removed and place in an Eppendorf tube on ice. The lower aqueous layer was then subjected to two more cycles of extraction. The organic layers from the 3 cycles of extraction were combined in an Eppendorf tube and stored on ice. The samples were then evaporated under Nitrogen gas and re-suspended in 300µl of ethanol. These samples could be stored at -80˚c until HPLC analysis.

11.3. HPLC Quantification

The cellular CoQ_{10} concentration was determined using reverse-phase HPLC with an Ultraviolet (UV) detector at 275 nm according to the method set out Duncan et al. (2005). Separation and quantification were achieved using a reverse phase C18 column (Phenomenex) and a mobile phase comprised of methanol, ethanol and perchloric acid (700:300:1.2) at a flow rate of 0.7 ml/min. CoQ_{10} detection was achieved using an Agilent 1200 series UV detector at 275 nm. (Figure 18)

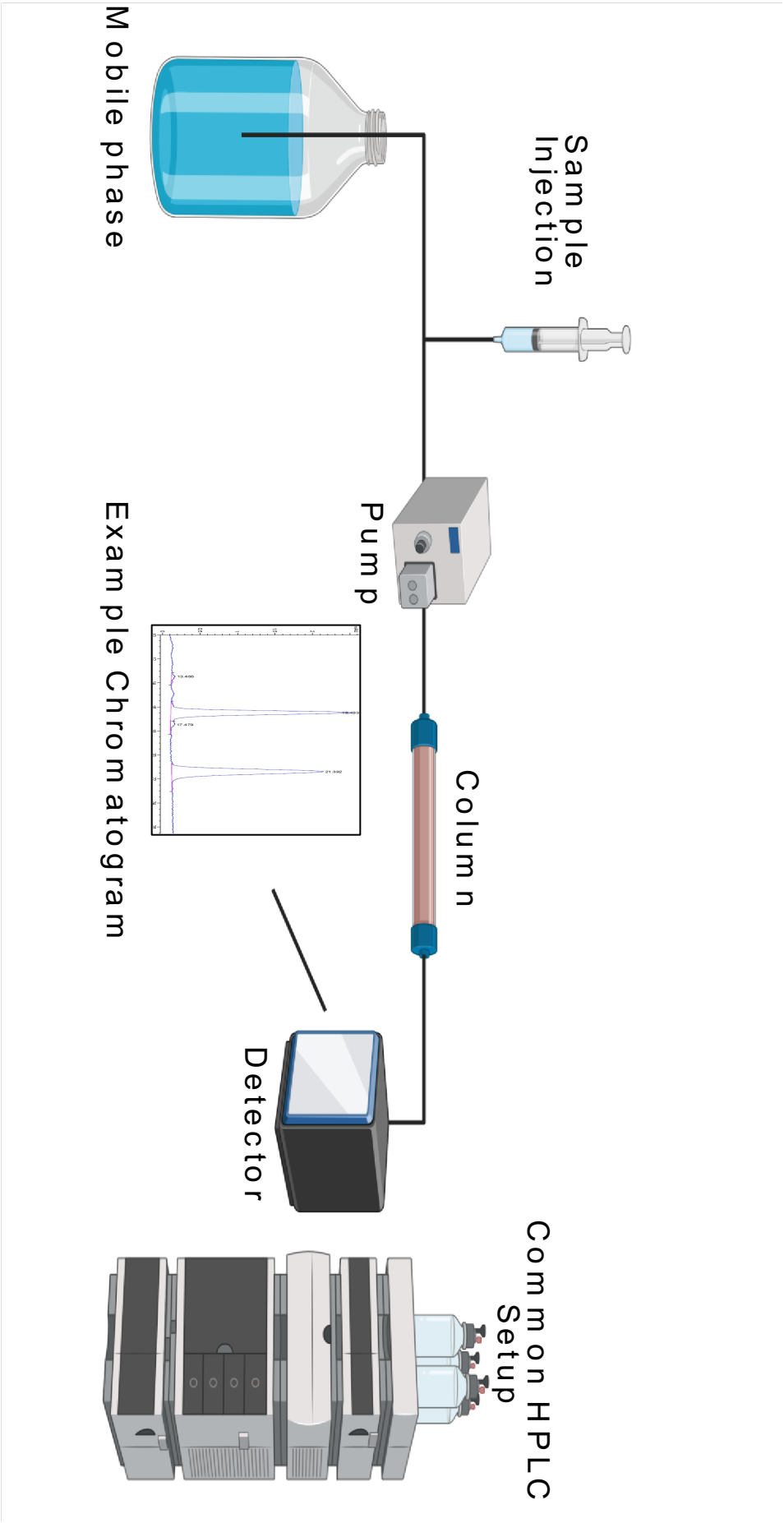

Figure 18. Basic layout of a Common HPLC Apparatus.

For each experiment prior to sample injection, 50µl of blank (ethanol) was injected followed by 50µl of a working standard comprising of 2µM I.S and 2µM of CoQ_{10} for calibration and followed by another blank run to remove any residual CoQ_{10} from the column. The samples were then injected (50µl) using an auto-sampler at 30-minute intervals.

Separation was achieved using a C18 reverse phase 5µ, 150 x 4.6mm column (Phenomenex), maintained at ambient temperature (25˚C). CoQ_{10} was detected using and inline UV detector (Adgulent 1200 series) at a wavelength of 275nm. The efficiency of the column was checked regularly by performing a calibration curve with varying concentrations of CoQ_{10} as shown in figure 19.

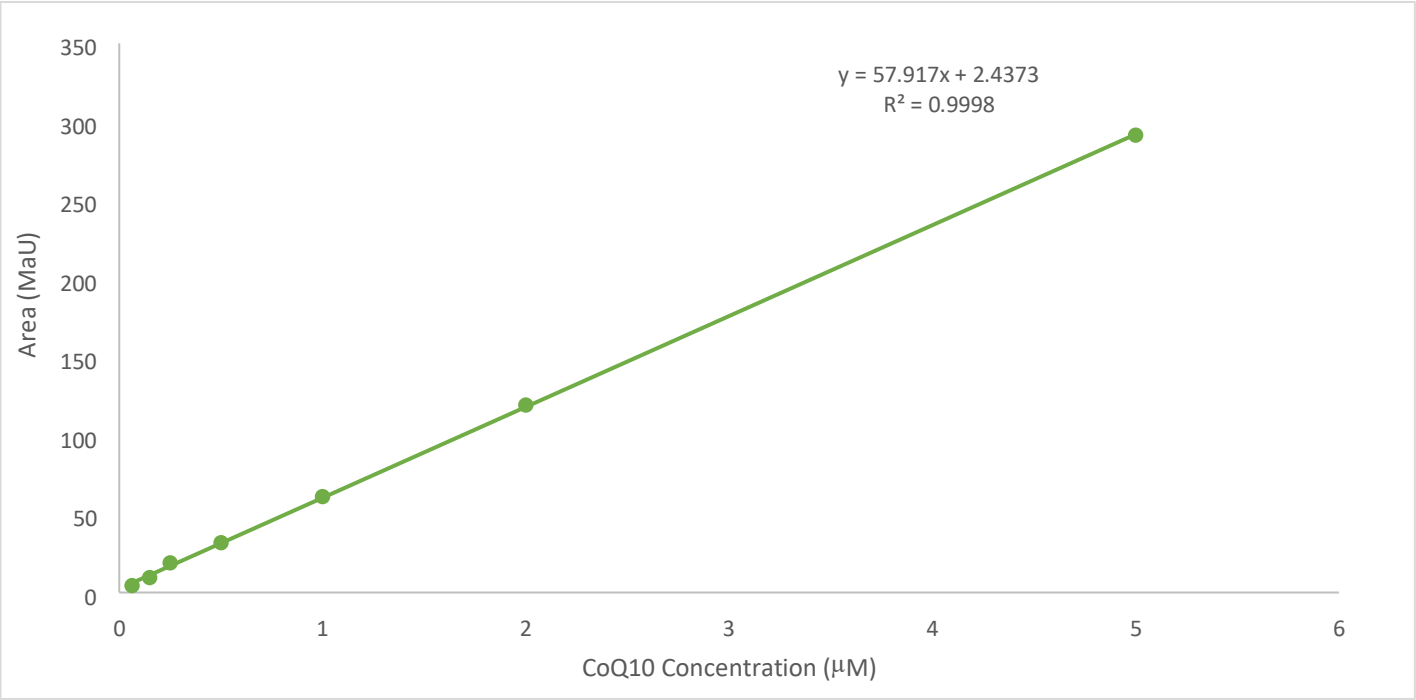

Figure 19. The Concentration Curve for CoQ10 on HPLC-UV Detection Method.

11.4 CoQ_{10} concentration calculation

CoQ_{10} concentration was calculated using the following equation:

Conc CoQ_{10} (pmol/ml) =

(Sample peak height /internal standard peak height) x internal standard conc. (μM) Dilution factor:

Conc CoQ_{10} (pmol/ml) =

(Conc CoQ_{10} (pmol/ml) x resuspension volume) / volume of extracted sample

Cellular CoQ_{10} status was calculated by dividing the CoQ_{10} concentration (pmol/ml) by the total protein (mg/mL) (section 10) for the sample and expressed as pmol/mg of total protein.

12. Flow Cytometry

Flow cytometry is a laser basted technique used to measure and evaluate an array of different biological materials; the method can be used to measure whole cell preparations or even individual cellular components such as organelles or nuclei (Radcliff and Jaroszeski, 1998). The basic principle of flow cytometry is that the molecule in question will scatter and/or emit light as its moves through a known beam of light; this can then be measured using an array of detectors (Figure 20)(Goetz et al., 2018).

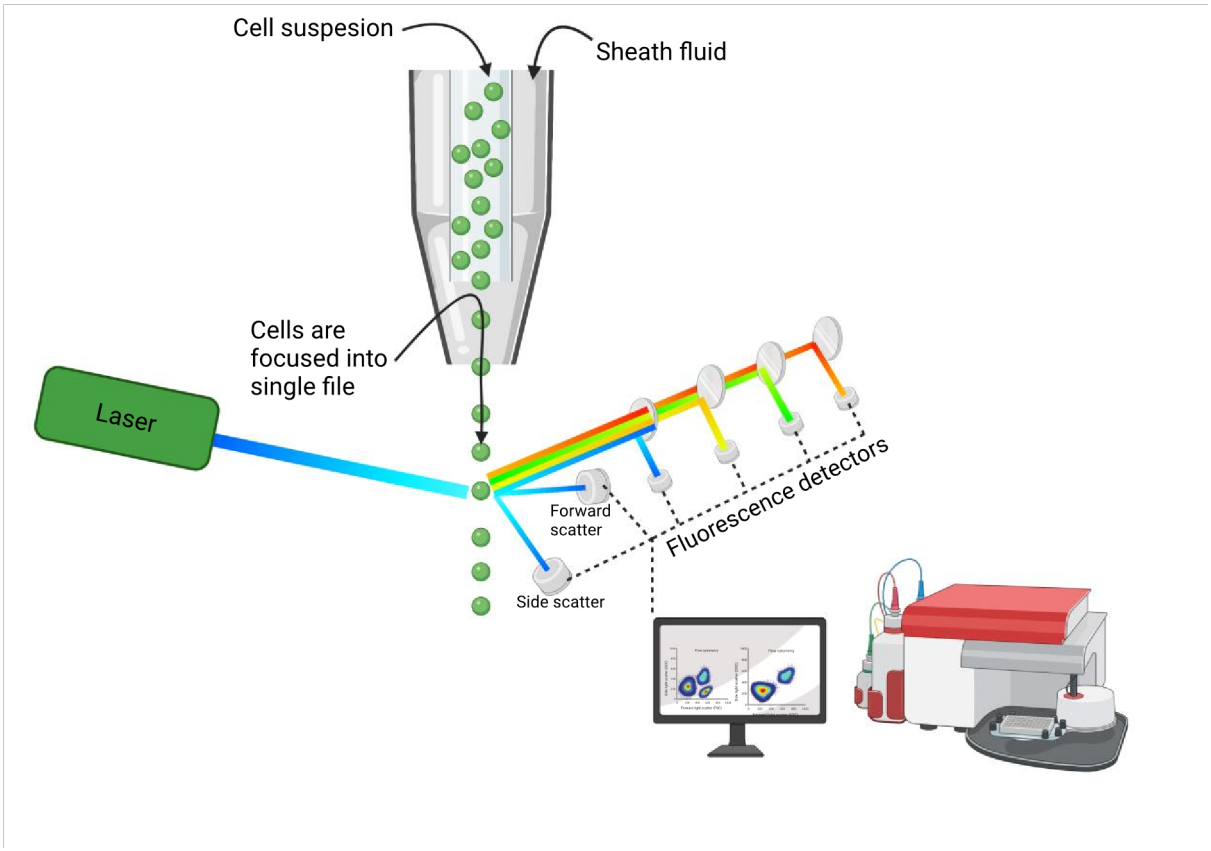

Figure 20. The Basic Layout of Basic layout of a flow cytometer apparatus.

In order to accurately determine the properties of individual cells, the suspension must first be passed through a stream of fluid (sheath fluid), which will hydrodynamically focus the cells into a single file as they pass the laser. Prior to any fluorescent probe analysis, the flow cytometer will first measure two dynamics of the light, forward scatter (FSC) and side scatter (SSC) (Figure 21). The FSC detector sits in line with the beam of light from the laser, as the cell moves through the laser beam it deflects the light, creating a "shadow" on the detector behind (figure 21). This can then be used to determine the size of the cell, the bigger the cell the bigger the shadow created. In contrast, the SSC detector sits perpendicular to the laser beam (figure 20 and 21), as light hits the cell it is scattered by internal cellular components. The more light that is scattered the more granulated (complex) the cell. These two components are then compiled in a dot plot, where populations of similarly sized cells will group together, as with cells of a similar complexity (figure 22). From this plot the nature of the cellular population can be determined as shown in figure 22 Healthy cells will group together in a particular region of the graph whereas cells undergoing apoptosis tend to shrink in size yet become more complex moving them into another region of

the plot (figure 22).

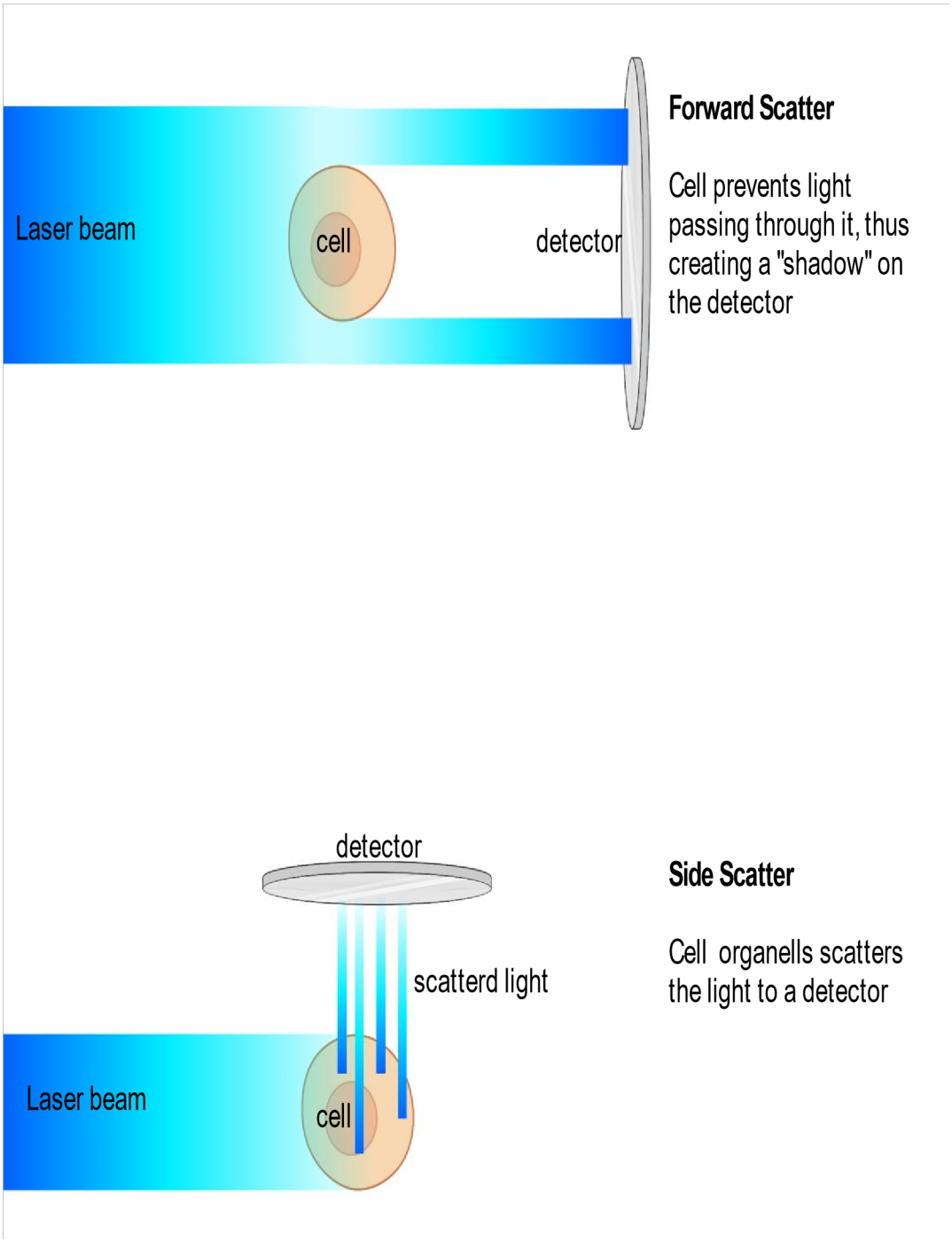

Figure 21. Shows Forward Scatter VS Side Scatter on the Flow cytometer.

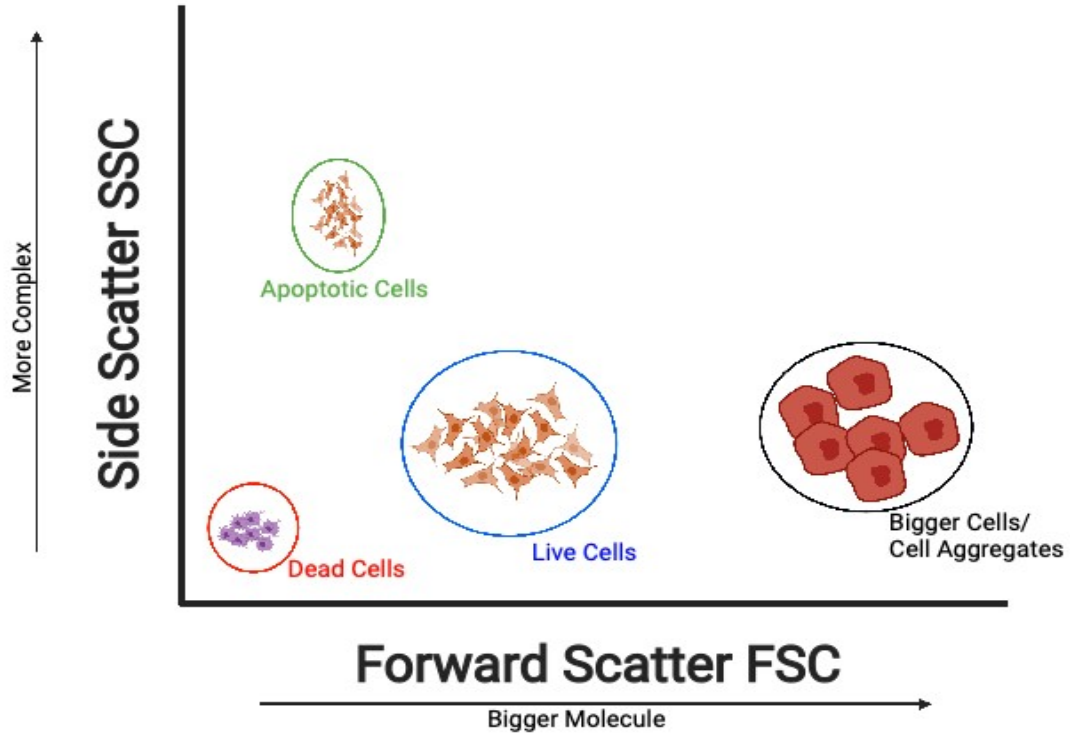

Figure 22. Shows FSC SSC Dot plot on the Flow Cytometer used to distinguish between different cells.

In addition to the FFS and SSC data gathered, the flow cytometer also measures cellular fluorescence as shown in figure 20 The flow cytometer can detect and accurately measure minute changes in individual cellular fluorescence. This can then be utilised to accurately measure changes in emission from fluorescent probes that have been added to the cells, allowing for the measurement of specific aspects of cellular homeostasis.

Each flow cytometer can be equipped with an array of different detectors with some flow cytometers measuring up to sixteen different channels. The machine utilised in this study was a BD accuri C6 with four channels for fluorescence intensity (figure 20), FL-1, FL-2, FL-3, and FL-4.

Prior to each experimental procedure a control group of cells were measured to create a background profile for the cells, whereby the SSC and FSC population will be gated, and the background fluorescence measured (Figure 23 and 24). 1 ml of cellular suspension (10^6 p/ml) was introduced into the flow cytometer and gated based on their

properties as previously discussed (FFS and SSC). The dense cell population was gated as shown in figure 23 and the parameters of each experiment were created as shown in figures 23, 24 and 25 … Once their parameters were established, they were maintained to ensure the experiments were comparable. For example, cells were gated and the number of events within the gate could then be kept the same (figure 25). Additionally, the background fluorescence for the cells on each detector was noted, this would allow for assessment of the uptake of the probes used in this study.

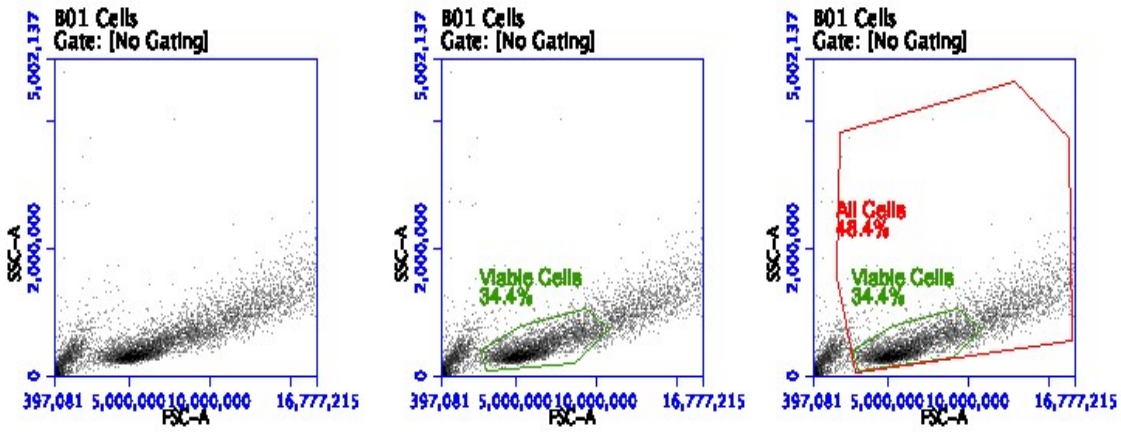

Figure 23. Figure shows the normal gating of SH-SY5Y cells on the flow cytometer

Shows how the cells were generally gated for each experiment.

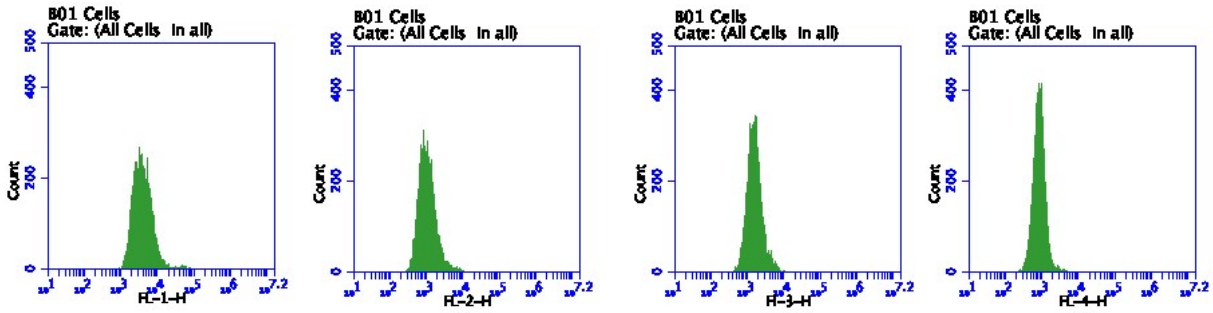

Figure 24. Normal Background Fluorescence profile of SH-SY5Y.

Shows the normal background fluorescence for the SH-SY5Y cells without any probes. Shows the cells have very little auto fluorescence.

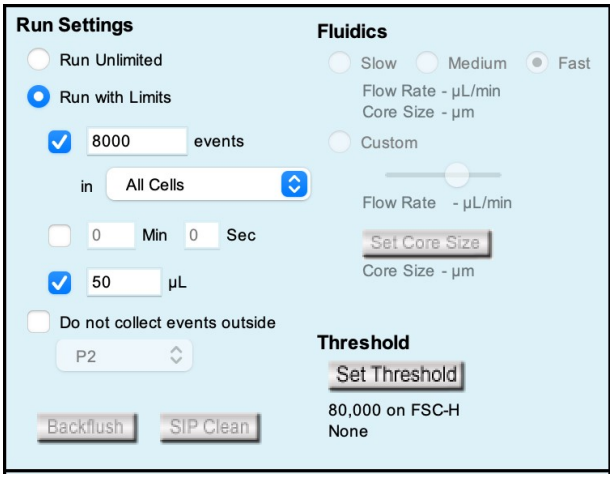

Figure 25. The Parameters used on the Flow cytometer

Shows the general limits setup for the flow cytometer; particularly shows that the limit for the number of events was set based upon the events ins ide the 'All Cells' gate.

13. Cell Death/ Viability

In order to investigate the potential cytotoxic effect of PABA treatment on SHS-S5Y cells, cell viability was assed post PABA treatment. This assessment was performed using the Propidium Iodide (PI) (ThermoFisher Scientific) and flow cytometry. PI is able to bind to double stranded DNA through intercalating between the bases, with little to no sequence preference (Lecoeur, 2002). However, it is excluded from cells with an intact plasma membrane (viable cells) and thus dead cells have a significantly increased fluorescence intensity when compared to live cells (Riccardi and Nicoletti, 2006).

For viability assessment cells were seeded into 96 well plates at a density of 5 x 10^4 cells/cm^2 and treated with PABA according to the method set out in (section 9.4). After a five-day incubation with PABA, the media was removed and kept in an Eppendorf tube. The cells were then washed with 1xPBS and then lifted with 50µl trypsin-EDTA at 37°C for 3 min. Trypsin was then inhibited by the addition of 150µl of fresh media. The cell solution was transferred to an Eppendorf tube to which 4µl of 1 mg/ml PI was then added (1 µg/mL). The solution was then mixed and quickly assayed by flow

cytometry as outlined in section 12 and longer incubation period could lead to inflated cellular death results. PI was only added to the sample once the sample was ready to be analysed (1 minute before analysis). This was imperative to ensure reproducible results given PIs toxicity. Control cells without PI were ran as well as PI with no organic matter to account for background fluorescence. Flow cytometry gating was performed as shown in figure 23 The dye has an excitation/emission maxima of 493/636 nm. Upon bindings its fluorescence is enhanced 20- to 30-fold, resulting in an excitation/emission maximum of 535 nm/617nm.

14. Lysosomal pH Measurements

14.1. LysoTracker DND-99

The LysoTracker (LT) probe is made up of a fluorophore linked to a weak base (figure 26) that is only partially protonated at a neutral pH, and when in a more acidic pH environment becomes more protonated, increasing the relative fluorescence of the probe, the protonation of the probe also gives it a more positive charge meaning the probe becomes unable cross the lysosomal membrane; thus, it can be used to measure acidic compartments such as the lysosome (Kang et al., 2013, Avrahami et al., 2013, Guha et al., 2014, Pierzyńska-Mach et al., 2014). As this probe is sensitive to photobleaching, the LT staining media was prepared on the day and kept in the dark at 37°C. The LT staining media was prepared by adding the stock LT solution (thermoscientific) to normal cell culture media to get a final working concentration of 1μM as
per manufactures instructions.

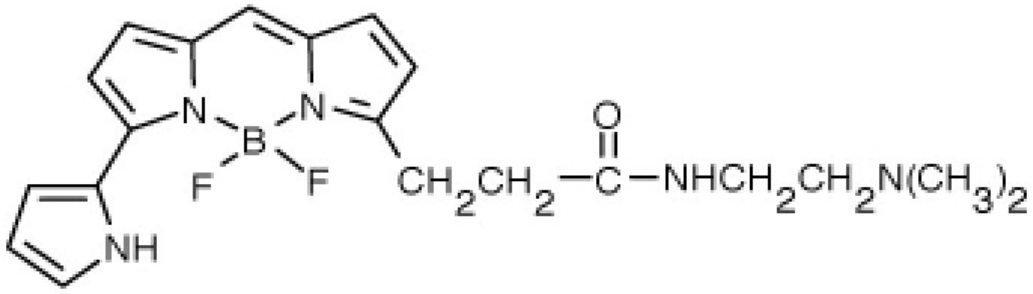

Figure 26. Chemical Structure of LysoTracker DND-99.

Cells were cultured in 96 well plates and treated with PABA/CoQ_{10} as described in section 9.4 Following the incubation period, PABA/CoQ_{10} treatment media was removed, and cells were washed twice with PBS (50 µl). The LT staining media was added (200µL), 96 well plates were then wrapped in tinfoil (to protect from photobleaching) and cells incubated at 37˚c for 20 minutes. After incubation, the staining media was removed, and cells washed with 1xPBS to remove any excess staining material. Cells were then lifted with 50µl trypsin-EDTA at 37°C for 3 min. fresh media was then added (150µL) to inhibit the trypsin. Cells were then transferred to fresh Eppendorf tubes and their fluorescence was assessed on the flow cytometer as per section 12 Lysotracker has an excitation and emission of 577/590 respectively, as such the fluorescence detector (FL-3) was used to analyse the fluorescence emission. Flow cytometry gating was undertaken as shown in figure 23.

14.2. LysoSensor DND-167

The LysoSensor DND-167 (LS) probe is a member of the same family of probes as the LT and consists of a fluorophore attached to a weak base that is protonated in an acidic environment (Figure 27). However, it has previously been reported that the fluorescence intensity of this probe is proportional to pH and thus can be used to determine pH (pKa ~5.2 to ~7.5) (Altan et al., 1998, Anway et al., 2004, Ma et al., 2017, Papakrivos et al., 2012).

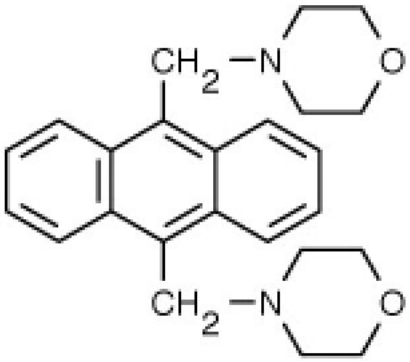

Figure 27. Chemical Structure of LysoSensor DND-167

As with LT, LS is sensitive to photobleaching, so all experiments were kept in the dark were possible and cell cultures were kept in tinfoil during and after staining. The LS staining media was prepared on the day with standard culture media, with a final working concentration of 1μM; this was then kept in the dark at 37°C until staining. At the end of the PABA and CoQ_{10} treatment experiments, the media was removed, and the cells were washed with 1 XPBS twice (50 μl). The LS staining media was then added (200μl) and the cells were incubated for 1 hour at 37°C. Following this incubation, the media was then removed, and cells were washed twice with PBS (50 μl). Cells were then left in 100μl of fresh PBS and the fluorescence was measured within five minutes to prevent photobleaching or unwarranted cellular stress. All LS measurements were made on a Clariostar plate reader with excitation at wavelength 373nm and emission detection at 425nm.

14.3. LysoSensor DND-160

The LysoSensor DND-160 (LS-160) is also a member of the same family as the LT and LS probes with made up with a similar structure (Figure *28)*. However, LS-160 is unique because of its ratiometric properties; this means it has dual excitation and emission peak wavelengths that are both pH dependent. In more acidic environments LS-160 exhibits a yellow fluorescence (4-5) and in less acidic environments, has a blue

fluorescence (5-7). As a result of this, a ratio of the two emission wavelengths can be used to give a more accurate assessment of lysosomal pH.

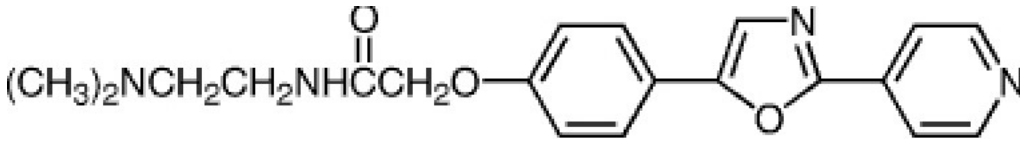

Figure 28. Chemical Structure of LysoSensor DND-160.

As with the previous probes the LS-160 is particularly sensitive to photo bleaching, thus precautions such as dimming lights and keeping the probe in dark during transit were made to prevent this from occurring. On the day of experiment, the LS-160 staining media was made up to a final working concentration of 1μM, in standard cell culture media; this was then kept in the dark at 37°C until staining. Post treatment with PABA or CoQ_{10}, media was removed, and the cells were washed twice with PBS (100 μL) LS staining media was then added (200μl – 96 well plate) and cells were incubated for 15 minutes at 37°C. Following this incubation, the media was removed, and the cells were washed twice with PBS. Cells were then suspended in 100μl of fresh PBS and the fluorescence measured. For standard pH measurements, after media was removed and cells washed twice with PBS, the desired pH standard solution was then added (100 μl) and cells incubated for 15 minutes at 37°C before measurements were taken. All LS-160 measurements were made on a Clariostar plate reader and measured at both the excitation and emission wavelengths (Abs- 329, 284: Em – 440, 540) sequentially.

It was determined that the background fluorescence of the PBS was higher than that of the standard pH solutions thus giving a false indication of high pH in the cells. To account for this, in each experiment three wells of each pH standard solution and three wells of PBS with no cells or probe were measured, an average was then taken, and this removed from the measured fluorescence in each sample.

Additionally, in order to fully evaluate LS-160s ability to measure lysosomal pH the V-ATPase inhibitor Bafilomycin A1 (BAF) was used. BAF is a member of a chemicals that can specifically target vacuoles-type H+ -ATPase (V-ATPase) inhibiting their function thus altering the pH of the lysosomal lumen (Yoshimori et al., 1991, Ponsford et al., 2021). BAF stock solution was made prior to experiment in DMSO at 2/100 volume of BAF and stored at -20°C. For these experiments cells were grown for five days as previously described, without treatment. On day of experiments BAF was thawed and kept at room temperature. Once grown media was removed and cells washed with 1XPBS twice. Fresh media was added (100 µl), BAF solution was then added to a final working solution containing 1/100 volume of BAF; control cells were treated with DMSO alone with the same volume. Cells were then incubated for 1 hour at 37°C. Staining could commence during the end stages of this period as previously set out.

15. ROS Measurements

In order to assess changes in total cellular ROS concentration the probe CMH2DCFDA was used (Invitrogen). CM-H2DCFDA is a chloromethyl derivative of the probe, H2DCFDA, although it has a considerably better live cell retention allowing for better analysis (Ameziane-El-Hassani and Dupuy, 2013). CM-H2DCFDA is able to passively diffuse into cells where intracellular este

rase's cleave its acetate groups, this then liberates the chloromethyl group to react with glutathione and other intracellular thiols; successive oxidation of the probe produces a fluorescent product trapped within the cells. As a result of this, it can be assumed that the fluorescent intensity of the cells post staining is directly proportional to the concentration of ROS within the cells.

Cells were counted and plated in clear 96 well plates and treated with PABA as previously described in section *9.4* On the day of experiment a stock solution of CMH2DCFDA was prepared in PBS with a final concentration of 1 µM. Post PABA/CoQ_{10} treatment, the media was then removed from the 96 well plate and the

cells washed twice with PBS. Trypsin was then added to the cells (50 µl) and the cells were left to incubate for 5 minutes. Once the cells had trypsinized, media was then added (150 µl), and the contents of the well transferred into Eppendorf tubes. The cells were spun down for 5 minutes at 100 g and the media was then removed. 200µl of the CMH2DCFDA staining solution was added to the cells, the cells were mixed and left to incubate for 15 minutes. Eppendorf tubes were then vortexed, and the fluorescence intensity was measured on the flow cytometer on FL-1.

To evaluate the relationship between the probe and ROS concentration a standard curve was crated between cells treated with 1mM H2O2 and time. H2O2 was used as it has previously been reported to induce oxidative stress in cells. The data shows a linear relationship with amount of time incubated with 1mM H2O2 and median fluorescence (figure 29). This suggests that the probe is indeed measuring the production of ROS in the cells as suggested.

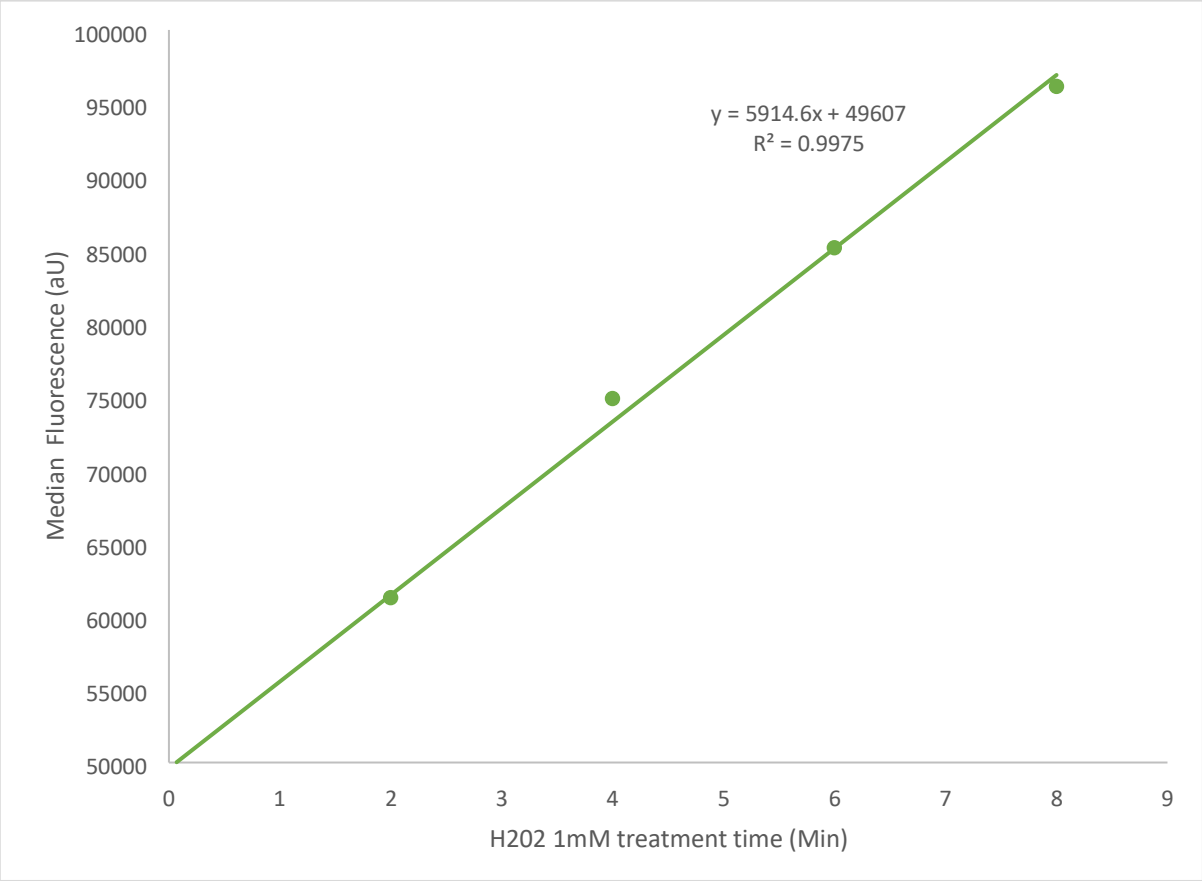

Figure 29. Shows the Linear Relationship Between Median Cellular Fluorescence and Cells Treated with H_2O_2 (positive control).

16. Cellular ATP Measurements

In order to *assess* the effect of a cellular CoQ_{10} deficiency on general cellular health, this study assessed changes in cellular ATP concentration; this was achieved using a CellTiter-Glo bioluminescence assay (Promega). This assay utilises *the reaction* of ATP with luciferin-luciferase. The lysis of *cells releases* free intracellular ATP, and as a result, the luciferase enzyme *catalyses* the mono-oxygenation of luciferin in the presence of Mg2+, ATP and molecular oxygen (Figure *30*) (Crouch et al., 1993). This reaction results in the production of oxyluciferin along with the *emission* of light (luminescence); the amount of light produced is directly proportional to the total ATP concentration and can be measured using a luminometer (Campbell, 1988).

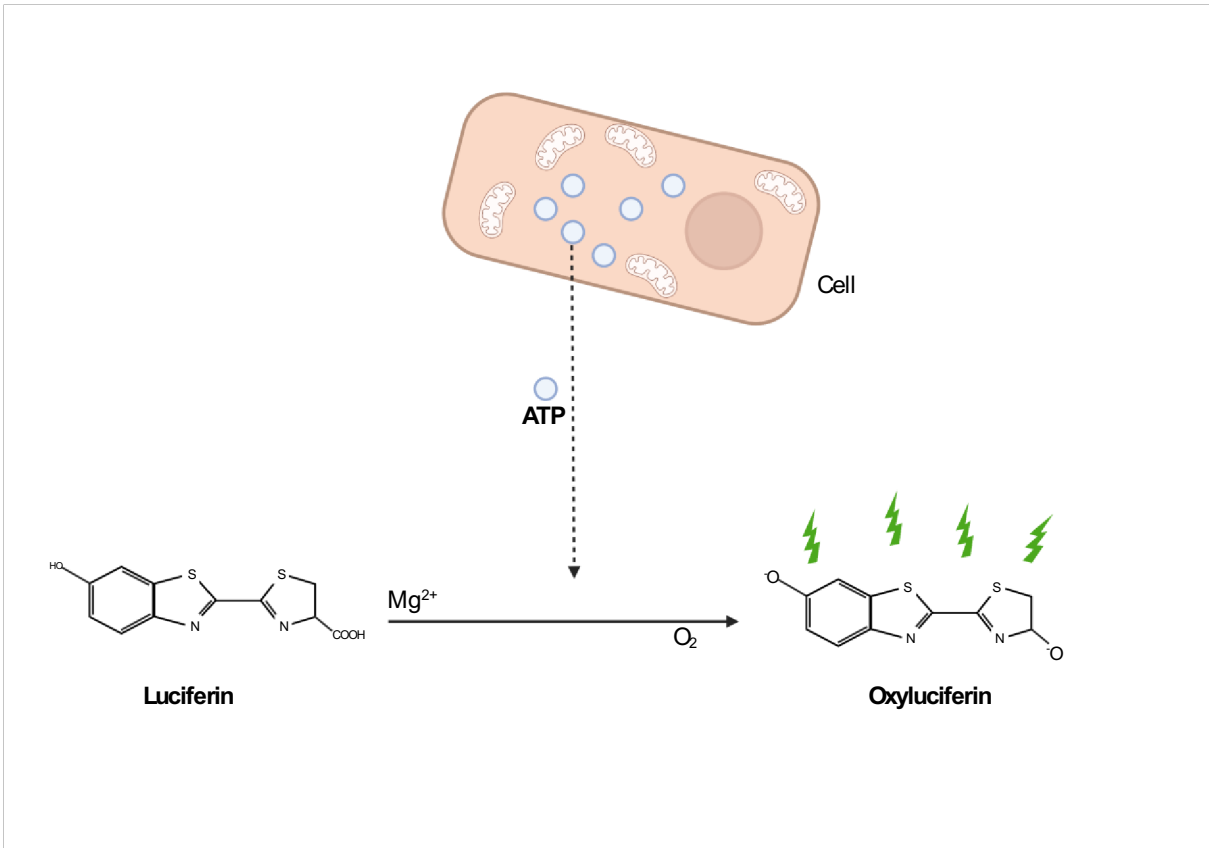

Figure 30. The basic chemical interaction for the CellTiter-Glo assay

Highlights that the luminescent chemical Oxyluciferin, can only be formed in the presence of ATP, thus the amount of light produced is proportional to the amount of ATP presence.

Cells were counted and plated into an opaque white 96 well plate and treated with PABA as previously described in section *9.4* On the day of *measurement CellTiter*-Glo® Buffer and substrate was thawed and equilibrated to room temperature. 10ml of the cellTiter-Glo® Buffer was transferred into the CellTiter-Glo® Substrate and mixed gently by *vertexing* to reconstitute the lyophilized enzyme/substrate mixture, thus forming the CellTiter-Glo® Reagent (It is unclear what *exactly* constitutes the buffer provided in the kit, however it can be *assumed that* it is a lysis buffer in order to release the ATP from the cells). The media was then removed from the cells *and the* cells were washed twice with PBS. Fresh media (50 µl, room temperature) was added, and the plate was equilibrated to room *temperature*. 50 µl of the CellTiter-Glo® Reagent was added and cells mixed on an orbital plate shaker for 2 *minutes* to induce cell lysis. Once mixed the plate was placed into the plate reader and left at room temperature for 10

minutes to stabilize the luminescent signal. The signal could then be measured using the Tecan plate reader luminometer. *To* assess the total cellular ATP concentration for each experiment, an ATP standard curve was created, this also displays the relationship between luminescence and total ATP *(Figure 31).*

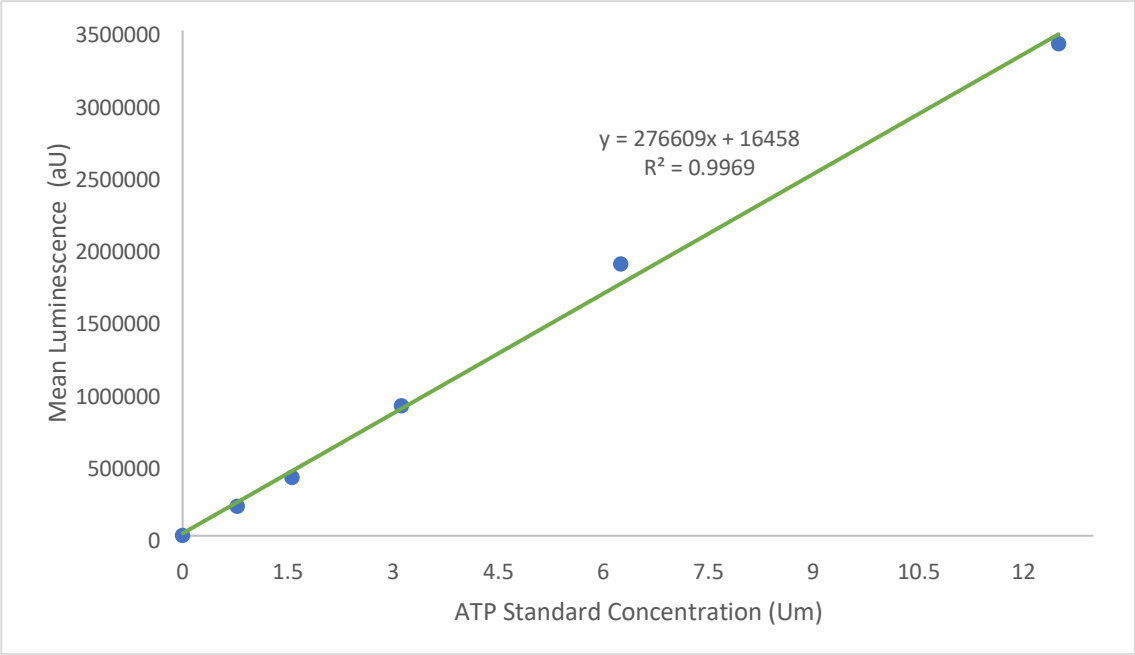

Figure 31. The standard curve showing the relationship between Luminescence and ATP concentration.

In addition to the ATP standards, analysis of 20 µl aliquots of each sample was undertaken, and the total protein was determined as described in section *10.* This was done to normalise the results of the cellular ATP concentrations which were expressed in µM/mg of protein.

17. Mitotraker green

MitoTracker green (MTG) is a membrane permeable probe consisting of a thiolreactive chloromethyl commonly used to label mitochondria in live cells (figure 32) (Presley et al., 2003). MTG has been utilized in a number of previous studies to determine cellular mitochondrial mass changes (Agnello et al., 2008, Cottet-Rousselle et al., 2011). MTG is able to cross the plasma membrane and selectively accumulate within active mitochondria where it covalently binds to mitochondrial proteins by reacting with the free thiol groups of cysteine residues (Presley et al., 2003). This reaction takes place independent of the mitochondrial membrane potential ($\Delta\Psi_m$) and thus can be used to determine changes in mitochondrial protein mass.

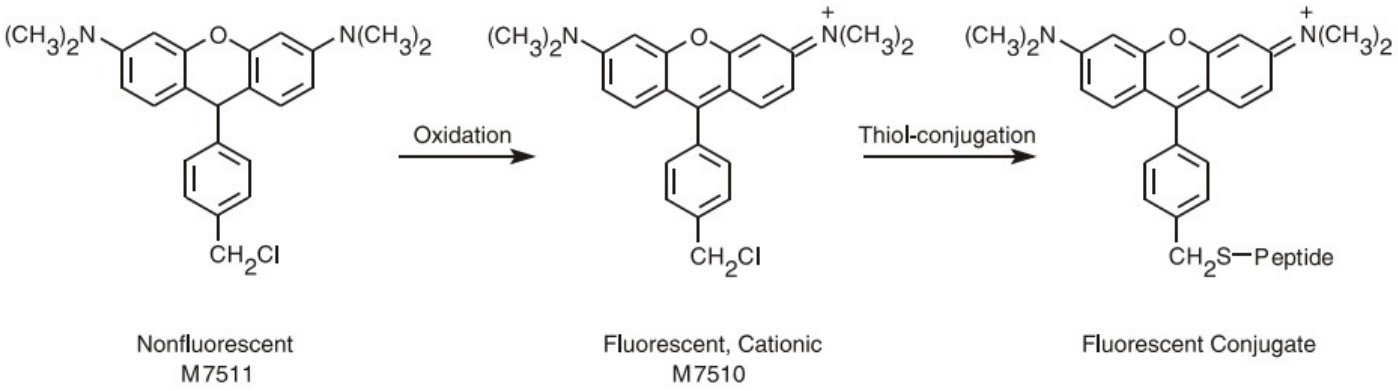

Figure 32. The chemical structure of MTG and the reaction leading to increased fluorescence.

However, there is a debate as to whether this is indeed true with studies such as Xiao et al. (2016) suggesting that MTG fluorescence can be affected by $\Delta\Psi_m$ changes. In contrast, the overwhelming evidence suggests this is not true and a number of studies have found that MTG fluorescence intensity is unaffected by $\Delta\Psi_m$ changes (Pendergrass et al., 2004)

On the day of experiment MTG was diluted from stock into a 100 μM solution in PBS. To prevent photobleaching this was kept in the dark until required. Post treatment with PABA/CoQ_{10}, the media was removed, and the cells were washed with PBS (50 ul). 100 ul of PBS stain was then added to each well (allowing for at least 3 wells without stain in each treatment). Cells were then incubated for 30 minutes at 37°C in the dark. Once incubated staining PBS was removed and the cells were washed with fresh PBS (100 μl). Cells were then lifted from the wells using 50 ul of pre-warmed trypsin and incubating for five minutes at 37°C. Once lifted 50 μl of fresh media was added and the cells were transferred into Eppendorf tubes. Cellular fluorescence could then be analysed on the flow cytometer as outlined in section 12.

18. JC-1

The importance of the mitochondrion in research has led to the development of a plethora of tools for understanding and measuring its function. In more recent years there has been a development of a number of fluorescent stains to specifically measure $\Delta\Psi_m$ (Cossarizza and Salvioli, 1998). One such probe is JC-1 (5,5,6,6'tetrachloro-1,1',3,3' tetraethylbenzimi- dazoylcarbocyanine iodide), which has been manufactured to measure the $\Delta\Psi_m$ in both healthy and apoptotic cells in an array of different cell types for example; neurons, myocytes, and endothelial cells (Sivandzade et al., 2019).

JC-1 is a lipophilic dye that emits a green fluorescence and is able to enter the mitochondrion where it naturally accumulates. Here, the probe forms reversible complexes called J aggregates in a concentration-dependent manner (Reers et al., 1991). The newly formed J aggregates differ from the JC-1 probe in that they emit fluorescence in the red portion of the visible spectrum (maximum at ~590 nm). Therefore, in healthy cells the JC-1 probe enters the cells and accumulates in the mitochondria, where due to the negative charge within the mitochondrial membrane it forms red fluorescent J aggregates. However, in cells with compromised $\Delta\Psi_m$ (such as apoptotic cells) the JC-1 probe will enter the cell and accumulate inside the mitochondria, but to a lesser extent as the inner mitochondrial space is less negative; under these conditions the JC-1 probe will not accumulate enough to induce the formation of the red j aggregates and thus, will retain the original green fluorescence (figure 33).

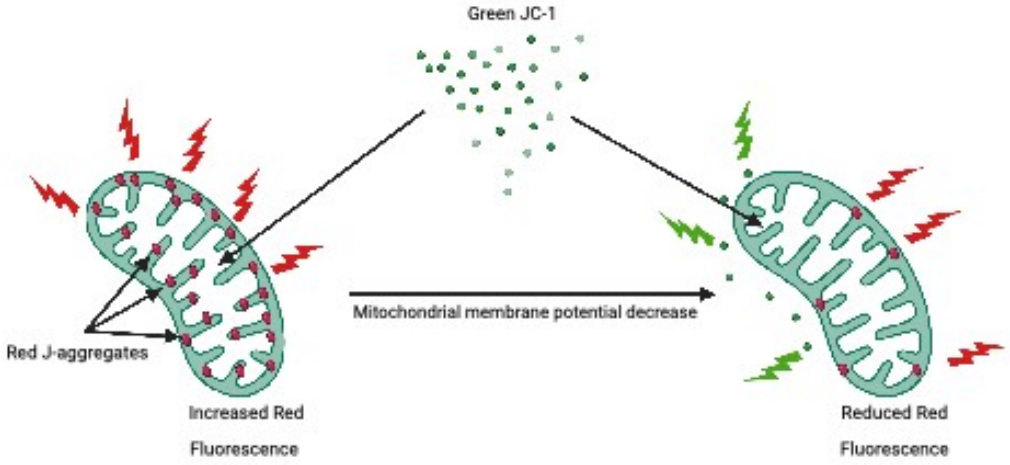

Figure 33. The Relationship between Red/Green JC-1 Fluorescence and ΔΨm.

As a result of this dependent change in fluorescence, the JC-1 probe can be utilized to measure mitochondrial $\Delta\Psi_m$ by ratioing the red to green fluorescence. It can be assumed that the higher the red fluorescence compared to the green the higher the $\Delta\Psi_m$ and vice-versa; the more green fluorescence the lower the $\Delta\Psi_m$.

On the day of the experiment, JC-1 was diluted from the stock into a 2µM solution in fresh media. To prevent photobleaching, this was kept in the dark until required. Post treatment, media was removed from cells and washed twice with PBS (50 µl). 100 µl of the JC-1 stain was then added to each well (allowing for at least 3 wells without stain in each treatment) and the cells were then incubated for 30 minutes at 37°C in the dark. Once incubated staining media was removed and cells were washed twice with fresh PBS. Cells were then lifted from the wells using 50 µl of pre-warmed trypsin and then incubating for five minutes at 37°C. Once lifted 150 µl of fresh media was added and the cells transferred to an Eppendorf tube. Cellular fluorescence could then be analysed on the flow cytometer.

19. Assessment of citrate synthase activity

Citrate Synthase (CS) is an enzyme involved in the citric acid cycle, where it facilitates the condensation of oxaloacetate and acetyl-coenzyme A to form citric acid and coenzyme A. Originally described by Shepherd and Garland (1969) the CS method has since been used to assess changes in mitochondrial cell content (Hargreaves et al., 1999). CS itself is located within the mitochondrial matrix and the assay measures the creation of coenzyme A through the reaction with 5, 5'-dithio-bis (2-nitrobenzoic acid) (DTNB). Thionitrobenzoate, mercaptide ion formed in this reaction absorbs light at 412 nm. The rate of change in absorbance at 412 nm is proportional to CS activity.

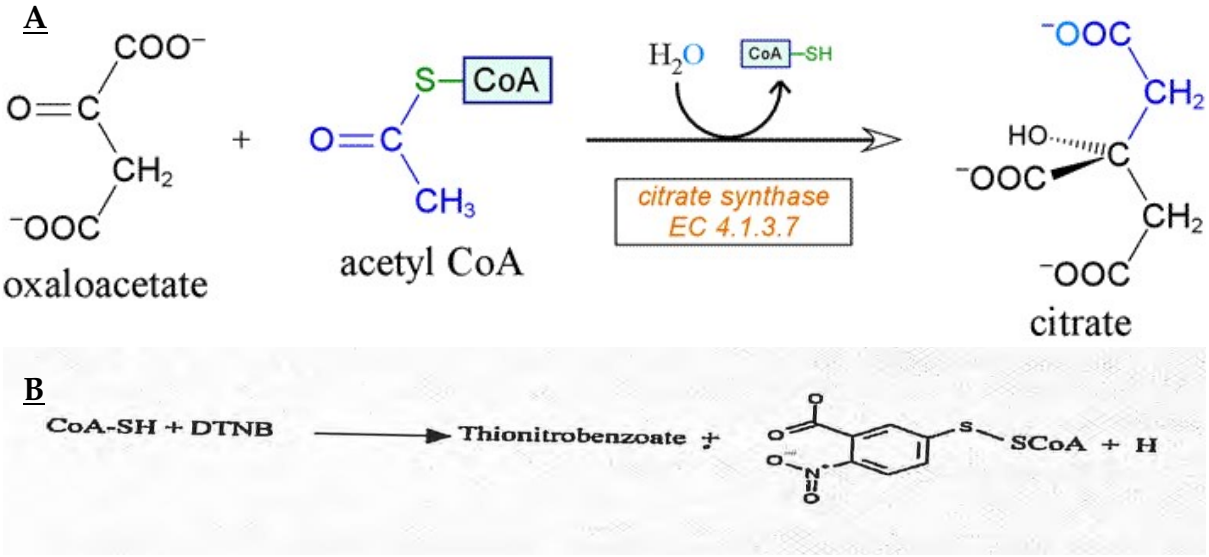

Figure 34. Schematic of the citrate synthase activity Assay.

A: The activity of CS is measured by the reaction of free Co-ASH with DTNB [5, 5` dithio-bis (2-nitrobenzoic acid)]. B: thionitrobenzoate, a mercaptide ion absorbs light at 412 nm. Therefore, the activity of CS can be followed spectrophotometrically in the presence of DTNB. The rate of change in absorbance at 412 nm is proportional to the enzyme activity.

20ul of previously described sample preparation for CoQ_{10} extraction in section 11.2 was taken and added to two corresponding cuvettes both containing 0.1mM acetylcoenzyme A, 1 g/L triton X-100 and 0.2mM SNTB in tris buffer (pH 8); with a final volume of 1 mL in each cuvette. The cuvettes were then gently mixed by inverting each four times with parafilm. The cuvettes were then placed in the Uvikon 941 spectrophotometer (Northstar Scientific, Potton, UK).

The reaction was initiated by adding 10ul (20mM) oxaloacetate to the sample cuvette and inverting with parafilm. The reaction was then measured at 412nm for 5 minutes at 30 second intervals at +30 ˚C. The absorbance could then be converted to a molar concentration using Beer-Lambert law. the extinction coefficient of DTNB is 13.6 x 10^3 M^{-1} cm^{-1} (path length 1 cm, total volume 1mL). Cellular CS activities were expressed as nmol/min/mg of protein similar (section 10). The linearity of CS activity shown in figure 35 was assessed for method validation.

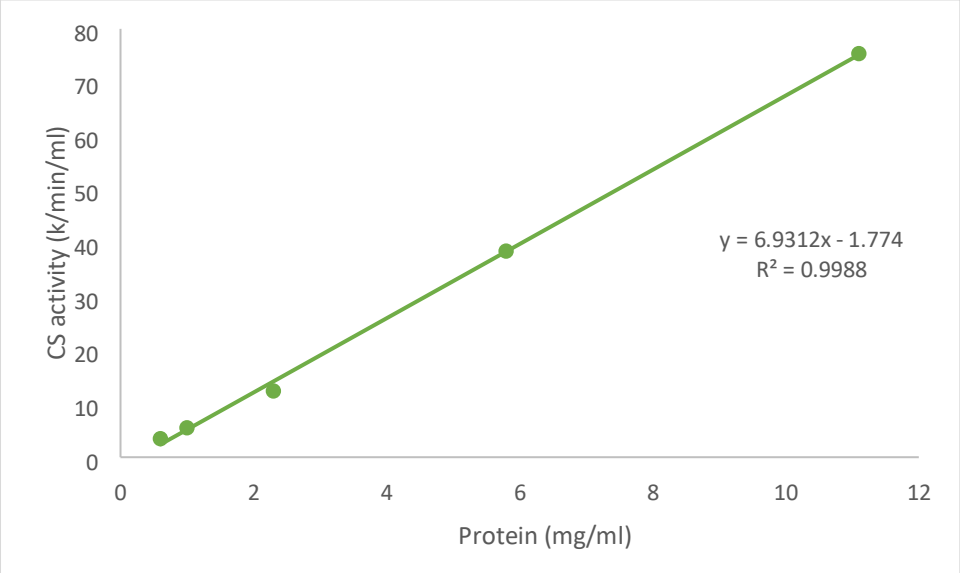

Figure 35. Standard curve of CS activity Vs Protein concentration in standards.

20. Lysosomal mass assessments

In this study it was necessary to assess whether changes in the LysoSensor fluorescence was indeed associated with changes in pH or changes in total cellular lysosomal content. In order to do this, we measured the lysosomal enzyme βgalactosidase (β-gal). β-gal is a eukaryotic, hydrolytic enzyme responsible for the cleavage of β-linked terminal galactosyl residues on a plethora of substrates bound for digestion in the lysosome (Higaki et al., 2011, Wallenfels and Weil, 1972). Generally, β-gal has been associated with determining age-related replicative senescence in cell culture, with it becoming known as senescence associated βgalactosidase (SA-β-

galactosidase) (Dimri et al., 1995, Sigal et al., 1999). However, more recent studies have shown that the total cellular β-gal can be associated with changes in lysosomal mass. For example, Kurz et al. (2000) demonstrated that changes in cellular lysosomal content directly correlated with a changes in β-gal activity. In this study the assay kit, Beta Galactosidase, Fluorescence (ab228562) from Abcam, UK was used to determine β-gal activity.

Cells were counted and plated in clear 12 (50,000 cells p/ml initial ceding density) well plates and treated with PABA as previously described in section 9.4 On the day of experiment all kit reagents were thawed and brought to room temperature. Stock staining solution was prepared by adding 1.5 µl of Senescence Dye per 500 µl of media, this was kept warm in the water bath until required. Post PABA treatment, media was removed from cells and washed with 1x PBS twice. The previously described senescence staining media was then added (500 µl) and cells incubated for 1 hour 30 minutes at 37°C, 5% CO_2.

Once staining was complete, media was removed, and cells washed twice with 500 µl wash buffer. Cells were then lifted by trypsinization as described in section 9 Cells were then centrifuged (100 g for five minutes), media removed, and the resulting pellet was re-suspended in 500 µl of wash buffer. Cells were then analysed using flow cytometry. In addition to control cells without PABA, cells without PABA and without senescence dye in wash buffer were also ran to generate gating parameters. It was unclear as to the exact composition of the provided wash buffer as the company were unwilling to provide that information.

21. Cell Harvesting for Microscopy

For confocal microscopy imagery, cells needed to be alive and attached to 22mm cover slips. Prior to seeding cells, the coverslips were sterilized by completely submerging them in 100% ethanol, then placing them into a clear 6 well plate to dry (one coverslip per well, for around 10 minutes). Once dry the cells could be seeded onto the coverslip (cells pipetted onto the middle of the coverslip) at a density of 1×10^4 cells p/ml. Cells were then left to adhere to the coverslip by leaving them to incubate for around 15 minutes at 37°C, 5% CO_2. This was to ensure that when the media was added to the coverslips the cells were not washed off the coverslip into the space around in the well.

Once incubated, cells could be treated with PABA as described in section 9.4
Once treatment and appropriate staining had been undertaken the media was removed, and the cells were washed twice with 1xPBS. The coverslip was then lifted using sterilised tweezers and placed cell side down onto a glass slide. The coverslip was fixed to the slide by a flouro-mount solution, this also reduced the amount of photobleaching that could take place during the imaging process.

22. Statistical analysis

All results are expressed as mean ± standard error of the mean (SEM), error bars represent SEM. Data was subjected to Normality testing and once confirmed appropriate parametric analyses, ANOVAs (groups ≥3) with Tukey's post-hoc test or Paired T tests as indicated, were used to compare data sets. In all cases an alpha value of 0.05 was considered significant. The `n` number represents the number of individual observations. The groups compared by statistical analysis are shown in the figure legends of the results section of the manuscript. Statistical analysis was carried out using both R studio and Graphpad Prism analysis software. Graphs were created using Graphpad Prism

22. The effect of CoQ_{10} deficiency on Lysosomal pH

22.1 Introduction

As previously alluded to, CoQ_{10} deficiency currently represents the only treatable mitochondrial disorder, with ever expanding links to a plethora of diseases particularly in neurodegeneration (Manzar et al., 2020). A number of previous patient studies and reviews have discussed the relationship between CoQ_{10} deficiency and the development of neurological dysfunction and have suggested that this is a common clinical feature associated with primary CoQ_{10} deficiency (Quinzii et al., 2014, Emmanuele et al., 2012b). In a study by Rötig et al. (2000) three siblings were reported whom presented shortly after birth with a number of neurological symptoms such as: optic atrophy, sensorineural hearing loss, ataxia, dystonia, weakness, and rapidly progressive nephropathy. The neurological symptoms were associated with a severe CoQ_{10} deficiency: skeletal muscle: 4.6 μg/g tissue (mean ± SD); controls: 32.1 ± 6.8 μg/g and fibroblasts patient 6.7 ± 2.6 ng/mg protein ((mean ± SD); controls: 52.2 ± 9.1 ng/mg protein. This CoQ_{10} deficiency was found to be caused by a mutation (nonsynonymous nucleotide changes) in the *PDSS2* gene (Rötig et al., 2000). Neurological impairment was also reported in patient with neonatal CoQ_{10} deficiency who presented with seizures and dystonia. An MRI scan of the patient's brain revealed evidence of cerebral and cerebellar atrophy with the patient passing away at two years of age following a period of incurrent infection. Post-mortem gene mapping was undertaken and a novel mutation in the *CoQ9* gene of the CoQ_{10} biosynthetic pathway (see section 4.1.6) (Rahman et al., 2001, Duncan et al., 2009). Additionally, Quinzii et al. (2006) reported a patient who first displayed severe nephrotic syndrome and mild psychomotor delay at 12 months old. This patient was subsequently found to have a mutation in the *CoQ2* gene which is required for CoQ_{10} biosynthesis (see section 4.1.3) (Mollet et al., 2007). An MRI of the patient's brain displayed stroke-like lesions and cerebral and cerebellar atrophy.

Generally, patients with a CoQ_{10} deficiency respond positively to CoQ_{10} supplementation, with around 78% of non-neurological symptoms being significantly alleviated (Emmanuele et al., 2012b). However, neurological dysfunction appears to be more refractory to CoQ_{10} treatment, with only 46% of neurological symptoms being reported to show any significant improvement following supplementation (Emmanuele et al., 2012b, Rahman et al., 2001). The exact reason for the refractory nature of neurological dysfunction associated with CoQ_{10} deficiency to CoQ_{10} supplementation has yet to be fully elucidated, but may result from irreversible neurological impairment prior to CoQ_{10} treatment or poor penetrance of CoQ_{10} across the blood brain barrier (Duncan et al., 2009).

As previously discussed, the lysosome plays a pivotal role in normal cellular homeostasis. These organelles have been reported to contain > 50 different hydrolytic enzymes that are designed to digest a myriad of cellular waste products such as proteins, DNA, RNA, polysaccharides and lipids (Figure 10) (Aronson and de Duve, 1968, Wartosch et al., 2015, Thelen and Zoncu, 2017). For these enzymes to work at optimally they require an acidic pH (between 4 and 5) environment. Previous studies have reported that changes in lysosomal pH may be a pathological factor in a number of diseases, with de-acidification specifically being associated with the pathogenesis of LSDs (Folts et al., 2016, Parkinson-Lawrence et al., 2010).

In a study by Coffey et al. (2014) it was found that lysosomal alkalization (an increase of 0.2 - 0.3 pH units) was associated with pathologic build-up of partially degraded material and bloated lysosomes. This is of particular interest as the change in pH was also found to be associated with mutations in the presenilin 1 (PS_1) gene, which has been associated with the progression of familial Alzheimer's disease (Kelleher and Shen, 2017, Coffey et al., 2014).

The lysosome has previously been reported to be a major site of CoQ_{10} localisation with around 20% of cellular CoQ_{10} residing in its membrane (Gille and Nohl, 2000, Turunen et al., 2004). Here it is thought to play several roles to facilitate the normal functioning of the lysosome, such as maintaining the acidic environment of the

lysosomal lumen and protecting the membrane from oxidative stress induced impairment.

Proton translocation into the interior of the lysosome (lumen) is linked to the activity of the tentative ETC of this organelle where CoQ_{10} is believed to act as both an electron carrier as well as a proton translocator. As discussed in section 3 it is believed that the oxidation reduction cycle of CoQ_{10} is utilised in proton translocation whereby lysosomal CoQ_{10} is oxidised by lysosomal cytochrome b, then CoQ_{10} can move into the lumen donating an electron to a final electron acceptor (figure 10). Although, it is thought that lysosomal acidification takes place predominantly due to activity of the V-ATPase as discussed in section 5.3. However, this process does require ATP synthesized by the METC whose activity is dependent upon the level of cellular CoQ_{10} (discussed in section 3).

The acidic environment maintained in the lumen by the joint action of the lysosomal ETC and the V-ATPase is essential for the activity of the lysosomal enzymes which are acidic hydrolases and active at a pH 4 to 5 rather than the neutral, pH 7.2 of the cytosol. Thus, an increase in lysosomal pH can lead to suboptimal performance/dysfunction of the lysosome. In a study by Coffey et al. (2014) it was found that the chemical chloroquine (a known inhibitor of lysosomal acidification) led to a build-up of numerous proteins leading to impairment of normal cellular function.

22.2 Aims

In view of the important role CoQ_{10} plays in the maintenance of lysosomal pH, the aim of the work outlined in this chapter was to investigate the effect of a CoQ_{10} deficiency on the acidification of the organelle and whether a deficit in CoQ_{10} status results in an increase in the pH of the lysosome.

22.3 Methods

22.3.1 Cell culture

SH-SY5Y cells were grown and maintained as described in Section 9 all CoQ_{10} concentration assessments were carried out in T75 cell culture flasks.

22.3.2 PABA treatment

cells were subject to a sing 1mM PABA treatment over a 5-day period, as outlined in section 9.4

22.3.3. Quantification of cellular CoQ_{10} Concentration

Cellular CoQ_{10} was extracted, and concentration was calculated using reverse phase HPLC with a C18 column, as described in sections 11.2 and 11.3

22.3.4. Assessment of cell viability

Flow cytometry assessment of cell viability after PABA treatment was carried out as outlined in section 12

22.3.5. Total protein assessment

The total protein of the cells was determined using an adapted version of the Lowry method, as outlined section 10

22.3.6. Lysosomal pH determinations

In order to assess changes in lysosomal lumen pH, this study deployed three acidotropic lysosomal specific fluorescent probes: LysoTracker red DND, LysoSensor yellow-blue DND-167, and LysoSensor yellow DND-160. Each of these probes have marginally different method for assaying the lysosomal pH as discussed in section 20 all lysosomal pH assessments were carried out following section 14.1, 14.2, and 14.3 respectively.

22.3.7. Lysosomal mass

Total cellular lysosomal mass comparisons were carried out using measuring the lysosomal enzyme β-gal as previously outlined in section 20. Analysis was carried out using the flow cytometer as described in section 12.

22.3.8. Statistical analysis

Statistical analysis was carried out as described in section 22.

22.4. Results

It was found that after PABA treatment cellular CoQ_{10} status was significantly reduced ($p < 0.005$) when compared to the control levels (untreated cells) after a five-day incubation with 1mM PABA. Results show that 1mM PABA induced a maximal 56% decrease in cellular CoQ_{10} (Figure 36), this result is comparable to those found by Duberley et al. (2013a) and was reproducible. Additionally, it was found that higher concentrations did not induce a further decrease in CoQ_{10} status (2mM, 56% decrease). In view this 1mM was selected as the appropriate concentration of PABA to induce a neuronal CoQ_{10} deficiency in this study.

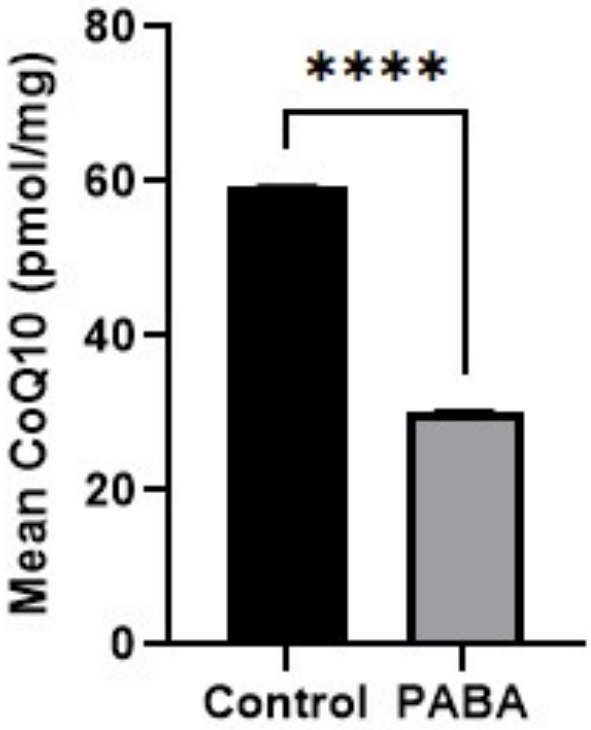

Figure 36. The Effect of Para-Aminobenzoic Acid (PABA) Treatment on total cellular CoQ10 Concentration.

*Error bars represent standard error of the mean (SEM); statistical analysis was carried out using T-test; levels of significance: ****: p<0.0005; n=20.*

Turunen et al. (2004) reported that the half-life of ubiquinone in rat brain (CoQ9) is roughly 90 hours or 3.75 days. As a result of this study an incubation period of five

days with 1mM PABA was selected for this study as this would enable accurate estimate of the inhibitory effect of the pharmaceutical on CoQ_{10} biosynthesis. Additionally, an incubation period of 10 day with PABA (1 mM) was also assessed but was found to induce a similar level of neuronal CoQ_{10} deficiency to that of a 5-day incubation in PABA (figure 37).

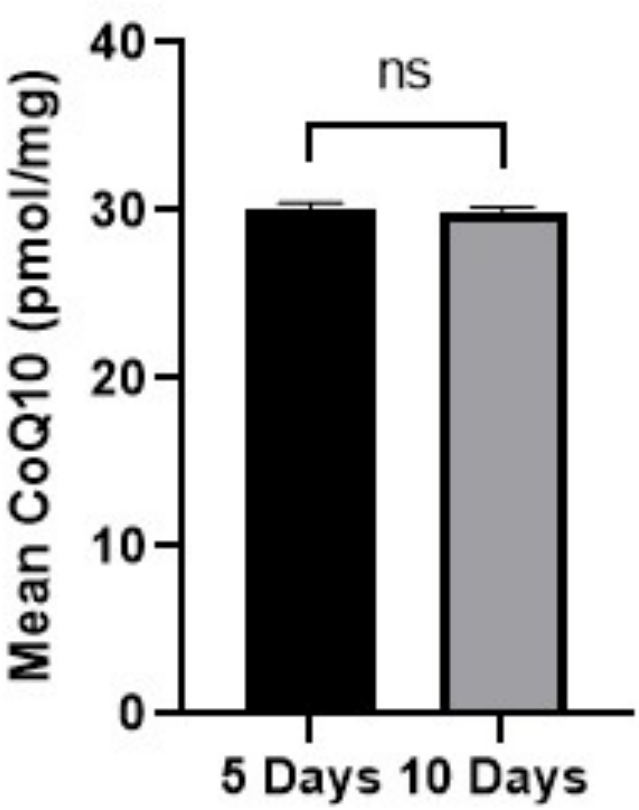

Figure 37. The Effect of Five- and Ten-day Para-Aminobenzoic Acid (PABA) Treatment on total cellular CoQ10 Concentration.

Error bars represent standard error of the mean (SEM); statistical analysis was carried out using T-test; n=20.

22.4.2. Assessment of Lysosomal pH

22.4.2.1 Lysotracker

Analysis of the flow cytometer LT results showed there was a significant decrease ($p < 0.005$) in fluorescence in the CoQ_{10} deficient cell line (PABA-treated) cells (figure 39). It was found that there was a 35% ($p < 0.05$) decrease in median fluorescence on average in the CoQ_{10}-deficent cells in comparison to the control cells (untreated).

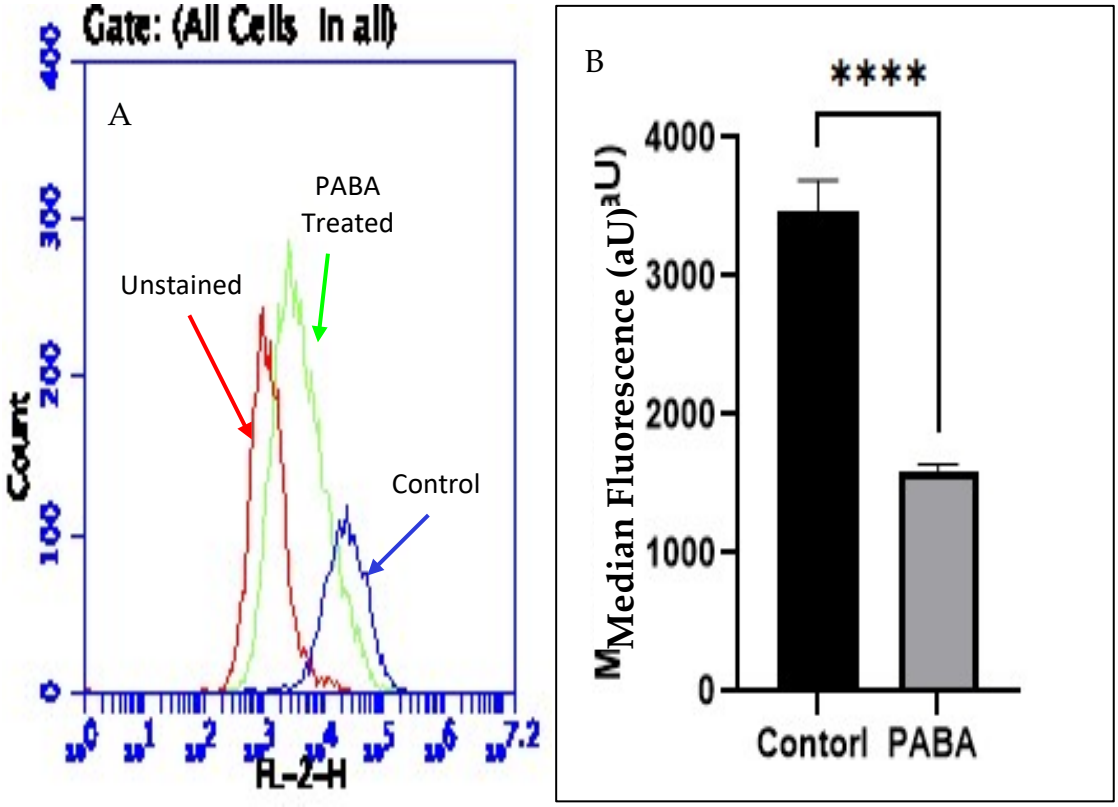

Figure 39. The Effect of CoQ10 deficiency on LysoTracker fluorescence.

*A) represents the florescence shift on the FL -2 detector, shows the cell population significantly increases in fluorescence after LysoTracker staining sowing the cells have successfully been stained. B) shows the median fluorescence pre CoQ10 deficiency (Control) and post (PABA). Error bars represent standard error of the mean (SEM); statistical analysis was carried out using T-test; levels of significance: ****: p<0.0005; n=26.*

Additionally, an assessment was made as to whether the PABA treatment had any interaction with the LT probe itself which may have impacted on the results. However, it was found that when both PABA and LT were tested simultaneously PABA itself did not hinder the uptake of the probe or effect the measurements in the control cells.

22.4.2.2 LysoSensor – 167

In order to evaluate the efficiency of the LS-167 probe`s ability to quantify the lysosomal pH, a calibration curve was constructed prior to each experiment; fluorescence was also compared between each calibrant and PBS alone (figure 40). It was found that the auto fluorescence of PBS was slightly above that of the calibrants. In order to combat this the measurements of each were taken of empty well (containing only PBS or calibrants) and background was taken away from results for each experiment.

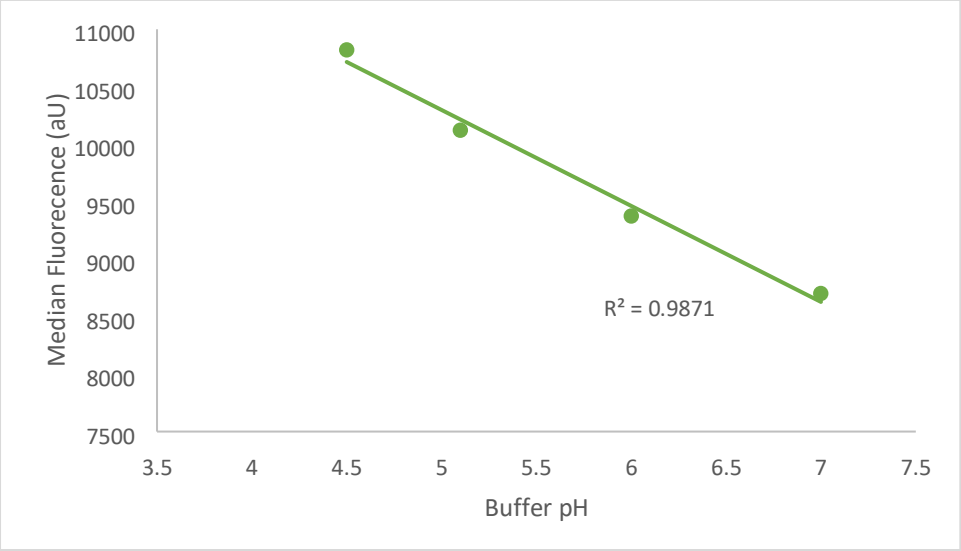

Figure 40. Standard curve of pH calibrants VS median LS-167 fluorescence.

It was found that the CoQ_{10} deficient cell line (PABA-treated) had a significantly decreased LS-167 fluorescence compared to the control (untreated) ($p < 0.05$). The results of this study show on average a 23% decrease in fluorescence (figure 41). This corresponded with an approximate increase in pH from 4.1 to 6.2 (figure 41).

Figure 41. The Effect of CoQ10 deficiency on LysoSensor-167 fluorescence.

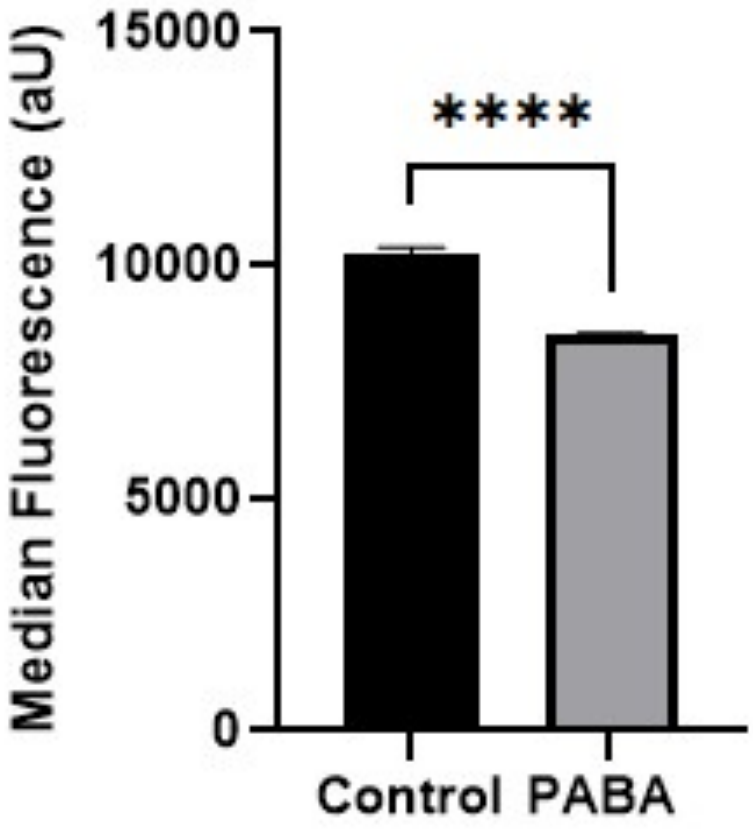

*Error bars represent standard error of the mean (SEM); statistical analysis was carried out using T-test; levels of significance: ****: p<0.0005; n=25.*

22.4.2.3 LysoSensor 160

To determine the lysosomal pH for each experiment a standard curve of pH was constructed as outlined in section 14.3 (Figure 42).

Analysis of the LS-160 fluorescence for the CoQ_{10} deficient neuronal cells revealed a decrease of around 15% on average compared to control levels. Using the standard curve (Figure 41), it was found that this correlated with a significant increase in pH from around 4.2 (untreated cells) to 6.3 (PABA-treated) ($p < 0.05$) (figure 43).

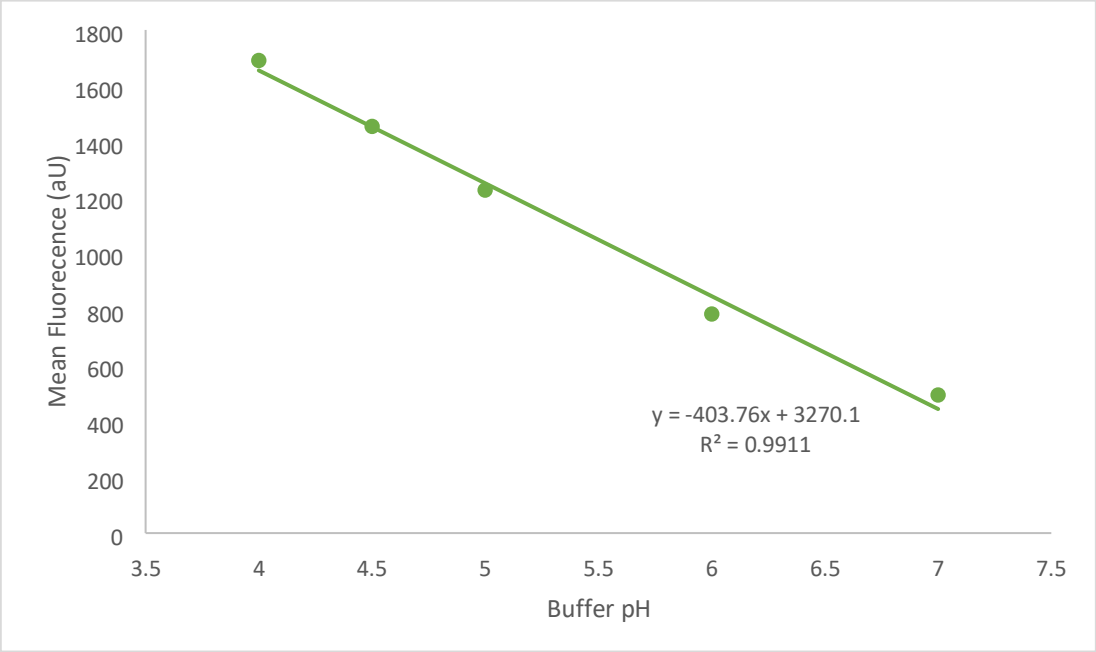

Figure 42. Shows the relationship between LS-160 and standard pH buffers

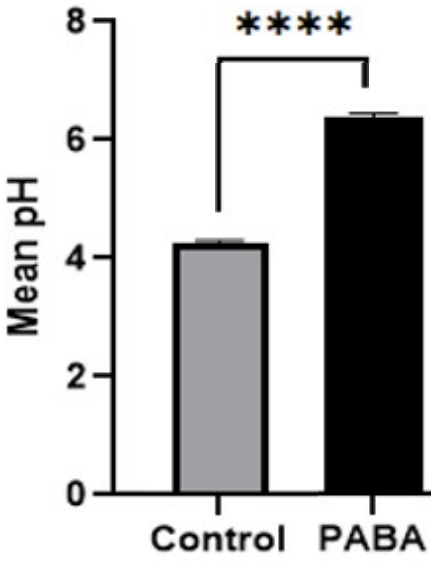

Figure 43. The Effect of CoQ10 deficiency on Lysosomal pH.

*Error bars represent standard error of the mean (SEM); statistical analysis was carried out using T-test; levels of significance: ****: p<0.0005; n=48.*

Additionally, analysis of the BAF treated cells (positive control of lysosomal alkalization) also showed a significant increase in lysosomal pH when compared to the controls with an increase from 4.1 to around 7.1 respectively ($p < 0.05$). It was also found that BAF treatment had a more profound effect on the lysosomal pH than that of the CoQ_{10} deficiency as shown in figure 43.

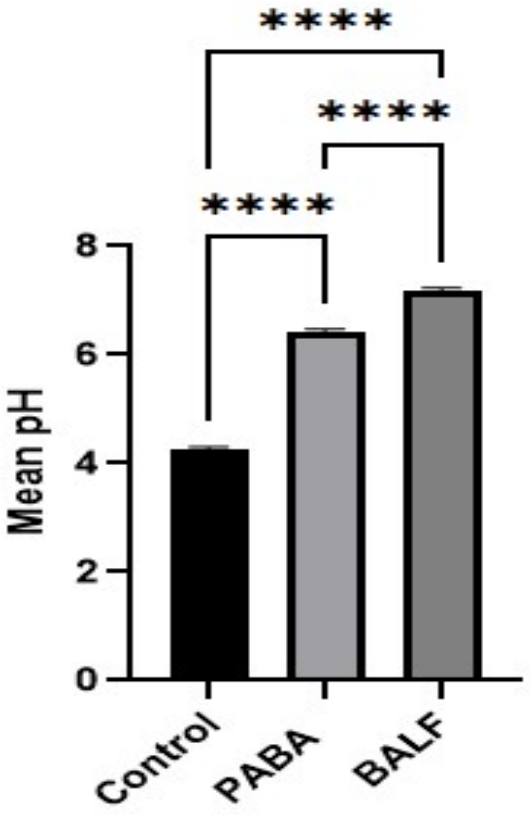

Figure 43. The Effect of CoQ10 deficiency and BAF on Lysosomal pH.

*Error bars represent standard error of the mean (SEM); statistical analysis was carried out using T-test; levels of significance: ****: p<0.0005; n=48.*

22.4.3. Lysosomal mass

To ensure that the results of both the LysoSensor and LysoTracker experiments were not influenced by changes in total cellular lysosomal mass, the senescence assay kit was used to assess changes in the lysosomal enrichment of the cells.

It was found that there was no significant difference between the fluorescence of the control cells (un-treated) and the CoQ_{10} deficient cells (PABA treated) ($p < 0.05$) (figure 44). Although not significant, it was found that there was a slight increase in fluorescence in the PABA treated cells compared to the controls (figure 44).

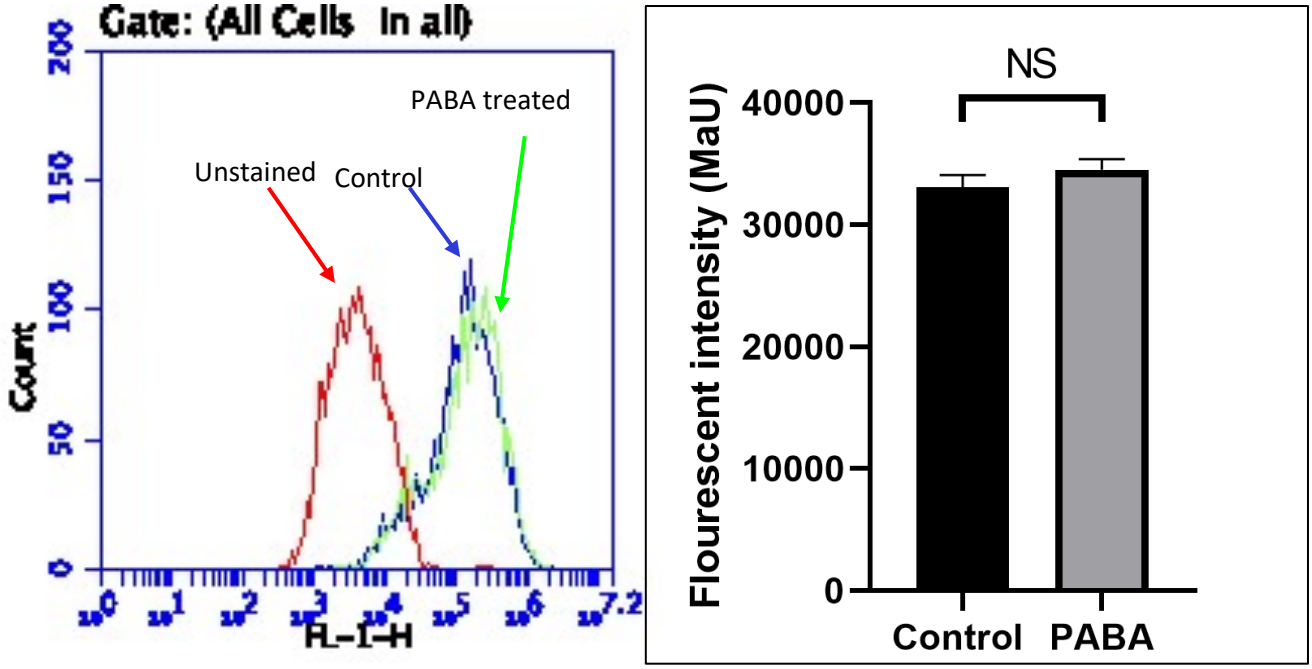

Figure 44. The Effect of CoQ10 deficiency on Lysosomal Mass.

A) represents the florescence shift on the FL -2 detector, shows the cell population significantly increases in fluorescence after staining sowing the cells have successfully been stained. B) shows the median fluorescence pre CoQ10 deficiency (Control) and post (PABA). Error bars represent standard error of the mean (SEM); statistical analysis was carried out using T -test; levels of significance: n=26.

22.4.4. Visualisation of the probes

To assess and ensure that the probes had indeed been taken up by the cells and localised in the lysosome, fluorescent imaging was undertaken using a confocal live imaging microscope.

It was found that the LS-167 probe did not produce images of sufficient quality at X40 (objective) to fully evaluate the uptake of the probe; therefore, future analysis of this probe will be required.

Analysis of the cellular distribution of the LT probe showed a significant uptake by the cells corresponding with the results from the flow cytometer (section 22.4.1) assay. Additionally, it was found that the fluorescence was held in small pockets within the cellular membrane (figure 45); this would indicate that the probe was being held within acidic organelles inside the cell. Importantly, there was minimum fluorescence across the cell outside of these pockets. Visualisation of the control cells (untreated) vs the PABA-treated cells also indicates that PABA itself was not affecting the distribution of the probe. Figure 46 also shows the distribution of the LS-160 probe pre and post PABA treatment. It was found that the LS-160 probe also showed significant uptake into the cells displaying a similar distribution as the LT probe.

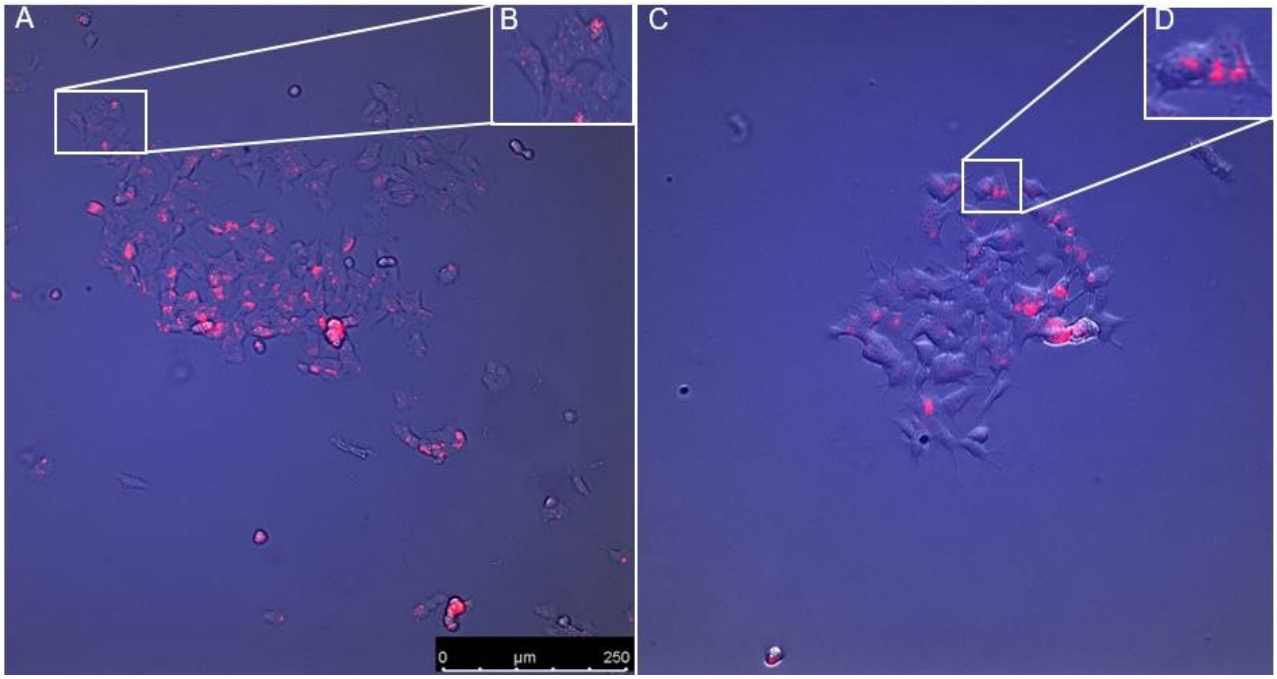

Figure 45. Distribution of the LysoTracker DND-99 probe in both control cells (A) and PABA-treated cells (B).

***C** and **D** show small localisation of LysoTracker in the cells. Suggests that PABA has little to no effect on the cellular distribution of the probe. Images taken using the Leica DMI6000 fluorescent microscope, with the Leica LAS X software, at x40 (objective).*

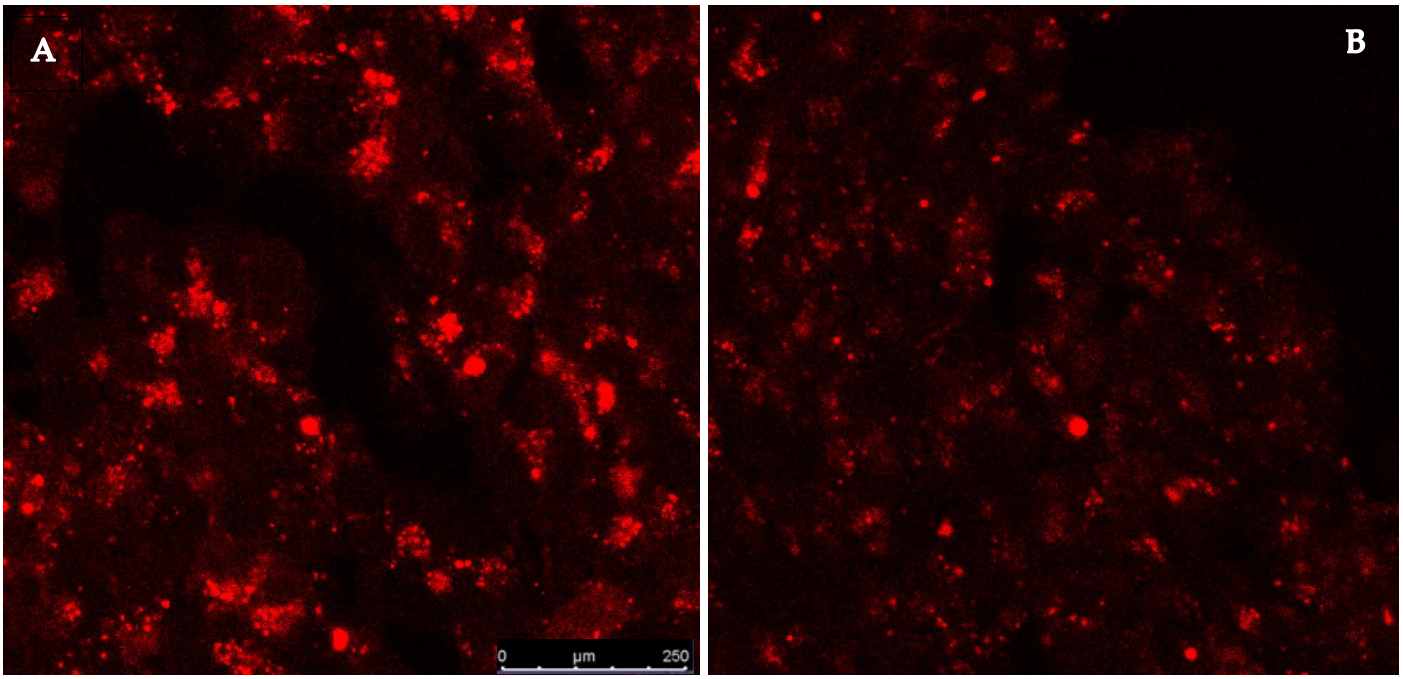

Figure 46. Distribution of the LysoSensor DND-160 probe in both control cells (A) and PABA-treated cells (B).

Images taken using the Leica DMI6000 fluorescent microscope, with the Leica LAS X software, at x40 (objective).

22.5. Discussion

The results of the present chapter have indicated that a 56% decrease in cellular CoQ_{10} status is associated with a rise in lysosomal pH from 4.2 to 6.2 (figure 43). To induce a neuronal cell model of CoQ_{10} deficiency SHS-S5Y cells were treated with PABA – (a competitive inhibitor of the enzyme COQ2). In agreement with the work of Duberley et al. (2013a), treatment of the SHS-S5Y cells with 1mM PABA was found to induce a 56% decrease in cellular CoQ_{10} status which was consistent and reproducible. In this study a treatment period of five days with 1mM PABA was chosen for a number of reasons, firstly, five days was chosen as the reported half-life of CoQ_{10} is around 3.5 days (Turunen et al., 2004). Thus, five days would be enough time for any endogenous CoQ_{10} synthesised prior to treatment to dissipate. Secondly, in the present and in previous studies higher concentrations of PABA and longer periods of incubation have been assessed and found not to induce a further deficit in CoQ_{10} status than that of a 5-day incubation with 1mM PABA CoQ_{10} (Duberley et al., 2013a). A 5-day period of incubation also allows for the normal growth of the cells without becoming overconfluent prior to harvesting.

In this study several probes were used to assess changes in lysosomal pH, LT, LS-167 and LS-160. LT has previously been used in a number of studies in the investigation of lysosomal pH and has proven to be a useful tool in the investigation of the lysosome (Guha et al., 2014, Yamada et al., 2016). The lysotracker probe is made up of a basic amine fluorescent fluorophore (Figure 26), the amine selectively accumulates in the lysosome where the fluorescence is released due to the acidic environment (see section 14.1) (Pierzyńska-Mach et al., 2014). It was found that the reduction in endogenous CoQ_{10} (56% reduction) correlated with a 35% decrease in LT fluorescence using flow cytometry. This decrease in fluorescence was found to reflect an increase in lysosomal pH. Although, the LT probe alone is unable to accurately determine the change in pH;

previous studies have successfully indicated that changes in LT fluorescence can be attributable to a substantial alteration in lysosomal pH. However, with more subtle changes accuracy may be lost making it challenging to determine the exact pH (Guha et al., 2014).

The LS-167 and LS-160 probes are members of the same family of probes as LT utilising a similar method of analysis lysosomal pH whereby, they selectively accumulate in the lysosome due to acidotropic properties. Here the probes are protonated because of the low pH, leading to accumulation in the lysosome. The
protonation also leads directly to the release of fluorescence; fluorescence intensity in this case is a direct result of the pH (Lin et al., 2001) (see section 14.2 and 14.1) Analysis of the LS-167 probe found there was little background fluorescence on the emission wavelength of LS-167 (590nm) in the cells prior to staining. additionally, it was found that when introduced to pH standard solutions the fluorescence intensity changed proportionally to the change in standard solution as shown in figure 40 Consequently, it can be assumed that changes in LS-167 fluorescence can be attributed to lysosomal lumen pH alterations. Analysis of the LS-167 probe sowed significant ($p < 0.005$, 23%) decrease in florescence (Figure 40). Using the standard curve, (Figure 39) it was determined that this change in fluorescence was associated with an average increase in lysosomal pH from 4.1 (control cells) to 6.2 (CoQ_{10} deficient cells).

The LS-160 probe as discussed is a member of the same family as LT and LS-167, however, can be considered to be the most interesting of the three. This is because it is a ratiometric probe, meaning it has two excitation and emission wavelengths (ext. 329, 384: emission. 440, 540). This is particularly useful in determining small changes in lysosomal pH as the dual wavelength properties can be used to ratio alkaline to acidic environments (Lin et al., 2001) (see section 14.3). As with the LS-167 a pH curve was constructed to determine the relationship between LS-160 fluorescence and pH (figure 42), it was determined that there was a strong linear relationship between the fluorescence intensity and thus LS-160 could be used to determine lysosomal pH. Analysis of the LS-160 probe showed an average significant increase in lysosomal pH from 4.2 to 6.3 associated with the neuronal CoQ_{10} deficiency (figure 43).

To ensure the probes had indeed been taken into the cells confocal microscopy was deployed to image the live stained cells. Inspection of Figure 45 shows LT was taken up by the cells and had been localised in small pockets within the cytoplasm. Following the data provided both by the manufacturer (Thermo Fisher) and previous studies, it is not unreasonable to assume that this localisation of the probe is within acidic organelles, such as the lysosome. Multiple attempts were made to image the LS167 probe but to no avail with no clear images of the probe being available. A possible reason for this could be the use of insufficient magnification or the probes excitation being out of range of the laser on the confocal microscope. As a result of this, more studies will be required to image this probe to ensure the increase in cellular fluorescence is indeed due to the uptake of the probe. into the lysosome.

As a result of the accumulative nature of the fluorescent probes used, it was important to exclude changes in lysosomal mass as a contributor to the increase in pH determined in the CoQ_{10} deficient neuronal cells. In order to do this the senescence assay kit was used to measure changes in the lysosomal enzyme β-gal (a lysosomal marker enzyme). It was found that a CoQ_{10} deficiency was not associated with any significant decrease in β-gal activity compared to the control (Figure 44). This would suggest that the neuronal CoQ_{10} deficiency was not associated with any significant decrease in lysosomal mass. Interestingly however, there is a slight increase in the fluorescent intensity of CoQ_{10} deficient cells (PABA treated, figure 45). This could be a result of some lysosomal swelling due to increased storage of undigested material, however more information is required to confirm this hypothesis.

To confirm the ability of LS-160 to accurately measure lysosomal pH the BAF inhibitor of V-ATPase activity was used to induce lysosomal alkalisation. BAF is a strong inhibitor of the lysosomal V-ATPase and has been previously reported to cause significant lysosomal lumen alkalisation (Yamamoto et al., 1998, Halcrow et al., 2019). In this study we found that treatment with BAF was associated with a significant decrease in LS-160 mean fluorescence, which suggested an increase in lysosomal lumen pH from 4.1 to 7.1 (figure 44). This finding corresponds to previously reported changes in lysosomal pH post BAF treatment (Klionsky et al., 2008). In addition to

further solidifying the finding that the impairment of the V-ATPase leads to alkalisation of the lysosomal lumen. This result also shows that the probes used in this study appear to be able to accurately determine alterations in lysosomal pH. Interestingly, this finding may also indicate that the V-ATPase plays a more significant role in the acidification of the lysosome compared to the LETC (Colacurcio and Nixon, 2016). However, a more severe CoQ_{10} deficiency will be needed to assess the comparability of the two results.

As previously discussed, the lysosome plays a pivotal role in normal cellular homeostasis. These organelles have been reported to contain > 50 different hydrolytic enzymes that are designed to digest a myriad of cellular waste products such as proteins, DNA, RNA, polysaccharides and lipids (Figure 8) (Aronson and de Duve, 1968, Wartosch et al., 2015, Thelen and Zoncu, 2017). For these enzymes to work at optimum activity, they require an acidic pH (between 4 and 5). Previous studies have reported that changes in lysosomal pH may be protagonists in the progression of diseases, with de-acidification specifically being associated with the pathogenesis of LSDs (Folts et al., 2016, Parkinson-Lawrence et al., 2010).

In a study by Coffey et al. (2014) it was found that lysosomal alkalization (an increase of 0.2 - 0.3 pH units) was associated with a pathologic build-up of partially degraded material and bloated lysosomes. Thus, the acidification the lysosome is imperative for maintaining its function and in turn cellular homeostasis (Ishida et al., 2013). Currently, the primary focus of the preponderance studies on CoQ_{10} deficiency have been upon its effects on mitochondrial function (Ben-Meir et al., 2015, Shults et al., 2002) However, given the reported high concentration of CoQ_{10} in the lysosomal fraction of the cell (Turunen et al., 2004)and its ability to navigate freely through membranes both in its oxidized and reduced state this study attempted to investigate how CoQ_{10} deficiency may impact the lysosomal lumen pH, which has yet to be explored outside of this study.

The cause of the increase in lysosomal pH associated with a CoQ_{10} deficiency in the present study is yet uncertain but may result from an impairment of the LETC as well

as a loss in activity of the V-ATPase. The results from the positive control (BAF treated cells) show that the lysosomal pH can be significantly increased due to inhibition of the V-ATPase proton translocators and as such, it would not be irrational to suggest that a CoQ_{10} deficiency may deprive the V-ATPase of ATP significantly reducing its efficiency. Additionally, given the reported role of CoQ_{10} in the LETC, a CoQ_{10} deficiency would also be expected to impede the flow of protons in the lumen of the organelle via the reduced activity of the LETC.

22.6 Conclusion

The results from the study outlined in this chapter have indicated that a cellular CoQ_{10} deficiency has the potential to increase lysosomal pH which may impair the function of the organelle. Therefore, the possibility arises that lysosomal dysfunction may contribute to the pathophysiology of diseases associated with CoQ_{10} deficiency.

23. Cellular CoQ10 deficiency and its effects on mitochondrial metabolism

23.1 Introduction

CoQ_{10} deficiency currently represents the only treatable disorder of the METC, and can have quite a heterogeneous clinical presentations which can be divided into five distinct phenotypes: encephalomypathy, severe infantile multisystemic disease, nephropathy, cerebellar ataxia, and isolated myopathy (Yubero et al., 2014). A primary CoQ_{10} deficiency is an inherited autosomal recessive disease, and has been associated with mutations in ten of the CoQ_{10} biosynthetic pathway genes: *PDSS1 and PDSS2 (*López et al., 2006, Mollet et al., 2007*), COQ2* (Mollet et al., 2007), *COQ4 (Salviati et al., 2012), COQ6* (Heeringa et al., 2011), *COQ7 (Hashemi et al., 2021), COQ8A/B (Liu et al., 2020), COQ9* (Duncan et al., 2009), and *ADCK3* (Mollet et al., 2008).

A number of studies have indicated that the development of neurological dysfunction is a common clinical feature associated with a CoQ_{10} deficiency (Emmanuele et al., 2012b, Quinzii et al., 2014). Rötig et al. (2000) described three siblings whom, shortly after birth presented with neurological symptoms such as: optic atrophy, sensorineural hearing loss, ataxia, dystonia, weakness, and rapidly progressive nephropathy. These symptoms were associated with a profound CoQ_{10} deficiency (4 nmol/g protein) compared to controls (29 nmol/g protein) in patient cultured fibroblasts, associated with a mutation in the *PDSS2* gene (Rötig et al., 2000). Rahman et al. (2001) reported a male neonate whom after displaying a number of nonneurological symptoms developed severe seizures and dystonia; MRI of his brain showed cerebral and cerebellar atrophy. The patient died at two years of age following a period of intercurrent infection. Post-mortem gene mapping revealed a mutation in the *COQ9* gene. Quinzii et al. (2006) reported a patient with a mutation in the *COQ2* gene, with the first patient displaying symptoms of severe nephrotic syndrome and mild psychomotor delay at twelve months old. MRI of his brain revealed cerebral and

cerebellar atrophy and stroke-like lesions (Quinzii et al., 2014).

In most cases, treatment of CoQ_{10} deficient patients with CoQ_{10} supplementation may improve their clinical symptoms. However, whilst symptoms relating to muscle issues and other non-neurological issues can improve significantly, neurological symptoms appear to be refractory to treatment in some cases (Rahman et al., 2001). A review by Emmanuele et al. (2012b) stated that whilst around 79% of non-neurological symptoms are alleviated by CoQ_{10} treatment, only 46% of neurological issues are responsive to supplementation. Currently, the exact reason for this discrepancy in treatment response is unknown; thus it is important to understand how a CoQ_{10} deficiency may impact upon neuronal function.

As previously alluded to, one of the mitochondria's most prominent roles is to produce ATP, the energy currency of the cell and for this reason this organelle is often dubbed "the powerhouse of the cell" (Siekevitz, 1957). The Mitochondrion is the site of both the tricarboxylic acid (TCA) cycle as well as the ETC, the latter utilising oxidative phosphorylation (OXPHOS). This is the process by which ATP can be created by ATP synthase (complex V) from ADP and inorganic phosphate (Pi), utilising the proton gradient formed across the inner mitochondrial membrane as the result of electron passage in the ETC (Chen, 1988). Yet, impairment to mitochondrial function and health can affect biological processes far beyond just changes in cellular ATP status; in fact, the idea that mitochondria were just the powerhouses of the cell was debunked when a study by Liu et al. (1996) showed that the release of cytochrome c from the organelle was able to mediate apoptosis. Given the complex nature of mitochondria, damage or impairment to this organelle can manifest itself within the cell in several different ways (Beal, 1998, Castellani et al., 2002, Exner et al., 2012, Kasote et al., 2013, Pessayre et al., 1999, Trifunovic and Larsson, 2008).

For example, alterations in mitochondrial homeostasis can cause an increase in mitochondrial ROS (mtROS) generation, or even result in a loss of mitochondrial membrane potential ($\Delta\Psi_m$), both having specific downstream signalling effects on cellular homeostasis (Sena and Chandel, 2012). Since, mitochondria are a major site of ROS production within the cell they are also susceptible to oxidative damage which

can cause mtDNA mutations and result in specific downstream signalling, leading to cell death (Scheibye-Knudsen et al., 2015). Another example of how the mitochondria can affect cellular function is through calcium signalling. The mitochondria are able to rapidly take in and store free calcium ions (Ca^{2+}) from the cytosol (Rossier, 2006). Ca^{2+} itself is extremely important in cell signalling and uptake or release of Ca^{2+} in response to changes in mitochondrial membrane potential can lead to changes in cellular homeostasis (Santulli et al., 2015, Miller, 1998). One example of how Ca^{2+} can influence cellular homeostasis is in programmed cell death (PCD); increased cytoplasmic Ca^{2+} concentrations lead to accumulation of Ca^{2+} in the mitochondria, under oxidative stress conditions mitochondrial Ca^{2+} accumulation leads to cell death signalling (Ermak and Davies, 2002). Additionally, study by Stout et al. (1998) found that the inhibition of mitochondrial Ca^{2+} uptake during stress conditions (glutamatestimulated cells) prevented cell PCD. This suggests that mitochondrial Ca^{2+} uptake
may be a necessity for PCD in some stress conditions (Stout et al., 1998).

Interestingly, in recent years several studies have reported significant cross talk between the mitochondria and lysosomes, suggesting changes in the homeostasis of one of these organelles can lead to changes in the other. For example, TFAM is a protein essential in the transcription of mtDNA, providing stability and protection to mtDNA not dissimilar to histones and DNA (Bonawitz et al., 2006). A study by Baixauli et al. (2015) reported that in lymphocytes without the TFAM genes, lysosomal number was significantly increased, however, their pH was higher than the wild type cells (less acidic) and thus their function may have been significantly impaired (Baixauli et al., 2015). It was suggested that the increase in lysosomal number was due to the activation of Transcription Factor EB (TFEB), which was found to be a regulator in lysosomal biogenesis. However, it was not addressed as to why this leads to dysfunctional lysosomes. In another study by Nezich et al. (2015) the effect of mitophagy on lysosomal biogenesis was explored by inducing myopathy in cell culture. The study found that after myopathy was induced, TFEB relocated into the nucleus, presumably for transcriptional activation (Nezich et al., 2015). The relocation of TFEB to the nucleus correlated with an increased in lysosomal biogenesis along

with mitochondrial biogenesis. Another study by Ivankovic et al. (2016) also assessed the effect of mitophagy on lysosomal biogenesis and found that TFEB accumulation in the nucleus resulted in increased lysosomal biogenesis, along with comparable mitochondrial biogenesis. Demers-Lamarche et al. (2016) reported that in PINK1 knock out (PINK1 KO) neurons both mitochondrial and lysosomal function were impaired. The PINK1 gene is responsible for protecting cells from mitochondrial dysfunction by causing the parkin protein to bind to depolarised mitochondria leading to mitophagy of the damaged mitochondria (Poole et al., 2008). DemersLamarche et al. (2016) found that in cells with this gene removed (PINK1 KO cells) not only was mitochondrial function impaired, but also lysosomal acidification was also negatively affected, and the lysosomal protease cathepsin B activity was significantly reduced. Interestingly, this was found to increase total lysosomal number, but as with the previous studies, these lysosomes were swollen and dysfunctional (DemersLamarche et al., 2016).

PABA has previously been used to induce a CoQ_{10} deficiency in cell culture (Duberley et al., 2014, Duberley et al., 2013b). Originally devised in 1975 by Alam et al. (1975) this method works through the competitive inhibition of COQ_{10}; specifically PABA competes with the enzyme, para-hydroxybenzoate for the active site of polyprenyl4-hydroxybenzoate transferase in the CoQ_{10} biosynthesis pathway (Alam et al., 1975) (figure 9.4). As previously shown (section 22) PABA is able to significantly reduce (up to 58% reduction) endogenous CoQ_{10} concentrations in cells.

As previously discussed in section 5 the lysosome has multiple mechanisms in order to transport protons into the lumen of the organelle and against a concentration gradient, to maintain the acidic environment required for optimal functioning of the lysosome (figure 8). One of these methods involves the lysosomal V-ATPase which is found on the lysosomal membrane (figure 9). The V-ATPase closely resembles the ATPase found in the METC, although the V-ATPase uses the energy liberated from the hydrolysis of ATP to pump protons into the lumen of the organelle (figure 9). In addition to the V-ATPase, the lysosomal electron transport chain (LECT) also contributes to the maintenance of lysosomal acidity via its proton transporting

capacity (Gille and Nohl, 2000). In the LETC CoQ_{10} plays a significant role in the movement of electrons across the membrane (figure 10), thanks to its ability to cycle through the REDOX states so readily in addition to functioning as a proton carrier (Gille and Nohl, 2000).

Given the plethora of information showing that lysosomal function is extensively linked to mitochondrial health (Baixauli et al., 2015, Demers-Lamarche et al., 2016, Ivankovic et al., 2016) it would be prudent to assess whether the increase in lysosomal pH observed following PABA treatment, induced cellular CoQ_{10} deficiency (see section 22.4.1) can be attributable to an impairment in METC, or whether it is directly linked to deficit in cellular CoQ_{10} status.

The lysosome requires a source of ATP in order for the V-ATPase to be able transport protons into the lysosomal lumen (Brown and Breton, 2000). Consequently, the lysosomal pH may be influenced by changes in cellular ATP availability. During "normal" homeostasis the mitochondria is the main source of ATP producing 36 ATP molecules per glucose molecule when compared to glycolysis, which only produces two (Yetkin-Arik et al., 2019). Given CoQ_{10}'s role in the METC it would be reasonable to assume that a PABA induced cellular CoQ_{10} deficiency would be expected to deprive the cell of ATP which may impact on the activity of the V-ATPase reducing the import of protons into the lysosome. Additionally, impairment of the METC may also result in an increase in OS (Ott et al., 2007). this increase in OS may lead to damage of the lysosomal membrane, as previously discussed in section 5 the lysosome is particularly sensitive to changes in OS concentration.

23.2 Aims

In order to fully investigate if the effect on the lysosomal pH is exclusively due to cellular CoQ_{10} concentration aberrations, we have investigated the effect of the PABA induced CoQ_{10} deficiency on general mitochondrial health and cellular growth. Following induction of neuronal CoQ_{10} deficiency mitochondrial function and number was investigated via the assessment of total cellular ATP, total cellular ROS assessment, CS activity, and the fluorescent mitochondrial probes JC-1 and MTG.

1. Assessing whether a deficit in CoQ_{10} deprives the cell of ATP.
2. Determining whether because of a CoQ_{10} deficiency there is an increase in cellular oxidative stress.

23.4 Methods

23.4.1. Cell culture

SH-SY5Y cells were grown and maintained as described in Section 9 all CoQ_{10} concentration assessments were carried out in T75 cell culture flasks.

23.4.2. PABA treatment

cells were subject to a single 1mM PABA treatment over a 5-day period, as outlined in section 9.4.

23.4.3. Quantification of cellular CoQ_{10} Concentration

Cellular CoQ_{10} was extracted, and concentration was calculated using reverse phase HPLC with a C18 column, as described in sections 11 and 11.3.

23.4.4. Assessment of cell viability

Flow cytometry assessment of cell viability after PABA treatment was carried out as outlined in section 12.

23.4.5. Total protein assessment

The total protein of the cells was determined using an adapted version of the Lowry method, as outlined section 10.

23.4.6. Cellular ATP assessment

The total cellular ATP concentration was carried out using the Cell Titer-Glo assay as outlined in section 16.

23.4.7. Mitochondrial membrane potential assessment

Mitochondrial membrane potential changes were assessed by the fluorescent probe JC-1 using flow cytometry, as outlined in section 18.

23.4.6. Mitochondrial membrane mass assessment

Total mitochondrial membrane protein concentration was assessed by deployment of the fluorescent probe Mitotraker Green using flow cytometry, as outlined in section 17.

23.4.7. CS activity

The activity of the mitochondrial enzyme citrate synthase was also measured as a marker of mitochondrial enrichment. This was done using a spectrophotometer method as set out in section 19.

23.4.8. Cellular ROS concentration assessment

Total cellular ROS was assessed using the fluorescent probe using flow cytometry, as outlined in section 15.

23.4.9. Statistical analysis

Statistical analysis was carried out as outlined in section 22.

23.5 Results

23.5.1 COQ_{10} concentration

The result of this study found that post PABA treatment cellular CoQ_{10} status was significantly decreased ($p< 0.005$), when compared to the controls (untreated cells) after a five-day incubation with 1mM PABA. Results show that 1mM PABA induced a maximal 58% decrease in cellular CoQ_{10} (Figure 36), this result is comparable to those reported by Duberley et al. (2013a). Additionally, it was found that higher concentrations of PABA did not lead to a further decrease in CoQ_{10} status (2mM, 56% decrease). As a result of this it was deemed that 1mM PABA would be suitable for this study.

23.5.2 Cellular viability

Two different cellular viability assays were deployed in this experiment in order to assess the effect of a CoQ_{10} deficiency on neuronal cellular viability. The results of the PI experiment show that a CoQ_{10} deficiency did not significantly reduce overall cell viability ($P < 0.05$, $N = 21$) as shown in figure 47. Additionally, figure 48 shows the relationship between PI fluorescence and cell death induced by hydrogen peroxide (H_2O_2), as a positive control for cellular death. Figure 49 also shows the data obtained from the flow cytometry experiment showing how the cellular fluorescence changes over time when cells were killed using H_2O_2 1mM.

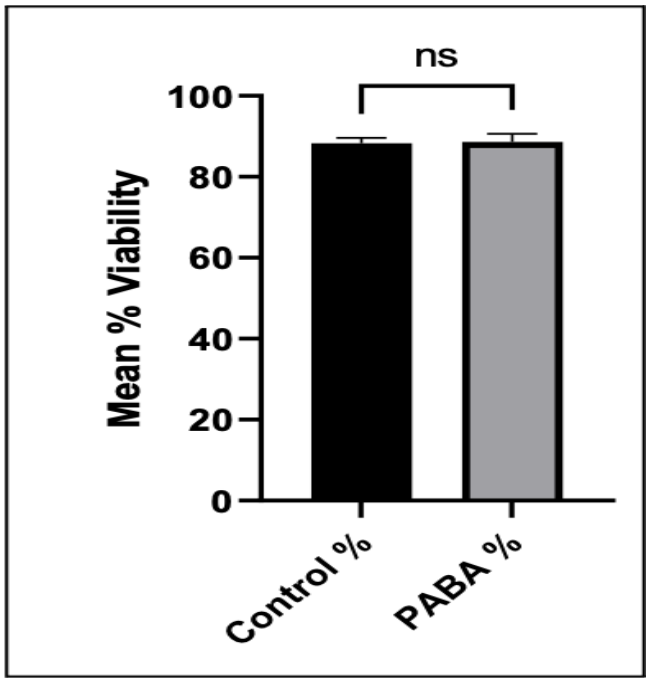

Figure 47. Mean Cellular Viability Post PABA Treatment determined via PI.

Error bars represent standard error of the mean (SEM); statistical analysis was carried out using a t test; N = 21.

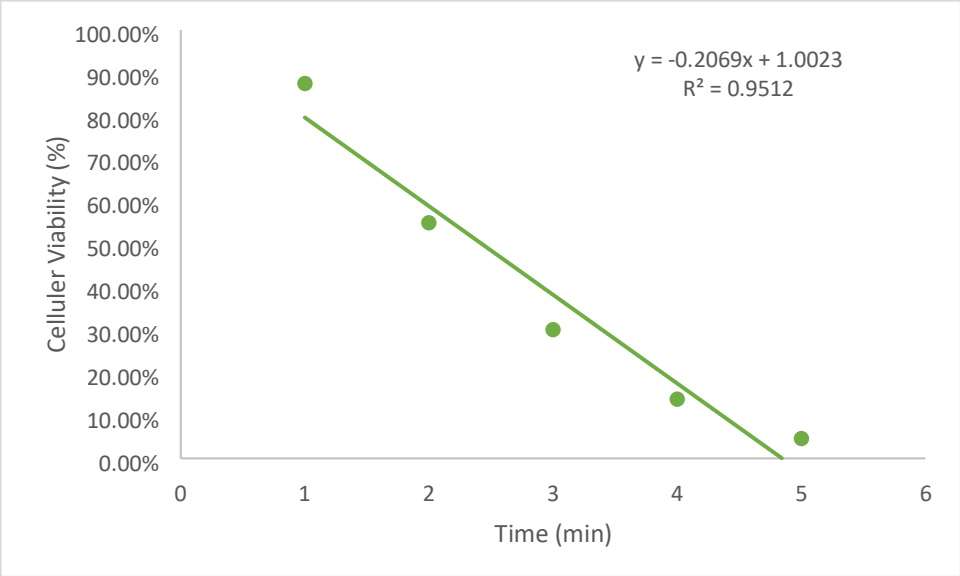

Figure 48. Shows cellular death Vs incubation time with H2O2.

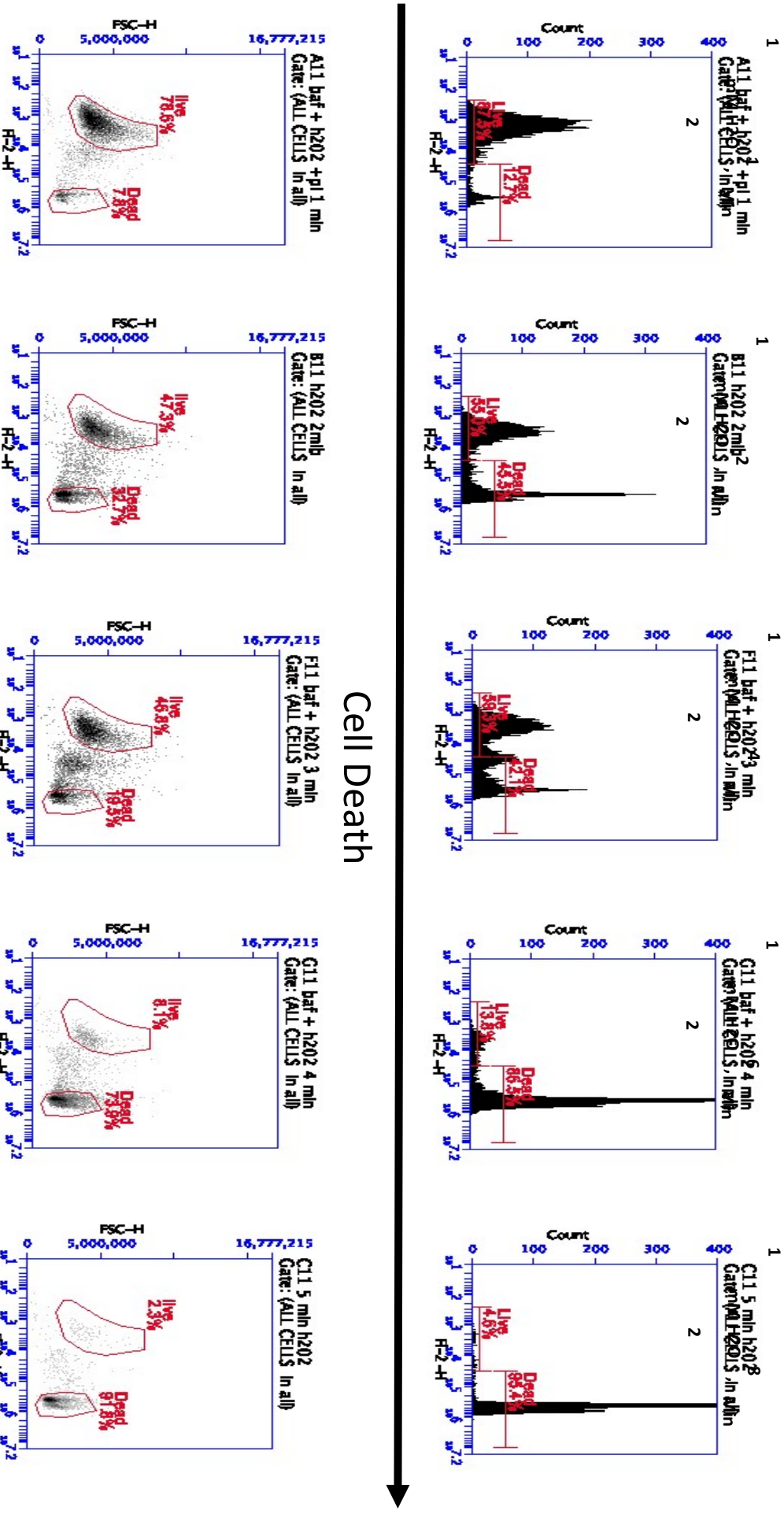

Figure 49. Shows the relationship between PI fluorescence and cellular death.

23.5.3 Cellular Growth

Total protein concentration of cellular culture was determined to investigate how PABA treatment affected cellular growth over time. Results in figure 50 show that cellular growth was unaffected by the decrease in CoQ_{10} status over the five-day treatment with 1 mM PABA.

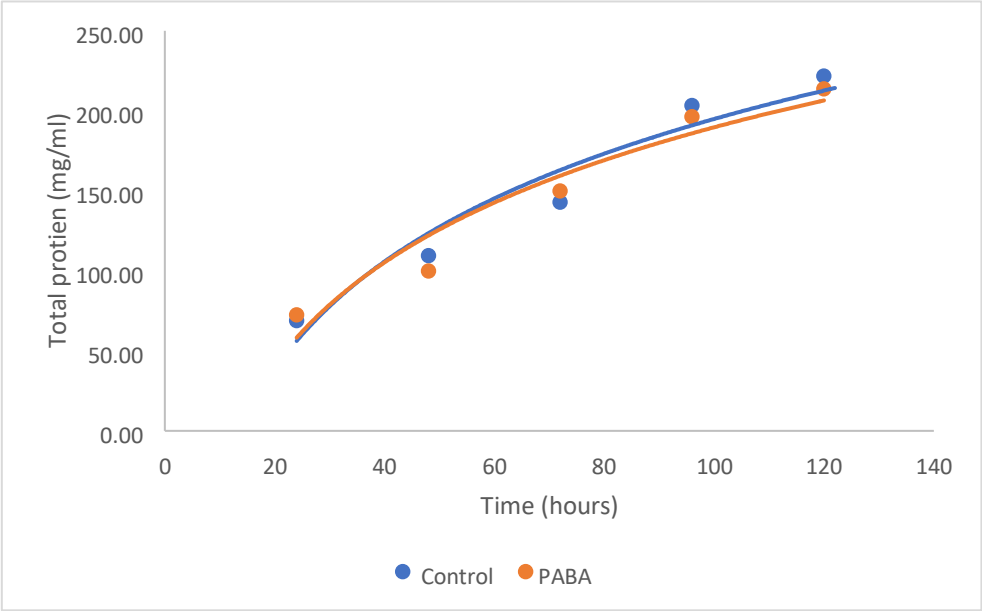

Figure 50. Shows Total Protein concentration over five-day treatment with PABA.

23.5.4 Mitochondrial membrane potential Δψm

23.5.4.1 JC-1

Mitochondrial membrane potential (Δψm) was measured using the probe JC-1 as discussed previously. It was found that there was no change in cellular fluorescence pre or post PABA treatment, suggesting no interference with the assay was caused by the PABA treatment itself. Figure 51 Shows raw data obtained from flow cytometry, showing little to no change in fluorescent peaks on FL-1, in the same population of cells against FSC and SSC. Figure 54 shows a significant increase population fluorescence intensity that is associated with JC-1 staining, showing significant uptake of the probe. It was found that there was no significant difference ($P = 0.876$, $N = 12$) in the median fluorescence between PABA (1mM) treated cells and control cells

(figure 52).

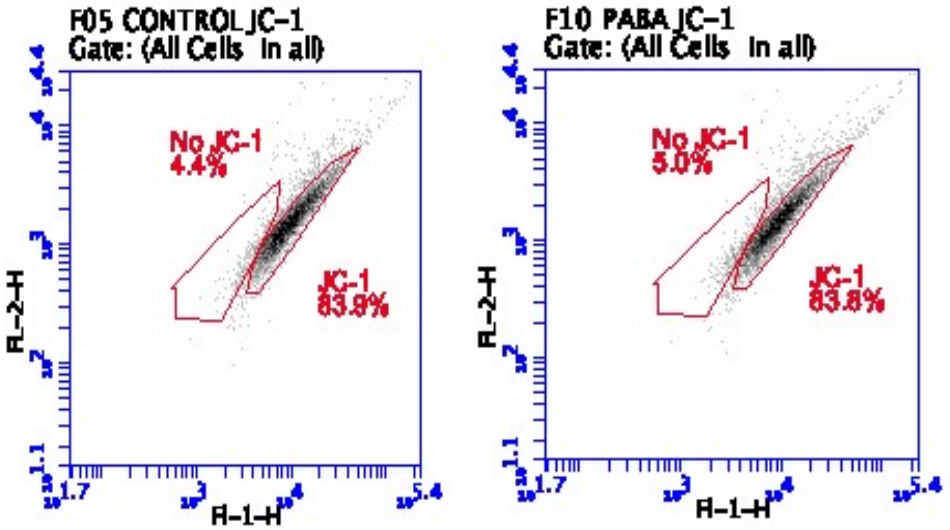

Figure 51. Shows FL-1 vs FL-2 Data for JC-1 staining in both control and PABA treated cells.

Data shows how there is no change in the population fluorescence pre and post PABA treatment, suggesting there is no significant alterations in $\Delta\psi m$.

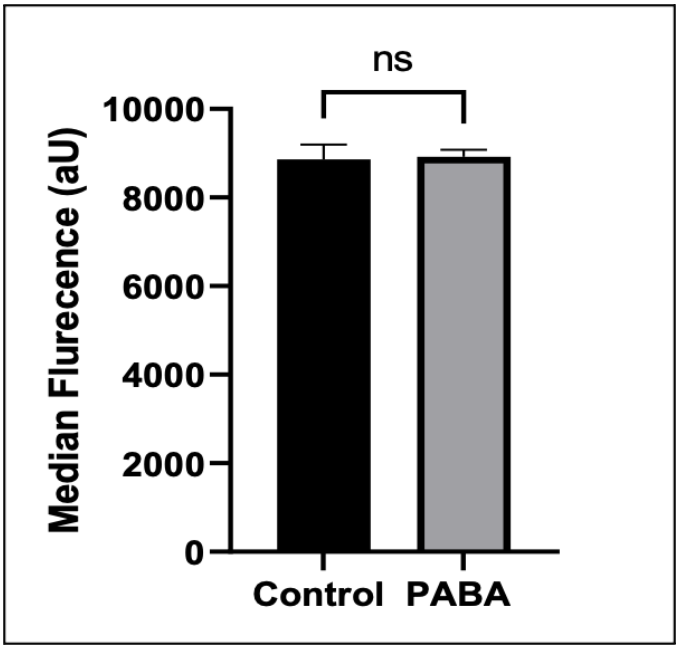

Figure 52. Median cellular FL-1 fluorescence of JC-1.

Error bars represent standard error of the mean (SEM); statistical analysis was carried out using a t test; N = 12.

23.5.5 Mitochondrial mass

23.5.5.1 MTG

Total cellular mitochondrial mass was determined using the flow cytometry probe MTG. It was found that there was no change in cellular fluorescence pre or post PABA

(1mM) treatment suggesting no interference with the assay. Results show that PABA did not significantly affect the total cellular mitochondrial mass (Figure 53).

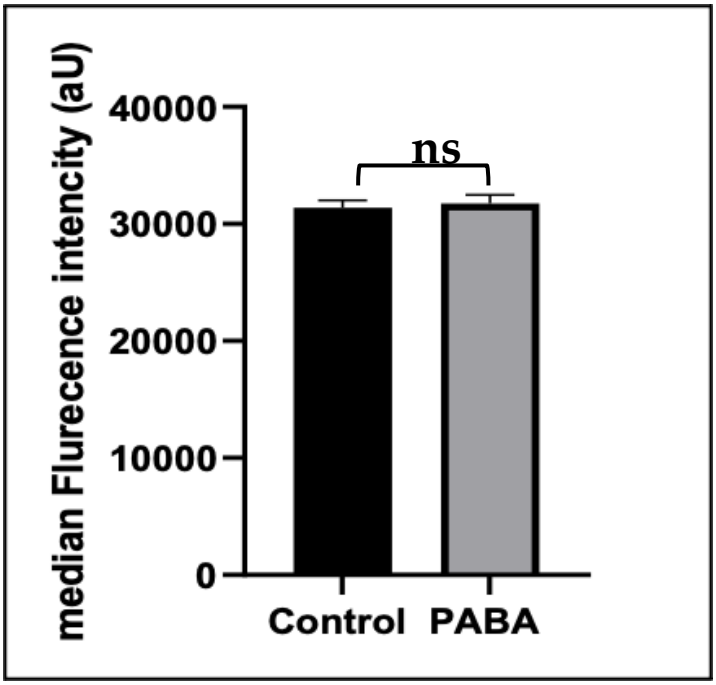

Figure 53. The effect of CoQ10 deficiency on Median MTG fluorescence.

Error bars represent standard error of the mean (SEM); statistical analysis was carried out using a t test; N = 12.

23.5.5.2 CS Activity

As an additional measurement of mitochondrial enrichment/ depletion, CS activity was assessed as described in section 19 analysis of CS activity found that there was a significant increase in CS activity post treatment with PABA (1mM) (29%, $p<0.005$, figure 54). This suggests that PABA induced CoQ_{10} deficiency leads to an amelioration of mitochondrial mass.

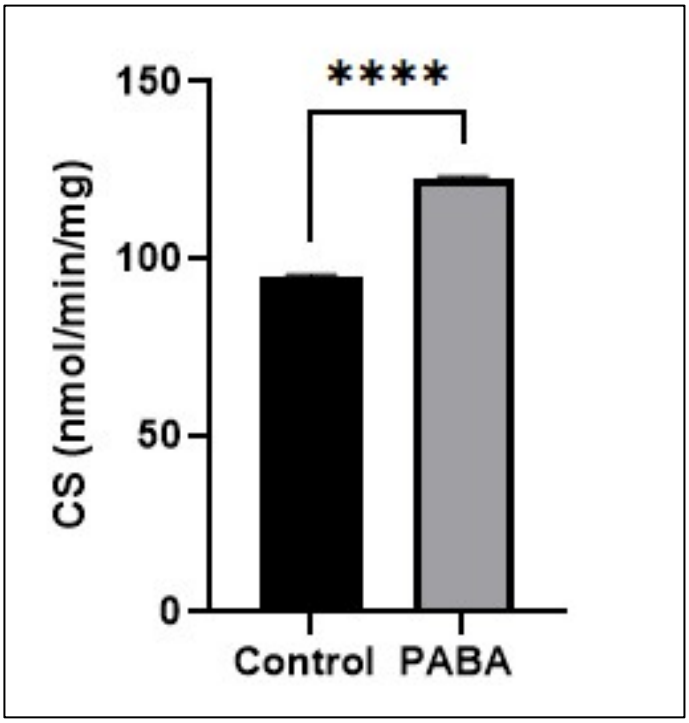

Figure 54. The effect of CoQ10 deficiency on mean CS activity.

*Error bars represent standard error of the mean (SEM);statistical analysis was carried out using a t test; ****:p<0.0005; N = 12.*

23.6 Cellular ATP concentration

Results show that the decrease in cellular CoQ_{10} concentration can be associated with a significant decrease in total cellular ATP concentration (P <0.0005, N = 30) (figure 55). It was observed that the decrease in cellular CoQ_{10} concentration led to a 15% decrease in cellular ATP concentration (figure 55).

Figure 31 shows the linear relationship between luminescence and ATP concentration used to calculate the cellular ATP concentration. ATP results were normalised to a protein bassline as shown as with CoQ_{10} concentration data (section 11.4).

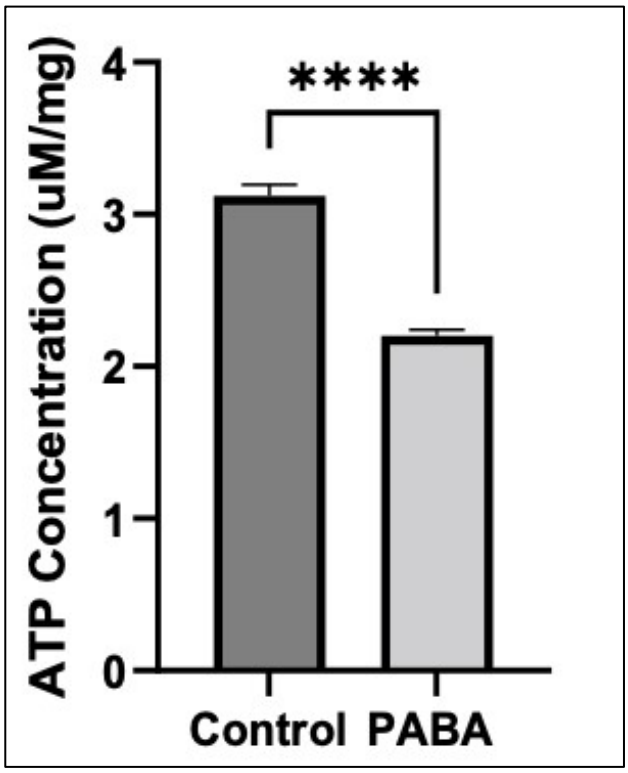

Figure 55. The effect of PABA on mean cellular ATP concentration.

*Error bars represent standard error of the mean (SEM); statistical analysis was carried out using a t test; ****: p<0.0001, N = 30.*

23.7 Cellular ROS

Given the antioxidant role of CoQ_{10} and the reported lysosomal sensitivity to changes in cellular ROS, it was prudent to assess changes in cellular ROS. This was undertaken using the probe CM-H2DCFDA. Oxidation of this probe leads to the entrapment of a fluorescent molecule leading to an increased cellular fluorescence proportional to the cellular concentration of ROS (Ameziane-El-Hassani and Dupuy, 2013). In this study it was found that PABA treatment was associated with a one-fold increase in cellular fluorescence, indicating a significant increase in cellular ROS concentration (figure 56). Figure 29 also shows the relationship between cellular ROS brought about by increasing concentrations of hydrogen peroxide and population fluorescence.

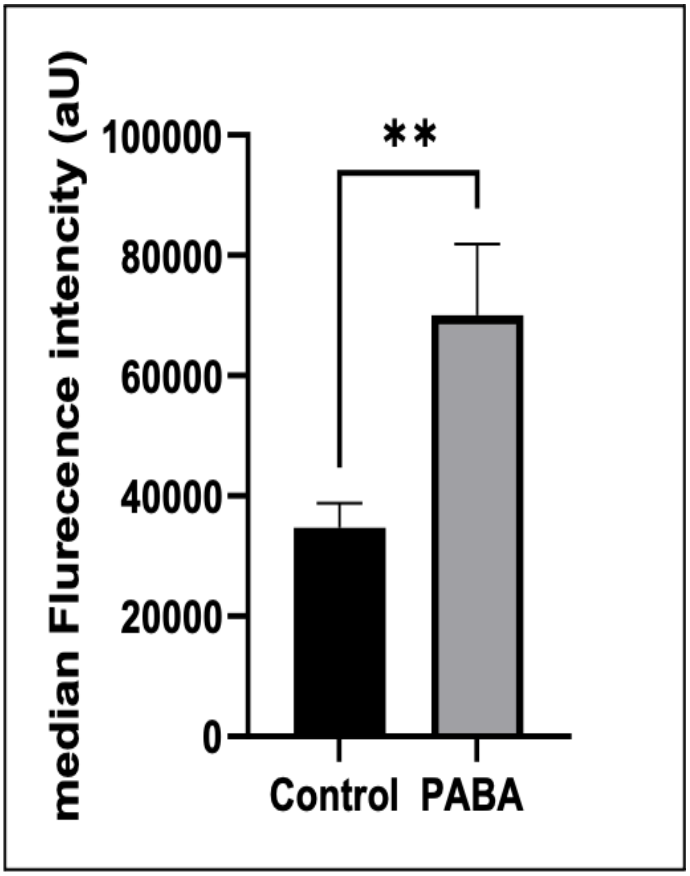

Figure 56. The effect of PABA on cellular ROS concentration.

*Error bars represent standard error of the mean (SEM); statistical analysis was carried out using a t test; **: p<0.005, N = 39.*

23.8 Discussion

In order to fully elucidate the mechanism responsible for the increase in lysosomal pH associated with a CoQ_{10} deficiency, it is important to assess the impact of this deficit in CoQ_{10} status upon mitochondrial function together with cellular ROS generation. Both lysosomal and mitochondrial function have previously been shown to be interconnected, thus affecting one may lead to changes in the other (Wong et al., 2018, Deus et al., 2020).

Cellular viability is an important measurement of how a treatment is affecting cellular health. This study deployed two assays to assess cellular viability, the more commonly used MTT assay and the dye exclusion PI experiment. The MTT experiment described in section 13, is a colorimetric assay measuring the activity of the mitochondrial enzyme NAD(P)H and is often considered the "gold standard" for cellular viability

assessment. However, in this study it was felt that given that PABA may be indirectly interfering with the METC, meaning any results obtained using MTT may not be reliable. Due to this, the current study focused on another cell viability probe PI. The results from the PI experiment show no significant difference in cellular viability in PABA treated cells when compared to the control. This suggests that the PABA induced CoQ_{10} deficiency has not significantly impacted cellular viability after the five-day treatment. PI as described in section 13 is a dye exclusion assay and is independent of any cellular processes. The results from both assays indicate that the CoQ_{10} deficiency does not appear to be detrimentally impacting cellular viability and therefore this should not be influencing the results of the study.

In addition to cellular viability, this study assessed the total protein concentration throughout PABA treatment to determine if cellular growth is affected during treatment. The results from the Lowry assay show that cellular growth is unaffected by CoQ_{10} deficiency when compared to controls (Figure 50). This shows that the results found in section 23.5.3 were unaffected by an increases/decreases in cellular mass, thus it can be assumed there is no significant increase/decrease in cellular mass.

MTG is a probe used in the determination of mitochondrial membrane mass; the probe selectively accumulates within the mitochondrial matrix, where it is able to covalently bind to mitochondrial proteins through interacting with free thiol groups of cysteine residues (Presley et al., 2003). Unlike other probes, MTG is known to selectively stain mitochondrial proteins regardless of membrane potential and because of this it can be used to measure total mitochondrial mass (Pendergrass et al., 2004). Results from this study show no significant difference between control and treated cells fluorescence. This suggest that PABA induced CoQ_{10} deficiency does not appear to be causing increased mitophagy or mitochondrial biogenesis during treatment. However, results from the CS study (figure 54) show a significant increase in CS activity ($p < 0.005$). This contradicts the results from the MTG probe as it suggests that mitochondrial enrichment has taken place. Currently there is no solid footing for an explanation for this discrepancy and the results are most likely due to issues with the MTG probe

staining. In a recent study by Doherty and Perl (2017) it was found that while under normal physiological conditions, MTG can accurately determine mitochondrial mass; however, alterations in ROS and reactive nitrogen species (RNS) in the mitochondria itself can alter MTG's accuracy in measuring mitochondrial mass.

This study also deployed the mitochondrial membrane probe JC-1. JC-1 is a lipophilic molecule which is able to enter and accumulate within the mitochondrial membrane, this exhibits a green fluorescence (527nm). However, when under the conditions of the mitochondrial membrane the formation of complexes called J aggregates takes place (Reers et al., 1991). J aggregates exhibit a red fluorescence (590 nm) and formation is dependent on the mitochondrial membrane potential; thus in healthy cells with "normal" mitochondria the probe fluorescence is changed from green to red (Sivandzade et al., 2019). The results show there is no significant difference in JC-1 red fluorescence between control and PABA treated cells (Figure 52). This indicates that the PABA induced CoQ_{10} deficiency does not appear to have impaired the $\Delta\Psi_m$ of the neuronal cells.

In this study, figure 51 shows in comparison how the fluorescent population of cells is unaltered post PABA treatment. The results determined in this study suggest that the mitochondrial membrane potential is not significantly impaired by a PABA induced CoQ_{10} deficiency. Additionally, the MTG results show that there is no significant difference in mitochondrial protein mass post PABA treatment; suggesting that the decrease in CoQ_{10} status does not result from a loss in mitochondrial enrichment (Figure 53). Furthermore, there is no diminution in mitochondrial number following a PABA induced CoQ_{10} deficiency. The results from both the JC-1 and MTG assays together with the results from the cell viability assays suggest that the PABA induced CoQ_{10} deficiency does not appear to be significantly affecting mitochondrial function and/or cellular homeostasis.

This study also investigated the effect of the reported CoQ_{10} deficiency on total cellular ATP concentration which was assessed using the Cell-titer Glo Assay kit. The assay

utilises the ATP dependent conversion of luciferin to oxyluciferin, as described in section 16 a buffer solution was added to induce apoptosis and release endogenous ATP; the ATP along with Mg2+ can then facilitate the enzyme luciferase (figure 30) (Hannah et al., 2001). Given the reaction is dependent on the presence of ATP and only the product of the reaction oxyluciferin is luminescent, we can assume the luminescence produced is directly proportional to the concentration of ATP as shown in the concentration curve in figure 31 (Conti et al., 1996). Previous to this study, a study by Duberley et al. (2013a) had reported that a CoQ_{10} deficiency is associated with a significant decrease in cellular ATP concentration. This corresponds to the results observed in the present study where it was observed that the PABA induced CoQ_{10} deficiency resulted in 15% decrease in total cellular ATP (Figure 55). This decrease in cellular ATP concentration was not found to be significant enough to effect cell viability (Figure 47). Additionally, Duberley et al. (2013a) similarly reported no effect of a CoQ_{10} deficiency on cellular growth in SHS-5Y neuroblastoma cells. In view of this, the 15% decrease in cellular ATP level may not be sufficient to impair "normal" cellular processes.

Furthermore, given previous evidence of the lysosome's susceptibility to ROS induced organelle dysfunction (Kurz et al., 2008) an assessment was made on the effect of a PABA induced CoQ_{10} deficiency on total cellular ROS levels. This study deployed the fluorescent probe CM-H_2DCFDA. CM-H_2DCFDA passively diffuses into the cell where it is cleaved by cellular esterase's, rendering it unable to leave (Oparka et al., 2016). In it reduce form, CM-H_2DCFDA is non-fluorescent, however, when oxidised by cellular ROS it is converted into the fluorescent 2', 7'- dichlorofluorescein (DCF) (Ameziane-El-Hassani and Dupuy, 2013). Thus, an increased fluorescence corresponds to an increased cellular concentration of ROS. The fluorescence of this probe was assayed using Flow cytometry, allowing for the assessment of individual cell populations including dead/dying and healthy cells as shown in figure's 22 and 49. The results from this study show significantly increased cellular fluorescence in CoQ_{10} deficient cells (PABA- treated) (Figure 56), indicating an increase in cellular ROS concentration. This result corresponds to findings in previous studies (Duberley et al.,

2013b) and given CoQ_{10}'s role as an antioxidant, this result was to be expected. Furthermore, as discussed, it has previously been reported that the lysosome is susceptible to changes in cellular ROS concentration (Kurz et al., 2008). Kurz et al. (2008) suggested that exposure to enhanced ROS concentrations can lead to damage to the lysosomal membrane causing leakage of the contents, thus altering the lysosomal lumen pH and function.

Due to CoQ_{10}'s role in the METC, a deficient state would be expected to impair its function and as a result cause an increase in ROS, as demonstrated in a study by Duberley et al. (2013a). In addition, given CoQ_{10}'s protective nature, it could also be hypothesised that the reduction in cellular CoQ_{10} status found in this study, may negatively impact upon the amount of protection the lysosomal membrane has against ROS damage. As a potential future research option, it would be interesting to assess how a cellular COQ_{10} deficiency alters the CoQ_{10} content on the lysosome and how this impacts the degree of peroxidation taking place at the lysosomal membrane. This could be done by extracting the lysosomes form the cells post treatments, then using a lipid peroxidation assay such as a thiobarbituric acid assay to determine changes in peroxidation of the lysosome.

23.9 Conclusion

Results from this chapter found that a PABA induced deficit in CoQ_{10} status appears to result in a 15% decrease in cellular ATP concentration and a 1-fold increase in cellular ROS generation, which may contribute to a dysregulation of lysosomal pH as outlined in section 22. Interestingly, the decrease in cellular CoQ_{10} status did not appear to impair mitochondrial membrane potential, cause a loss of mitochondrial enrichment, or induce a loss of cellular viability. With this in mind, the current study has highlighted evidence that a CoQ_{10} deficiency can be associated with increased mitochondrial derived oxidative stress and decreased cellular ATP concentration. Given the lysosomes susceptibility to ROS changes and requirements for cytosolic ATP it may be that a CoQ_{10} deficiency is negatively impacting lysosomal acidification

via multiple pathways. Figure 66 (section 25) shows some hypothesised mechanisms of action, based upon the results found in this study.

24 CoQ10 Supplementation

24.1 Introduction

As previously alluded to in the introductory chapter to this thesis, CoQ_{10} deficiency currently represents the only treatable METC disorder, with a number of diseases associated with primary and secondary CoQ_{10} deficiency showing some clinical improvement following CoQ_{10} supplementation (Hargreaves et al., 2020).

One example of a primary CoQ_{10} deficiency reported to respond positively to CoQ_{10} supplementation, is the cerebellar ataxia (CA) clinical phenotype associated with this disorder (Mantle and Hargreaves, 2018). A clinical study by Musumeci et al. (2001) found that CoQ_{10} supplementation (200-3000 mg/day) was able to significantly improve cerebellar function in patients that had been identified in the early stages of the disease. Another example of a positive response to CoQ_{10} supplementation was reported in a study by Müller et al. (2003a) in which supplementation with CoQ_{10} (360 mg over 4 weeks in 28 PD patients) was found to significantly improve PD patients scores on the Farnsworth–Munsell 100 Hue test (FMT), a colour vison test in which a patients ability to isolate and arrange differences in colour targets, where PD patients results often differ to controls due to motor impairment (Müller et al., 2003b). This would suggest that CoQ_{10} supplementation is able to improve some of the cerebral symptoms associated with PD, although the cause of this therapeutic efficacy is at present uncertain.

In a more recent study by Ramezani et al. (2020) it was found that CoQ_{10} supplementation (300 mg/day over four weeks) was able to improve National Institute of Health Stroke Scale (NIHSS) scores in patients after an acute ischemic stroke. The NIHSS is a toll used to evaluate the neuronal impairment caused by a stroke (Appelros and Terént, 2004). Interestingly, although there is some evidence that CoQ_{10} supplementation is effective in the treatment of certain neurological disorders such as PD and Huntington's disease (Flint Beal and Shults, 2003, Müller et al., 2003a), the preponderance of neurological diseases have been reported to show little or no response to CoQ_{10} treatment in clinical studies to date. This lack of response could be due to the poor transference of CoQ_{10} across the BBB and its reported poor

bioavailability in general (Hargreaves, 2014, Emmanuele et al., 2012a, Hargreaves et al., 2020). Patients with non-neurological/systemic CoQ_{10} deficiencies appear to respond better to CoQ_{10} supplementation with clinical improvement being reported such as in the study by Mortensen et al. (2014), in which patients with chronic heart failure were treated with CoQ_{10} in addition to conventional treatments. Mortensen et al. (2014) reported that supplementation with CoQ_{10} (300 mg/day over two years) was able to significantly reduce the risk of cardiac associated deaths by around 43%. Additionally, there have been a number of reports suggesting that CoQ_{10} supplementation may have a beneficial effect on the clinical status of patients suffering with type II diabetes (El-ghoroury et al., 2009). In a study by HosseinzadehAttar et al. (2013) it was reported that CoQ_{10} supplementation (200 mg/day over three months) was able to significantly reduce fasting blood serum HbA1c (glycated heamoglobin) (Hargreaves et al., 2020, Hosseinzadeh-Attar et al., 2013).

In Chapter 22 of this thesis it was reported that a CoQ_{10} deficiency may also play a role in the de-acidification of the lysosome, and therefore together with mitochondrial dysfunction, an impairment in lysosomal function may also contribute to the pathogenesis of diseases associated with a deficit in CoQ_{10} status (Heaton et al., 2020). However, although CoQ_{10} supplementation has been reported to ameliorate METC impairment in CoQ_{10} deficient neuronal cells (Duberley et al., 2014), it is at present uncertain whether CoQ_{10} treatment would also be able to restore lysosomal pH to control levels in these CoQ_{10} deficient cells. This possible lysosomal impairment may be a contributory factor to the refractory nature of the neurological symptoms associated with a CoQ_{10} deficiency to CoQ_{10} supplementation. Furthermore, at present the factors responsible for the increase in lysosomal pH associated with a neuronal CoQ_{10} deficiency are uncertain and include; oxidative stress, impairment of organelle function or LETC dysfunction and a deficit in ATP status which is required for lysosomal V-ATPase activity. Thus, further studies will be required to elucidate the cause of this de-acidification associated with a CoQ_{10} deficiency.

24. 2 Aims

The aims of this chapter were to assess whether the increase in lysosomal pH associated with a PABA induced CoQ_{10} deficiency, could be reversed by CoQ_{10} supplementation. Also, to investigate some of the possible factors responsible for the de-acidification of this organelle, following the decrease in neuronal CoQ_{10} status.

24.3 Methods

22.3.1. Cell culture

SH-SY5Y cells were grown and maintained as described in Section 9 all CoQ_{10} concentration assessments were carried out in T75 cell culture flasks.

22.3.2. PABA treatment

cells were subject to a sing 1mM PABA treatment over a 5-day period, as outlined in section 9.4

23..3.3. CoQ10 Supplementation

Following PABA treatment (see section), cells were co-incubated with 5 μM CoQ_{10} over three days as described in section 9.4

23.3.4. Quantification of cellular CoQ_{10} Concentration

Cellular CoQ_{10} was extracted, and concentration was calculated using reverse phase HPLC with a C18 column, as described in sections 11.2 and 11.3

23.3.5. Assessment of cell viability

Flow cytometry assessment of cell viability after PABA treatment was carried out as outlined in section 12

23.3.6. Total protein assessment

The total protein of the cells was determined using an adapted version of the Lowry method, as outlined section 10

23.3.7. Lysosomal pH determinations

In order to assess changes in lysosomal lumen pH, this study deployed three acidotropic lysosomal specific fluorescent probes; LysoSensor yellow-blue DND-167 and LysoSensor yellow DND-160. Each of these probes have marginally different method for assaying the lysosomal pH as discussed in section 20 all lysosomal pH assessments were carried out following section 14.1, 14.2, and 14.3 respectively.

23.3.8. Lysosomal mass

Total cellular lysosomal mass comparisons were carried out using measuring the lysosomal enzyme β-gal as previously outlined in section 20. Analysis was carried out using the flow cytometer as described in section 12.

23.3.7. Cellular ATP assessment

The total cellular ATP concentration was carried out using the Cell Titer-Glo assay as outlined in section 16.

23.3.8. Mitochondrial membrane potential assessment

Mitochondrial membrane potential changes were assessed by the fluorescent probe JC-1 using flow cytometry, as outlined in section 18.

23.3.9. Mitochondrial membrane mass assessment

Total mitochondrial membrane protein concentration was assessed by deployment of the fluorescent probe Mitotraker Green using flow cytometry, as outlined in section 17.

23.3.10. CS activity

The activity of the mitochondrial enzyme citrate synthase was also measured as a marker of mitochondrial enrichment. This was done using a spectrophotometer method as set out in section 19.

23.3.11. Cellular ROS concentration assessment

Total cellular ROS was assessed using the fluorescent probe using flow cytometry, as outlined in section 15.

22.3.12. Statistical analysis

Statistical analysis was carried out as described in section 22.

24.4 Results

24.4.1 CoQ10 Treatment

HPLC analysis of the CoQ_{10} status of the CoQ_{10} deficient neuronal cells (PABAtreated) following CoQ_{10} supplementation revealed that the cellular CoQ_{10} concentration was significantly increased (from 59 pmol/mg to 1463 pmol/mg) following a three-day co-incubation with 5 μM CoQ_{10} ($p < 0.0001$) (figure 57). Coincubation with CoQ_{10} resulted in an average 25-fold increase in CoQ_{10} status, which is consistent with previous studies (Duberley et al., 2014). As with previous CoQ_{10} determinations, the CoQ_{10} concentration was normalised on a protein baseline and expressed as pmol/mg.

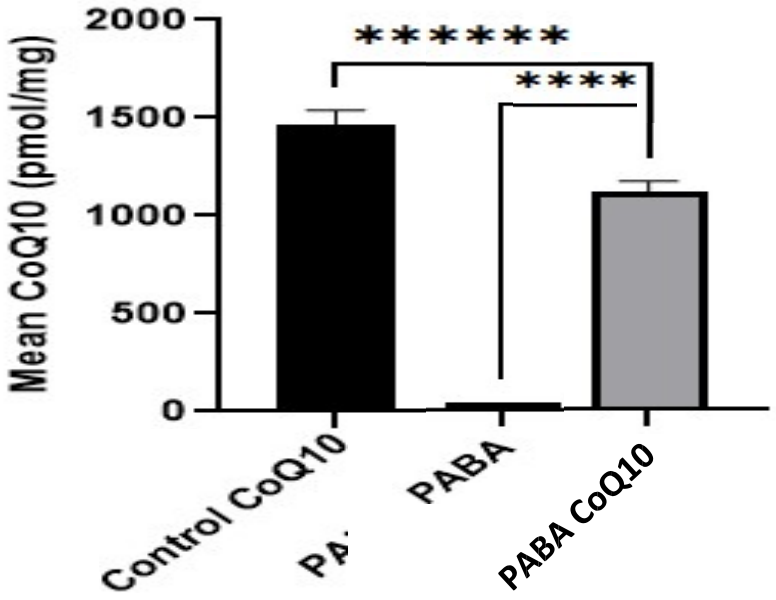

Figure 57. The cellular CoQ10 Concentration pre and post CoQ10 supplementation.

*Figure shows the total cellular CoQ_{10} concentration both after PABA treatment (1 μM over five days) and CoQ_{10} supplementation (5μM over three days). Additionally, the data shows the total cellular CoQ_{10} concentration in control cells post CoQ_{10} supplementation. Error bars represent standard error of the mean (SEM); statistical analysis was carried out using a t test; ****: p<0.0001, N = 20.*

Flow cytometry analysis of the cellular viability post co-incubation with CoQ_{10} (5 μM, three days) was undertaken. Analysis of the PI staining showed that there was no significant difference in the cellular viability post CoQ_{10} supplementation when compared to either the CoQ_{10} deficient (PABA treated) cells or the control cells (figure 58).

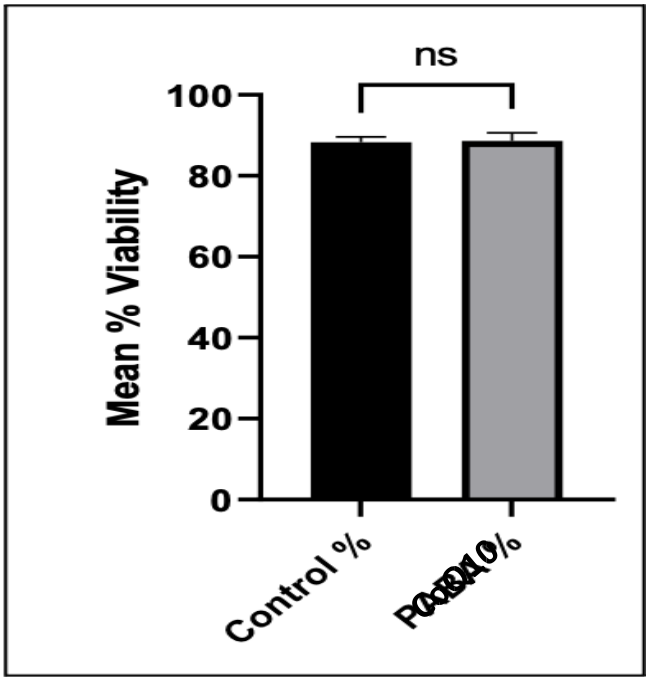

Figure 58. Mean Cellular Viability Post PABA Treatment.
Error bars represent standard error of the mean (SEM); statistical analysis was carried out using a t test; N = 21.

Analysis of the Cell Titer-Glo ATP results show that post co-incubation with CoQ_{10} the cellular ATP concentration was significantly increased ($p < 0.05$) (figure 59). The results show that a PABA induced 50% decrease in neuronal cell CoQ_{10} status was found to be associated with a 30% reduction in total cellular ATP concentration from a mean of 3.19 μM/mg (± 0.1073) in controls to 2.2 μM/mg (± 0.1220) in CoQ_{10} deficient cells, as shown in section 22 Post CoQ_{10} supplementation, the total cellular ATP concentration was found to be a mean result of 3.39 μM/mg (± 0.637), a 42% increase in cellular ATP levels when compared to the CoQ_{10} deficient neuronal cells.

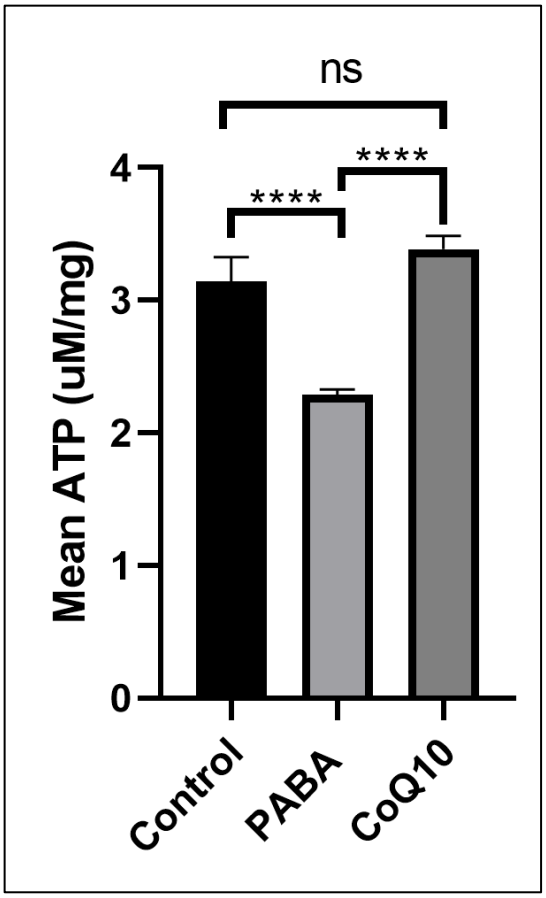

Figure 59. The cellular ATP Concentration pre and post CoQ10 supplementation.

Figure shows the total cellular ATP concentration (μg/mg) both after PABA treatment (1 μM over five days) and CoQ_{10} supplementation (5μM over three days). Error bars represent standard error of the mean (SEM); statistical analysis was carried out using a t test; ****: $p<0.0001$, N = 30.

Analysis of the mitochondrial membrane potential using the JC-1 probe showed that there was a slight increase in JC-1 median fluorescence following CoQ_{10} supplementation, however, there was no significant difference when compared to either the control cells (untreated) or the CoQ_{10} deficient cells (PABA treated, figure 60).

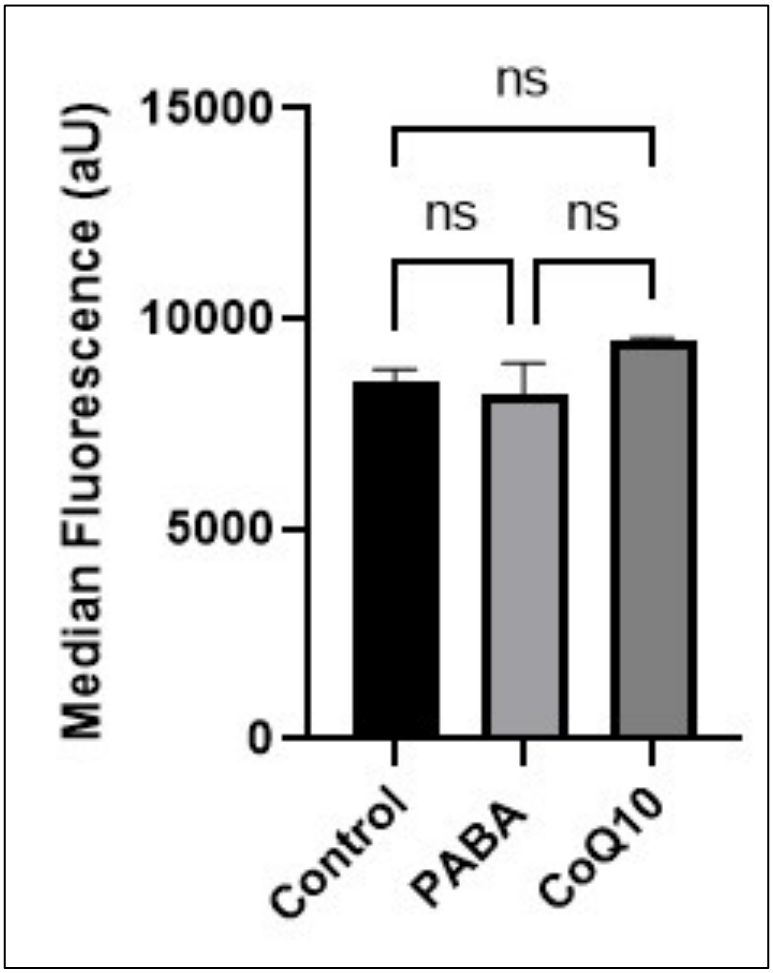

Figure 60. The Median JC-1 Fluorescence Pre and Post CoQ10 supplementation.

Figure shows the median JC-1 fluorescence pre and post CoQ_{10} supplementation (5μM over three days) as a marker of MMP. Error bars represent standard error of the mean (SEM); statistical analysis was carried out using an Anova; N = 16.

The MTG probe was used as a marker of mitochondrial mass, analysis showed there was no significant difference in MTG fluorescence between the CoQ_{10} deficient cells

(PABA treated) and the CoQ_{10} supplemented cells (figure 61). Although there was a slight increase in MTG fluorescence when comparing control cells and CoQ_{10} treated cells, it was found to not be statistically significant (figure 61).

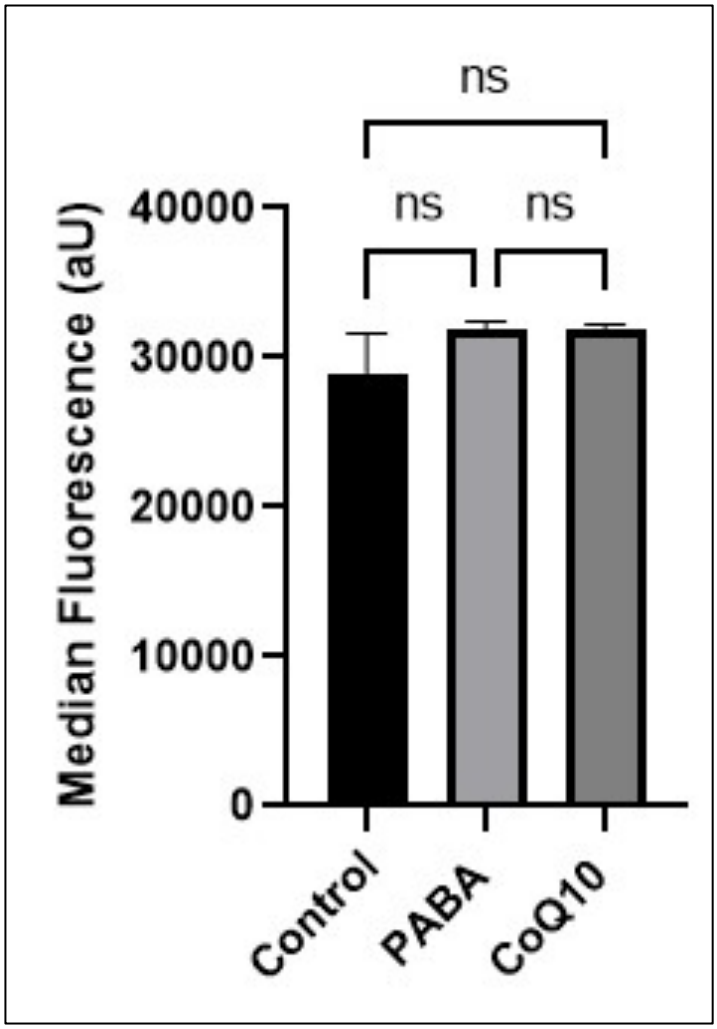

Figure 61. The Median MTG Fluorescence Pre and Post CoQ10 supplementation.

Figure shows the median MTG fluorescence pre and post CoQ_{10} supplementation (5μM over three days) as a marker of mitochondrial mass. Error bars represent standard error of the mean (SEM); statistical analysis was carried out using an Anova; N = 11.

24.4.5 Cellular ROS

Analysis of the general ROS concentration in the cells revealed that CoQ_{10} supplementation was able to significantly reduce the concentration of ROS in the CoQ_{10} deficient neuronal cells (PABA treated). Following supplementation with CoQ_{10}, the median Fluorescence was significantly reduced ($p < 0.0001$) when compared to the CoQ_{10} deficient cells (PABA treated) (figure 62). Additionally, it was found that CoQ_{10} supplementation was able to restore the fluorescence intensity to almost control levels. Although the fluorescence was not fully restored, there was no significant difference between the control cells (untreated) and CoQ_{10} supplementation cells (figure 62).

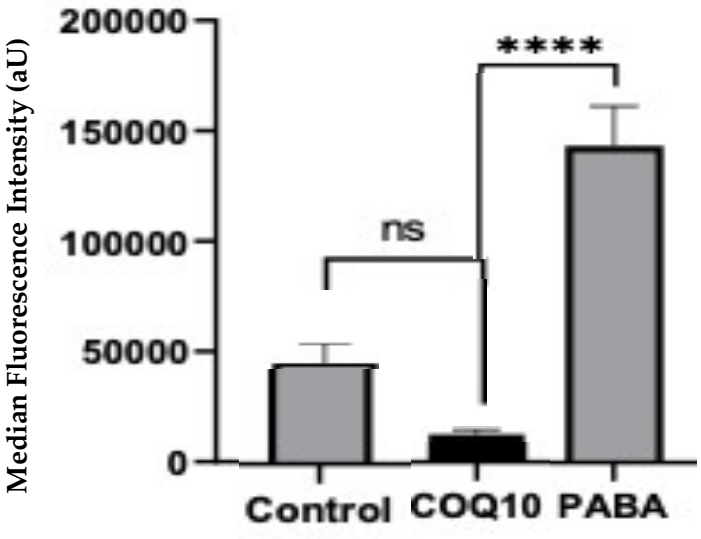

Figure 62. The Median Florescence of the ROS indicator CM-H2DCFDA Pre and Post CoQ10 supplementation.

Shows the median fluorescence of the ROS indicator probe pre and post CoQ_{10} Co-incubation (5 μM over three days) with PABA (1 μM over five days, A). Also shows the median fluorescence of Control cells vs CoQ_{10} supplemented cells (B). Error bars represent standard error of the mean (SEM); statistical analysis was carried out using a t test; ****: $p<0.0001$, N = 30.

Analysis of the LS-167 fluorescence post co-incubation with CoQ_{10} (5 μM for 3 days), showed there was a significant increase in LS-167 mean fluorescence ($p < 0.05$) compared to the CoQ_{10} deficient cells (PABA-treated) (figure 63). Interestingly, results show that the fluorescence did not exceed 90% of the mean fluorescence of the control cells.

Additionally, using the constructed calibration curve (Figure 40), it was calculated that the LS-167 probe suggested the lysosomal pH was 5.4 following CoQ_{10} supplementation.

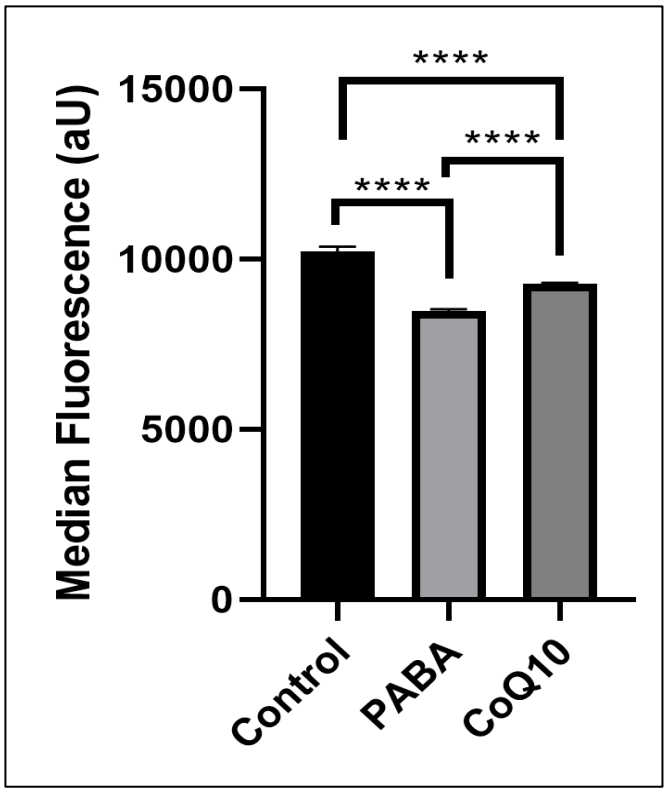

Figure 63. Median Fluorescence of LS-167 pre and post CoQ10 supplementation.

*Mean fluorescence of control, PABA-treated cells (CoQ_{10} deficient cells) and CoQ_{10} supplemented cells (5 μM treated cells in the presence of PABA). PABA-treated and CoQ_{10} –supplemented cells (in the presence of PABA) following 3 days of incubation. Following incubation with CoQ_{10}, the LysoSensor-167 (LS-167) fluorescence is significantly increased when compared to the PABA-treated cells. Comparisons of groups was carried out as follows: Control cells vs. PABA-treated cells, control cells vs. CoQ_{10} -treated cells, PABA-treated cells vs. CoQ_{10} -treated cells. Data available in supplemental data under table S7/8. Significance level; * ***p < 0.001; n = 94, **** p < 0.001, n = 94.*

Assessment of the LS-160 probe post CoQ_{10} supplementation found that there was a significant increase in LS-160 fluorescence and thus a significant decrease (more acidic) in lysosomal pH ($p < 0.0001$). It was found that CoQ_{10} supplementation (5 μM for 3 days) was associated with a decrease in pH from 6.3 (PABA-treated) to 4.7 (Figure 64). Interestingly, the pH of the lysosomal lumen was still significantly higher (pH 4.7) than that of the control cells (pH 4.2) following CoQ_{10} supplementation. This suggests that CoQ_{10} supplementation has not fully resorted the lysosomal pH (figure 64).

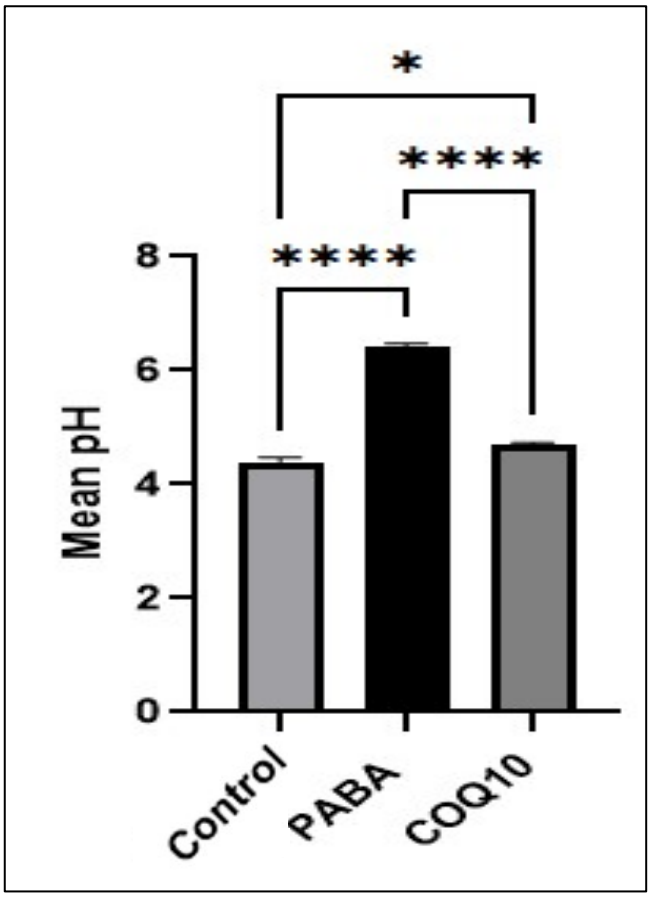

Figure 64. The Mean Lysosomal pH Pre and Post CoQ10 Co-incubation.

*Shows the Mean lysosomal lumen pH both after PABA treatment (1 μM over five days) and CoQ_{10} co-incubation (5 μM over three days). Error bars represent standard error of the mean (SEM); statistical analysis was carried out using a t test; *: $p<0.05$, ****: $p<0.0001$, N = 24.*

24.4.8 GBA assessments

Analysis of the lysosomal mass on the flow cytometer showed no significant difference in fluorescence when CoQ_{10} treated cells were compared to the CoQ_{10} deficient cells (PABA-treated) (Figure 65). It was also found that there was no significant difference when CoQ_{10} treated cells were compared to the control cells (untreated).

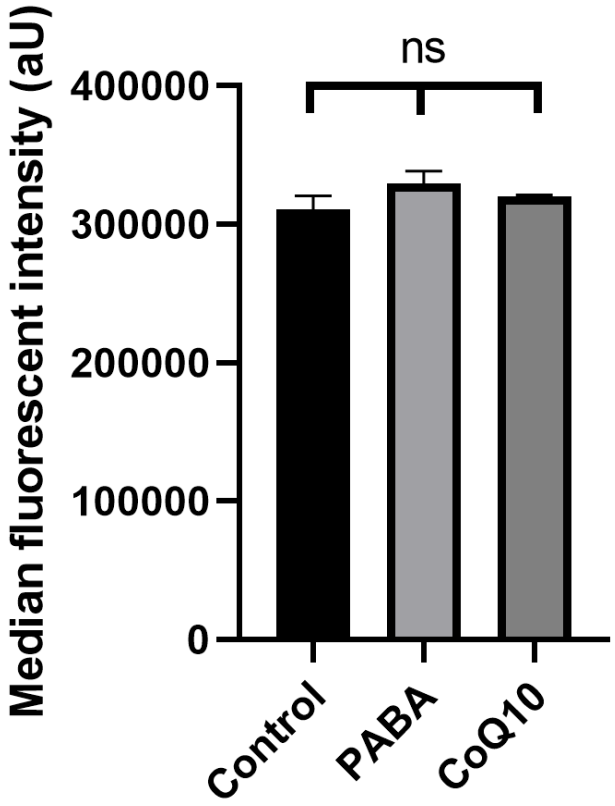

Figure 65. The Median Fluorescence intensity of the … probe representative of lysosomal mass pre and post co-incubation with CoQ10.

Shows the median fluorescence intensity of the lysosomal mass indicator, pre and post CoQ_{10} supplementation. Error bars represent standard error of the mean (SEM); statistical analysis was carried out using an anova N = 24.

24.9 Discussion

CoQ_{10} deficiency is a relatively uncommon disease with an estimated prevalence of 1 in 100,000 (Acosta et al., 2016), if identified in the early stages of life, patients may respond positively to CoQ_{10} supplementation. Although, the neurological symptoms associated with a CoQ_{10} deficiency seem to be more refractory to treatment for reasons that have not yet been fully resolved. This chapter investigated the ability of CoQ_{10} supplementation to restore lysosomal pH in a neuronal cell model of CoQ_{10} deficiency.

Treatment of SHS-SY5Y neuroblastoma cells with 1mM PABA for five days resulted in a reproducible (58%) decrease in cellular CoQ_{10} status (section 22). This deficiency was found to be associated with an alkalisation of the lysosomal lumen, of which the pH increased from 4.2 to 6.3 (section 22).

Following CoQ_{10} supplementation (5 μM over three days) the intracellular CoQ_{10} status was assessed and found to be significantly increased from 59.29 pmol/mg to 1463 pmol/mg ($p < 0.001$, figure 57). It was found that there was an average 25-fold increase in the cellular CoQ_{10} content (figure 57) following CoQ_{10} supplementation. This increase in neuronal cellular CoQ_{10} concentration following CoQ_{10} supplementation was consistent with that previously reported by Duberley et al. (2014). A □□□M concentration of CoQ_{10} was used for the supplementation experiment as this corresponds to the concentration of CoQ_{10} reported to improve mitochondrial function in CoQ_{10} deficient patient fibroblasts (López et al., 2010).

Assessment of cellular viability was also undertaken pre and post CoQ_{10} supplementation and no significant difference between the control and CoQ_{10} treated cells was identified. This was undertaken to ensure that the CoQ_{10} supplementation was not significantly impacting cell number or health, thus having a negative impact on the biochemical results. This finding also corresponds with previous CoQ_{10} supplementation studies, where almost all have found little to no toxic effects of CoQ_{10} treatment in cellular models; additionally, CoQ_{10} supplementation in human trials have reported very little adverse side effects, with CoQ_{10} being generally well

tolerated at even the highest of doses (Duberley et al., 2013a).

CoQ_{10} supplementation also appeared to be particularly effective at restoring cellular ATP content (50% figure 59). As previously discussed, (section 5) the lysosome has a cytoplasmic ATP dependent mechanism for maintaining the lysosomal lumen (VATPase), because of this it has been suggested that the lysosome may be inherently susceptible to changes in cellular ATP concentration. Therefore, the increase in cellular ATP status following CoQ_{10} supplementation determined in this study may be a contributing factor to the partial restoration of lysosomal pH.

However, in a study focusing on the V-ATPase it was reported that the K_m value for V-ATPase was 450 ± 80 nM/ml and interestingly the K_m for ADP being much lower at 4.7 ± 0.5 nM/ml (Yokoyama et al., 2003, Nakano et al., 2008). Moreover, the general reported cellular ATP concentration is around 1 to 10 μM/ml (Zimmerman et al., 2011). This would suggest that the V-ATPase is quite efficient in utilising the available ATP and that the reported reduction in ATP from this study is still above the minimum requirement for V-ATPase activity. Thus, the changes in total ATP may not have as much of an impact as initially hypothesised; however, more understanding of the dynamics of the V-ATPase itself is needed.

Additionally, cellular ATP concentration has also been previously reported as a marker for METC activity (López et al., 2010). In view of this, the change in cellular ATP concentration determined in this study may also show that CoQ_{10} supplementation is able to restore METC activity post PABA (1 mM) treatment. Although more in-depth measurements of the METC enzyme activity is needed to confirm or refute this assumption. However, it must be stressed that a decrease in cellular ATP levels has been associated with METC dysfunction and has been reported in previous studies (Duberley et al., 2014). Additionally, Duberley et al. (2014) reported that CoQ_{10} supplementation is unable to fully restore $\Delta\Psi_m$ only reaching around 90% of the controls.

Analysis of both MTG and JC-1 mitochondrial homeostasis probes showed no significant difference post supplementation with CoQ_{10} compared to either controls or CoQ_{10} deficient cells (figure 60 and 61), suggesting that CoQ_{10} supplementation is not having a significant impact on the $\Delta\Psi m$ or the mitochondrial enrichment of the cell. However, as previously discussed in section 23 these findings may be unreliable given the conflicting result found in the CS activity (mitochondrial matrix marker) found in section 23, whereby CS activity was elevated in CoQ_{10} deficiency cells (Figure 54). Additionally, from previous studies (Duberley et al., 2014). Duberley et al. (2013a) reported that a CoQ_{10} deficiency was associated with a significant decrease in $\Delta\Psi m$ of up to 40% in a similar CoQ_{10} deficient state. There is no clear reason for this discrepancy other than the methods used may have differences in sensitivity.

Given the antioxidant function of CoQ_{10} it was no surprise that the neuronal CoQ_{10} deficiency was associated with an increase in cellular ROS concentration (figure 56). This could also have implications on lysosomal function given the lysosome`s susceptibility to oxidative stress induced dysfunction (Kurz et al., 2008) (see section 23.8). CoQ_{10} supplementation was able to significantly decrease the total ROS concentration in the cell ($p< 0.0001$ Figure 62). It was thought that the excess CoQ_{10} post supplementation may have reduced total cellular ROS in view of its potent antioxidant capability. The findings are also collaborated by previous studies using a similar concentration of CoQ_{10} supplementation, where a reduction in cellular ROS was also associated with CoQ_{10} supplementation although the studies are not directly comparable due to differences in the detections methods used (Duberley et al., 2014).

The results determined in this chapter have indicated that the pharmacologicallyinduced CoQ_{10} deficiency was associated with a significant increase in lysosomal pH (more alkaline; see section 22) from 4.2 in control cells to 6.2 in CoQ_{10} deficient cells; this was then decreased to a pH of 4.7 following CoQ_{10} supplementation (5 μM). However, this pH value is still above the pH found in control cells (4.2), although, it is within the normal working range of the lysosome previously reported by Ohkuma and Poole (1978). A possible reason for the inability of CoQ_{10}

supplementation to restore lysosomal pH to control levels may be related to the ineffectiveness of CoQ_{10} supplementation to fully ameliorate METC dysfunction in CoQ_{10} deficient neurons (Duberley et al., 2014). Interestingly, in the present study it was found that CoQ_{10} supplementation was able to restore cellular ATP levels to that of the control, although the activity of the METC enzyme complexes was not assessed. Therefore, other factors such as ROS induced damage of the lysosome must be brought into consideration as CoQ_{10} supplementation was not able to decrease ROS levels to that of the control in the CoQ_{10} deficient neurons. Therefore, in addition to the ineffectiveness of CoQ_{10} supplementation to restore METC activities to control levels reported by Duberley et al (2014), the inability of CoQ_{10} treatment to fully restore lysosomal pH in CoQ_{10} deficient neurones may also contribute to the refractory nature of neurological symptoms associated with CoQ_{10} deficiency to CoQ_{10} supplementation.

24.10 Conclusion

To conclude the findings of this chapter are particularly interesting and have provided some possible insight into how effective CoQ_{10} supplementation (5 μM over five days) may be in the restoration of lysosomal pH in CoQ_{10} deficient neuronal cells. In particular, the results have provided evidence that CoQ_{10} treatment may be able to mitigate the impact of a CoQ_{10} deficiency on the lysosome. However, the results also show that CoQ_{10} supplementation is unable to fully restore the lysosomal pH to that of the control levels, although, it fell within what is considered to be normal pH range compatible with the function of the organelle, although no studies were undertaken to assess lysosomal function in the present study. Therefore, concentrations of CoQ_{10} above 5 μM may be required to fully restore lysosomal pH in these CoQ_{10} deficient cells. The results also suggest that when diagnosing an LSD, it may be judicious to also assess the CoQ_{10} status of the patient, as this may open an avenue of treatment

previously unidentified. However, more solid evidence is required before this can be confirmed or refuted.

25 General Discussion

CoQ_{10} is the principal form of ubiquinone in humans (Hargreaves et al., 2020). It serves numerous roles in the cell, most notably as an electron carrier in the METC and as a potent lipid soluble antioxidant (Crane, 2001, Hargreaves, 2003, Neergheen et al., 2017). Consequently, a CoQ_{10} deficiency (either primary or secondary) could be a contributing factor to the pathogenesis of a plethora of diseases associated with a failure in mitochondrial energy generation as well as impaired cellular antioxidant status (Hargreaves, 2003). Since the first reported cases of CoQ_{10} deficiency by Ogasahara et al. (1989) who described two sisters who presented with seizures with accompanying rhabdomyolysis and mental retardation, a number of other patients have been reported with a deficit in this isoprenoid, although the estimated prevalence of a primary CoQ_{10} deficiency is thought to be less than 1 in 100, 000. However, this condition is thought to be under diagnosed (Hargreaves et al., 2020). The clinical presentations of a primary CoQ_{10} deficiency are particularly heterogeneous, although it can be divided into five distinct phenotypes as shown in table (Table 1).

Phenotype	Clinical Aspects
Encephalomypathy	Juvenile-onset mitochondrial myopathy, recurrent myoglobinuria, encephalopathy.
Isolated myopathy	Juvenile- or adult-onset muscle weakness, myoglobinuria, exercise intolerance, cramps, myalgias, elevated creatine kinase level.
Nephropathy	Infantile- or early childhood-onset steroidresistant nephrotic syndrome. Infantile- or juvenile-onset steroid-resistant nephrotic syndrome typically with congenital sensorineural deafness.
Infantile multisystemic	Infantile-onset psychomotor regression, encephalopathy, optic atrophy, retinopathy, hearing loss, renal dysfunction (mainly nephrotic syndrome).
Cerebellar ataxia	Typically, juvenile-onset cerebellar ataxia, additional manifestations may occur.

Table 1. Table depicting the Phenotypes Associated with a CoQ10 Deficiency.

taken from (Emmanuele et al., 2012a).

At present, the factors responsible for the heterogeneous clinical nature of a primary CoQ_{10} deficiency are uncertain. The major focus of the preponderance of clinical research associated with CoQ_{10} deficiencies has been to investigate their effect on mitochondrial metabolism (Hargreaves et al., 2020). However, together with the

mitochondria, the lysosomes are also a major site of CoQ_{10} localisation within the cell, where this isoprenoid is thought to play an essential role in the transport of protons across the lysosomal membrane required for maintaining the acidity of the organelle and for preserving lysosomal function (Coffey et al., 2014). The acidic environment of the lumen is essential for lysosomal function with alterations in pH being associated with lysosomal impairment (Altan et al., 1998, Coffey et al., 2014). The pH dependence of the lysosome arises because of the numerous (50 or more) hydrolytic enzymes found in the lumen of the organelle that require an acidic environment to maintain their optimal activity (Lübke et al., 2009). In view of the essential role lysosomes play in the degradation of biological debris as well as non-fragmented subcellular entities (Gille and Nohl, 2000, Wartosch et al., 2015), an impairment of lysosome function would be anticipated to contribute to cellular morbidity. However, at present no studies have assessed the effect of a CoQ_{10} deficiency on lysosomal function. Furthermore, there have been no reports of secondary LSDs in patients with CoQ_{10} deficiencies.

The lysosome is a single membrane organelle and as with CoQ_{10} is found in almost all eukaryotic cells where their foremost responsibility is the digestion of waste products from normal metabolic processes (De Duve, 1963, Wartosch et al., 2015). Additionally, the lysosome is implicated in several other roles in the cell such as a signalling hub for the cell and as a monitor of the availably of a multitude of cellular resources (Ballabio and Bonifacino, 2020). Subsequently, damage or malfunction to the lysosome have been associated with disease (Cox and Cachón-González, 2012). Lysosomal dysfunction has been implicated in a plethora of diseases with neurodegenerative phenotypes being prevalent in many LSDs, which undoubtedly connects the organelle to the survival of neurones (Fraldi et al., 2016). Fascinatingly, there are also a number of mutations known to be implicated in the pathogenesis of neurodegenerative diseases which also implicate the lysosome as a key conspirator in disease progression (Fraldi et al., 2016).

The overarching aim of the work reported in this thesis was to study how a CoQ_{10} deficiency may affect lysosomal homeostasis, particularly focusing on its impact on the maintenance of the pH of the organelle. This is the first study of its kind, and it has provided insights into how CoQ_{10} may contribute to the pathogenesis of lysosomal dysfunction. The results of this study have indicated that a CoQ_{10} deficiency can result in an increase in lysosomal pH. This rise in pH may then impair the lysosomal hydrolytic enzymes present in the lumen of the organelle which require an acidic environment for optimal activity.

To assess the effect of a CoQ_{10} deficiency on lysosomal pH we established a neuronal cell model of CoQ_{10} deficiency according to the study of Duberley et al. (2013a). Using SH-SY5Y neuroblastoma cells. This PhD research project used this cell type in view of the predominant neurological presentation of CoQ_{10} deficiencies in patients (López et al., 2006, Balreira et al., 2014, Navas et al., 2021). PABA (1mM, treatment for five days) which is a competitive inhibitor of the COQ2 (Alam et al., 1975) was found to induce a consistent and reproducible 56% decrease in neuronal cell CoQ_{10} status. It was felt that this would provide a good platform for assessing the effects of CoQ_{10} deficiency on lysosomal pH as the deficit in cellular CoQ_{10} status induced by PABA treatment is comparable to that of patient tissues.

In order to assess the effect of the CoQ_{10} deficiency on lysosomal pH three pH sensitive probes were used LT, LS-167, and LS-160, all with slightly different aspects in an attempt to create a full picture of the lysosomal pH. Firstly, the LT flow cytometry probe was used. LT is a single wavelength probe often used as a quantitative measure of lysosomal pH, however, due to sensitivity issues should be considered more as a qualitative measure of lysosomal pH as with this study (Guha et al., 2014).

In this study we found that a CoQ_{10} deficiency was associated with a 35% decrease in LT fluorescence indicating an increase in lysosomal pH. However, due to the limitations in the sensitivity of LTs, the actual change in pH cannot be accurately determined.

The second probe used was the LS-167 probe, another single wavelength probe with promising results shown in previous studies in determining lysosomal pH. It was found that the reported CoQ_{10} deficiency was associated with a 23% reduction in LS167 fluorescence. This also indicates that there is a significant increase in lysosomal pH. Unlike the LT probe we attempted to create a standard curve of pH using the LS167 probe in order to determine the lysosomal pH with some success. It was found that a CoQ_{10} deficiency led to an increase in lysosomal pH from 4.1 to 6.2. However, there was some considerable day-to-day variation in the data from this probe, and upon inspection of the literature other researchers have also reported inconsistencies in the readings form this probe (Lin et al., 2001, Guha et al., 2014, Ma et al., 2017). Higher concentrations and/or longer periods of incubation with the probe itself were found to cause a significant alkalisation of the lysosomal lumen, therefore, a third probe was employed in this study, LS-160. LS-160 is again from the same family of probes as the previous, however, it differs in that it is a radiometric probe. This means that it has a dual wavelength for both excitation and emission and is fluorescent in both alkali and acidic environments at different wavelengths. This allowed for more accurate measurements as an alkali to acidic ratio could be used to measure lysosomal pH. A concentration curve was created using standard pH buffers using LS-160 with much more consistency than the LS-167 probe. Using the LS-160 probe we found that a CoQ_{10} deficiency was associated with an increase of lysosomal pH from 4.1 to 6.3. This is consistent with the findings from the previous probes and provides evidence that CoQ_{10} deficiency is associated with lysosomal alkalisation. To ensure the validity of the LS-160 probe we treated the cells with the V-ATPase inhibitor (known to increase lysosomal pH) to ensure the validity of the LS-160 probe and found that it led to an increase in pH from 4.1 to 7.1. This is in conjunction with previous published works, further solidifying the findings from this study.

In this study, we were able to reduce the cellular CoQ_{10} status by up to 56%, similar to that reported in patients with the cerebellar ataxia clinical phenotype of CoQ_{10}

deficiency (Musumeci et al., 2001, Malicdan et al., 2018). Taking these findings into consideration, it could be assumed that these patients may also have an increase in lysosomal pH. One limitation to the nature of a PABA induced CoQ_{10} deficiency, was that we were not able to elicit a further decrease in cellular CoQ_{10} status. This meant we were not able to investigate whether a more severe CoQ_{10} deficiency (as reported in some primary forms of the disease) would result in a further alkalinisation of the lysosome.

In order to establish whether the rise in pH induced by a CoQ_{10} deficiency was caused by a diminution in cellular lysosomal content the activity of the lysosomal marker enzyme, β-gal was determined. The activity of β-gal was found to be comparable to control levels following an induced CoQ_{10} deficiency in the neuronal cells indicating that the increase in pH was not the result of a decrease in the lysosomal content of the cell. Given the requirement of the lysosomal hydrolases for the acidic environment, it would be reasonable to speculate that this increase in pH would impair the function of these enzymes. This could imply that a CoQ_{10} deficiency may be a factor to consider in the pathogenesis of some LSDs, however, further studies are required to confirm or refute this possibility

Another aim of this study was to assess whether CoQ_{10} supplementation can reverse the increase in lysosomal pH associated with a CoQ_{10} deficiency. This is an important aspect of the study, as it not only provides evidence for the relationship between CoQ_{10} and the lysosome but also as a potential treatment avenue in diseases relating to lysosomal dysfunction. In this study 5 μM CoQ_{10} supplementation over three days was chosen, this was because it has previously been reported to elicit some biochemical improvement in CoQ_{10}-deficent fibroblasts in the study by López et al. (2010); where supplementation was able to increase cellular ATP concentration and ameliorate oxidative stress. It was found that CoQ_{10} supplementation was able to increase LT and LS-167 fluorescence (90% of control levels). Analysis of LS-160 also showed restoration of the lysosomal pH from 6.3 in the CoQ_{10} deficient cells (PABA treated) to around 4.7 in the supplemented cells. Interestingly, in all cases lysosomal

pH was not fully restored to control levels. The failure to fully restore lysosomal pH could be due to several reasons such as, irreversible damage to the lysosomal membrane from OS resulting in leakage, or inadequate transport of protons which are required to maintain lysosomal acidification. In a study by Duberley et al. (2013a) it was also reported that CoQ_{10} supplementation was not able to fully restore the activity of the METC following PABA-induced CoQ_{10} deficiency (around 90% of control levels). The possibility arises that the reduced METC capacity is hindering the lysosomal proton gradient via some undisclosed mechanism, however, this is merely speculation, and the most likely cause is the aforementioned damage via increased OS.

To further elucidate the causes of the increase in pH associated with a neuronal cell CoQ_{10} deficiency an assessment was made of cellular ATP status and OS. As to be expected, given CoQ_{10}'s role in the METC, the CoQ_{10} deficiency was associated with a significant decrease in cellular ATP concentration (30% decrease compared to control levels). Additionally, following CoQ_{10} supplementation there was a 40% increase in cellular ATP concentration. Therefore, during a CoQ_{10} deficiency there may be insufficient cytoplasmic ATP available for the lysosomal V-ATPase to function optimally; following the restoration of the cellular ATP supply commensurate with CoQ_{10} supplementation, the V-ATPase can again translocate protons adequately into the lumen of the organelle. When investigating the validity of the LS-160 probe a specific inhibitor of the V-ATPase was used (BAF). It was found that BAF was also able to induce significant lysosomal alkalisation, leading to a lysosomal pH of around 7.1. This finding could indicate that the reduction in V-ATPase activity rather than an impairment of LETC function as the main factor causing the rise in lysosomal pH following the deficit in neuronal CoQ_{10} status. Although further work is required to fully ascertain the contribution of the LETC/V-ATPase in the maintenance of the lysosomal pH.

In this study we also assessed the effect of a CoQ_{10} deficiency on the level of total cellular ROS. It was found that there was a one-fold increase in the level of cellular

ROS associated with a neuronal CoQ_{10} deficiency, significantly increasing the potential for OS induced lysosomal impairment. The possibility arises that the significant increase in ROS may be causing damage to the lysosomal membrane resulting in a proton leak into the cytoplasm. Again, this is merely speculation, however, it is yet another avenue for a potential mechanism leading to lysosomal alkalisation during a CoQ_{10} deficiency. Figure 66 depicts some of the mechanisms which may link CoQ_{10} deficiency to lysosomal dysfunction.

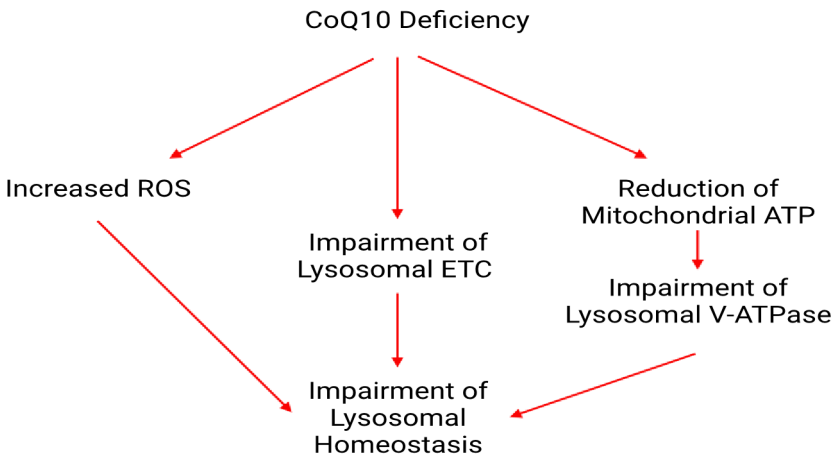

Figure 66. Proposed schematic of how CoQ10 deficiency may influence the acidification of lysosomes.

Taken from (Heaton et al., 2020).

25.1 Conclusion

The results of this study have provided insights into the relationship between the ubiquitous molecule, CoQ_{10} and the lysosome and their possible involvement in disease. However, whilst there is evidence that strongly links the two, the exact mechanism(s) is yet to be fully elucidated (Figure 66). As previously discussed, (section 3) CoQ_{10} is a major contributor to the synthesis of ATP and the lysosome has an inherent requirement for cytoplasmic ATP. It could be that CoQ_{10} deficiency exerts its effects on the lysosome via reducing the freely available ATP required for normal V-ATPase activity. Furthermore, it is uncertain at present whether the observed increase in lysosomal pH following the deficit in cellular CoQ_{10} status would be sufficient to impair the activity of the hydrolase enzymes present in the lumen of the organelle.

Figure 66 shows some possible ways in which a CoQ_{10} deficiency may impair lysosomal function. In addition, studies will need to be undertaken to assess evidence of secondary LSD in patients with primary CoQ_{10} deficiency, to fully understand the relationship between a CoQ_{10} deficiency and LSD's.

Although these are important factors when considering the data from this study, they do not subtract from the overarching finding of this investigation which is that a CoQ_{10} deficiency has now been linked to the de-acidification of the lysosome and that CoQ_{10} supplementation has the potential to restore lysosomal pH.

26 Future work

Given the implications of this study so far, there are several future investigations that would add to the current body of work.

26.1 Advancing the cellular model of CoQ10 deficiency

The cellular model of neuronal CoQ_{10} deficiency used in this study has proven to be of particular use in assessing the deficiency in particular relation to secondary CoQ_{10} deficiency. However, development of a more sophisticated model may be in sight given the advancement in gene editing. It may now be possible to develop a model of a primary CoQ_{10} deficiency via alterations in genes relating to CoQ_{10} deficiency. It may also be possible to develop this as a 'switch' mechanism whereby the cells are grown without a deficiency and when needed the genetic change can be simply 'switched on' through some chemical stimulation creating a 'true deficient' cell model. This could then be developed to each individual gene involved in CoQ_{10} synthesis, meaning it would be possible to understand the effects of each specific genotype. On top of this, the current study has only investigated the effect in one cell type, it would be prudent to investigate how/if the same CoQ_{10} deficiency impacts lysosomal pH in other cell types. This would give a clearer idea of how a CoQ_{10} deficiency may impact the body globally.

26.2 Investigating lysosomal pH in patient cells

Additionally, it would be enlightening to investigate how lysosomal pH may be impacted in actual patient cells. Fibroblasts from patients with a primary CoQ_{10} deficiency could be assessed to see if a CoQ_{10} deficiency impacts "real world" cells in the same way as in this study.

26.3 Investigating the exact mechanism(s) of how CoQ10 deficiency impacts the lysosome

The evidence of the current study has shown that CoQ_{10} is able to significantly impact the normal acidification of the lysosome, however, we are yet to fully understand by which mechanism or mechanisms. To further understand the link between a CoQ_{10} deficiency and diseases linked to lysosomal dysfunction it would be interesting to investigate the exact mechanism/mechanisms by which CoQ_{10} is impacting the lysosome. This could be done using some of the aforementioned techniques in conjunction with assessments such as the peroxidation. Additionally, it would be interesting to measure the effect of CoQ_{10} supplementation alongside the inhibition of the V-ATPase, this would give insight into the mechanism of how effective CoQ_{10} is at maintaining the pH alone.

26.4 Analysis of an array of lysosomal enzyme activities

In this study we have been successful in establishing a link between CoQ_{10} deficiency and lysosomal de-acidification. However, we have been unable to fully understand the effects of the pH change on the lysosomal enzymes. Assessing different aspects of lysosomal function such as total cellular GAG build-up may also be sensible.

To further strengthen the findings of this study, assessment of a variety of lysosomal enzymes would be prudent. Furthermore, assessment of how CoQ_{10} supplementation effects these enzymes would also be of clinical consequence.

27 References:

ÅBERG, F., APPELKVIST, E.-L., DALLNER, G. & ERNSTER, L. 1992. Distribution and redox state of ubiquinones in rat and human tissues. *Archives of biochemistry and biophysics,* 295**,** 230-234.

ACKRELL, B. A. 2000. Progress in understanding structure–function relationships in respiratory chain complex II. *FEBS letters,* 466**,** 1-5.

ACOSTA, M. J., FONSECA, L. V., DESBATS, M. A., CERQUA, C., ZORDAN, R., TREVISSON, E. & SALVIATI, L. 2016. Coenzyme Q biosynthesis in health and disease. *Biochimica et Biophysica Acta (BBA)-Bioenergetics,* 1857**,** 1079-1085.

AGNELLO, M., MORICI, G. & RINALDI, A. M. 2008. A method for measuring mitochondrial mass and activity. *Cytotechnology,* 56**,** 145-149.

ALAEI, M. R., TABRIZI, A., JAFARI, N. & MOZAFARI, H. 2019. Gaucher disease: new expanded classification emphasizing neurological features. *Iranian journal of child neurology,* 13**,** 7.

ALAM, S. S., NAMBUDIRI, A. & RUDNEY, H. 1975. 4-Hydroxybenzoate: polyprenyl transferase and the prenylation of 4-aminobenzoate in mammalian tissues. *Archives of biochemistry and biophysics,* 171**,** 183-190.

ALBERTS, B. 2002. *Molecular Biology of the Cell: Hauptbd*, Garland.

ALTAN, N., CHEN, Y., SCHINDLER, M. & SIMON, S. M. 1998. Defective acidification in human breast tumor cells and implications for chemotherapy. *Journal of Experimental Medicine,* 187**,** 1583-1598.

AMEZIANE-EL-HASSANI, R. & DUPUY, C. 2013. Detection of intracellular reactive oxygen species (CM-H2DCFDA). *Bio-protocol,* 3**,** e313.

ANDERSON, R. F., HILLE, R., SHINDE, S. S. & CECCHINI, G. 2005. Electron transfer within complex II succinate: ubiquinone oxidoreductase of Escherichia coli. *Journal of Biological Chemistry,* 280**,** 33331-33337.

ANWAY, M. D., WRIGHT, W. W., ZIRKIN, B. R., KORAH, N., MORT, J. S. & HERMO, L. 2004. Expression and localization of cathepsin k in adult rat sertoli cells. *Biology of reproduction,* 70**,** 562-569.

APPELROS, P. & TERÉNT, A. 2004. Characteristics of the National Institute of Health Stroke Scale: results from a population-based stroke cohort at baseline and after one year. *Cerebrovascular Diseases,* 17**,** 21-27.

ARONSON, N. N. & DE DUVE, C. 1968. Digestive activity of lysosomes II. The digestion of macromolecular carbohydrates by extracts of rat liver lysosomes. *Journal of Biological Chemistry,* 243**,** 4564-4573.

ARROYO, M. & CRAWFORD, J. M. 2009. Pediatric liver disease and inherited, metabolic, and developmental disorders of the pediatric and adult liver. *Surgical Pathology of the GI Tract, Liver, Biliary Tract, and Pancreas (Second Edition).* Elsevier.

AU - SHIPLEY, M. M., AU - MANGOLD, C. A. & AU - SZPARA, M. L. 2016. Differentiation of the SH-SY5Y Human Neuroblastoma Cell Line. *JoVE*, e53193.

AVRAHAMI, L., FARFARA, D., SHAHAM-KOL, M., VASSAR, R., FRENKEL, D. & ELDAR-FINKELMAN, H. 2013. Inhibition of Glycogen Synthase Kinase-3 Ameliorates β-Amyloid Pathology and Restores Lysosomal Acidification and

Mammalian Target of Rapamycin Activity in the Alzheimer Disease Mouse Model IN VIVO AND IN VITRO STUDIES. *Journal of Biological Chemistry,* 288**,** 1295-1306.

BAIXAULI, F., ACÍN-PÉREZ, R., VILLARROYA-BELTRÍ, C., MAZZEO, C., NUÑEZANDRADE, N., GABANDÉ-RODRIGUEZ, E., LEDESMA, M. D., BLÁZQUEZ, A., MARTIN, M. A. & FALCÓN-PÉREZ, J. M. 2015. Mitochondrial respiration controls lysosomal function during inflammatory T cell responses. *Cell metabolism,* 22**,** 485-498.

BALLABIO, A. & BONIFACINO, J. S. 2020. Lysosomes as dynamic regulators of cell and organismal homeostasis. *Nature reviews Molecular cell biology,* 21**,** 101-118.

BALREIRA, A., BOCZONADI, V., BARCA, E., PYLE, A., BANSAGI, B., APPLETON, M., GRAHAM, C., HARGREAVES, I. P., RASIC, V. M. & LOCHMÜLLER, H. 2014. ANO10 mutations cause ataxia and coenzyme Q 10 deficiency. *Journal of neurology,* 261**,** 2192-2198.

BARTLETT, K. & EATON, S. 2004. Mitochondrial β-oxidation. *European Journal of Biochemistry,* 271**,** 462-469.

BASSET, G. J., QUINLIVAN, E. P., RAVANEL, S., RÉBEILLÉ, F., NICHOLS, B. P., SHINOZAKI, K., SEKI, M., ADAMS-PHILLIPS, L. C., GIOVANNONI, J. J. & GREGORY, J. F. 2004. Folate synthesis in plants: the p-aminobenzoate branch is initiated by a bifunctional PabA-PabB protein that is targeted to plastids. *Proceedings of the National Academy of Sciences,* 101**,** 1496-1501.

BEAL, M. F. 1998. Mitochondrial dysfunction in neurodegenerative diseases. *Biochimica et Biophysica Acta (BBA)-Bioenergetics,* 1366**,** 211-223.

BEN-MEIR, A., BURSTEIN, E., BORREGO-ALVAREZ, A., CHONG, J., WONG, E., YAVORSKA, T., NARANIAN, T., CHI, M., WANG, Y. & BENTOV, Y. 2015. Coenzyme Q10 restores oocyte mitochondrial function and fertility during reproductive aging. *Aging cell,* 14**,** 887-895.

BEZAWORK-GELETA, A., ROHLENA, J., DONG, L., PACAK, K. & NEUZIL, J. 2017. Mitochondrial complex II: at the crossroads. *Trends in biochemical sciences,* 42**,** 312-325.

BIEDLER, J. L., HELSON, L. & SPENGLER, B. A. 1973. Morphology and growth, tumorigenicity, and cytogenetics of human neuroblastoma cells in continuous culture. *Cancer research,* 33**,** 2643-2652.

BIEDLER, J. L., ROFFLER-TARLOV, S., SCHACHNER, M. & FREEDMAN, L. S. 1978. Multiple neurotransmitter synthesis by human neuroblastoma cell lines and clones. *Cancer research,* 38**,** 3751-3757.

BLANZ, J., ZUNKE, F., MARKMANN, S., DAMME, M., BRAULKE, T., SAFTIG, P. & SCHWAKE, M. 2015. Mannose 6-phosphate-independent Lysosomal Sorting of LIMP-2. *Traffic,* 16**,** 1127-1136.

BONAWITZ, N. D., CLAYTON, D. A. & SHADEL, G. S. 2006. Initiation and beyond: multiple functions of the human mitochondrial transcription machinery. *Molecular cell,* 24**,** 813-825.

BOYER, P. D. 1997. The ATP synthase—a splendid molecular machine. *Annual review of biochemistry,* 66**,** 717-749.

BRADY, R. O., PENTCHEV, P. G., GAL, A. E., HIBBERT, S. R. & DEKABAN, A. S. 1974. Replacement Therapy for Inherited Enzyme Deficiency: Use of Purified Glucocerebrosidase in Gaucher's Disease. *New England Journal of Medicine,* 291**,** 989-993.

BRANDT, U. 1999. Proton translocation in the respiratory chain involving ubiquinone–a hypothetical semiquinone switch mechanism for complex I. *Biofactors,* 9**,** 95-101.

BREA-CALVO, G., HAACK, T. B., KARALL, D., OHTAKE, A., INVERNIZZI, F., CARROZZO, R., KREMER, L., DUSI, S., FAUTH, C. & SCHOLL-BÜRGI, S. 2015. COQ4 mutations cause a broad spectrum of mitochondrial disorders associated with CoQ10 deficiency. *The American Journal of Human Genetics,* 96**,** 309-317.

BRIGHTMAN, A. O., WANG, J., MIU, R. K.-M., SUN, I. L., BARR, R., CRANE, F. L. & MORRÉ, D. J. 1992. A growth factor-and hormone-stimulated NADH oxidase from rat liver plasma membrane. *Biochimica et Biophysica Acta (BBA)Biomembranes,* 1105**,** 109-117.

BROWN, D. & BRETON, S. 2000. H (+) V-ATPase-dependent luminal acidification in the kidney collecting duct and the epididymis/vas deferens: vesicle recycling and transcytotic pathways. *Journal of Experimental Biology,* 203**,** 137-145.

BROWN, M. S. & GOLDSTEIN, J. L. 1986. A receptor-mediated pathway for cholesterol homeostasis. *Science,* 232**,** 34-47.

BRZEZINSKI, P. & GENNIS, R. B. 2008. Cytochrome c oxidase: exciting progress and remaining mysteries. *Journal of bioenergetics and biomembranes,* 40**,** 521-531.

BUHAESCU, I. & IZZEDINE, H. 2007. Mevalonate pathway: a review of clinical and therapeutical implications. *Clinical biochemistry,* 40**,** 575-584.

CADENAS, E., BOVERIS, A., RAGAN, C. I. & STOPPANI, A. O. 1977. Production of superoxide radicals and hydrogen peroxide by NADH-ubiquinone reductase and ubiquinol-cytochrome c reductase from beef-heart mitochondria. *Archives of biochemistry and biophysics,* 180**,** 248-257.

CADENAS, E. & DAVIES, K. J. 2000. Mitochondrial free radical generation, oxidative stress, and aging. *Free Radical Biology and Medicine,* 29**,** 222-230.

CARSTEA, E. D., MORRIS, J. A., COLEMAN, K. G., LOFTUS, S. K., ZHANG, D., CUMMINGS, C., GU, J., ROSENFELD, M. A., PAVAN, W. J. & KRIZMAN, D. B. 1997. Niemann-Pick C1 disease gene: homology to mediators of cholesterol homeostasis. *Science,* 277**,** 228-231.

CASTELLANI, R., HIRAI, K., ALIEV, G., DREW, K. L., NUNOMURA, A., TAKEDA, A., CASH, A. D., OBRENOVICH, M. E., PERRY, G. & SMITH, M. A. 2002. Role of mitochondrial dysfunction in Alzheimer's disease. *Journal of neuroscience research,* 70**,** 357-360.

CATALDO, A. M., HAMILTON, D. J. & NIXON, R. A. 1994. Lysosomal abnormalities in degenerating neurons link neuronal compromise to senile plaque development in Alzheimer disease. *Brain research,* 640**,** 68-80.

CHEN, L. B. 1988. Mitochondrial membrane potential in living cells. *Annual review of cell biology,* 4**,** 155-181.

CHINOPOULOS, C. 2011. Mitochondrial consumption of cytosolic ATP: not so fast. *FEBS letters,* 585**,** 1255-1259.

COFFEY, E. E., BECKEL, J. M., LATIES, A. M. & MITCHELL, C. H. 2014. Lysosomal alkalization and dysfunction in human fibroblasts with the Alzheimer's disease-linked presenilin 1 A246E mutation can be reversed with cAMP. *Neuroscience,* 263**,** 111-124.

COLACURCIO, D. J. & NIXON, R. A. 2016. Disorders of lysosomal acidification—The emerging role of v-ATPase in aging and neurodegenerative disease. *Ageing Research Reviews,* 32**,** 75-88.

COLLINS, M. P., STRANSKY, L. A. & FORGAC, M. 2020. AKT Ser/Thr kinase increases V-ATPase–dependent lysosomal acidification in response to amino acid starvation in mammalian cells. *Journal of Biological Chemistry,* 295**,** 94339444.

CONTI, E., FRANKS, N. P. & BRICK, P. 1996. Crystal structure of firefly luciferase throws light on a superfamily of adenylate-forming enzymes. *Structure,* 4**,** 287298.

COSSARIZZA, A. & SALVIOLI, S. 1998. Analysis of mitochondrial membrane potential with the sensitive fluorescent probe JC-1. *Purdue Cytometry CD-ROM Series,* 4.

COTTET-ROUSSELLE, C., RONOT, X., LEVERVE, X. & MAYOL, J. F. 2011. Cytometric assessment of mitochondria using fluorescent probes. *Cytometry Part A,* 79**,** 405-425.

COUTINHO, M. F., PRATA, M. J. & ALVES, S. 2012. Mannose-6-phosphate pathway: a review on its role in lysosomal function and dysfunction. *Molecular genetics and metabolism,* 105**,** 542-550.

COX, T. M. & CACHÓN-GONZÁLEZ, M. B. 2012. The cellular pathology of lysosomal diseases. *The Journal of pathology,* 226**,** 241-254.

CRANE, F., SUN, I., CROWE, R., ALCAIN, F. & LÖW, H. 1994. Coenzyme Q10, plasma membrane oxidase and growth control. *Molecular aspects of medicine,* 15**,** s1-s11.

CRANE, F. L. 1957. Isolation of a quinone from beef heart mitochondria. *Biochim Biophys Acta.,* 25**,** 220-221.

CRANE, F. L. 2001. Biochemical functions of coenzyme Q10. *Journal of the American College of Nutrition,* 20**,** 591-598.

CRANE, F. L. & LÖW, H. 2012. The oxidative function of diferric transferrin. *Biochemistry research international,* 2012.

CRIVARO, A. N., MUCCI, J. M., BONDAR, C. M., ORMAZABAL, M. E., CECI, R., SIMONARO, C. & ROZENFELD, P. A. 2019. Efficacy of pentosan polysulfate in in vitro models of lysosomal storage disorders: Fabry and Gaucher Disease. *Plos one,* 14**,** e0217780.

CROFTS, A. R. 2004. The cytochrome bc 1 complex: function in the context of structure. *Annu. Rev. Physiol.,* 66**,** 689-733.

DE DUVE, C. 1963. The lysosome. *Scientific American,* 208**,** 64-73.

DE DUVE, C., PRESSMAN, B., GIANETTO, R., WATTIAUX, R. & APPELMANS, F. 1955. Tissue fractionation studies. 6. Intracellular distribution patterns of enzymes in rat-liver tissue. *Biochemical Journal,* 60**,** 604.

DEMERS-LAMARCHE, J., GUILLEBAUD, G., TLILI, M., TODKAR, K., BÉLANGER, N., GRONDIN, M., NGUYEN, A. P., MICHEL, J. & GERMAIN, M. 2016. Loss of mitochondrial function impairs lysosomes. *Journal of biological chemistry,* 291**,** 10263-10276.

DESBATS, M. A., LUNARDI, G., DOIMO, M., TREVISSON, E. & SALVIATI, L. 2015. Genetic bases and clinical manifestations of coenzyme Q 10 (CoQ 10) deficiency. *Journal of inherited metabolic disease,* 38**,** 145-156.

DEUS, C. M., YAMBIRE, K. F., OLIVEIRA, P. J. & RAIMUNDO, N. 2020. Mitochondria–lysosome crosstalk: from physiology to neurodegeneration. *Trends in molecular medicine,* 26**,** 71-88.

DIMRI, G. P., LEE, X., BASILE, G., ACOSTA, M., SCOTT, G., ROSKELLEY, C., MEDRANO, E. E., LINSKENS, M., RUBELJ, I. & PEREIRA-SMITH, O. 1995. A biomarker that identifies senescent human cells in culture and in aging skin in vivo. *Proceedings of the National Academy of Sciences,* 92**,** 9363-9367.

DOHERTY, E. & PERL, A. 2017. Measurement of Mitochondrial Mass by Flow Cytometry during Oxidative Stress. *Reactive oxygen species (Apex, N.C.),* 4**,** 275283.

DUBERLEY, K., HEALES, S., ABRAMOV, A., CHALASANI, A., LAND, J., RAHMAN, S. & HARGREAVES, I. 2014. Effect of Coenzyme Q10 supplementation on mitochondrial electron transport chain activity and mitochondrial oxidative stress in Coenzyme Q10 deficient human neuronal cells. *The international journal of biochemistry & cell biology,* 50**,** 60-63.

DUBERLEY, K. E., ABRAMOV, A. Y., CHALASANI, A., HEALES, S. J., RAHMAN, S. & HARGREAVES, I. P. 2013a. Human neuronal coenzyme Q10 deficiency results in global loss of mitochondrial respiratory chain activity, increased mitochondrial oxidative stress and reversal of ATP synthase activity: implications for pathogenesis and treatment. *Journal of Inherited Metabolic Disease: Official Journal of the Society for the Study of Inborn Errors of Metabolism,* 36**,** 63-73.

DUBERLEY, K. E., ABRAMOV, A. Y., CHALASANI, A., HEALES, S. J., RAHMAN, S. & HARGREAVES, I. P. 2013b. Human neuronal coenzyme Q 10 deficiency results in global loss of mitochondrial respiratory chain activity, increased mitochondrial oxidative stress and reversal of ATP synthase activity: implications for pathogenesis and treatment. *Journal of inherited metabolic disease,* 36**,** 63-73.

DUNCAN, A. J., BITNER-GLINDZICZ, M., MEUNIER, B., COSTELLO, H., HARGREAVES, I. P., LÓPEZ, L. C., HIRANO, M., QUINZII, C. M., SADOWSKI, M. I. & HARDY, J. 2009. A nonsense mutation in COQ9 causes autosomal-recessive neonatal-onset primary coenzyme Q10 deficiency: a potentially treatable form of mitochondrial disease. *The American Journal of Human Genetics,* 84**,** 558-566.

DUNCAN, A. J., HEALES, S. J., MILLS, K., EATON, S., LAND, J. M. & HARGREAVES, I. P. 2005. Determination of coenzyme Q10 status in blood mononuclear cells, skeletal muscle, and plasma by HPLC with di-propoxycoenzyme Q10 as an internal standard. *Clinical chemistry,* 51**,** 2380-2382.

DUNN, J. D., ALVAREZ, L. A., ZHANG, X. & SOLDATI, T. 2015. Reactive oxygen species and mitochondria: A nexus of cellular homeostasis. *Redox biology,* 6**,** 472-485.

DUTTON, P. L., OHNISHI, T., DARROUZET, E., LEONARD, M. A., SHARP, R. E., CIBNEY, B., DALDAL, F. & MOSER, C. C. 2000. Coenzyme Q oxidation reduction reactions in mitochondrial electron transport. *Coenzyme Q: Molecular mechanisms in health and disease***,** 65-82.

EL-GHOROURY, E. A., RASLAN, H. M., BADAWY, E. A., EL-SAAID, G. S., AGYBI, M. H., SIAM, I. & SALEM, S. I. 2009. Malondialdehyde and coenzyme Q10 in platelets and serum in type 2 diabetes mellitus: correlation with glycemic control. *Blood Coagulation & Fibrinolysis,* 20**,** 248-251.

ELTSCHINGER, S. & LOEWITH, R. 2016. TOR complexes and the maintenance of cellular homeostasis. *Trends in cell biology,* 26**,** 148-159.

EMMANUELE, V., LÓPEZ, L. C., BERARDO, A., NAINI, A., TADESSE, S., WEN, B., D'AGOSTINO, E., SOLOMON, M., DIMAURO, S., QUINZII, C. & HIRANO, M. 2012a. Heterogeneity of coenzyme Q10 deficiency: patient study and literature review. *Arch Neurol,* 69**,** 978-83.

EMMANUELE, V., LÓPEZ, L. C., BERARDO, A., NAINI, A., TADESSE, S., WEN, B., D'AGOSTINO, E., SOLOMON, M., DIMAURO, S. & QUINZII, C. 2012b. Heterogeneity of coenzyme Q10 deficiency: patient study and literature review. *Archives of neurology,* 69**,** 978-983.

ERICKSON, R., GARVER, W., CAMARGO, F., HOSSIAN, G. & HEIDENREICH, R. 2000. Pharmacological and genetic modifications of somatic cholesterol do not substantially alter the course of CNS disease in Niemann–Pick C mice. *Journal of inherited metabolic disease,* 23**,** 54-62.

ERMAK, G. & DAVIES, K. J. A. 2002. Calcium and oxidative stress: from cell signaling to cell death. *Molecular Immunology,* 38**,** 713-721.

ERNSTER, L. & DALLNER, G. 1995. Biochemical, physiological and medical aspects of ubiquinone function. *Biochimica et Biophysica Acta (BBA)-Molecular Basis of Disease,* 1271**,** 195-204.

ERNSTER, L. & FORSMARK-ANDREE, P. 1993. Ubiquinol: an endogenous antioxidant in aerobic organisms. *The clinical investigator,* 71**,** S60-S65.

ESKELINEN, E.-L. 2006. Roles of LAMP-1 and LAMP-2 in lysosome biogenesis and autophagy. *Molecular aspects of medicine,* 27**,** 495-502.

EXNER, N., LUTZ, A. K., HAASS, C. & WINKLHOFER, K. F. 2012. Mitochondrial dysfunction in Parkinson's disease: molecular mechanisms and pathophysiological consequences. *The EMBO journal,* 31**,** 3038-3062.

FASSONE, E. & RAHMAN, S. 2012. Complex I deficiency: clinical features, biochemistry and molecular genetics. *Journal of medical genetics,* 49**,** 578-590.

FEDELE, A. O. & HOPWOOD, J. J. 2010. Functional analysis of the HGSNAT gene in patients with mucopolysaccharidosis IIIC (Sanfilippo C Syndrome). *Human mutation,* 31**,** E1574-E1586.

FESTENSTEIN, G., HEATON, F., LOWE, J. & MORTON, R. 1955. A constituent of the unsaponifiable portion of animal tissue lipids (λmax. mμ.). *Biochemical Journal,* 59**,** 558.

FIGURA, K. V. & HASILIK, A. 1986. Lysosomal enzymes and their receptors. *Annual review of biochemistry,* 55**,** 167-193.

FISHER, J. E., RODAN, G. A. & RESZKA, A. A. 2000. In vivo effects of bisphosphonates on the osteoclast mevalonate pathway. *Endocrinology,* 141**,** 4793-4796.

FLINT BEAL, M. & SHULTS, C. W. 2003. Effects of Coenzyme Q10 in Huntington's disease and early Parkinson's disease. *Biofactors,* 18**,** 153-161.

FOLTS, C. J., SCOTT-HEWITT, N., PRÖSCHEL, C., MAYER-PRÖSCHEL, M. & NOBLE, M. 2016. Lysosomal re-acidification prevents lysosphingolipidinduced lysosomal impairment and cellular toxicity. *PLoS biology,* 14**,** e1002583.

FORGAC, M. 1989. Structure and function of vacuolar class of ATP-driven proton pumps. *Physiological reviews,* 69**,** 765-796.

FRALDI, A., KLEIN, A. D., MEDINA, D. L. & SETTEMBRE, C. 2016. Brain disorders due to lysosomal dysfunction. *Annual review of neuroscience,* 39**,** 277-295.

FRAUTSCHY, S. A., YANG, F., CALDERÓN, L. & COLE, G. M. 1996. Rodent models of Alzheimer's disease: Rat aβ infusion approaches to amyloid deposits. *Neurobiology of Aging,* 17**,** 311-321.

FREI, B., KIM, M. C. & AMES, B. N. 1990. Ubiquinol-10 is an effective lipid-soluble antioxidant at physiological concentrations. *Proceedings of the National Academy of Sciences,* 87**,** 4879-4883.

FU, R., YANJANIN, N. M., BIANCONI, S., PAVAN, W. J. & PORTER, F. D. 2010. Oxidative stress in Niemann-Pick disease, type C. *Mol Genet Metab,* 101**,** 214-8.

FULLER, M., MEIKLE, P. J. & HOPWOOD, J. J. 2006. Epidemiology of lysosomal storage diseases: an overview. *Fabry disease: perspectives from 5 years of FOS*.

GAHL, W., THOENE, J. & SCHNEIDER, J. 2001. Cystinosis: a disorder of lysosomal membrane transport. *The metabolic and molecular bases of inherited disease,* 4**,** 50855108.

GASPARRO, F. P., MITCHNICK, M. & NASH, J. F. 1998. A review of sunscreen safety and efficacy. *Photochemistry and photobiology,* 68**,** 243-256.

GAUCHER, P. 1882. De l'epithelioma primitif de la rate, hypertrophie la rate sans leucemie [thesis]. Paris.

GEGG, M. E., BURKE, D., HEALES, S. J., COOPER, J. M., HARDY, J., WOOD, N. W. & SCHAPIRA, A. H. 2012. Glucocerebrosidase deficiency in substantia nigra of parkinson disease brains. *Annals of neurology,* 72**,** 455-463.

GILLE, L. & NOHL, H. 2000. The existence of a lysosomal redox chain and the role of ubiquinone. *Archives of biochemistry and biophysics,* 375**,** 347-354.

GOETZ, C., HAMMERBECK, C. & BONNEVIER, J. 2018. *Flow cytometry basics for the non-expert*, Springer.

GOLDSTEIN, J. L. & BROWN, M. S. 1990. Regulation of the mevalonate pathway. *Nature,* 343**,** 425-430.

GÓMEZ-DÍAZ, C., RODRIGUEZ-AGUILERA, J. C., BARROSO, M. P., VILLALBA, J. M., NAVARRO, F., CRANE, F. L. & NAVAS, P. 1997. Antioxidant ascorbate is stabilized by NADH-coenzyme Q 10 reductase in the plasma membrane. *Journal of bioenergetics and biomembranes,* 29**,** 251-257.

GÓMEZ-SINTES, R., LEDESMA, M. D. & BOYA, P. 2016. Lysosomal cell death mechanisms in aging. *Ageing research reviews,* 32**,** 150-168.

GORDON, S. & MARTINEZ-POMARES, L. 2017. Physiological roles of macrophages. *Pflugers Archiv : European journal of physiology,* 469**,** 365-374.

GRABOWSKI, G. A. 2012. Gaucher disease and other storage disorders. *Hematology 2010, the American Society of Hematology Education Program Book,* 2012**,** 13-18.

GREEN, D. E. & TZAGOLOFF, A. 1966. The mitochondrial electron transfer chain. *Archives of biochemistry and biophysics,* 116**,** 293-304.

GUHA, S., COFFEY, E. E., LU, W., LIM, J. C., BECKEL, J. M., LATIES, A. M., BOESZEBATTAGLIA, K. & MITCHELL, C. H. 2014. Approaches for detecting lysosomal alkalinization and impaired degradation in fresh and cultured RPE cells: evidence for a role in retinal degenerations. *Experimental eye research,* 126**,** 68-76.

HACKENBROCK, C. R., CHAZOTTE, B. & GUPTE, S. S. 1986. The random collision model and a critical assessment of diffusion and collision in mitochondrial electron transport. *Journal of bioenergetics and biomembranes,* 18**,** 331-368.

HALCROW, P. W., KHAN, N., DATTA, G., OHM, J. E., CHEN, X. & GEIGER, J. D. 2019. Importance of measuring endolysosome, cytosolic, and extracellular pH in understanding the pathogenesis of and possible treatments for glioblastoma multiforme. *Cancer reports,* 2**,** e1193.

HANNAH, R., BECK, M., MORAVEC, R. & RISS, T. 2001. CellTiter-Glo™ luminescent cell viability assay: a sensitive and rapid method for determining cell viability. *Promega Cell Notes,* 2**,** 11-13.

HARDY, J. A. & HIGGINS, G. A. 1992. Alzheimer's disease: the amyloid cascade hypothesis. *Science,* 256**,** 184.

HARGREAVES, I. 2014. Coenzyme Q10 as a therapy for mitochondrial disease. *The international journal of biochemistry & cell biology,* 49**,** 105-111.

HARGREAVES, I., HEALES, S. & LAND, J. 1999. Mitochondrial respiratory chain defects are not accompanied by an increase in the activities of lactate dehydrogenase or manganese superoxide dismutase in paediatric skeletal muscle biopsies. *Journal of inherited metabolic disease,* 22**,** 925-931.

HARGREAVES, I., HEATON, R. A. & MANTLE, D. 2020. Disorders of human coenzyme q10 metabolism: An overview. *International Journal of Molecular Sciences,* 21**,** 6695.

HARGREAVES, I., SHEENA, Y., LAND, J. & HEALES, S. 2005. Glutathione deficiency in patients with mitochondrial disease: implications for pathogenesis and treatment. *Journal of inherited metabolic disease,* 28**,** 81.

HARGREAVES, I. P. 2003. Ubiquinone: cholesterol's reclusive cousin. *Annals of clinical biochemistry,* 40**,** 207-218.

HARPER, C. R. & JACOBSON, T. A. 2010. Evidence-based management of statin myopathy. *Current atherosclerosis reports,* 12**,** 322-330.

HASHEMI, S. S., ZARE-ABDOLLAHI, D., BAKHSHANDEH, M. K., VAFAEE, A., ABOLHASANI, S., INANLOO RAHATLOO, K., DANAEEFARD, F., FARBOODI, N., ROHANI, M. & ALAVI, A. 2021. Clinical spectrum in multiple families with primary COQ10 deficiency. *American Journal of Medical Genetics Part A,* 185**,** 440-452.

HEATON, R. A., HEALES, S., RAHMAN, K., SEXTON, D. W. & HARGREAVES, I. 2020. The Effect of Cellular Coenzyme Q(10) Deficiency on Lysosomal Acidification. *J Clin Med,* 9.

HEERINGA, S. F., CHERNIN, G., CHAKI, M., ZHOU, W., SLOAN, A. J., JI, Z., XIE, L. X., SALVIATI, L., HURD, T. W. & VEGA-WARNER, V. 2011. COQ6 mutations in human patients produce nephrotic syndrome with sensorineural deafness. *The Journal of clinical investigation,* 121**,** 2013-2024.

HIGAKI, K., LI, L., BAHRUDIN, U., OKUZAWA, S., TAKAMURAM, A., YAMAMOTO, K., ADACHI1, K., PARAGUISON, R. C., TAKAI, T. & IKEHATA, H. 2011. Chemical chaperone therapy: chaperone effect on mutant enzyme and cellular pathophysiology in β-galactosidase deficiency. *Human mutation,* 32**,** 843-852.

HILLE-REHFELD, A. 1995. Mannose 6-phosphate receptors in sorting and transport of lysosomal enzymes. *Biochimica et Biophysica Acta (BBA)-Reviews on Biomembranes,* 1241**,** 177-194.

HINKLE, P. C., BUTOW, R. A., RACKER, E. & CHANCE, B. 1967. Partial resolution of the enzymes catalyzing oxidative phosphorylation XV. Reverse electron transfer in the Flavin-cytochrome B region of the respiratory chain of beef heart submitochondrial particles. *Journal of Biological Chemistry,* 242**,** 5169-5173.

HINSON, D., CHAMBLISS, K., TOTH, M., TANAKA, R. & GIBSON, K. 1997. Posttranslational regulation of mevalonate kinase by intermediates of the cholesterol and nonsterol isoprene biosynthetic pathways. *Journal of lipid research,* 38**,** 2216-2223.

HINTON, A., BOND, S. & FORGAC, M. 2009. V-ATPase functions in normal and disease processes. *Pflügers Archiv - European Journal of Physiology,* 457**,** 589-598.

HIRST, J. 2010. Towards the molecular mechanism of respiratory complex I. *Biochemical Journal,* 425**,** 327-339.

HOSSEINZADEH-ATTAR, M., ESHRAGHIAN, M., NAKHJAVANI, M., KHORAMI, E. & ESTEGHAMATI, A. 2013. The effect of coenzyme Q10 supplementation on metabolic status of type 2 diabetic patients. *Minerva gastroenterologica e dietologica,* 59**,** 231-236.

HUIZING, M. & GAHL, W. A. 2020. Inherited disorders of lysosomal membrane transporters. *Biochimica et Biophysica Acta (BBA)-Biomembranes,* 1862**,** 183336.

HUNZIKER, W., SIMMEN, T. & HÖNING, S. 1996. Trafficking of lysosomal membrane proteins in polarized kidney cells. *Nephrologie,* 17**,** 347-350.

ISHIDA, Y., NAYAK, S., MINDELL, J. A. & GRABE, M. 2013. A model of lysosomal pH regulation. *The Journal of general physiology,* 141**,** 705-720.

ISTVAN, E. S. & DEISENHOFER, J. 2001. Structural mechanism for statin inhibition of HMG-CoA reductase. *Science,* 292**,** 1160-1164.

IVANKOVIC, D., CHAU, K. Y., SCHAPIRA, A. H. & GEGG, M. E. 2016. Mitochondrial and lysosomal biogenesis are activated following PINK1/parkin-mediated mitophagy. *J Neurochem,* 136**,** 388-402.

JADOT, M., LIN, L., SLEAT, D. E., SOHAR, I., HSU, M.-S., PINTAR, J., DUBOIS, F., WATTIAUX-DE CONINCK, S., WATTIAUX, R. & LOBEL, P. 1999. Subcellular localization of mannose 6-phosphate glycoproteins in rat brain. *Journal of Biological Chemistry,* 274**,** 21104-21113.

JEYAKUMAR, M., DWEK, R. A., BUTTERS, T. D. & PLATT, F. M. 2005. Storage solutions: treating lysosomal disorders of the brain. *Nature Reviews Neuroscience,* 6**,** 713-725.

JMOUDIAK, M. & FUTERMAN, A. H. 2005. Gaucher disease: pathological mechanisms and modern management. *British journal of haematology,* 129**,** 178188.

KABUTA, T., FURUTA, A., AOKI, S., FURUTA, K. & WADA, K. 2008. Aberrant interaction between Parkinson disease-associated mutant UCH-L1 and the lysosomal receptor for chaperone-mediated autophagy. *The Journal of biological chemistry,* 283**,** 23731-23738.

KAGAN, V., FABISIAK, J. & QUINN, P. 2000. Coenzyme Q and vitamin E need each other as antioxidants. *Protoplasma,* 214**,** 11-18.

KALEN, A., NORLING, B., APPELKVIST, E. & DALLNER, G. 1987. Ubiquinone biosynthesis by the microsomal fraction from rat liver. *Biochimica et Biophysica Acta (BBA)-General Subjects,* 926**,** 70-78.

KANG, C.-C., HUANG, W.-C., KOUH, C.-W., WANG, Z.-F., CHO, C.-C., CHANG, C.-C., WANG, C.-L., CHANG, T.-C., SEEMANN, J. & HUANG, L. J.-S. 2013. Chemical principles for the design of a novel fluorescent probe with high cancer-targeting selectivity and sensitivity. *Integrative Biology,* 5**,** 1217-1228.

KASOTE, D. M., HEGDE, M. V. & KATYARE, S. S. 2013. Mitochondrial dysfunction in psychiatric and neurological diseases: cause (s), consequence (s), and implications of antioxidant therapy. *Biofactors,* 39**,** 392-406.

KAWAMUKAI, M. 2009. Biosynthesis and bioproduction of coenzyme Q10 by yeasts and other organisms. *Biotechnology and applied biochemistry,* 53**,** 217-226.

KELLEHER, R. J. & SHEN, J. 2017. Presenilin-1 mutations and Alzheimer's disease. *Proceedings of the National Academy of Sciences,* 114**,** 629-631.

KHOLODENKO, B. N., CASCANTE, M. & WESTERHOFF, H. V. 1995. Control theory of metabolic channelling. *Molecular and cellular biochemistry,* 143**,** 151-168.

KLIONSKY, D. J. 2008. Autophagy revisited: a conversation with Christian de Duve. *Autophagy,* 4**,** 740-743.

KLIONSKY, D. J., ELAZAR, Z., SEGLEN, P. O. & RUBINSZTEIN, D. C. 2008. Does bafilomycin A1 block the fusion of autophagosomes with lysosomes? *Autophagy,* 4**,** 849-850.

KOLE, A. J., ANNIS, R. P. & DESHMUKH, M. 2013. Mature neurons: equipped for survival. *Cell death & disease,* 4**,** e689-e689.

KRÖGER, A., KLINGENBERG, M. & SCHWEIDLER, S. 1973. Further evidence for the pool function of ubiquinone as derived from the inhibition of the electron transport by antimycin. *European journal of biochemistry,* 39**,** 313-323.

KURZ, D. J., DECARY, S., HONG, Y. & ERUSALIMSKY, J. D. 2000. Senescenceassociated (beta)-galactosidase reflects an increase in lysosomal mass during replicative ageing of human endothelial cells. *Journal of cell science,* 113**,** 36133622.

KURZ, T., TERMAN, A., GUSTAFSSON, B. & BRUNK, U. T. 2008. Lysosomes and oxidative stress in aging and apoptosis. *Biochimica et Biophysica Acta (BBA) - General Subjects,* 1780**,** 1291-1303.

LACHMANN, R., GRANT, I., HALSALL, D. & COX, T. 2004. Twin pairs showing discordance of phenotype in adult Gaucher's disease. *Qjm,* 97**,** 199-204.

LAGIER-TOURENNE, C., TAZIR, M., LÓPEZ, L. C., QUINZII, C. M., ASSOUM, M., DROUOT, N., BUSSO, C., MAKRI, S., ALI-PACHA, L. & BENHASSINE, T. 2008. ADCK3, an ancestral kinase, is mutated in a form of recessive ataxia associated with coenzyme Q10 deficiency. *The American Journal of Human Genetics,* 82**,** 661-672.

LARM, J. A., VAILLANT, F., LINNANE, A. W. & LAWEN, A. 1994. Up-regulation of the plasma membrane oxidoreductase as a prerequisite for the viability of human Namalwa rho 0 cells. *Journal of Biological Chemistry,* 269**,** 30097-30100.

LAWRENCE, R. E. & ZONCU, R. 2019. The lysosome as a cellular centre for signalling, metabolism and quality control. *Nature cell biology,* 21**,** 133-142.

LE BER, I., DUBOURG, O., BENOIST, J.-F., JARDEL, C., MOCHEL, F., KOENIG, M., BRICE, A., LOMBES, A. & DÜRR, A. 2007. Muscle coenzyme Q10 deficiencies in ataxia with oculomotor apraxia 1. *Neurology,* 68**,** 295-297.

LECOEUR, H. 2002. Nuclear Apoptosis Detection by Flow Cytometry: Influence of Endogenous Endonucleases. *Experimental Cell Research,* 277**,** 1-14.

LEE, R. E. 1968. The fine structure of the cerebroside occurring in Gaucher's disease. *Proceedings of the National Academy of Sciences,* 61**,** 484-489.

LIJNEN, P. J., VAN PELT, J. F. & FAGARD, R. H. 2012. Stimulation of reactive oxygen species and collagen synthesis by angiotensin II in cardiac fibroblasts. *Cardiovascular therapeutics,* 30**,** e1-e8.

LIN, H.-J., HERMAN, P., KANG, J. S. & LAKOWICZ, J. R. 2001. Fluorescence lifetime characterization of novel low-pH probes. *Analytical biochemistry,* 294**,** 118-125.

LITON, P. B., LIN, Y., LUNA, C., LI, G., GONZALEZ, P. & EPSTEIN, D. L. 2008. Cultured porcine trabecular meshwork cells display altered lysosomal function when subjected to chronic oxidative stress. *Investigative ophthalmology & visual science,* 49**,** 3961-3969.

LIU, G., MA, D., LI, J., LUO, C., SUN, Y., ZHANG, J., HU, P., TANG, W. & XU, Z. 2020. A novel COQ8A missense variant associated with a mild form of primary coenzyme Q10 deficiency type 4. *Clinical Biochemistry,* 84**,** 93-98.

LIU, X., KIM, C. N., YANG, J., JEMMERSON, R. & WANG, X. 1996. Induction of apoptotic program in cell-free extracts: requirement for dATP and cytochrome c. *Cell,* 86**,** 147-157.

LIU, Y.-T., HERSHESON, J., PLAGNOL, V., FAWCETT, K., DUBERLEY, K. E. C., PREZA, E., HARGREAVES, I. P., CHALASANI, A., LAURÁ, M., WOOD, N. W., REILLY, M. M. & HOULDEN, H. 2014. Autosomal-recessive cerebellar ataxia caused by a novel ADCK3 mutation that elongates the protein: clinical, genetic and biochemical characterisation. *Journal of Neurology, Neurosurgery & Psychiatry,* 85**,** 493-498.

LOHMAN, D. C., FOROUHAR, F., BEEBE, E. T., STEFELY, M. S., MINOGUE, C. E., ULBRICH, A., STEFELY, J. A., SUKUMAR, S., LUNA-SÁNCHEZ, M. & JOCHEM, A. 2014. Mitochondrial COQ9 is a lipid-binding protein that associates with COQ7 to enable coenzyme Q biosynthesis. *Proceedings of the National Academy of Sciences,* 111**,** E4697-E4705.

LÓPEZ, L. C., QUINZII, C. M., AREA, E., NAINI, A., RAHMAN, S., SCHUELKE, M., SALVIATI, L., DIMAURO, S. & HIRANO, M. 2010. Treatment of CoQ10 deficient fibroblasts with ubiquinone, CoQ analogs, and vitamin C: time-and compound-dependent effects. *PLoS One,* 5**,** e11897.

LÓPEZ, L. C., SCHUELKE, M., QUINZII, C. M., KANKI, T., RODENBURG, R. J., NAINI, A., DIMAURO, S. & HIRANO, M. 2006. Leigh syndrome with nephropathy and CoQ10 deficiency due to decaprenyl diphosphate synthase subunit 2 (PDSS2) mutations. *The American Journal of Human Genetics,* 79**,** 11251129.

LÖW, H., CRANE, F. L. & MORRÉ, D. J. 2012. Putting together a plasma membrane NADH oxidase: a tale of three laboratories. *The international journal of biochemistry & cell biology,* 44**,** 1834-1838.

LOWRY, O. H., ROSEBROUGH, N. J., FARR, A. L. & RANDALL, R. J. 1951. Protein measurement with the Folin phenol reagent. *Journal of biological chemistry,* 193**,** 265-275.

LÜBKE, T., LOBEL, P. & SLEAT, D. E. 2009. Proteomics of the lysosome. *Biochimica et Biophysica Acta (BBA)-Molecular Cell Research,* 1793**,** 625-635.

LUDWIG, T., MUNIER-LEHMANN, H., BAUER, U., HOLLINSHEAD, M., OVITT, C., LOBEL, P. & HOFLACK, B. 1994. Differential sorting of lysosomal enzymes in mannose 6-phosphate receptor-deficient fibroblasts. *The EMBO journal,* 13**,** 3430-3437.

MA, L., OUYANG, Q., WERTHMANN, G. C., THOMPSON, H. M. & MORROW, E. M. 2017. Live-cell Microscopy and Fluorescence-based Measurement of Luminal pH in Intracellular Organelles. *Frontiers in cell and developmental biology,* 5**,** 71.

MALICDAN, M. C. V., VILBOUX, T., BEN-ZEEV, B., GUO, J., ELIYAHU, A., PODESHAKKED, B., DORI, A., KAKANI, S., CHANDRASEKHARAPPA, S. C. & FERREIRA, C. R. 2018. A novel inborn error of the coenzyme Q10 biosynthesis pathway: cerebellar ataxia and static encephalomyopathy due to COQ5 Cmethyltransferase deficiency. *Human mutation,* 39**,** 69-79.

MALONEY, P. C., KASHKET, E. & WILSON, T. H. 1974. A protonmotive force drives ATP synthesis in bacteria. *Proceedings of the National Academy of Sciences,* 71**,** 3896-3900.

MANNING-BOĞ, A. B., SCHÜLE, B. & LANGSTON, J. W. 2009. Alpha-synucleinglucocerebrosidase interactions in pharmacological Gaucher models: a biological link between Gaucher disease and parkinsonism. *Neurotoxicology,* 30**,** 1127-1132.

MANTLE, D. & HARGREAVES, I. P. 2018. Ataxia and coenzyme Q10: An overview. *British Journal of Neuroscience Nursing,* 14**,** 108-114.

MANZAR, H., ABDULHUSSEIN, D., YAP, T. E. & CORDEIRO, M. F. 2020. Cellular Consequences of Coenzyme Q10 Deficiency in Neurodegeneration of the Retina and Brain. *International Journal of Molecular Sciences,* 21**,** 9299.

MARBOIS, B., GIN, P., GULMEZIAN, M. & CLARKE, C. F. 2009. The yeast Coq4 polypeptide organizes a mitochondrial protein complex essential for coenzyme Q biosynthesis. *Biochimica et Biophysica Acta (BBA)-Molecular and Cell Biology of Lipids,* 1791**,** 69-75.

MARTIN, K. & BARRETT, J. 2002. Reactive oxygen species as double-edged swords in cellular processes: low-dose cell signaling versus high-dose toxicity. *Human & experimental toxicology,* 21**,** 71-75.

MARTINEFSKI, M. R., CONTIN, M. D., RODRIGUEZ, M. R., GERÉZ, E. M., GALLEANO, M. L., LUCANGIOLI, S. E., BIANCIOTTI, L. G. & TRIPODI, V. P. 2014. Coenzyme Q in pregnant women and rats with intrahepatic cholestasis. *Liver International,* 34**,** 1040-1048.

MASTERS, C. L., SIMMS, G., WEINMAN, N. A., MULTHAUP, G., MCDONALD, B. L. & BEYREUTHER, K. 1985. Amyloid plaque core protein in Alzheimer disease and Down syndrome. *Proceedings of the National Academy of Sciences of the United States of America,* 82**,** 4245-4249.

MATTERA, R., BOEHM, M., CHAUDHURI, R., PRABHU, Y. & BONIFACINO, J. S. 2011. Conservation and diversification of dileucine signal recognition by adaptor protein (AP) complex variants. *Journal of Biological Chemistry,* 286**,** 20222030.

MEGANATHAN, R. 2001. Ubiquinone biosynthesis in microorganisms. *FEMS microbiology letters,* 203**,** 131-139.

MENZ, R. I., WALKER, J. E. & LESLIE, A. G. 2001. Structure of bovine mitochondrial F1-ATPase with nucleotide bound to all three catalytic sites: implications for the mechanism of rotary catalysis. *Cell,* 106**,** 331-341.

MILLER, R. J. 1998. Mitochondria–the Kraken wakes! *Trends in neurosciences,* 21**,** 9597.

MITCHELL, P. 1961. Coupling of phosphorylation to electron and hydrogen transfer by a chemi-osmotic type of mechanism. *Nature,* 191**,** 144-148.

MITCHELL, P. 1966. Chemiosmotic coupling in oxidative and photosynthetic phosphorylation. *Biological Reviews,* 41**,** 445-501.

MITCHELL, P. 1975. The protonmotive Q cycle: a general formulation. *FEBS letters,* 59**,** 137-139.

MOIRÉ, D. J., BRIGHTMAN, A. O., WU, L. Y., BARR, R., LEAK, B. & CRANE, F. L. 1988. Role of plasma membrane redox activities in elongation growth in plants. *Physiologia Plantarum,* 73**,** 187-193.

MOKHTARIYE, A., HAGH-NAZARI, L., VARASTEH, A.-R. & KEYFI, F. 2019. Diagnostic methods for Lysosomal storage disease. *Reports of biochemistry & molecular biology,* 7**,** 119.

MOLLET, J., DELAHODDE, A., SERRE, V., CHRETIEN, D., SCHLEMMER, D., LOMBES, A., BODDAERT, N., DESGUERRE, I., DE LONLAY, P. & DE BAULNY, H. O. 2008. CABC1 gene mutations cause ubiquinone deficiency with cerebellar ataxia and seizures. *The American Journal of Human Genetics,* 82**,** 623-630.

MOLLET, J., GIURGEA, I., SCHLEMMER, D., DALLNER, G., CHRETIEN, D., DELAHODDE, A., BACQ, D., DE LONLAY, P., MUNNICH, A. & RÖTIG, A. 2007. Prenyldiphosphate synthase, subunit 1 (PDSS1) and OH-benzoate polyprenyltransferase (COQ2) mutations in ubiquinone deficiency and oxidative phosphorylation disorders. *The Journal of clinical investigation,* 117**,** 765-772.

MONTERO, R., GRAZINA, M., LÓPEZ-GALLARDO, E., MONTOYA, J., BRIONES, P., NAVARRO-SASTRE, A., LAND, J. M., HARGREAVES, I. P., ARTUCH, R. & MARIA DEL MAR, O. C. 2013. Coenzyme Q10 deficiency in mitochondrial DNA depletion syndromes. *Mitochondrion,* 13**,** 337-341.

MORGAN, A. J., PLATT, F. M., LLOYD-EVANS, E. & GALIONE, A. 2011. Molecular mechanisms of endolysosomal Ca2+ signalling in health and disease. *Biochemical Journal,* 439**,** 349-378.

MORTENSEN, S. A., ROSENFELDT, F., KUMAR, A., DOLLINER, P., FILIPIAK, K. J., PELLA, D., ALEHAGEN, U., STEURER, G., LITTARRU, G. P. & INVESTIGATORS, Q.-S. S. 2014. The effect of coenzyme Q10 on morbidity and mortality in chronic heart failure: results from Q-SYMBIO: a randomized double-blind trial. *JACC: Heart Failure,* 2**,** 641-649.

MÜLLER, T., BÜTTNER, T., GHOLIPOUR, A.-F. & KUHN, W. 2003a. Coenzyme Q10 supplementation provides mild symptomatic benefit in patients with Parkinson's disease. *Neuroscience Letters,* 341**,** 201-204.

MÜLLER, T., MEISEL, M., RUSS, H. & PRZUNTEK, H. 2003b. Motor impairment influences Farnsworth-Munsell 100 Hue test error scores in Parkinson's disease patients. *J Neurol Sci,* 213**,** 61-5.

MURPHY, M. P. & LEVINE, H., 3RD 2010. Alzheimer's disease and the amyloid-beta peptide. *Journal of Alzheimer's disease : JAD,* 19**,** 311-323.

MUSUMECI, O., NAINI, A., SLONIM, A., SKAVIN, N., HADJIGEORGIOU, G., KRAWIECKI, N., WEISSMAN, B., TSAO, C.-Y., MENDELL, J. & SHANSKE, S. 2001. Familial cerebellar ataxia with muscle coenzyme Q10 deficiency. *Neurology,* 56**,** 849-855.

NAKANO, M., IMAMURA, H., TOEI, M., TAMAKOSHI, M., YOSHIDA, M. & YOKOYAMA, K. 2008. ATP hydrolysis and synthesis of a rotary motor VATPase from Thermus thermophilus. *Journal of Biological Chemistry,* 283**,** 2078920796.

NALYSNYK, L., ROTELLA, P., SIMEONE, J. C., HAMED, A. & WEINREB, N. 2017. Gaucher disease epidemiology and natural history: a comprehensive review of the literature. *Hematology,* 22**,** 65-73.

NAVARRO, F., ARROYO, A., MARTÍN, S. F., BELLO, R. I., DE CABO, R., BURGESS, J. R., NAVAS, P. & VILLALBA, J. M. 1999. Protective role of ubiquinone in vitamin E and selenium-deficient plasma membranes. *Biofactors,* 9**,** 163-170.

NAVAS, P., CASCAJO, M. V., ALCÁZAR-FABRA, M., HERNÁNDEZ-CAMACHO, J. D., SÁNCHEZ-CUESTA, A., RODRÍGUEZ, A. B. C., BALLESTEROSSIMARRO, M., ARROYO-LUQUE, A., RODRÍGUEZ-AGUILERA, J. C. & FERNÁNDEZ-AYALA, D. J. 2021. Secondary CoQ10 deficiency, bioenergetics unbalance in disease and aging. *BioFactors*.

NEERGHEEN, V., CHALASANI, A., WAINWRIGHT, L., YUBERO, D., MONTERO, R., ARTUCH, R. & HARGREAVES, I. 2017. Coenzyme Q10 in the treatment of mitochondrial disease. *Journal of Inborn Errors of Metabolism and Screening,* 5**,** 2326409817707771.

NEUFELD, E. B., WASTNEY, M., PATEL, S., SURESH, S., COONEY, A. M., DWYER, N. K., ROFF, C. F., OHNO, K., MORRIS, J. A. & CARSTEA, E. D. 1999. The Niemann-Pick C1 protein resides in a vesicular compartment linked to retrograde transport of multiple lysosomal cargo. *Journal of Biological Chemistry,* 274**,** 9627-9635.

NEZICH, C. L., WANG, C., FOGEL, A. I. & YOULE, R. J. 2015. MiT/TFE transcription factors are activated during mitophagy downstream of Parkin and Atg5. *Journal of Cell Biology,* 210**,** 435-450.

NIXON, R. A., MATHEWS, P. M. & CATALDO, A. M. 2001. The neuronal endosomallysosomal system in Alzheimer's disease. *Journal of Alzheimer's Disease,* 3**,** 97107.

NIXON, R. A., YANG, D.-S. & LEE, J.-H. 2008. Neurodegenerative lysosomal disorders: A continuum from development to late age. *Autophagy,* 4**,** 590-599.

NOHL, H. & GILLE, L. 2002. The bifunctional activity of ubiquinone in lysosomal membranes. *Biogerontology,* 3**,** 125-131.

NOHL, H. & GILLE, L. 2005. Lysosomal ROS formation. *Redox Report,* 10**,** 199-205.

ODDO, S., CACCAMO, A., SHEPHERD, J. D., MURPHY, M. P., GOLDE, T. E., KAYED, R., METHERATE, R., MATTSON, M. P., AKBARI, Y. & LAFERLA, F. M. 2003. Triple-transgenic model of Alzheimer's disease with plaques and tangles: intracellular Aβ and synaptic dysfunction. *Neuron,* 39**,** 409-421.

OGASAHARA, S., ENGEL, A. G., FRENS, D. & MACK, D. 1989. Muscle coenzyme Q deficiency in familial mitochondrial encephalomyopathy. *Proceedings of the National Academy of Sciences,* 86**,** 2379-2382.

OHKUMA, S. & POOLE, B. 1978. Fluorescence probe measurement of the intralysosomal pH in living cells and the perturbation of pH by various agents. *Proceedings of the National Academy of Sciences,* 75**,** 3327-3331.

OKADA, K., KAINOU, T., MATSUDA, H. & KAWAMUKAI, M. 1998. Biological significance of the side chain length of ubiquinone in Saccharomyces cerevisiae. *FEBS letters,* 431**,** 241-244.

OKOUCHI, M., EKSHYYAN, O., MARACINE, M. & AW, T. Y. 2007. Neuronal apoptosis in neurodegeneration. *Antioxidants & redox signaling,* 9**,** 1059-1096.

OKUNO, D., IINO, R. & NOJI, H. 2011. Rotation and structure of FoF1-ATP synthase. *The Journal of Biochemistry,* 149**,** 655-664.

OPARKA, M., WALCZAK, J., MALINSKA, D., VAN OPPEN, L. M., SZCZEPANOWSKA, J., KOOPMAN, W. J. & WIECKOWSKI, M. R. 2016. Quantifying ROS levels using CM-H2DCFDA and HyPer. *Methods,* 109**,** 3-11.

OTT, M., GOGVADZE, V., ORRENIUS, S. & ZHIVOTOVSKY, B. 2007. Mitochondria, oxidative stress and cell death. *Apoptosis,* 12**,** 913-922.

PAPAKRIVOS, J., SA, J. M. & WELLEMS, T. E. 2012. Functional characterization of the Plasmodium falciparum chloroquine-resistance transporter (PfCRT) in transformed Dictyostelium discoideum vesicles. *PLoS One,* 7.

PARKINSON-LAWRENCE, E. J., SHANDALA, T., PRODOEHL, M., PLEW, R., BORLACE, G. N. & BROOKS, D. A. 2010. Lysosomal storage disease: revealing lysosomal function and physiology. *Physiology,* 25**,** 102-115.

PASTORES, G. M. & HUGHES, D. A. 2018. Gaucher disease. *GeneReviews®[Internet].* University of Washington, Seattle.

PATRICK, A. 1965. A deficiency of glucocerebrosidase in Gaucher's disease. *Biochemical Journal,* 97**,** 17C-24C.

PATTERSON, M. C., HENDRIKSZ, C. J., WALTERFANG, M., SEDEL, F., VANIER, M. T., WIJBURG, F. & GROUP, N.-C. G. W. 2012. Recommendations for the diagnosis and management of Niemann–Pick disease type C: an update. *Molecular genetics and metabolism,* 106**,** 330-344.

PENDERGRASS, W., WOLF, N. & POOT, M. 2004. Efficacy of MitoTracker Green™ and CMXrosamine to measure changes in mitochondrial membrane potentials in living cells and tissues. *Cytometry Part A: the journal of the International Society for Analytical Cytology,* 61**,** 162-169.

PERRY, S. W., NORMAN, J. P., BARBIERI, J., BROWN, E. B. & GELBARD, H. A. 2011. Mitochondrial membrane potential probes and the proton gradient: a practical usage guide. *Biotechniques,* 50**,** 98-115.

PESSAYRE, D., MANSOURI, A., HAOUZI, D. & FROMENTY, B. 1999. Hepatotoxicity due to mitochondrial dysfunction. *Cell biology and toxicology,* 15**,** 367-373.

PIERZYŃSKA-MACH, A., JANOWSKI, P. A. & DOBRUCKI, J. W. 2014. Evaluation of acridine orange, LysoTracker Red, and quinacrine as fluorescent probes for long-term tracking of acidic vesicles. *Cytometry Part A,* 85**,** 729-737.

PLATT, F. M., BOLAND, B. & VAN DER SPOEL, A. C. 2012. Lysosomal storage disorders: The cellular impact of lysosomal dysfunction. *J Cell Biol,* 199**,** 723734.

PONSFORD, A. H., RYAN, T. A., RAIMONDI, A., COCUCCI, E., WYCISLO, S. A., FRÖHLICH, F., SWAN, L. E. & STAGI, M. 2021. Live imaging of intra-lysosome pH in cell lines and primary neuronal culture using a novel genetically encoded biosensor. *Autophagy,* 17**,** 1500-1518.

POOLE, A. C., THOMAS, R. E., ANDREWS, L. A., MCBRIDE, H. M., WHITWORTH, A. J. & PALLANCK, L. J. 2008. The PINK1/Parkin pathway regulates mitochondrial morphology. *Proceedings of the National Academy of Sciences,* 105**,** 1638-1643.

POON, W. W., DO, T. Q., MARBOIS, B. N. & CLARKE, C. F. 1997. Sensitivity to treatment with polyunsaturated fatty acids is a general characteristic of the ubiquinone-deficient yeast coq mutants. *Molecular aspects of medicine,* 18**,** 121127.

PRAVST, I., RODRÍGUEZ AGUILERA, J. C., CORTES RODRIGUEZ, A. B., JAZBAR, J., LOCATELLI, I., HRISTOV, H. & ŽMITEK, K. 2020. Comparative Bioavailability of Different Coenzyme Q10 Formulations in Healthy Elderly Individuals. *Nutrients,* 12**,** 784.

PRESLEY, A. D., FULLER, K. M. & ARRIAGA, E. A. 2003. MitoTracker Green labeling of mitochondrial proteins and their subsequent analysis by capillary electrophoresis with laser-induced fluorescence detection. *Journal of Chromatography B,* 793**,** 141-150.

QUINZII, C., KATTAH, A., NAINI, A., AKMAN, H., MOOTHA, V., DIMAURO, S. & HIRANO, M. 2005. Coenzyme Q deficiency and cerebellar ataxia associated with an aprataxin mutation. *Neurology,* 64**,** 539-541.

QUINZII, C., NAINI, A., SALVIATI, L., TREVISSON, E., NAVAS, P., DIMAURO, S. & HIRANO, M. 2006. A mutation in para-hydroxybenzoate-polyprenyl transferase (COQ2) causes primary coenzyme Q10 deficiency. *The American Journal of Human Genetics,* 78**,** 345-349.

QUINZII, C. M., EMMANUELE, V. & HIRANO, M. 2014. Clinical presentations of coenzyme q10 deficiency syndrome. *Molecular syndromology,* 5**,** 141-146.

QUINZII, C. M. & HIRANO, M. 2011. Primary and secondary CoQ10 deficiencies in humans. *Biofactors,* 37**,** 361-365.

QUINZII, C. M., LÓPEZ, L. C., GILKERSON, R. W., DORADO, B., COKU, J., NAINI, A. B., LAGIER-TOURENNE, C., SCHUELKE, M., SALVIATI, L. & CARROZZO, R. 2010. Reactive oxygen species, oxidative stress, and cell death correlate with level of CoQ10 deficiency. *The FASEB Journal,* 24**,** 3733-3743.

RADCLIFF, G. & JAROSZESKI, M. J. 1998. Basics of flow cytometry. *Flow Cytometry Protocols.* Springer.

RAHAL, R., DANIELE, S., HUBERT-PFALZGRAF, L. G., GUYOT-FERRÉOL, V. & TRANCHANT, J. F. 2008. Synthesis of para-Amino Benzoic Acid–TiO2 Hybrid Nanostructures of Controlled Functionality by an Aqueous One-Step Process. Wiley Online Library.

RAHMAN, S., HARGREAVES, I., CLAYTON, P. & HEALES, S. 2001. Neonatal presentation of coenzyme Q10 deficiency. *The Journal of pediatrics,* 139**,** 456-458.

RAMEZANI, M., SAHRAEI, Z., SIMANI, L., HEYDARI, K. & SHAHIDI, F. 2020. Coenzyme Q10 supplementation in acute ischemic stroke: Is it beneficial in short-term administration? *Nutritional Neuroscience,* 23**,** 640-645.

RAO, S. P., ALONSO, S., RAND, L., DICK, T. & PETHE, K. 2008. The protonmotive force is required for maintaining ATP homeostasis and viability of hypoxic, nonreplicating Mycobacterium tuberculosis. *Proceedings of the National Academy of Sciences,* 105**,** 11945-11950.

REERS, M., SMITH, T. W. & CHEN, L. B. 1991. J-aggregate formation of a carbocyanine as a quantitative fluorescent indicator of membrane potential. *Biochemistry,* 30**,** 4480-4486.

RICCARDI, C. & NICOLETTI, I. 2006. Analysis of apoptosis by propidium iodide staining and flow cytometry. *Nature protocols,* 1**,** 1458.

RIESKE, J. S. 1976. Composition, structure, and function of complex III of the respiratory chain. *Biochimica et Biophysica Acta (BBA)-Reviews on Bioenergetics,* 456**,** 195-247.

RIJNBOUTT, S., AERTS, H., GEUZE, H., TAGER, J. & STROUS, G. 1991. Mannose 6phosphate-independent membrane association of cathepsin D, glucocerebrosidase, and sphingolipid-activating protein in HepG2 cells. *Journal of Biological Chemistry,* 266**,** 4862-4868.

ROLFE, D. & BROWN, G. C. 1997. Cellular energy utilization and molecular origin of standard metabolic rate in mammals. *Physiological reviews,* 77**,** 731-758.

ROSEN, W. G., MOHS, R. C. & DAVIS, K. L. 1984. A new rating scale for Alzheimer's disease. *The American journal of psychiatry*.

ROSSIER, M. F. 2006. T channels and steroid biosynthesis: in search of a link with mitochondria. *Cell Calcium,* 40**,** 155-164.

RÖTIG, A., APPELKVIST, E.-L., GEROMEL, V., CHRETIEN, D., KADHOM, N., EDERY, P., LEBIDEAU, M., DALLNER, G., MUNNICH, A. & ERNSTER, L. 2000. Quinone-responsive multiple respiratory-chain dysfunction due to widespread coenzyme Q10 deficiency. *The Lancet,* 356**,** 391-395.

RUBINSZTEIN, D. C. 2006. The roles of intracellular protein-degradation pathways in neurodegeneration. *Nature,* 443**,** 780.

SACCONI, S., TREVISSON, E., SALVIATI, L., AYMÉ, S., RIGAL, O., REDONDO, A. G., MANCUSO, M., SICILIANO, G., TONIN, P. & ANGELINI, C. 2010. Coenzyme Q10 is frequently reduced in muscle of patients with mitochondrial myopathy. *Neuromuscular Disorders,* 20**,** 44-48.

SAFTIG, P. & KLUMPERMAN, J. 2009. Lysosome biogenesis and lysosomal membrane proteins: trafficking meets function. *Nature reviews Molecular cell biology,* 10**,** 623.

SAFTIG, P., SCHRÖDER, B. & BLANZ, J. 2010. Lysosomal membrane proteins: life between acid and neutral conditions. Portland Press Ltd.

SAIKI, R., NAGATA, A., KAINOU, T., MATSUDA, H. & KAWAMUKAI, M. 2005. Characterization of solanesyl and decaprenyl diphosphate synthases in mice and humans. *The FEBS journal,* 272**,** 5606-5622.

SAKAKURA, Y., SHIMANO, H., SONE, H., TAKAHASHI, A., INOUE, K., TOYOSHIMA, H., SUZUKI, S. & YAMADA, N. 2001. Sterol regulatory element-binding proteins induce an entire pathway of cholesterol synthesis. *Biochemical and biophysical research communications,* 286**,** 176-183.

SALVIATI, L., TREVISSON, E., HERNANDEZ, M. A. R., CASARIN, A., PERTEGATO, V., DOIMO, M., CASSINA, M., AGOSTO, C., DESBATS, M. A. & SARTORI, G. 2012. Haploinsufficiency of COQ4 causes coenzyme Q10 deficiency. *Journal of medical genetics,* 49**,** 187-191.

SANTORO, M. M. 2020. The antioxidant role of non-mitochondrial CoQ10: mystery solved! *Cell metabolism,* 31**,** 13-15.

SANTULLI, G., PAGANO, G., SARDU, C., XIE, W., REIKEN, S., D'ASCIA, S. L., CANNONE, M., MARZILIANO, N., TRIMARCO, B. & GUISE, T. A. 2015. Calcium release channel RyR2 regulates insulin release and glucose homeostasis. *The Journal of clinical investigation,* 125**,** 1968-1978.

SARDIELLO, M., PALMIERI, M., DI RONZA, A., MEDINA, D. L., VALENZA, M., GENNARINO, V. A., DI MALTA, C., DONAUDY, F., EMBRIONE, V. & POLISHCHUK, R. S. 2009. A gene network regulating lysosomal biogenesis and function. *Science,* 325**,** 473-477.

SCHÄGGER, H. & PFEIFFER, K. 2000. Supercomplexes in the respiratory chains of yeast and mammalian mitochondria. *The EMBO journal,* 19**,** 1777-1783.

SCHAPIRA, A. H. 2015. Glucocerebrosidase and Parkinson disease: recent advances. *Molecular and Cellular Neuroscience,* 66**,** 37-42.

SCHEDIN, S., SINDELAR, P. J., PENTCHEV, P., BRUNK, U. & DALLNER, G. 1997. Peroxisomal impairment in Niemann-Pick type C disease. *J Biol Chem,* 272**,** 6245-51.

SCHEIBYE-KNUDSEN, M., FANG, E. F., CROTEAU, D. L., WILSON III, D. M. & BOHR, V. A. 2015. Protecting the mitochondrial powerhouse. *Trends in cell biology,* 25**,** 158-170.

SCHMELZLE, T. & HALL, M. N. 2000. TOR, a central controller of cell growth. *Cell,* 103**,** 253-262.

SCHNEIDER, D. & ELSTNER, E. F. 2000. Coenzyme Q10, vitamin E, and dihydrothioctic acid cooperatively prevent diene conjugation in isolated lowdensity lipoprotein. *Antioxidants & redox signaling,* 2**,** 327-333.

SCHÖNDORF, D. C., AURELI, M., MCALLISTER, F. E., HINDLEY, C. J., MAYER, F., SCHMID, B., SARDI, S. P., VALSECCHI, M., HOFFMANN, S. & SCHWARZ, L. K. 2014. iPSC-derived neurons from GBA1-associated Parkinson's disease patients show autophagic defects and impaired calcium homeostasis. *Nature communications,* 5**,** 1-17.

SCHWAKE, M., SCHRÖDER, B. & SAFTIG, P. 2013. Lysosomal membrane proteins and their central role in physiology. *Traffic,* 14**,** 739-748.

SENA, L. A. & CHANDEL, N. S. 2012. Physiological roles of mitochondrial reactive oxygen species. *Molecular cell,* 48**,** 158-167.

SETTEMBRE, C., DI MALTA, C., POLITO, V. A., ARENCIBIA, M. G., VETRINI, F., ERDIN, S., ERDIN, S. U., HUYNH, T., MEDINA, D. & COLELLA, P. 2011. TFEB links autophagy to lysosomal biogenesis. *science***,** 1204592.

SHEPHERD, D. & GARLAND, P. 1969. The kinetic properties of citrate synthase from rat liver mitochondria. *Biochemical Journal,* 114**,** 597-610.

SHULTS, C. W., BEAL, M. F., SONG, D. & FONTAINE, D. 2004. Pilot trial of high dosages of coenzyme Q10 in patients with Parkinson's disease. *Experimental neurology,* 188**,** 491-494.

SHULTS, C. W., OAKES, D., KIEBURTZ, K., BEAL, M. F., HAAS, R., PLUMB, S., JUNCOS, J. L., NUTT, J., SHOULSON, I. & CARTER, J. 2002. Effects of coenzyme Q10 in early Parkinson disease: evidence of slowing of the functional decline. *Archives of neurology,* 59**,** 1541-1550.

SIDRANSKY, E., NALLS, M. A., AASLY, J. O., AHARON-PERETZ, J., ANNESI, G., BARBOSA, E. R., BAR-SHIRA, A., BERG, D., BRAS, J. & BRICE, A. 2009. Multicenter analysis of glucocerebrosidase mutations in Parkinson's disease. *New England Journal of Medicine,* 361**,** 1651-1661.

SIEKEVITZ, P. 1957. Powerhouse of the cell. *Scientific American,* 197**,** 131-144.

SIES, H. 2000. What is oxidative stress? *Oxidative stress and vascular disease.* Springer.

SIGAL, S. H., RAJVANSHI, P., GORLA, G. R., SOKHI, R. P., SAXENA, R., GEBHARD JR, D. R., REID, L. M. & GUPTA, S. 1999. Partial hepatectomy-induced polyploidy attenuates hepatocyte replication and activates cell aging events. *American Journal of Physiology-Gastrointestinal and Liver Physiology,* 276**,** G1260G1272.

SIVANDZADE, F., BHALERAO, A. & CUCULLO, L. 2019. Analysis of the mitochondrial membrane potential using the cationic JC-1 dye as a sensitive fluorescent probe. *Bio-protocol,* 9.

SKULACHEV, V. P. 1998. Uncoupling: new approaches to an old problem of bioenergetics. *Biochimica et Biophysica Acta (BBA)-Bioenergetics,* 1363**,** 100-124.

SLOCK, J., STAHLY, D., HAN, C., SIX, E. & CRAWFORD, I. 1990. An apparent Bacillus subtilis folic acid biosynthetic operon containing pab, an amphibolic trpG gene, a third gene required for synthesis of para-aminobenzoic acid, and the dihydropteroate synthase gene. *Journal of bacteriology,* 172**,** 7211-7226.

SOLMAZ, S. R. & HUNTE, C. 2008. Structure of complex III with bound cytochrome c in reduced state and definition of a minimal core interface for electron transfer. *Journal of Biological Chemistry,* 283**,** 17542-17549.

STEFANIS, L. 2012. α-Synuclein in Parkinson's disease. *Cold Spring Harbor perspectives in medicine,* 2**,** a009399-a009399.

STIRPE, F., HIGGINS, T., TAZZARI, P. L. & ROZENGURT, E. 1991. Stimulation by xanthine oxidase of 3T3 Swiss fibroblasts and human lymphocytes. *Experimental cell research,* 192**,** 635-638.

STOUT, A. K., RAPHAEL, H. M., KANTEREWICZ, B. I., KLANN, E. & REYNOLDS, I. J. 1998. Glutamate-induced neuron death requires mitochondrial calcium uptake. *Nature neuroscience,* 1**,** 366-373.

STOYANOVSKY, D. A., OSIPOV, A. N., QUINN, P. J. & KAGAN, V. E. 1995. Ubiquinone-dependent recycling of vitamin E radicals by superoxide. *Archives of Biochemistry and Biophysics,* 323**,** 343-351.

SUN, A. 2018. Lysosomal storage disease overview. *Annals of translational medicine,* 6.

TAKAHASHI, T., OKAMOTO, T., MORI, K., SAYO, H. & KISHI, T. 1993. Distribution of ubiquinone and ubiquinol homologues in rat tissues and subcellular fractions. *Lipids,* 28**,** 803-809.

TAUCHE, A., KRAUSE-BUCHHOLZ, U. & RÖDEL, G. 2008. Ubiquinone biosynthesis in Saccharomyces cerevisiae: the molecular organization of O-methylase Coq3p depends on Abc1p/Coq8p. *FEMS yeast research,* 8**,** 1263-1275.

THELEN, A. M. & ZONCU, R. 2017. Emerging roles for the lysosome in lipid metabolism. *Trends in cell biology,* 27**,** 833-850.

THOMAS, S. R., WITTING, P. K. & STOCKER, R. 1999. A role for reduced coenzyme Q in atherosclerosis? *Biofactors,* 9**,** 207-224.

TRAN, U. C. & CLARKE, C. F. 2007. Endogenous synthesis of coenzyme Q in eukaryotes. *Mitochondrion,* 7**,** S62-S71.

TRIFUNOVIC, A. & LARSSON, N. G. 2008. Mitochondrial dysfunction as a cause of ageing. *Journal of internal medicine,* 263**,** 167-178.

TURRENS, J. F., ALEXANDRE, A. & LEHNINGER, A. L. 1985. Ubisemiquinone is the electron donor for superoxide formation by complex III of heart mitochondria. *Archives of biochemistry and biophysics,* 237**,** 408-414.

TURUNEN, M., OLSSON, J. & DALLNER, G. 2004. Metabolism and function of coenzyme Q. *Biochimica et Biophysica Acta (BBA)-Biomembranes,* 1660**,** 171-199.

VAN DIJCK, P., DE KRUIJFF, B., VAN DEENEN, L., DE GIER, J. & DEMEL, R. 1976. The preference of cholesterol for phosphatidylcholine in mixed phosphatidylcholine-phosphatidylethanolamine bilayers. *Biochimica et Biophysica Acta (BBA)-Biomembranes,* 455**,** 576-587.

VANIER, M. T., DUTHEL, S., RODRIGUEZ-LAFRASSE, C., PENTCHEV, P. & CARSTEA, E. D. 1996. Genetic heterogeneity in Niemann-Pick C disease: a study using somatic cell hybridization and linkage analysis. *Am J Hum Genet,* 58**,** 118-25.

VÁZQUEZ, M. C., BALBOA, E., ALVAREZ, A. R. & ZANLUNGO, S. 2012. Oxidative stress: a pathogenic mechanism for Niemann-Pick type C disease. *Oxidative medicine and cellular longevity,* 2012.

VILLALBA, J. M. & NAVAS, P. 2000. Plasma membrane redox system in the control of stress-induced apoptosis. *Antioxidants & redox signaling,* 2**,** 213-230.

VITNER, E. B., PLATT, F. M. & FUTERMAN, A. H. 2010. Common and uncommon pathogenic cascades in lysosomal storage diseases. *Journal of Biological Chemistry***,** jbc. R110. 134452.

VON BALLMOOS, C., COOK, G. M. & DIMROTH, P. 2008. Unique rotary ATP synthase and its biological diversity. *Annu. Rev. Biophys.,* 37**,** 43-64.

WALLENFELS, K. & WEIL, R. 1972. 20 β-Galactosidase. *The enzymes.* Elsevier.

WARTOSCH, L., BRIGHT, N. A. & LUZIO, J. P. 2015. Lysosomes. *Current Biology,* 25**,** R315-R316.

WATMOUGH, N. J. & FRERMAN, F. E. 2010. The electron transfer flavoprotein: ubiquinone oxidoreductases. *Biochimica et Biophysica Acta (BBA)-Bioenergetics,* 1797**,** 1910-1916.

WEBER, L. W., BOLL, M. & STAMPFL, A. 2004. Maintaining cholesterol homeostasis: sterol regulatory element-binding proteins. *World journal of gastroenterology: WJG,* 10**,** 3081.

WIKSTROM, M. K. 1977. Proton pump coupled to cytochrome c oxidase in mitochondria. *Nature,* 266**,** 271-273.

WOLF, D. E., HOFFMAN, C. H., TRENNER, N. R., ARISON, B. H., SHUNK, C. H., LINN, B. O., MCPHERSON, J. F. & FOLKERS, K. 1958. Coenzyme QI Structure studies on the coenzyme Q group. *Journal of the American Chemical Society,* 80**,** 4752-4752.

WONG, Y. C., YSSELSTEIN, D. & KRAINC, D. 2018. Mitochondria–lysosome contacts regulate mitochondrial fission via RAB7 GTP hydrolysis. *Nature,* 554**,** 382-386.

XIAO, B., DENG, X., ZHOU, W. & TAN, E.-K. 2016. Flow cytometry-based assessment of mitophagy using MitoTracker. *Frontiers in cellular neuroscience,* 10**,** 76.

XILOURI, M., VOGIATZI, T. & STEFANIS, L. 2008. alpha-synuclein degradation by autophagic pathways: a potential key to Parkinson's disease pathogenesis. *Autophagy,* 4**,** 917-919.

YAMADA, D., SAIKI, S., FURUYA, N., ISHIKAWA, K.-I., IMAMICHI, Y., KAMBE, T., FUJIMURA, T., UENO, T., KOIKE, M. & SUMIYOSHI, K. 2016. Ethambutol neutralizes lysosomes and causes lysosomal zinc accumulation. *Biochemical and biophysical research communications,* 471**,** 109-116.

YAMAMOTO, A., TAGAWA, Y., YOSHIMORI, T., MORIYAMA, Y., MASAKI, R. & TASHIRO, Y. 1998. Bafilomycin A1 prevents maturation of autophagic vacuoles by inhibiting fusion between autophagosomes and lysosomes in rat hepatoma cell line, H-4-II-E cells. *Cell structure and function,* 23**,** 33-42.

YETKIN-ARIK, B., VOGELS, I. M. C., NOWAK-SLIWINSKA, P., WEISS, A., HOUTKOOPER, R. H., VAN NOORDEN, C. J. F., KLAASSEN, I. & SCHLINGEMANN, R. O. 2019. The role of glycolysis and mitochondrial respiration in the formation and functioning of endothelial tip cells during angiogenesis. *Scientific Reports,* 9**,** 12608.

YOKOYAMA, K., NAKANO, M., IMAMURA, H., YOSHIDA, M. & TAMAKOSHI, M. 2003. Rotation of the proteolipid ring in the V-ATPase. *Journal of Biological Chemistry,* 278**,** 24255-24258.

YOSHIMORI, T., YAMAMOTO, A., MORIYAMA, Y., FUTAI, M. & TASHIRO, Y. 1991. Bafilomycin A1, a specific inhibitor of vacuolar-type H(+)-ATPase, inhibits acidification and protein degradation in lysosomes of cultured cells. *Journal of Biological Chemistry,* 266**,** 17707-17712.

YU, L., MCPHEE, C. K., ZHENG, L., MARDONES, G. A., RONG, Y., PENG, J., MI, N., ZHAO, Y., LIU, Z. & WAN, F. 2010. Termination of autophagy and reformation of lysosomes regulated by mTOR. *Nature,* 465**,** 942.

YUBERO, D., MONTERO, R., ARTUCH, R., LAND, J. M., HEALES, S. J. & HARGREAVES, I. P. 2014. Biochemical diagnosis of coenzyme q10 deficiency. *Molecular syndromology,* 5**,** 147-155.

ZHANG, Y., TURUNEN, M. & APPELKVIST, E.-L. 1996. Restricted uptake of dietary coenzyme Q is in contrast to the unrestricted uptake of α-tocopherol into rat organs and cells. *The Journal of nutrition,* 126**,** 2089-2097.

ZIMMERMAN, J. J., VON SAINT ANDRÉ-VON ARNIM, A. & MCLAUGHLIN, J. 2011. Chapter 74 - Cellular Respiration. *In:* FUHRMAN, B. P. & ZIMMERMAN, J. J. (eds.) *Pediatric Critical Care (Fourth Edition).* Saint Louis: Mosby.

ZONCU, R., BAR-PELED, L., EFEYAN, A., WANG, S., SANCAK, Y. & SABATINI, D. M. 2011. mTORC1 senses lysosomal amino acids through an inside-out mechanism that requires the vacuolar H+-ATPase. *Science,* 334**,** 678-683.

Appendix

Turton, N., Bowers, N., Khajeh, S., Hargreaves, I. P., & Heaton, R. A. (2021). Coenzyme Q10 and the exclusive club of diseases that show a limited response to treatment. *Expert opinion on orphan drugs*, 1-10. doi:10.1080/21678707.2021.1932459

Mantle, D., Heaton, R., & Hargreaves, I. (2021). Coenzyme Q10 and Immune Function: An Overview. *Antioxidants*, *10*(5). doi:10.3390/antiox10050759

Lund, M., Andersen, K. G., Heaton, R., Hargreaves, I. P., Gregersen, N., & Olsen, R. K. J. (2021). Bezafibrate activation of PPAR drives disturbances in mitochondrial redox bioenergetics and decreases the viability of cells from patients with VLCAD deficiency. *Biochimica et Biophysica Acta (BBA): Molecular Basis of Disease*, 166100. doi:10.1016/j.bbadis.2021.166100

Maguire, Á., Mooney, C., Flynn, G., Ferguson, Y., O'Keane, V., O'Rourke, D., . . . Hargreaves, A. (2021). No Effect of Coenzyme Q10 on Cognitive Function, Psychological Symptoms, and Health-related Outcomes in Schizophrenia and Schizoaffective Disorder: Results of a Randomized, Placebo-Controlled Trial. *Journal of Clinical Psychopharmacology*, *41*(1), 53-57. doi:10.1097/JCP.0000000000001330

Hufnagel, A., Fernandez-Twinn, D. S., Blackmore, H. L., Ashmore, T. J., Heaton, R. A., Jenkins, B., . . . Ozanne, S. E. (2021). Maternal but not fetoplacental health can be improved by metformin in a murine diet-induced model of maternal obesity and glucose intolerance. *Journal of Physiology*. doi:10.1113/JP281902

Hargreaves, I. (n.d.). Effects of Feeding Coenzyme Q10-Ubiquinol on Plasma Coenzyme Q10 Concentrations and Semen Quality in Stallions. *Journal of Equine Veterinary Science*.

Proctor, E. C., Turton, N., Boan, E. J., Bennett, E., Philips, S., Heaton, R., & Hargreaves, I. (2020). The Effect of Methylmalonic Acid Treatment on Human Neuronal Cell Coenzyme Q10 Status and Mitochondrial Function. *International Journal of Molecular Sciences*, *21*(23). doi:10.3390/ijms21239137

Hargreaves, I., Heaton, R. A., & Mantle, D. (2020). Disorders of Human Coenzyme Q10 Metabolism: An Overview. *International Journal of Molecular Sciences*, *21*(18), 6695. doi:10.3390/ijms21186695

Stepien, K. M., Roncaroli, F., Turton, N., Hendriksz, C. J., Roberts, M., Heaton, R., & Hargreaves, I. (n.d.). Mechanisms of Mitochondrial Dysfunction in Lysosomal Storage Disorders: A Review. *Journal of Clinical Medicine*.

Heaton, R. A., Heales, S., Rahman, K., Sexton, D., & Hargreaves, I. (2020). The Effect of Cellular Coenzyme Q10 Deficiency on Lysosomal Acidification. *Journal of Clinical Medicine*, *9*(6). doi:10.3390/jcm9061923

Hargreaves, A., Maguire, A., Mooney, C., Hargreaves, I., Heaton, R., Phillips, S., & Gill, M. (2020). T58. EFFECTIVENESS OF ORALLY ADMINISTERED CO-ENZYME Q10 FOR SCHIZOPHRENIA: COGNITIVE, FUNCTIONAL AND BIOCHEMICAL OUTCOMES FROM A DOUBLE BLIND, RANDOMISED, PLACEBO CONTROLLED TRIAL. In *Schizophrenia Bulletin* (Vol. 46, Iss. 1, pp. S253). Oxford University Press (OUP). doi:10.1093/schbul/sbaa029.618

Ghosh, R.; Wood-Kaczmar, A.; Dobson, L.; Smith, E. J.; Sirinathsinghji, E. C.; Kriston-Vizi, J.; Hargreaves, Iain; Heaton, R.; Hermann, F.; Abramov, A. Y. (2020). Expression of mutant exon 1 huntingtin fragments in human neural stem cells and neurons causes

inclusion formation and mitochondrial dysfunction. *The FASEB Journal*, *34*(6), 81398154. doi:10.1096/fj.201902277RR

Turton, N., Heaton, R., Ismail, F., Roberts, S., Nelder, S., Phillips, S., & Hargreaves, I. (2020). The Effect of Organophosphate Exposure on Neuronal Cell Coenzyme Q10 Status.. *Neurochemical Research*. doi:10.1007/s11064-020-03033-y

Hargreaves, I. (2020). Coenzyme Q10 Assessment and the Establishment of a Neuronal Cell Model of CoQ10 Deficiency. In P. guest (Ed.), *Clinical and Preclinical Models for Maximizing Healthspan* (pp. 277-287). Springer. Retrieved from https://doi.org/10.1007/978-1-0716-0471-7_19

Ceresa, C., Hutton, S., Lajarin-Cuesta, M., Heaton, R., Hargreaves, I., Fracchia, L., & Diaz, M. (2020). Production of Mannosylerythritol Lipids (MELs) to be Used as Antimicrobial Agents against S. aureus ATCC 6538. *Current Microbiology: an international journal*. doi:10.1007/s00284-020-01927-2

Heaton, R., Millichap, L., Saleem, F., Gannon, J., Begum, G., & Hargreaves, I. P. (2019). Current biochemical treatments of mitochondrial respiratory chain disorders. *Expert opinion on orphan drugs*, *7*(6), 277-285. doi:10.1080/21678707.2019.1638250

Thueson, E., Leadon, D. P., Heaton, R., Hargreaves, I. P., & Bayly, W. M. (2019). Effect of daily supplementation with ubiquinol on muscle coenzyme Q10 concentrations in Thoroughbred racehorses. *Comparative Exercise Physiology*, *15*(3), 219-226. doi:10.3920/CEP190023

Stepien, K. M., Heaton, R., Rankin, S., Murphy, A., Bentley, J., Sexton, D., & Hargreaves, I. (2017). Evidence of Oxidative Stress and Secondary Mitochondrial Dysfunction in Metabolic and Non-Metabolic Disorders. *Journal of Clinical Medicine*, *6*(7). doi:10.3390/jcm6070071